5-2018

The Intrinsic Properties of Reconstituted Soils

Nabeel Shaker Mahmood
University of Arkansas, Fayetteville

The Intrinsic Properties of Reconstituted Soils

A dissertation submitted in partial fulfillment of the
requirements for the degree of
Doctor of Philosophy in Engineering

by

Nabeel S. Mahmood
University of Anbar
Bachelor of Science in Civil Engineering, 2001
University of Baghdad
Master of Science in Civil Engineering, 2004

May 2018
University of Arkansas

This dissertation is approved for recommendation to the Graduate Council.

_____
Richard A. Coffman, Ph.D., P.E., P.L.S.
Dissertation Director

_____
Michelle Bernhardt-Barry, Ph.D., P.E.
Committee Member

_____
Paul Millett, Ph.D.
Committee Member

_____
Clinton Wood, Ph.D., P.E.
Committee Member

ABSTRACT

Reconstituted specimens are often utilized to characterize engineering properties of cohesive soils. A series of undrained triaxial tests were conducted on reconstituted soil specimens to evaluate 1) the influence of stress path, 2) the intrinsic shear strength behavior, and 3) the small-strain characteristics. The stress path tests were conducted on kaolinite specimens reconstituted from slurries with water content values of one and one-half times the liquid limit of the soil (1.5LL). To evaluate the intrinsic undrained shear strength and the intrinsic small-strain properties, the triaxial tests were performed on kaolinite and illite specimens that were reconstituted at two levels of slurry water content of 1.5LL and three times the corresponding liquid limit of the soil. Bender elements were employed with the triaxial device to measure shear wave velocity during the triaxial tests that were performed to evaluate the small-strain characteristics.

The stress-strain behavior of the normally consolidated kaolinite specimens was similar to the typical behavior of the overconsolidated specimens. Identical stress-strain behavior was observed from the stress paths tests at the same orientation of the principal stresses. A new interpretation method was proposed to normalize the undrained shear strength values of the overconsolidated specimens based on the concept of void index. By utilizing this method, better correlation was obtained between the undrained shear strength values and the intrinsic shear strength line. The values of the shear wave velocity and shear modulus were also normalized to the void index to evaluate the intrinsic small-strain characteristics. The values of both the shear wave velocity and the shear modulus did not normalize with respect to the void index values.

As discussed herein, the triaxial compression test and the reduced triaxial extension test are adequate to represent the different loading and unloading conditions in the field. Unlike

previous recommendations of preparing soil slurries at water contents of 1.25 times the liquid limit, soil slurries should be prepared at water content values of at least 3LL. By preparing soil slurries with a water content of 3LL, undrained shear strength and small-strain characteristics that are in better agreement with those for natural soils will be obtained.

ACKNOWLEDGEMENTS

I would like to express my deep appreciation and sincere gratitude to my academic advisor and committee chair, Dr. Richard Coffman for his continuous guidance, assistance, and motivation throughout my years at the University of Arkansas. Similarly, I would like to thank my committee members, Dr. Michelle Bernhardt-Barry, Dr. Paul Millett, and Dr. Clinton Wood for generously offering their time, support, guidance and advice along this project.

I want to also thank the Higher Committee for Education Development in Iraq (HCED) who granted me the financial support and to the University of Anbar who granted me a six-year study leave.

I would like to acknowledge my colleagues, including but not limited to: Yi Zhao, Elvis Ishimwe, Sean Salazar, and Cyrus Garner for their valuable assistance and friendship throughout the years.

Finally, I am very grateful to my mother, who passed away during my study. She was always there with unconditional love and encouragement. I am thankful to my father, parents-in-law, brothers and sisters for their encouragement and inspiration. Special thanks to my wife Noor, who provided me with love and strength to face the difficulties. Many thanks to my children, Zaid, Yousif, and Adam, who provided me hope to finish my degree.

TABLE OF CONTENTS

LIST OF FIGURES

LIST OF TABLES

LIST OF PUBLISHED OR SUBMITTED PAPERS

Chapter 4: Mahmood, N. S. and Coffman, R. A., (2017). "The Effects of Stress Path on the Characterization of Reconstituted Low Plasticity Kaolinite." Soils and Foundations, (Under Review, Manuscript Number: SANDF-D-17-00352-R1).

Chapter 5: Mahmood, N. S., and Coffman, R. A., (2018a). "Intrinsic Shear Strength Behavior of Reconstituted Kaolinite and Illite Soils." Quarterly Journal of Engineering Geology and Hydrogeology, (In Review, Manuscript Number: qjegh2018-056-R1).

Chapter 6: Mahmood, N. S., and Coffman, R. A., (2018b). "Small-strain of Reconstituted Soils: The Effect of Slurry Water Content." Geotechnical Testing Journal, (Under Review, Manuscript Number: GTJ-2018-0098-R1).

CHAPTER 1: Introduction

1.1. Chapter Overview

Reconstituted soil specimens are commonly utilized to characterize the geotechnical properties of natural soils. The compression, strength, and small-strain properties of reconstituted kaolinite and illite soils are introduced in this document. Specifically, four main items including: 1) shear strength parameters and stress-strain relationships under different loading conditions, 2) intrinsic undrained shear strength behavior, 3) small-strain stiffness, and 4) fabric anisotropy of illite and kaolinite soils are discussed. The aforementioned properties were determined by performing K_o-consolidated, undrained, triaxial tests with shear wave velocity measurements. The equipment, test materials, and methodology that were utilized to perform the experimental program are also described herein. The measured parameters were analyzed by utilizing the principles of soil mechanics and then compared with literature values to gain insight into the measured behavior of the reconstituted soils.

This chapter is divided into three sections. 1) An overview of the research project is described in Section 1.2. 2) The motivation for this research is presented in Section 1.3. 3) The organization of the entire dissertation is presented in Section 1.4.

1.2. Project Description and Objectives

The hypothesis of this research included *1) stress-strain and soil moduli parameters may be evaluated by performing triaxial testing under different loading conditions and 2) these parameters may be utilized to characterize the engineering behavior of reconstituted soils.* The three main objectives of this research were to 1) explore the relationship between the stress path and the shear strength parameters of various cohesive soils, 2) examine the intrinsic shear strength behavior of various cohesive soils, and to 3) examine the intrinsic small-strain behavior and fabric anisotropy of various cohesive soils. The flow chart of the research plan is presented

in Figure 1.1. Several tasks were completed to evaluate the hypothesis of this research, as described below.

- A series of K_o-reconsolidated, undrained, triaxial compression and extension tests were performed under different loading conditions on kaolinite specimens that were reconstituted at initial water content of the slurry (w_s) of one and one-half times the liquid limit (1.5LL) of the soil.
- A series of K_o-reconsolidated, undrained, triaxial compression tests were conducted on kaolinite and illite specimens that were reconstituted at w_s levels of 1.5LL and three times the liquid limit (3LL) to explore the intrinsic shear strength characteristics.
- Small-strain shear modulus values were determined for kaolinite and illite specimens during the reconsolidation and shearing stages of the triaxial compression tests. These values were computed based on the shear wave velocity values that were measured by utilizing bender elements. The specimens for this scope of work were reconstituted at w_s values of 1.5LL and 3LL.
- The values of shear wave velocity were compared with the shear wave velocity values that were obtained by utilizing bender elements within a constant rate of strain consolidation device.
- Problems associated with the test methods were discussed and new test procedures were proposed.

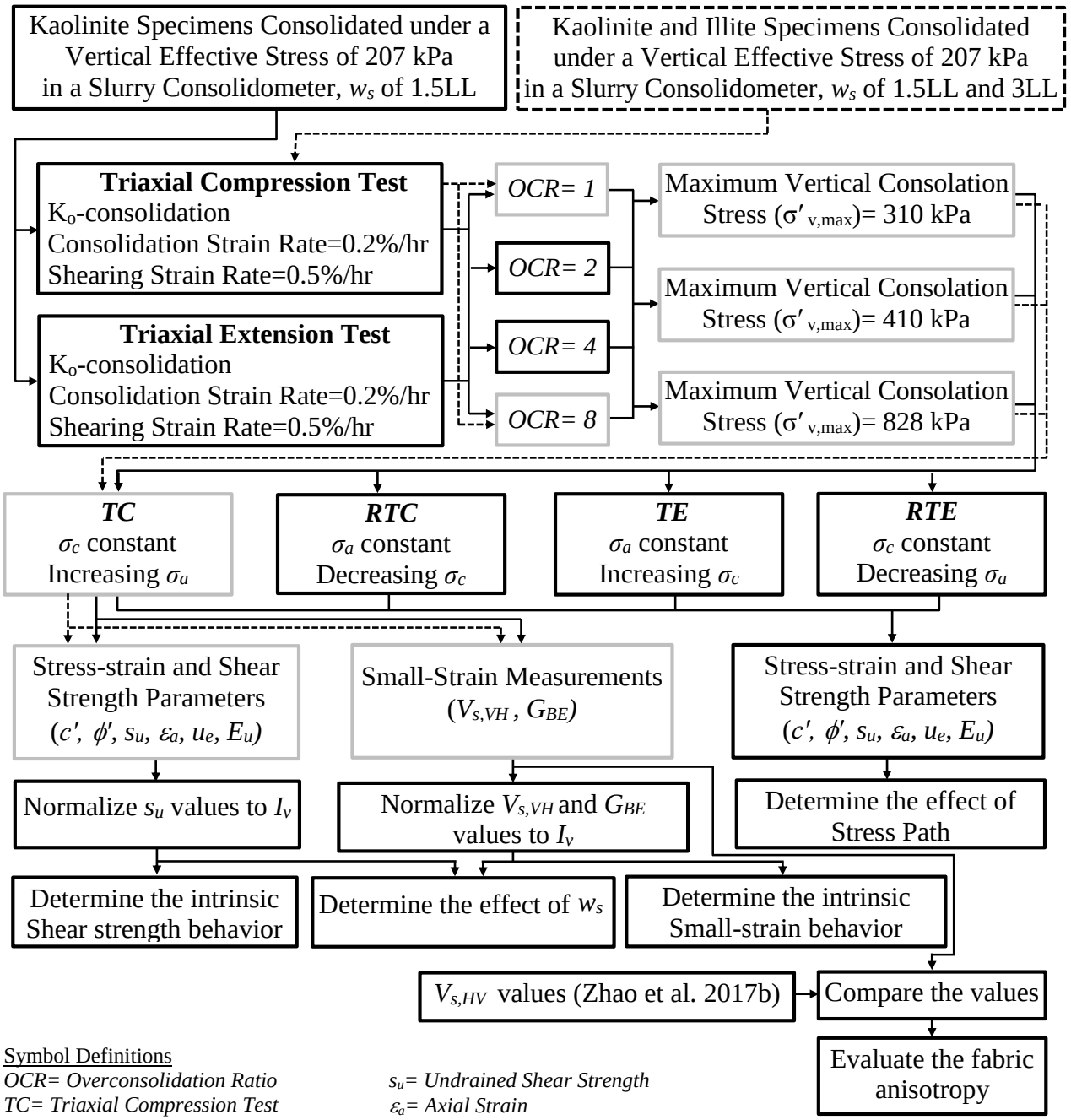

Symbol Definitions

OCR= Overconsolidation Ratio
TC= Triaxial Compression Test
RTC= Reduced Triaxial Compression
TE= Triaxial Extension Test
RTE= Reduced Triaxial Extension Test
σ_c = Cell Pressure
σ_a = Axial Stress
c' = Effective Cohesion
ϕ'= Effective Angle of Internal Friction
Gray outlines indicating tests performed on specimens with w_s of 1.5LL and 3LL

s_u= Undrained Shear Strength
ε_a= Axial Strain
u_e= Excess Pore Water Pressure
E_u= Undrained Young's Modulus
I_v= Void Index
G_{BE}= Small-strain Shear Modulus
$V_{s,VH}$= Vertically-propagated, Horizontally-polarized Shear Wave Velocity
$V_{s,HV}$= Horizontally -propagated, Vertically -polarized Shear Wave Velocity
w_s= Initial Water Content of the Slurry

Figure 1.1. The flow chart of the research plan.

1.3. Benefits to Geotechnical Engineering

Characterization of the shear strength of soil for engineering practice requires applying various stress paths to soil to represent loading field conditions. Based on the concept of stress path, different site characterization and design methods have been developed to account for different orientations of the major, minor, and intermediate principal stress states. These methods have been developed because the use of conventional triaxial testing has often led to either unsafe or over-conservative designs. The shear strength parameters, as obtained from controlled stress path triaxial testing, will aid in the solution of many instu stress path related problems. Furthermore, limited amounts of triaxial compression testing data are currently available to evaluate the parameters for advanced constitutive models. The data obtained from this research will be analyzed and compared to develop an understanding of the testing techniques required to represent certain field conditions. Moreover, these data will be useful to develop or validate advanced constitutive models.

A better understanding of the engineering behavior of the reconstituted soils will aid in the quantification and characterization of the engineering behavior of the natural soils. Few studies have investigated the correlations between the initial water content of a given slurry and the engineering characteristics of the reconstituted soils that were developed from the slurry. Specifically, the intrinsic shear strength of reconstituted specimens that were overconsolidated during the triaxial testing has not been previously evaluated. Furthermore, the influence of the initial water content of the slurry and fabric anisotropy on the small-strain behavior of reconstituted soil specimens has been studied by a limited number of researchers. Recommended w_s levels, that should be considered when reconstituting specimens of cohesive soils for shear strength small-strain measurements, will be provided. More representative values of shear

strength and small-strain characteristics of corresponding natural soils will be obtained as the result of this study by using the recommended slurry reconstitution procedures.

1.4. Dissertation Organization

The results from this research are described in seven chapters of this dissertation. The organization of the dissertation is described in this chapter (Chapter 1). A review the related literature, describing fundamental aspects of stress path, reconstituted soils, and small-strain measurements, is presented in Chapter 2. The contents of Chapters 4 through 6 have been submitted for publication. Information about the submissions is described below. The main conclusions drawn from the research are presented in Chapter 7.

A technical paper about the effect of the stress path on 1) the stress-strain behavior and 2) the shear strength characteristics of reconstituted low plasticity kaolinite soil, as obtained from a comprehensive triaxial testing program, is presented in Chapter 4. The paper was submitted to *Soils and Foundations*. The full reference is: Mahmood, N. S. and Coffman, R. A., (2017). "The Effects of Stress Path on the Characterization of Reconstituted Low Plasticity Kaolinite." *Soils and Foundations*, Under Review, Manuscript Number: SANDF-D-17-00352-R1.

The observed relationships between the initial water content of the slurry and the corresponding shear strength characteristics of reconstituted kaolinite and illite soils, is presented in Chapter 5. The paper was submitted to *Quarterly Journal of Engineering Geology and Hydrogeology*. The full reference is: Mahmood, N. S. and Coffman, R. A., (2018a). "Intrinsic shear strength behavior of reconstituted kaolinite and illite soils." *Quarterly Journal of Engineering Geology and Hydrogeology*, Under Review, Manuscript Number: qjegh2018-056-R1.

The shear wave velocity and small-strain shear stiffness of reconstituted kaolinite and illite specimens were investigated by utilizing triaxial apparatus instrumented with bender elements. The results obtained from this investigation were documented in a technical paper which is presented in Chapter 6. The paper was submitted to the *Geotechnical Testing Journal*. The full reference is: Mahmood, N. S. and Coffman, R. A., (2018b). "Small-strain of Reconstituted Soils: The Effect of Slurry Water Content." *Geotechnical Testing Journal*, Under Review, Manuscript Number: GTJ-2018-0098-R1.

1.5. References

Mahmood, N. S. and Coffman, R. A., (2017). "The Effects of Stress Path on the Characterization of Reconstituted Low Plasticity Kaolinite." Soils and Foundations, (Under Review, Manuscript Number: SANDF-D-17-00352-R1).

Mahmood, N. S., and Coffman, R. A., (2018a). "Intrinsic Shear Strength Behavior of Reconstituted Kaolinite and Illite Soils." Quarterly Journal of Engineering Geology and Hydrogeology, (In Review, Manuscript Number: qjegh2018-056-R1).

Mahmood, N. S., and Coffman, R. A., (2018b). "Small-strain of Reconstituted Soils: The Effect of Slurry Water Content." Geotechnical Testing Journal, (Under Review, Manuscript Number: GTJ-2018-0098-R1).

CHAPTER 2: Literature Review

2.1. Chapter Overview

A review of literature on the key areas of the research is presented in this chapter. Specifically, consideration is given to the stress-strain behavior and small-strain properties of cohesive soils under different loading conditions in undrained triaxial testing. An overview of the concept and the importance of stress path in triaxial testing, as well as the effects of stress path on the measurements engineering parameters is presented in Section 2.2. The engineering behavior of reconstituted soils, is discussed in Section 2.3. A description of the small-strain soil measurements and a discussion of the influences of stress history and fabric anisotropy on these measurements are presented in Section 2.4.

2.2. Stress Path in Triaxial Testing

Historically, triaxial testing has been the most utilized test method for reliable measurements of stress-strain relationships for soil. One of the factors that influences the stress-strain relationships, as obtained from triaxial testing, is the applied stress path. The concept and importance of stress path are presented in Section 2.2.1. The methods for applying stress paths during triaxial tests are discussed in Section 2.2.2. The effects of stress path on shear strength parameters are discussed in Section 2.2.3. The influences of stress path on 1) developed constitutive models and on 2) soil moduli are discussed in Sections 2.2.4 and Section 2.2.5, respectively.

2.2.1. *The Concept and Importance of Stress Path*

By definition, the stress path is the line that is developed by recording the direction and magnitude of the three principal stresses as a function of time during the consolidation and shearing stages of a triaxial test (Lambe 1967). Soil deformation during loading is mainly due to sliding between soil particles. Therefore, this deformation is highly irrecoverable and is

significantly dependent on the stress path (Lade and Duncan 1976). The amount of shear strength anisotropy, for a given soil, is influenced by the stress path that the soil experiences. Shear strength anisotropy is an important factor that may have significant effects on shear strength properties. In nature, anisotropic consolidation occurs during sedimentation of soil; this process is known as the inherent anisotropy. Examinations of the structure of clay samples following one-dimensional consolidation have led to the realization that clay particles tend to be oriented perpendicularly with respect to the direction of the major principal stress. Therefore, any change in the directions of the principal stress will affect the compressibility and shear strength of the clay (Hanse and Gibson 1949, Duncan and Seed 1966).

In addition to the inherent anisotropy, another form of anisotropy occurs as a result of the rotation of the three principal stresses during consolidation and shear. This rotation of the principal stresses is known as stress induced anisotropy (Hanse and Gibson 1949, Atkinson et al. 1987, Prashant and Penumadu 2005). It has been recognized by many researchers that different loading conditions encountered in the field result in a rotation of the principal stresses during shear (Figure 2.1). Therefore, the selected stress paths utilized during laboratory testing must be selected to represent the insitu loading conditions. Heave of soil at the bottom of an excavation, for instance, has been shown to be reproduced using triaxial extension tests while the bearing capacity of an embankment has been modeled by using a combination of plan strain active (PSA), plan strain passive (PSP), and direct simple shear (DSS) tests. For instance, the Earth Retaining Structures Manual (2007) distributed by the Federal Highway Administration (FHWA) states that triaxial extension tests should be conducted to evaluate the shear strength parameters in cases such as 1) deep excavations in soft clays or 2) soils in the passive zone. The manual also

states that the value of shear strength for soil in the passive zone is typically lower than the value of shear strength for soil in the active zone.

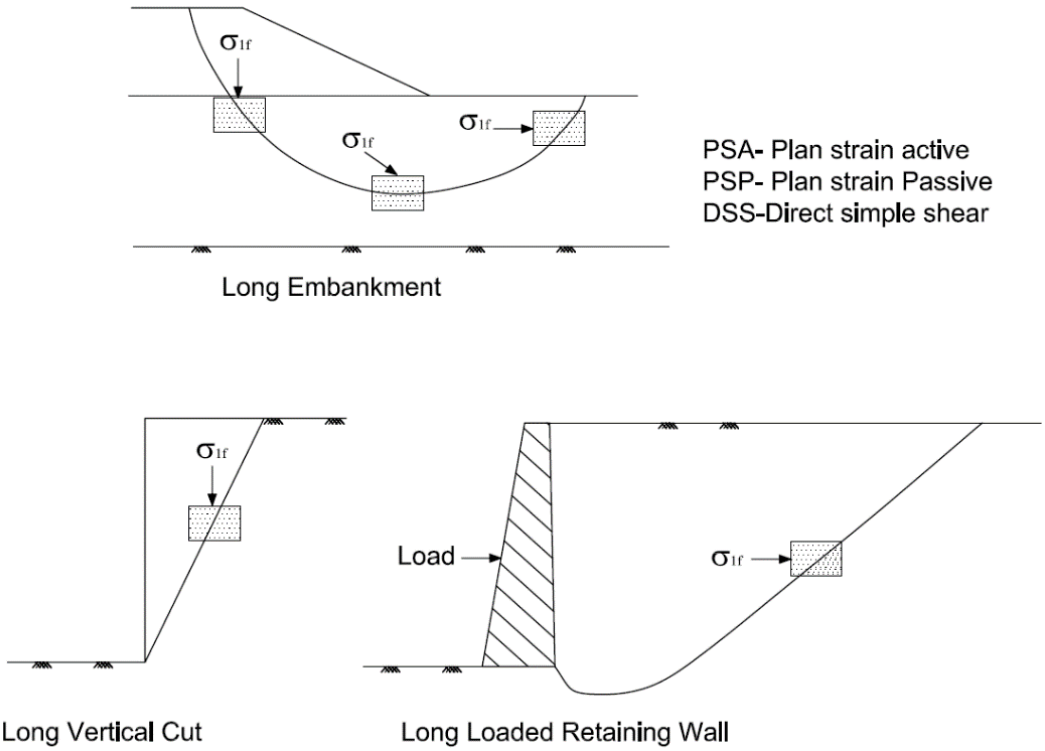

Figure 2.1. Orientation of the principal stresses and typical in situ modes of failure (modified from Ladd and Foott 1974).

Many different design methods have been employed to evaluate the stress-strain behavior of a given soil element soil when the soil is subjected to loading or unloading (e.g., Davis and Poulos 1968, Simons and Som 1970, Davis and Poulos 1972, Coffman et al. 2010). These methods have been developed to account for stress changes, in the field, that require representative laboratory obtained soil parameters, as obtained from laboratory stress path tests. Simons and Som (1970) stated that the modulus of elasticity value should be determined from an appropriate stress path to take in account the field stress conditions for settlement analyses.

In most design cases, the triaxial compression test (conventional triaxial) has been used to evaluate the undrained shear behavior of clay because of the simplicity and expediency of this test compared with other controlled stress path tests (Bishop and Henkel 1962, Kulhawy and

Mayne 1990, Bayoumi 2006). In the conventional triaxial compression test, the axial stress increased while the confining stress remains constant. However, the directions of the stresses induced by this test are not always representative of the directions of the principal stresses in the field.

Ladd and Foott (1974) stated that the undrained shear strength values obtained from PSA were greater than those obtained from DSS and the values obtained from the DSS were greater than those obtained from PSP. As described in Ladd and Foott (1974), the methods that have been commonly used in design to evaluate shear strength of soil have tended to self-compensate. Specifically, high values of undrained strength (s_u) that resulted from high levels of strain rate during the tests were compensated by the low s_u values that resulted from sample disturbance. This compensating error cannot to be controlled, so conservative or unsafe values of s_u may be mistakenly utilized for the design.

The SHANSEP (Stress History and Normalized Soil Engineering Properties) method, as based on the concept of normalization of the undrained shear strength (s_u) with respect to the in situ vertical effective stress (σ'_{vc}), has been utilized to ensure the use of representative values of undrained shear strength. As shown in Figure 2.2, the undrained shear strength is observed to increase with an increase in the over consolidation ratio (*OCR*). This relationship between the *OCR* and the undrained shear strength was formulated by the SHANSEP equation (Equation 2.1). This method was established by conducting a series of triaxial compression, triaxial extension, or direct simple shear tests, in addition to consolidation tests. Historically, the undrained shear strength has been characterized by using this procedure.

$$\frac{s_u}{\sigma'_{vc}} = S(OCR)^m \qquad \text{(after Ladd and Foott 1974)} \qquad \text{Equation 2.1}$$

Within Equation 2.1, *S* is the normalized undrained strength ratio for the respective stress paths at *OCR*=1 and *m* is the slope of the regression line for the respective stress paths.

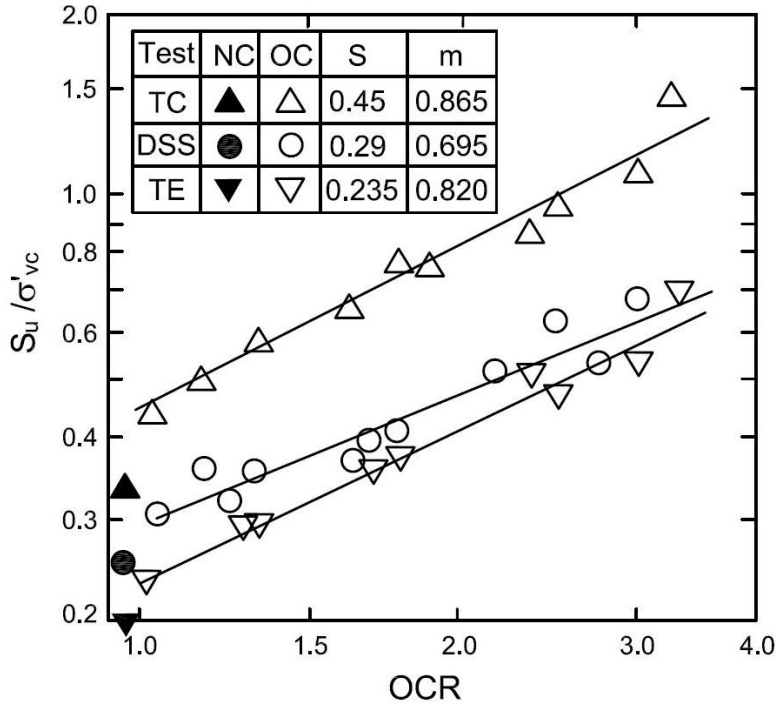

Figure 2.2. Undrained shear strength from three shear tests with different modes of shearing (data from Lefebrve et al. 1983, reproduced from Ladd 1991).

2.2.2. *Stress Path Methods in Triaxial Testing*

Triaxial testing is widely used, within the laboratory, to evaluate the strain-strain and strength properties of various soil types. One of the factors that influences the stress-strain and strength relationships obtained from triaxial testing is the applied stress path during the consolidation and shearing stages. Recent advances in the triaxial testing apparatus have led to stress path dependent triaxial tests being easier to conduct (Parry 2004, Holtz et al. 2011). The consolidation stage may consist of either isotropic or anisotropic consolidation (Bishop and Henkel 1962). Isotropic consolidation is achieved by applying equal vertical and horizontal effective stresses while anisotropic consolidation is achieved when the vertical effective stress is

greater than the horizontal effective stress. The purpose of the consolidation stage is to restore the original stress conditions before the sample is sheared.

Based on the assumption that the lateral stresses that are produced in the laboratory are the same as that in the field, the original field conditions, during the deposition process of natural soils, may be better represented using K_o-consolidation, (Hansen and Gibson 1949). Consolidation and reconsolidation may also be required to achieve certain overconsolidation values. Ladd and Foott (1974) recommended that soil specimens be reconsolidated to consolidation pressures that exceed the in situ preconsolidation pressures (σ'_c) by one and one-half to four times to eliminate the effects of sampling disturbance. Baldi et al. (1988) mentioned that 1) a suitable stress path must be selected to reconsolidate soil samples and that 2) the selected stress path should depend on the in situ effective stress, the overconsolidation ratio, and the clay type.

According to Salazar and Coffman (2014), during the shearing stage of triaxial testing, the specimen may be sheared in triaxial compression or triaxial extension by increasing or decreasing one or more of the three principal stresses. Accordingly, as listed in Table 2.1, there are six stress paths: conventional triaxial compression (CTC), reduced triaxial compression (RTC), triaxial compression (TC), conventional triaxial extension (CTE), reduced triaxial extension (RTE), and triaxial extension (TE).

Table 2.1. Shearing methods during triaxial compression and extension tests (modified from Salazar and Coffman 2014).

Triaxial Compression			Triaxial Extension		
Test	Axial Stress, σ_a	Cell Pressure, σ_c	Test	Axial Stress, σ_a	Cell Pressure, σ_c
CTC	Increase	Constant	CTE	Constant	Increase
RTC	Constant	Decrease	RTE	Decrease	Constant
TC	Increase by $\Delta\sigma_a$	Decrease by $1/2\Delta\sigma_a$	TE	Decrease by $1/2\Delta\sigma_c$	Increase by $\Delta\sigma_c$

Except for the K_o-consolidated specimens with K_o values greater than one, the major principal stress acts in the vertical direction and the minor principal stress acts in the horizontal direction at the end of consolidation stage. During the triaxial compression tests, the orientation of the principal stresses does not change during the shearing stage. The term "reorientation" of principal stresses was introduced by Duncan and Seed (1966) to describe the change in the state of stress when the orientation of the principal stresses, at the end of shearing stage, did not coincide with the orientation of the principal stresses prior to shearing. During triaxial extension testing, increasing the horizontal stress during the shearing or decreasing the vertical stress may cause the major principal stress to act in the horizontal direction and the minor principal stress to act in the vertical direction. Therefore, the principal stresses will be reoriented by 90 degrees at the end of shearing stage (Duncan and Seed 1966).

2.2.3. *Effect of Stress Path on Shear Strength Parameters*

The stress path that a sample is subjected to is one of the major factors that has a significant influence on both drained and undrained shear strength parameters. Based on the results from one of the earliest series of triaxial extension tests on clay, which were performed by Hirschfield (1958), the values of undrained strength (s_u) of extension tests were 20 to 25 percent less than those obtained from compression tests. More recently, Ladd and Foott (1974) reported that the shear strength values from the triaxial extension test (TE) were 10 to 25 percent less than those from (PSP) tests. Some examples of previous work concerning the effect of stress path on undrained shear strength values are presented in Table 2.2. Furthermore, the reported values of undrained shear strength were observed to decrease with an increase in the vertical stress level. Bishop (1966) attributed the lower values of undrained strength, that were obtained from triaxial extension tests, to differences in the amount of excess pore water pressure that developed during shearing.

Table 2.2. Undrained shear strength from compression and extension tests.

$s_{u(compression)}/s_{u(Extension)}$	Reference	Clay Type
1.25	Duncan and Seed (1966)	San Francisco Bay Mud
2.13	Ladd et al. (1971)	Resedimented Boston Blue Clay
2.5	Bjerrum et al. (1972)	Normally Consolidated Clay
1.75 to 3.78	Bjerrum (1973)	Bangkok Clay
1.2	Parry and Nadarajah (1974)	Fulford Clay
1.74 to 1.90	Moniz (2009)	Resedimented Boston Blue Clay

According to Bishop and Henkel (1962), Bishop (1966), and Lambe (1967), the drained shear strength parameters c′ and ϕ′ can be calculated from the undrained triaxial tests with pore water pressure measurements. Parry (2004) stated that there has been conflicting evidence presented in the available data regarding the effect of stress path on ϕ′ values. A few researchers have indicated that the effect of the stress path on the drained shear strength is insignificant. Duncan and Seed (1966) and Gens (1983) reported that the effective angle of internal friction in compression (ϕ'_c) and the effective angle of internal friction in extension (ϕ'_e) are approximately equal. Many other researchers (e.g. Parry 1960, Saada and Bianchanini 1977) reported that ϕ'_c is less than ϕ'_e by a few degrees. Atkinson et al. (1990) investigated the effect of stress history and stress path on kaolinite samples. Based on the Atkinson et al. (1990) results, the critical state lines for compression and extension test were symmetrical about p′ axis and the ϕ'_c values were significantly less than ϕ'_e values. Parry (2004) attributed the difference in the results to the instability of the sample during shearing in extension tests.

As discussed by Skempton (1954), the orientation of the principal stresses influences the amount of pore water pressure developed during shearing. The pore pressure parameter A_f, which represents the relationship between the change in pore pressure (Δu) and the change in

principal stresses ($\Delta\sigma_1$ and $\Delta\sigma_3$) at failure, can be determined from pore pressure measurements at failure, as presented in Equation 2.2.

$$A_f = \frac{\Delta u}{(\Delta\sigma_1 - \Delta\sigma_3)} \qquad \text{(after Skempton 1954)} \qquad \text{Equation 2.2}$$

The pore pressure parameter A_f is highly influenced by the stress history and principal stresses directions (Figure 2.3). Stipho (1978) reported that A_f values decreased with the increase in the stress anisotropy. Furthermore, A_f values obtained from compression tests were considerably greater than those obtained from extension tests (Simons and Som 1970). It has been shown by many researchers that the effective stress path and consequently the effective strength parameters are independent of the total stress path. Wroth (1984) reported that the difference between CTC and TC tests is only in terms of excess pore water pressure response (Δu), and that difference will not affect effective stress path (Figure 2.4).

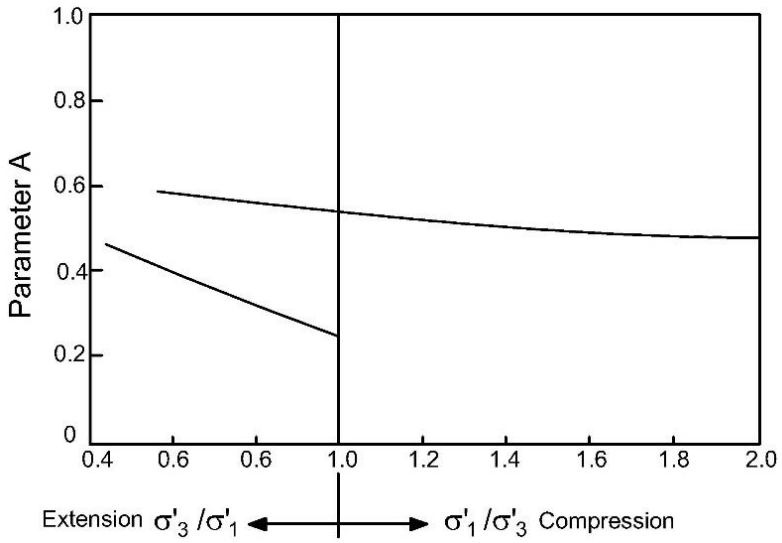

Figure 2.3. Pore water pressure parameter for compression and extension tests (reproduced from Simons and Som 1970).

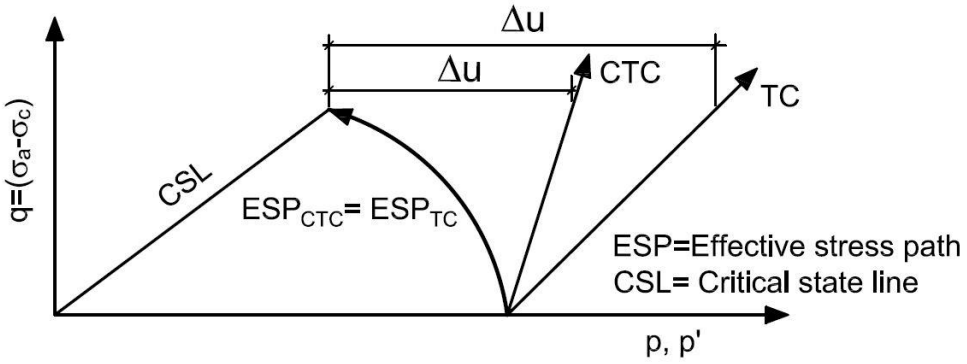

Figure 2.4. Total and effective stress paths from CTC and TC tests (reproduced from Wroth 1984).

2.2.4. *Stress Path Influences on Developed Constitutive Models*

Constitutive models are essential for numerical simulations of geotechnical problems such as ground deformation, slope and tunnels stability, and excavations. As mentioned in Hashash et al. (2002), over the last few decades, many constitutive models have been formulated based on elasto-plasticity theory to predict stress-strain behavior of soils during shearing (from the initial stress condition to the critical state condition). The loading conditions play a significant role in obtaining a realistic prediction of soil behavior using these models. Utilizing the classic elastoplastic theory and the critical state concept for soil, as defined by Roscoe et al. (1958) and later referred by Roscoe and Burland (1968), the Modified Cam Clay model (MCC) was developed to represent clay behavior. More recently, advanced soil models, such as MIT-E3 (Whittle and Kavvadas 1994) and S-CLAY1 (Wheeler et al. 2003), were developed to account for soil anisotropy and structure destruction. Lade (2005) mentioned that most of the current research related to constitutive modeling has focused on the effect of anisotropy and stress path.

Only a few of the aforementioned constitutive models were established based on comprehensive laboratory data (Wheeler et al. 2003). If laboratory data are available, constitutive parameters are typically obtained from triaxial tests. Therefore, these acquired parameters include shear strength parameters and soil moduli values. Most of the constitutive

models that were developed based on triaxial data were derived from conventional triaxial compression tests. The parameters from these tests are simple and provide only limited information. Therefore, there is still a lack of knowledge about the performance of the developed constitutive models when the soil is subjected to different loading conditions (Bayoumi 2006). Bryson and Salehian (2011) evaluated the performance of four constitutive models in predicting the behavior of medium plasticity remolded clay. As described by Bryson and Salehian (2011), the 3-SKH and Cam Clay models were the most suitable for predicting the stress-strain behavior of the remolded clay under different stress paths.

2.2.5. *Effect of Stress path on Soil Moduli*

Soil moduli including: shear modulus (G), Young's modulus (E), bulk modulus (K), and constrained modulus (M), are essential in the evaluation of soil deformation and stress distribution in a soil mass by using elastic solutions. These values can be determined from either field or laboratory tests. As shown in Figure 2.5, there are three types of the modulus of the elasticity which may be determined from triaxial testing: the initial tangent modulus (E_i), the tangent modulus (E_t), and the secant modulus (E_s). Simons and Som (1970) reported that modulus of elasticity for isotropically consolidated samples are significantly less than those for K_o-consolidated samples due to the effect of disturbance. Skempton and Hankel (1957) reported that large strain modulus of elasticity for extension is higher than that for compression. Clayton and Heymann (2001) also indicated that the stiffness at large strain for extension tests performed on London clay are higher than those for compression tests (Figure 2.6).

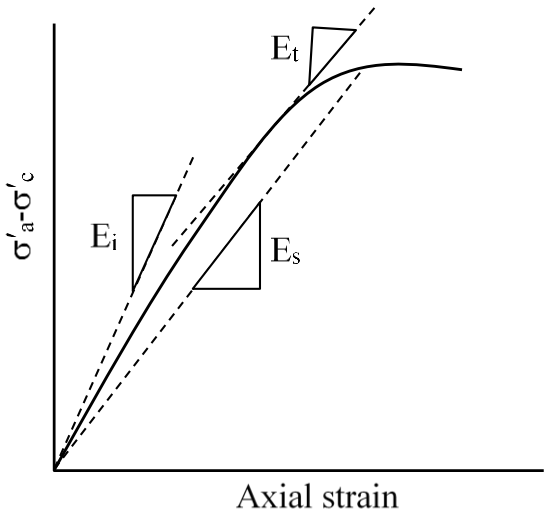

Figure 2.5. Definition of E_i, E_t, and E_s from triaxial testing (from Lambe and Whitman 1969, Atkinson 2000).

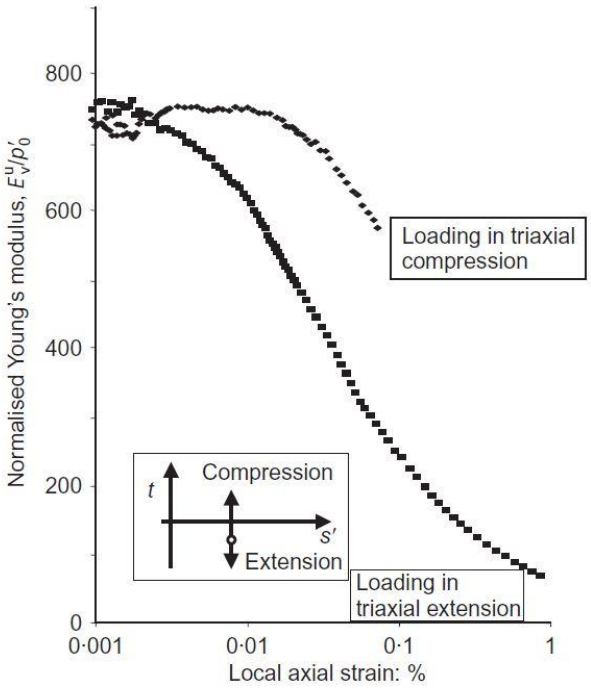

Figure 2.6. Degradation of vertical Young's modulus for specimens tested in triaxial compression and extension (from Clayton 2011).

The decrease in soil stiffness with increasing strain, is well known as stiffness degradation. Soil moduli as obtained from small shear strain ($<10^{-3}$%), including modulus of elasticity (E_o), constrained modulus (M) and shear modulus (G_o), are of great importance for estimating response of structures to dynamic loads, soil improvement, and liquefaction assessment (Hardin and Drnevich 1972, Woods and Partos 1981, Clayton 2011). However, measurements of small-stain stiffness utilizing triaxial tests with conventional external strain measurements may not be accurate because there are many sources of error in the measurement of small strain including seating, bedding, and alignment errors (Baldi et al. 1988).

2.2.6. *Problems Associated with the Triaxial Extension Test*

Recent advances in triaxial testing equipment, including load system control and stress strain measurements, have led to ease in conducting stress path dependent triaxial tests. However, there are some problems associated with the triaxial extension test that may prevent utilizing results obtained from the triaxial extension test in practice (Wu and Kolymbas 1991, Parry 2004). Specifically, the development of necking during shearing in extension test, may cause significant errors in the test results. Many researchers have argued that the greatest shortcoming of the triaxial test is the stress-strain nonuniformity that exists along the longitudinal direction of the sample due to the restriction of the sample ends. Necking during the test causes the shear stress levels to peak, which invalidates the data because of the inaccurate calculation of the cylindrical area. Sheahan (1991) reported that as the strain rate increased, the cross-sectional area decreased due to the effect of added dilation at high strain rates. Liu (2004) also reported that the necking associated with triaxial extension tests increased with an increase in the specimen height to the diameter ratio. Therefore, polished and lubricated end platens have been used to reduce the effect of ends restriction (Stipho 1978, Sheahan 1991, Liu 2004).

The deviatoric stress during shearing stage is calculated from the axial load and the average cross-sectional area. The conventional method to determine the corrected cross-sectional area (A_c) for a given value of axial strain, ε, and an initial average cross-sectional area of the specimen (A_o) is presented in Equation 2.3. This equation, as suggested in ASTM D4767 (2011), is limited because it only relies upon the axial strain measurements.

$$A_c = \frac{A_o}{(1 - \varepsilon)} \qquad \text{ASTM D4767} \qquad \text{Equation 2.3}$$

This conventional procedure relies on the assumption of uniform radial deformation throughout the sample. However, as illustrated in Figure 2.7, the radial deformation at the ends of the specimen is resisted by the end restraint. Therefore, this procedure provides imprecise determination of the sample cross-sectional area, specifically when failure occurs at large levels of strain (Bishop and Henkel 1962). As discussed in Scholey (1996), many localized measurements have been used to measure the radial deformation (such as local strain probes and digital imaging techniques). One of the digital imaging techniques consists of using small board cameras, within the triaxial cell, to measure the change in volume of the specimen (Salazar and Coffman 2015).

Another source of errors in triaxial extension tests is caused by the friction between the loading piston and the bearings within the top cap of the triaxial cell. Many methods have been attempted to eliminate the effect of piston friction. According to Bishop and Henkel (1962) the amount of this friction is between one to five percent of the applied axial load. Therefore, this friction may be a significant contribution of the load for soft samples. Race and Coffman (2011) utilized an internal load cell placed between the top platten and the loading piston to measure the applied axial force inside the triaxial cell to avoid the effect of piston friction.

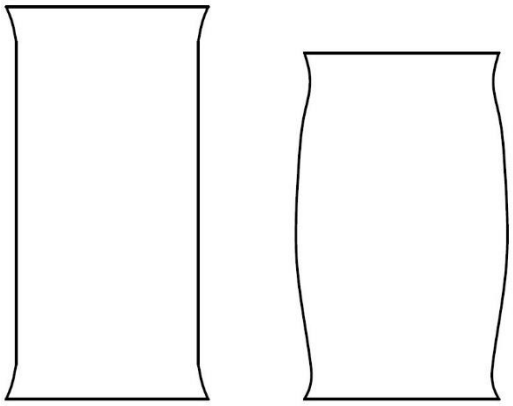

Figure 2.7. The effect of end restraint the radial deformation a specimen in triaxial testing a) Extension and b) Compression (reproduced from Bishop and Henkel 1962).

2.3. Reconstituted Soils

Natural and laboratory prepared specimens are used for laboratory testing to study and characterize the geotechnical properties of the field soils. According to the values of the initial water content that is used to mix the slurry (w_s), the laboratory prepared specimens can be categorized into: 1) "remolded" (Olson 1962), w_s values less than or slightly above the liquid limit of the soil (LL); 2) "reconstituted" (Burland 1990), w_s from one (1) to one and one-half (1.5) times the LL; and 3) "sedimented", w_s greater than two times the LL (Olson 1962).To form a reconstituted structure, Burland (1990) suggested that the water content of the mixed slurry should be between 1 and 1.5 times the liquid limit of the soil. The slurry is often consolidated in a slurry consolidometer to a certain consolidation stress that is related to the in-site effective stress (Henkel 1956, Olson 1962, Burland 1990).

Because of the way the reconstituted specimens are prepared, various fabrics may result, which may raise a question whether these specimens accurately duplicate the field soil properties. As documented by Allman and Atkinson (1992), sedimentation and aging of intact soils in the ground produced soils with void ratios higher than those for the reconstituted soils. According to Mitchell and Soga 2005, comprehensive investigation of the engineering behavior

of laboratory prepared specimens will result in better characterization of the properties of natural soils. The values of the initial water content of the slurry that are utilized to reconstitute cohesive soils may have significant effects on the compression and shear strength behavior of the soils due to the influence of w_s on the soil fabric. The term "intrinsic" was introduced by Burland (1990) to describe the properties for specimens that were reconstituted within the aforementioned water content values. Burland (1990) further reported that the shear strength and compressibility of reconstituted soils may be utilized to develop a reference framework to correlate the laboratory obtained properties from reconstituted soils with those from the intact soils.

2.3.1. *Fabric of Reconstituted Soils*

Previous studies (e.g., Olson 1962, Martin and Ladd 1978, Carrier and Beckman 1984) have shown that using different levels of initial water content (w_s) to remold or reconstitute soil specimens will affect the mechanical behavior of the specimens due to the significant changes in the soils structure. As describe by Mitchell and Soga (2005), soil structure is composed of fabric and bonding (interparticle force system). The term fabric refers to the arrangement of particles and the arrangement of pore space within a given soil. The term fabric, however, has been used interchangeably with the term structure. As presented in Figure 2.8, clay particles may have a flocculated (random arrangement) fabric or dispersed (parallel arrangement) fabric (Mitchell and Soga 2005).

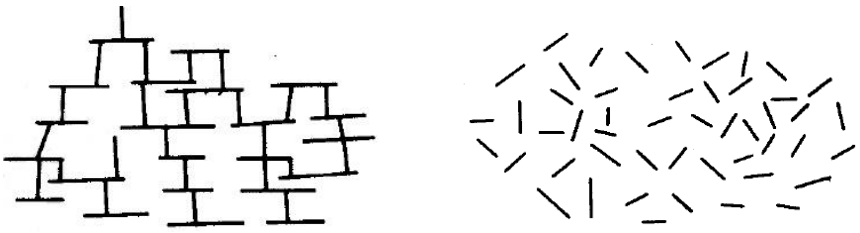

(a) (b)

Figure 2.8. Typical particle arrangement of cohesive soils: a) flocculated fabric, and b) dispersed fabric (from Mitchell and Soga 2005).

According to Olson (1962), Burland (1990), and Prashant and Penumadu (2007), soil fabric has been shown to play an essential role in the engineering behavior of clayey soils. Soil fabric can vary considerably as a result of using different water content values to reconstitute clay soils. Olson (1962) indicated that laboratory prepared specimens, at water content less than or slightly above liquid limit, may not represent the natural deposition process. Moreover, Olson (1962) mentioned that specimens at these low levels of water content will have dispersed microfabric and exhibit intrinsic properties of overconsolidated clayey soil regardless of the level of overconsolidation within the specimen. Olson (1962) also indicated that sedimentation of specimens from slurries with w_s values higher than two times the respective liquid limit will produce specimens with flocculated fabric. To obtain more representative specimens, Olson (1962) reported that the water content of the mixed slurry should be at least two times the liquid limit. However, sedimentation of specimens at such high water content requires an extended period of time. Moreover, it has been shown that these specimens are often difficult to extrude and trim. Therefore, the following researchers: Henkel (1956), Parry (1960), Bryson and Salehian (2011), Tiwari and Ajmera (2011), Zhao and Coffman (2016), Zhao et al. (2017), and Zhao et al. (2018) have instead prepared reconstituted clay specimens at lower water content values.

2.3.2. *Intrinsic Compression Behavior*

The results from many studies (e.g. Carrier and Beckman 1984, Cerato and Lutenegger 2004, Hong et al. 2010) indicated that both initial void ratio and compression behavior of reconstructed soils were affected by the initial water content. As shown in Figure 2.9, the compression curves of specimens prepared at a higher initial water content lied above the compression curves of the specimens prepared at a lower initial water content. Based on the results from these studies, increasing the initial water content of the slurry tended to increase the initial void ratio and to increase the compressibility of the reconstituted clays for a given vertical effective stress.

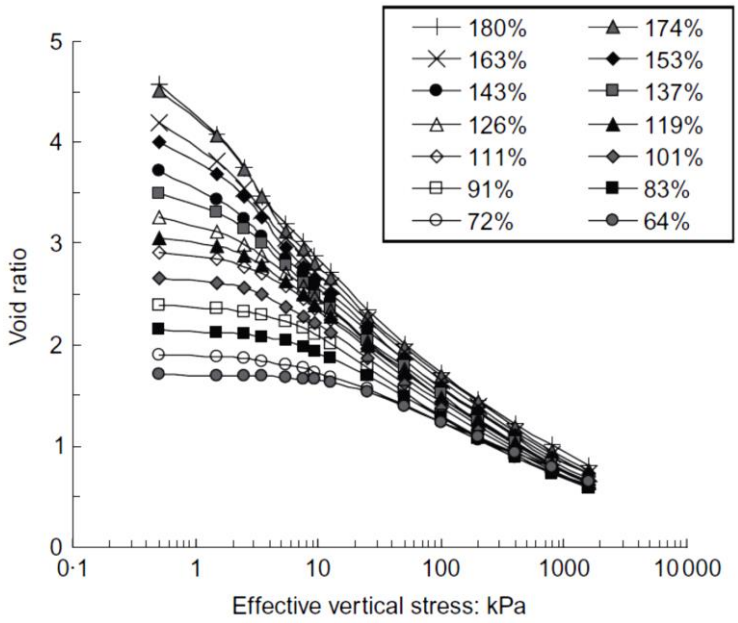

Figure 2.9. Compression curves of reconstituted Baimahu Clay at different initial water contents of the slurry (from Hong et al. 2010).

Many previous studies (e.g., Burland 1990, Hong et al. 2010, Tiwari and Ajmera 2011, Al Haj and Standing 2015) have indicated that the shape of the compression curve that was obtained from odometer tests conducted on reconstituted soils was different than the typical shape of the compression curve for natural soils. The shapes of the compression curve (as

presented previously in Figure 2.9), that were observed by these studies, tended to slightly concave upwards in a pattern similar to that for soft clays. Burland (1990) reported that intrinsic properties of the reconstituted soils were inherent and independent of the soil structure. Furthermore, the compression curves of different reconstituted clays with w_s values of 1.25 LL can be normalized by using the void index (I_v), as presented in Equations 2.4 and 2.5.

$$I_v = \frac{e - e^*_{100}}{C^*_c} \qquad \text{Burland (1990)} \qquad \text{Equation 2.4}$$

$$C^*_c = e^*_{100} - e^*_{1000} \qquad \text{Burland (1990)} \qquad \text{Equation 2.5}$$

Within Equations 2.4 and 2.5, e^*_{100} and e^*_{1000} are the void ratio of the reconstituted clay corresponded to vertical stress levels of 100 and 1000 kPa respectively; C^*_c is the intrinsic compression index.

When laboratory measurements are not available, Equations 2.6 and 2.7 can be used to estimate the e^*_{100} and C^*_c respectively, based on the values of the initial void ration at the liquid limit (e_L), as suggested by Burland (1990).

$$e^*_{100} = 0.109 + 0.679e_L - 0.089e_L^2 + 0.016e_L^3 \qquad \text{Burland (1990)} \qquad \text{Equation 2.6}$$

$$C^*_c = 0.256e_L - 0.04 \qquad \text{Burland (1990)} \qquad \text{Equation 2.7}$$

As shown in Figure 2.10, the normalized compression lines for three clays exhibited identical relationships. The normalized curves were represented by a unique line which was descried by Burland (1990) as the intrinsic compression line (ICL), as presented in Equation 2.8. In Equation 2.8, σ'_v is the vertical effective stress in kPa.

$$I_v = 2.45 - 1.285\log\sigma'_v + 0.015(\log\sigma'_v)^3 \qquad \text{Burland (1990)} \qquad \text{Equation 2.8}$$

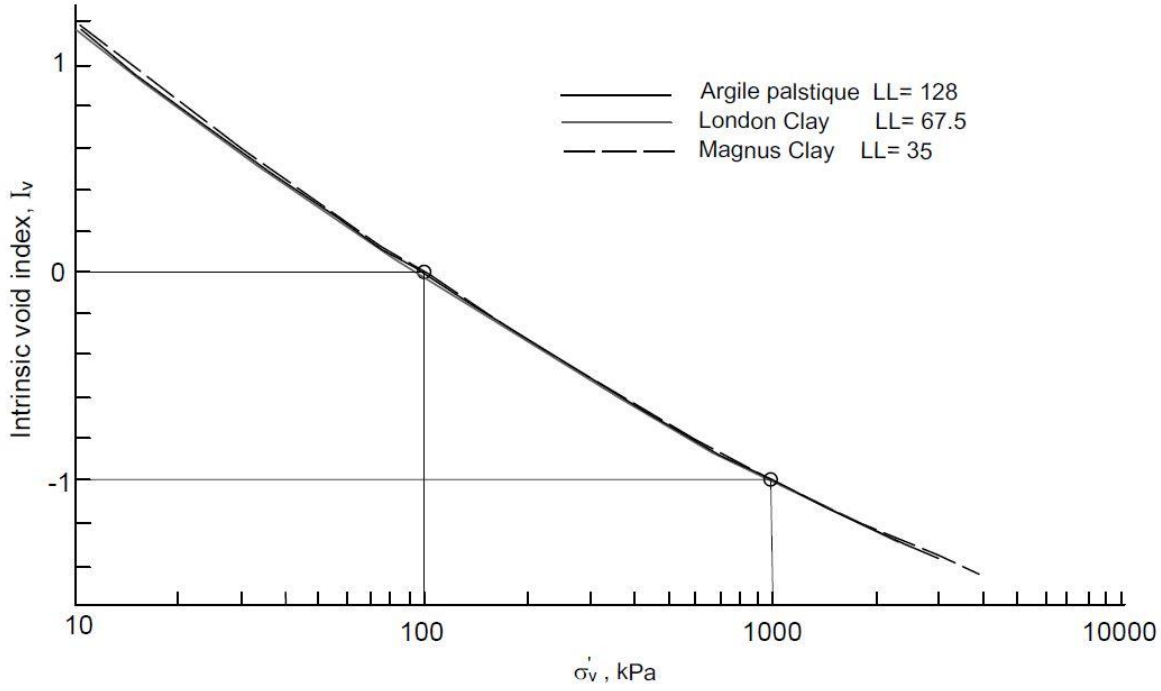

Figure 2.10. Intrinsic compression lines for three clays obtained by normalizing the compression curves to the void index (reproduced from Burland 1990).

As described by Burland (1990), the intrinsic properties of the reconstituted soils were inherent and should be independent of the natural state or structure of the soil. Therefore, if a given soil was disturbed and then reconstituted many times, the compression curves of the reconstituted specimens from this soil at each time would be identical when the specimens was reconstructed at the same w_s values. However, based on the results from (Cerato and Lutenegger 2004), the ICL lines for 35 natural clays, that were reconstituted at w_s of 1.25, were not identical. As shown in Figure 2.11, poor correlation was observed between the ICL and the normalized compression curves for these clays. Cerato and Lutenegger (2004) attributed the difference in the compression behavior to the difference in the mineralogical compositions of the soils. The intrinsic compression index C_c^* (slope of the linear portions of the loading curves) was greater for kaolinite and illite than for montmorillonite soil. Furthermore, Cerato and Lutenegger (2004)

indicated that the degree to which the w_s affected the compression behavior was also dependent on the soil mineralogy.

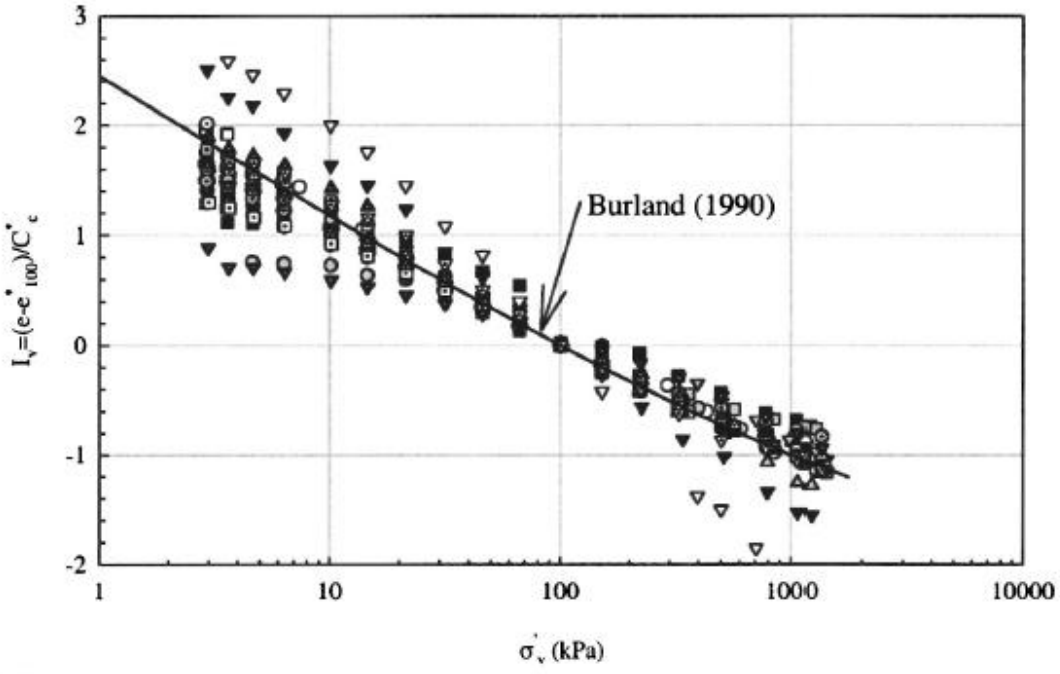

Figure 2.11. Normalized compression curves for natural clays (from Cerato and Lutenegger 2004).

2.3.3. *Intrinsic Undrained Shear Strength Behavior*

Based on previous research on reconstituted soils, the stress-strain behavior of these soils was significantly affected by the w_s levels (Henkel 1962, Burland 1990, Allman and Atkinson 1992, Chandler 2000, Hong et al. 2013). As documented by Allman and Atkinson (1992), at the same specific volume and water content, the undrained shear strength values of the intact samples were from 10 to 15 times greater than those for reconstituted soils. Allman and Atkinson (1992), attributed the higher values of the undrained shear strength for the intact soils to the aging of the naturally sedimented specimens. The pattern of behavior, during shearing of the normally consolidated reconstituted specimens, was different from the typical behavior that has been observed for normally consolidated soils. As described by Olson (1962), slurried specimens

that were prepared at w_s values less than or slightly above the liquid limit exhibited shear strength characteristics similar to the typical characteristics of the overconsolidated clay soils. Therefore, Olson (1962), suggested that a water content values of at least two times the liquid limit should be utilized to prepare the slurry.

Furthermore, as reported by Burland (1990) and Atkinson et al. (1987), postpeak shear planes were observed to develop in one-dimensional consolidated kaolinite specimens regardless of whether the soil was normally consolidated or overconsolidated. The difference in the magnitude of the shear induced pore water pressure during shear may explain the unusual behavior of normally consolidated specimens during shear. As discussed by Cerato and Lutenegger (2004), the double layer may have not completely been developed around the particles of the flocculated soils that were reconstituted at low values initial water content. Therefore, the particles may absorb additional water during shear, depending on the initial water content of the specimens (w_o).

Previous researchers have reported that the undrained shear strength values of the reconstituted soils decreased with increasing levels of the w_s (Chandler 2000, Hong et al. 2013, Al Haj and Standing 2015). As observed by Hong et al. (2013), the undrained shear strength values, obtained from isotropic consolidation undrained triaxial compression tests, decreased with the increasing values of the initial water content (Figure 2.12).

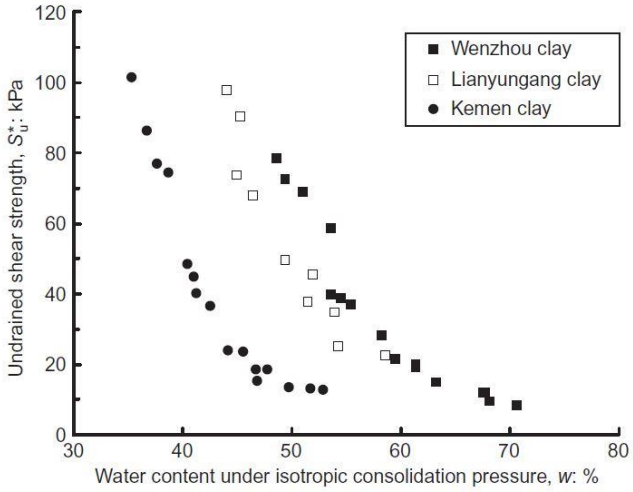

Figure 2.12. Undrained shear strength values as a function of initial water content (from Hong et al. 2013).

Following a normalization procedure that was similar to Burland (1990), the values of the undrained shear strength were normalized to the values of the I_v that corresponded to the vertical effective stress values prior to shear. The intrinsic shear strength behavior was introduced by Chandler (2000) to describe the relation between the w_s and the undrained shear strength of the reconstituted soils. As shown in Figure 2.13, the normalized line was defined by Chandler (2000) as the intrinsic strength line (IS_uL). However, this line was not unique for a given soil type, but it was developed based on a single value of 0.33 of the undrained shear strength ratio (R_{su}^*), which is defined as the ratio of the undrained shear strength of the reconstituted soil (s_u^*) to the preshear vertical effective stress (σ'_{vc}). As presented in Figure 2.14, similar procedure was successfully utilized by Hong et al. (2013) to normalize the values of the undrained shear strength, obtained from isotropically consolidated undrained triaxial tests that were conducted on of an illitic soil. However, Hong et al. (2013) utilized the values of effective isotropic consolidation stress instead of the values of vertical effective stress to determine the I_v values.

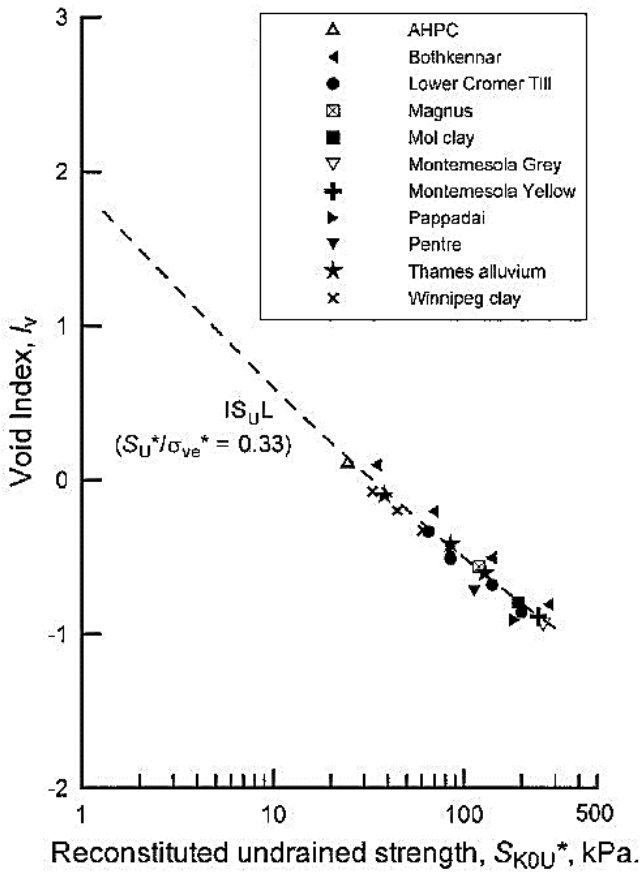

Figure 2.13. Normalized undrained shear strength and intrinsic strength line (from Chandler 2000).

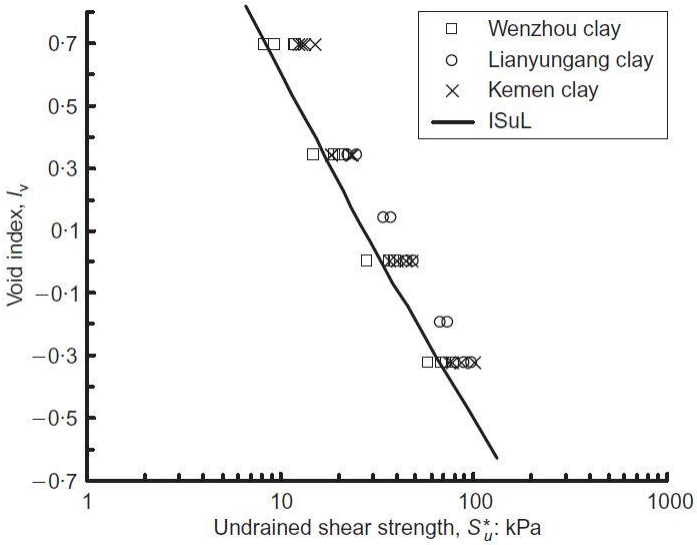

Figure 2.14. Normalized values of undrained shear strength obtained from isotropically consolidated undrained triaxial testes (from Hong et al. 2013).

2.4. Small-Strain Moduli of Reconstituted Soils

As previously mentioned, measurements of soil moduli by utilizing triaxial tests, with conventional external strain measurements, may not be accurate because of the errors that have been associated with these measurements. Alternately, bender elements and piezoelectric disks have been previously utilized to determine soil moduli based on the seismic wave velocity measurements. A brief description of the shear wave velocity measurements by utilizing bender elements technique is presented in Section 2.4.1. The effect of stress history and fabric anisotropy are discussed in Section 2.4.2 and Section 2.4.3, respectively.

2.4.1. *Bender Elements Technique*

During the last few decades, bender elements (BE) have been utilized to measure shear wave velocities for different types of soils. The BE technique has provided an inexpensive and reliable alternative to study small-strain soil properties (Clayton 2011). The velocity of a shear wave that travels through a soil specimen is computed by measuring the travel time of the wave from the transmitter BE to the receiver BE. As described in Equations 2.9, soil moduli G_o may be related to shear wave velocity (V_s) by utilizing the total mass density of the soil (ρ).

$$G_o = \rho V_s^2 \qquad \text{Richart et al. 1970} \qquad \text{Equation 2.9}$$

Bender elements have been employed within open odometer, floating wall consolidometer, and constant-rate-of-strain consolidometer devices to examine small-strain soil properties during consolidation. Some researchers (e.g., Fam and Santamarina 1995, Jovicic and Coop 1998, Kang et al. 2014) have incorporated bender elements within the top and bottom plates of an oedometer to measure shear waves in the vertical direction. As presented in Figure 2.15, bender elements have also been installed in the horizontal direction (Jamiolkowski et al. 1995, Kang et al. 2014, Zhao and Coffman 2016, Zhao et al. 2017) to acquire horizontally

propagated shear waves. Recently, a back-pressure saturated, constant rate-of-strain, consolidation device, with bender elements (BP-CRS-BE) was developed at the University of Arkansas by Zhao and Coffman (2016), as shown in Figure 2.16. Velocities of two types of shear waves were measured by utilizing the BP-CRS-BE device: 1) horizontally propagated-vertically polarized shear waves ($V_{s,HV}$), and 2) horizontally propagated-horizontally polarized shear waves ($V_{s,HH}$).

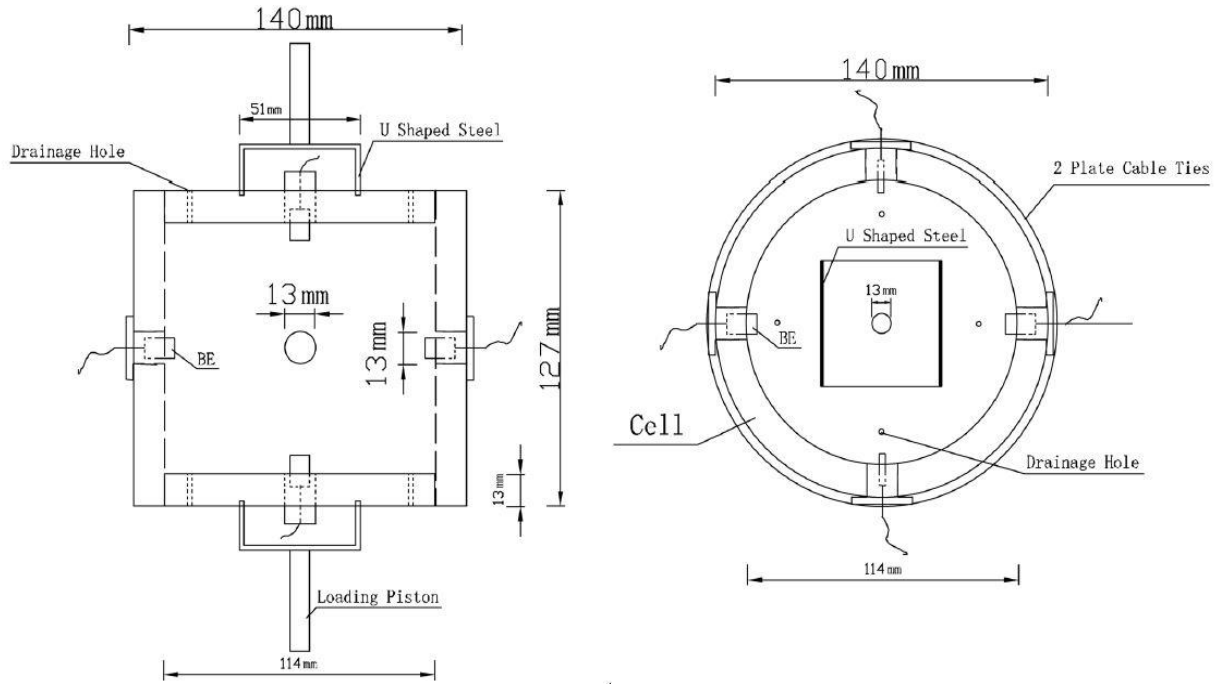

Figure 2.15. Bender elements installed in the vertical and horizontal directions within an oedometer device (after Kang et al. 2014).

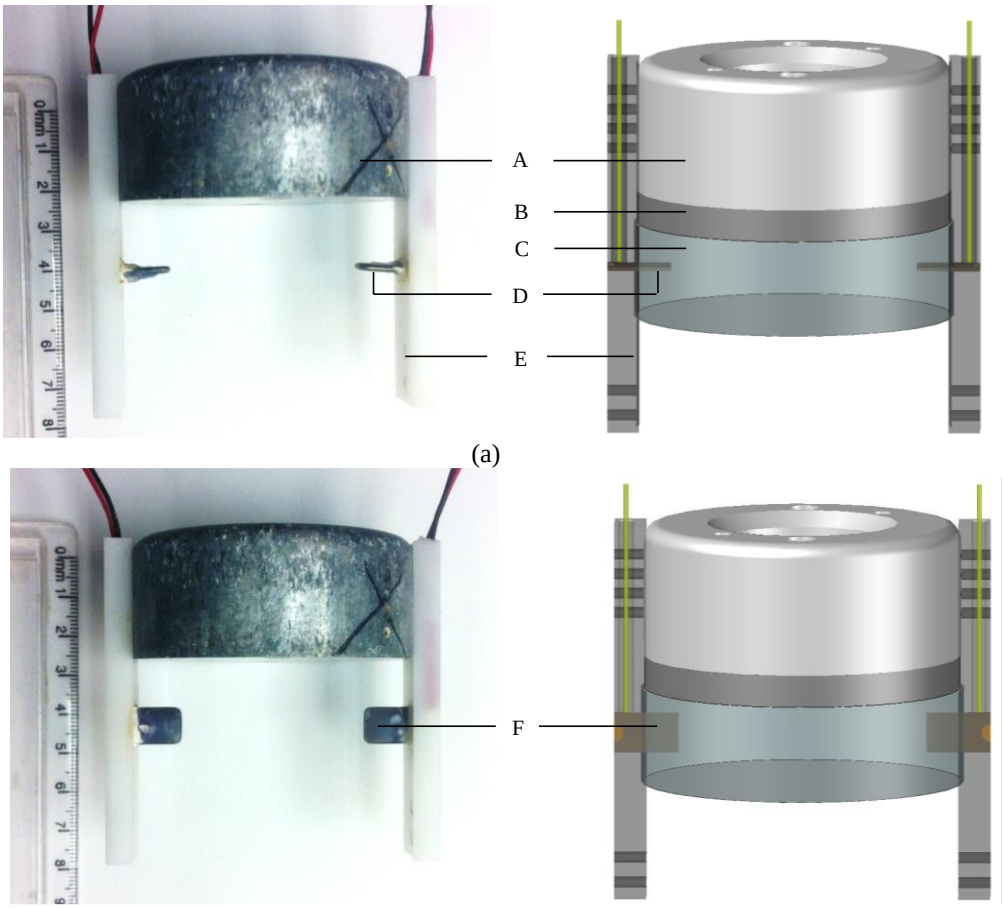

A. Alumimum loading cap. B. Porous stone. C. Soil sample. D. Horizontal bender element. E. Polyoxymethylene slide bar. F. Vertical bender element.

Figure 2.16. Photograph and schematic of bender elements within BP-CRS-BE device in the a) horizontal orientation, and b) vertical orientation (after Zhao et al 2017).

The bender elements technique has also been utilized within the triaxial apparatus (e.g., Viggiani and Atkinson 1995, Jovicic and Coop 1998, Gasparre and Coop 2006, Finno and Kim 2012, Choo 2013, Salazar and Coffman 2014) in different orientations, as presented in Figure 2.17. As discussed by Viggiani and Atkinson (1995) and Jovicic and Coop (1998), valuable measurements of small-strain stiffness were obtained by utilizing bender elements within the triaxial apparatus because of the different loading conditions that can be applied by the triaxial apparatus during the consolidation and shearing stages.

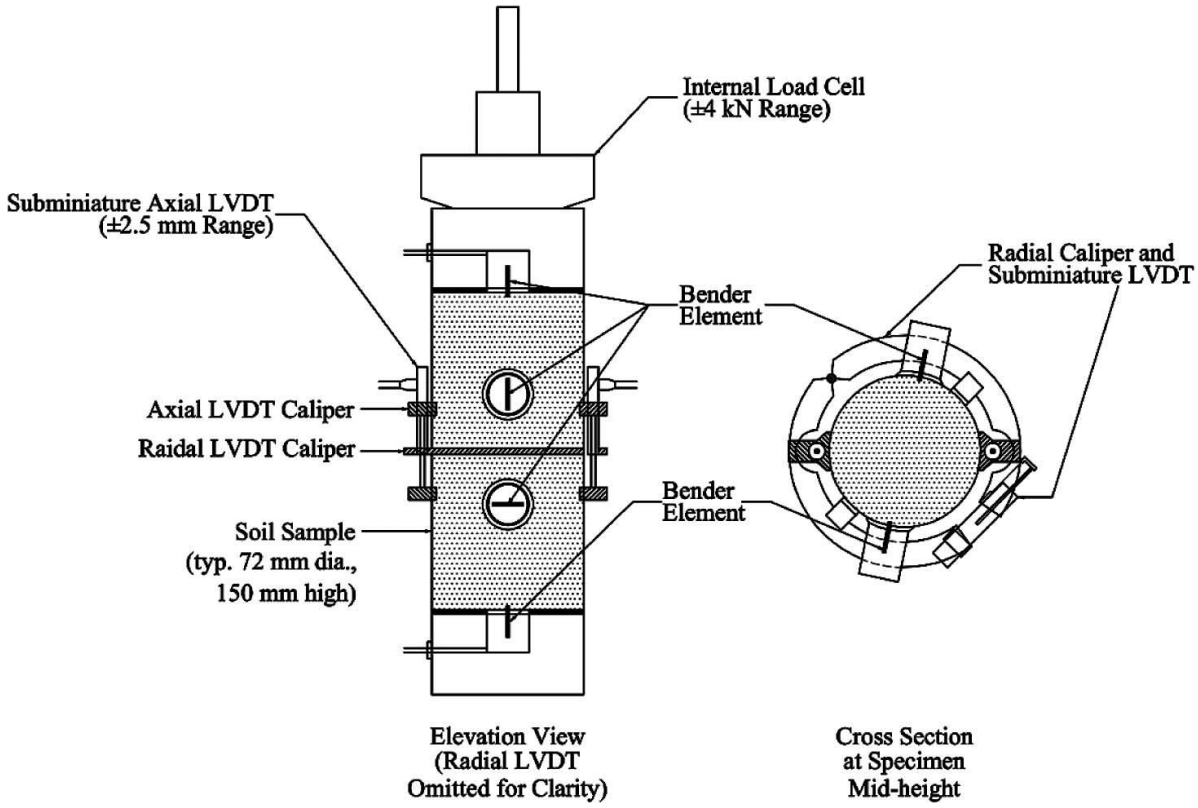

Figure 2.17. Schematic of a triaxial specimen instrumented with bender elements in the a) horizontal orientation, and b) vertical orientation (after Finno and Kim 2012).

2.4.2. *Effect of Stress History on Small-Strain Behavior*

The term "recent stress history" was first introduced by Atkinson et al. (1990) to describe the current applied stress path that has a direction different than the direction of the previous stress path. Atkinson et al. (1990) showed that the recent stress history has an impact on small-strain stiffness during consolidation and shearing stages of the triaxial tests. Simons and Som (1970) reported that the modulus of elasticity for isotropically consolidated samples are less than those obtained from K_o consolidated samples, due to the effect of disturbance. The relationship between shear modulus, specific volume (v), current effective stress (p'), and overconsolidation ratio (R_o) is provided in Equation 2.10 (Atkinson 2000).

$$\frac{G_o}{p_a} = A\left(\frac{p'}{p_a}\right)^n R_o^m \qquad \text{Atkinson (2000)} \qquad \text{Equation 2.10}$$

Within Equation 2.10, p_a is the atmospheric pressure; *A*, *n*, and *m* are material parameters. Amorosi et al. (1999) and Choo et al. (2013) showed that stress history during consolidation stage in triaxial testing has a significant effect on stiffness degradation during shear.

Although there have been many studies to investigate the effect of recent stress history on small-strain stiffness and the degradation of small-strain stiffness during shear, conflicting data has been presented in these studies (Finno and Cho 2011). Based on the experimental work performed by Atkinson et al. (1990), Zdravkovic (1996), and Lings et al. (2000), recent stress path has a strong impact on small-strain stiffness during shear. Similar observations were obtained from bender element tests on completely decomposed granite performed by Wang and Ng (2004). The shear modulus values measured in triaxial extension tests were about sixty percent higher than those measured in triaxial compression tests. Furthermore, Wang and Ng (2004) showed that the G_o value increased as the void ratio decreased and the mean effective stress increased. Likewise, Santagata (2008) reported that the small-strain stiffness, for sedimented Boston Blue Clay from undrained triaxial tests, was highly influenced by the recent stress history. In contrast to aforementioned results, Clayton and Heymann (2001) showed that the recent stress history in undrained triaxial tests has insignificant influences on the small-strain stiffness. Based on the small-strain results obtained from triaxial tests with bender elements, as conducted by Finno and Cho (2011) on lightly over consolidated samples, the stress path direction had no effect on small-strain stiffness at very small levels of shear strain (less than 0.001 percent). However, the direction of the stress path had a strong effect on the small-strain stiffness when the small-strains were measured by utilizing local small-strain measurements which detected shear strain greater than 0.002 percent. Finno and Cho (2011) also showed that

effect of stress path on the small-strain stiffness decreased as the shear strain increased, as shown in Figure 2.18.

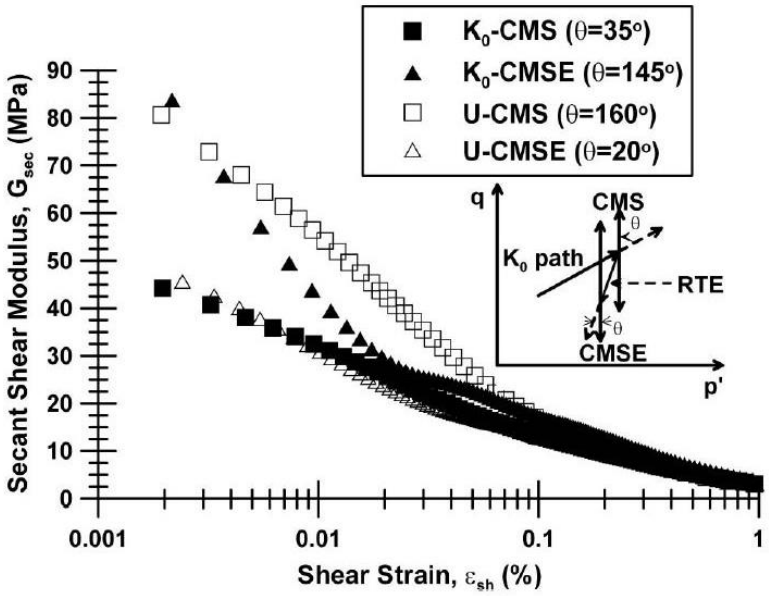

Figure 2.18. Secant shear modus degradation of constant mean normal stress compression (CMS), reduced constant mean normal stress (CMSE), and anisotropic unloading (AU) stress paths (from Finno and Cho 2011).

2.4.3. *Fabric Anisotropy*

As previously presented, using different levels of initial water content (w_s) to reconstitute specimens from cohesive soils will affect the initial void ratio, fabric, and initial water content (w_o) of the prepared specimens. The effect of void ratio and fabric of cohesive soils on the small-strain stiffness has been well documented in the previous studies. As reported by Atkinson et al. (1990), Lings et al. (2000), Clayton (2011), Finno and Cho (2011), small-strain stiffness increased with decreasing values of void ratio. Furthermore, Equation 2.11 was proposed by Hardin and Blandford (1989) to correlate shear modulus of a given soil to the inherent properties and state of stress of the soil.

$$G_{\max} = \frac{S \cdot OCR^{k}}{F(e)} P_a^{1-n} (p')^{n} \qquad \text{(after Hardin and Blandford 1989)} \qquad \text{Equation 2.11}$$

Within Equation 2.11, G_{max} is the small-strain shear modulus of soil; S is a non-dimensional material constant representing the fabric anisotropy; OCR is overconsolidation ratio; k is an empirical constant depends on the soil plasticity index; P_a is the atmospheric pressure; $n = 0.5$ is non-dimensional material constant; p' is the effective stress; and $F(e)$ is the void ratio function, $F(e) = 0.3 + 0.7e^2$.

Previous studies on soil anisotropy (e.g., Duncan 1966, Mitchell 1972, Martin and Ladd 1978, Jovicic and Coop 1998) have indicated that anisotropy of soil fabric occurred during deposition of soil particles (inherent anisotropy) or as a result of change in the stress conditions (stress-induced anisotropy). The importance of soil fabric as a factor influencing the small-strain stiffness has been discussed and illustrated by previous researchers (e.g, Hardin and Brandford 1989, Jovicic and Coop 1998, Zhao et al. 2017). The inherent anisotropy was determined to have a significant effect on the small-strain behavior, while the stress induced anisotropy was found to slightly affect this behavior (Jovicic and Coop 1998). The inherent fabric anisotropy for cohesive soils was essentially caused by the large strain levels during one-dimensional deposition (Jovicic and Coop 1998).

Bender elements can be installed in different positions within the specimen. As shown in Figure 2.19, velocities of three types of shear waves were measured from these positions: 1) vertically propagated-horizontally polarized shear waves $(V_{s,VH})$, 2) horizontally propagated-horizontally polarized shear waves $(V_{s,HH})$, and 3) horizontally propagated-vertically polarized shear waves $(V_{s,HV})$. For a given soil specimen, at the same stress state, different values of the three aforementioned types of shear wave velocities may be measured as a result of fabric anisotropy. Accordingly, different values of the shear modulus may be calculated for the specimens from these three types of shear wave velocities (Jovicic and Coop 1998, Yamashita et

al. 2005, Kang et al. 2014, Zhao et al. 2017). Kang et al. (2014) reported that the $V_{s,HH}/V_{s,HV}$ ratio was around 1.20, for reconstituted kaolinite soil. As also reported by Yamashita et al. (2000), the $V_{s,HH}/V_{s,HV}$ ratio was between 1.05 and 1.13 for Toyoura sand and Kussharo sand, respectively.

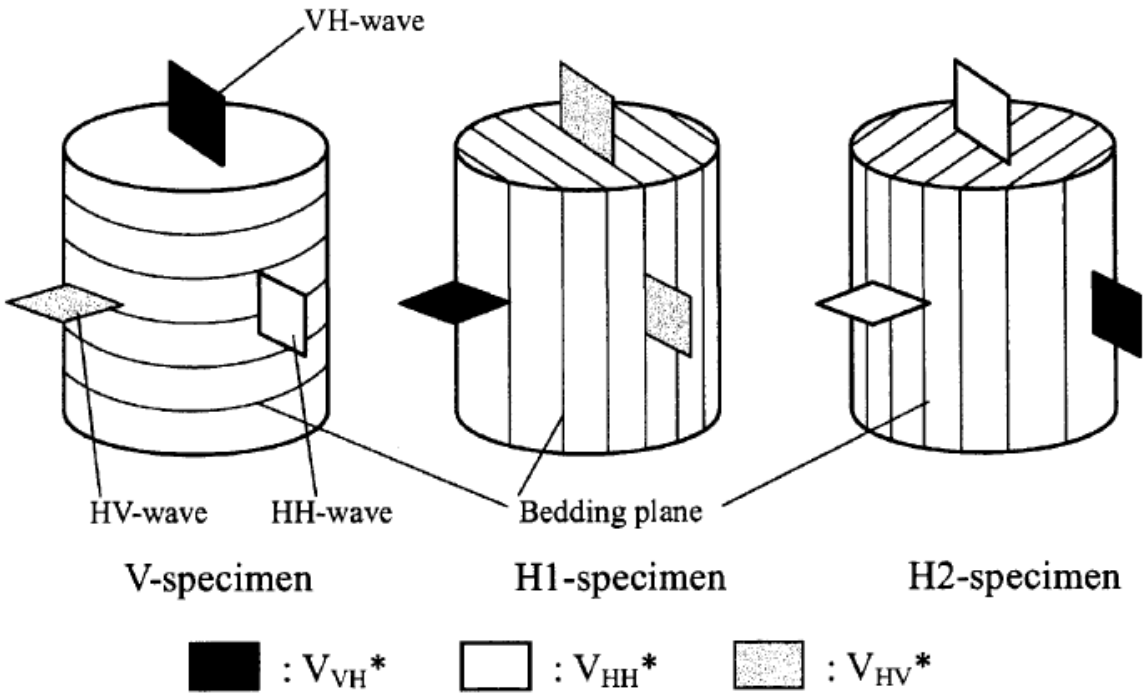

Figure 2.19. Different positions of bender elements within triaxial specimens and the corresponding shear wave velocity measurements (from Yamashita et al., 2000).

Previous research (e.g., Jovicic and Coop 1998, Lings et al. 2000, Yimsiri and Soga 2000, Cho and Finno 2010) has demonstrated that one-dimensionally deposited soils will essentially experience cross anisotropy ($V_{s,HV} \approx V_{s,VH}$). As also documented by Yamashita et al. (2000), insignificant difference between the $V_{s,HV}$ and $V_{s,VH}$ values was observed for sandy soils. In contrast to the aforementioned observations, the amount of fabric anisotropy of natural clays that have been observed by Pennington et al. (1997) and Lee et al. (2008) indicated that the $V_{s,HV}$ values were greater than the $V_{s,VH}$ values. Pennington et al. (1997) reported that for natural Gault clay, the $V_{s,HV}/V_{s,VH}$ ratio was around 1.17, while the $V_{s,HH}/V_{s,HV}$ ratio was around 1.2. Similarly,

for reconstituted kaolinite soil, Kang et al. (2014) observed that the $V_{s,HV}/V_{s,VH}$ ratio was around 1.14.

As a result of fabric anisotropy, the shear modulus has been found to be inherently anisotropic (Pennington et al. 1997). The values of stiffness anisotropy (also known as modulus ratio), refers to the ratio of shear modulus in the horizontal direction (G_{HH}) to the shear modulus in the vertical direction (G_{VH}), ranged from 1.2 to 1.7 for normally and lightly overconsolidated soils, as obtained from laboratory bender elements tests. For the overconsolidated soils, the stiffness anisotropy was greater than two (Roesler 1979, Jamiolkowski et al. 1995, Lings et al. 2000, Kang et al. 2014, Zhao et al. 2017). The modulus ratio (G_{HH}/G_{VH}) that was measured by Pennington et al. (1997) for reconstituted Gault clay was around 1.5.

As reported by Jovicic and Coop (1998), the G_{HH}/G_{VH} of natural clays was greater than the G_{HH}/G_{VH} of reconstituted soils. The values of G_{HH}/G_{VH} for natural London clay ranged from 1.5 to 1.7, while the values of G_{HH}/G_{VH} for the reconstituted London clay ranged from 1.24 to 1.33 (Jovicic and Coop 1998). Nash et al. (1999) reported that the values of the G_{HH}/G_{VH} for anisotropically consolidated specimens were between 1.5 and 1.9. For isotropically consolidated specimens, the values of G_{HH}/G_{VH} that were measured by Nash et al. (1999) were between 1.45 and 1.52.

2.5. References

Al Haj, K. M. A., Standing, J. R., (2015). "Mechanical Properties of Two Expansive Clay Soils from Sudan." Geotechnique, Vol. 65, No. 4, pp. 258-273.

Allman, M. and A., Atkinson, J. H., (1992). "Mechanical Properties of Reconstituted Bothkennar Soil." Geotechnique, Vol 42, No 2, pp. 289-301.

American Society for Testing and Materials (2011). "Standard Test Method for Unconsolidated-Undrained Triaxial Compression Test on Cohesive Soils." Annual Book of ASTM Standards, Designation D4767, Vol. 4.08, ASTM, West Conshohocken, PA.

Amorosi, A., Callisto, L., and Rampello, S., (1999). "Observed Behavior of Reconstituted Clay Along Stress Paths Typical of Excavations." Proceedings of the Second International Symposium on Pre-Failure Deformation Characteristics of Geomaterials, Torino, Italy, pp. 28-30. CRC Press.

Atkinson, J. H., (2000). "Non-linear Soil Stiffness in Routine Design." Geotechnique, Vol.50, No. 5, pp 487-508.

Atkinson, J. H., Richardson, D., and Robinson, P. J., (1987). "Compression and Extension of K_0 Normally Consolidated Kaolin Clay." Journal of Geotechnical Engineering, Vol.113. No. 12, pp. 1468-1482.

Atkinson, J.H., Richardson, D. and Stallebrass, S.E., (1990). "Effect of Recent Stress History on the Stiffness of Overconsolidated Soil." Geotechnique, Vol.40, No. 4, pp.531-540.

Baldi, G., Hight, D. W., and Thomas, G. E. (1988). "A Reevaluation of Conventional Triaxial Test Methods." Advanced Triaxial Testing of Soil and Rock." ASTM STP, 977, 219-263.

Bayoumi, A., (2006). "New Laboratory Test Procedure for the Enhanced Calibration of Constitutive Models." Doctoral Dissertation, Georgia Institute of Technology, GA.

Bishop, A.W., and Henkel, D.J. (1962). "The Measurement of Soil Properties in the Triaxial Test." Edward Arnold LTD, London.

Bishop, A. W., (1966). "The Strength of Soils as Engineering Materials." Geotechnique, Vol. 16, pp. 91-130.

Bjerrum, L., (1973). "Problems of Soil Mechanics and Construction on Soft Clays and Structurally Unstable Soils (Collapsible, Expansive and others)." In Proceeding of 8th International Conference on SMFE, Vol. 3, pp. 111-159.

Bjerrum, L., Frimann, L.J., Has, M. and Duncan, J.M., (1972). "Earth Pressures on Flexible Structures." A State-of-the-Art-Report; Procedding of the 5th European Conference on Soil Mechanics and Foundations Engineering, Madrid, Vol 2, pp.169 - 196.

Bryson, L. S., and Salehian, A. (2011). "Performance of Constitutive Models in Predicting Behavior of Remolded Clay." Acta Geotechnica, Vol. 6, No. 3, pp.143-154.

Burland, J. B., (1990). "On the Compressibility and Shear Strength of Natural Clays." Geotechnique 40 (3), 329-378.

Carrier, W. D., and Beckman, J. F., (1984). "Correlations Between Index Tests and the Properties of Remolded Clays." Geotechnique, Vol. 34, No. 2, pp. 211-228.

Cerato, A. B., and Lutenegger, A. J., (2004). "Determining Intrinsic Compressibility of Fine Grained Soils." Journal of Geotechnical and Geoenvironmental Engineering, Vol. 130, No. 8, pp. 872–877.

Chandler, R.J., (2000). “The Third Glossop Lecture Clay Sediments in Depositional Basins: the Geotechnical Cycle.” Quarterly Journal of Eng. Geology and Hydrogeology, Vol. 33, No. 1, pp.7-39.

Cho,W., and Finno, R. J. (2010). “Stress-strain Responses of Block Samples of Compressible Chicago Glacial Clays.” Journal of Geotechnical and Geoenvironmental Engineering, Vol. 136, No.1, pp 178–188.

Choo, J., Jung, Y.H., Cho, W. and Chung, C.K., (2013). “Effect of Pre-Shear Stress Path on Nonlinear Shear Stiffness Degradation of Cohesive Soils.” Geotechnical Testing Journal, Vol. 36, No. 2.

Clayton, C.R.I., (2011). “Stiffness at Small Strain: Research and Practice.” Geotechnique, Vol. 61, No. 1, pp. 5-37.

Clayton, C.R.I., and Heymann, G., (2001). “Stiffness of Geomaterials at Very Small Strains.” Geotechnique, Vol. 51, No. 3, pp 245–255.

Coffman, R. A., Bowders, J. J., and Burton, P. M., (2010). “Use of SHANSEP Design Parameters in Landfill Design: A Cost/Benefit Case Study.” ASCE Geotechnical Special Publication No. 199, Proceedings GeoFlorida 2010, Advances in Analysis, Modeling and Design, West Palm Beach, FL, Feb 20–24, pp. 2859–2866.

Davis, E. H., and Poulos, H. G., (1972). “Rate of Settlement Under Two-and Three-dimensional Conditions.” Geotechnique, Vol. 22, No. 1.

Davis, E.H. and Poulos, H.G., (1968). “The Use of Elastic Theory for Settlement Prediction under Three-dimensional Conditions.” Geotechnique, Vol.18, No. 1, pp.67-91.

Duncan, J. M., and Seed, H. B., (1966). “Anisotropy and Stress Reorientation in Clay.” Journal of the Soil Mechanics and Foundations Division, Vol. 92, No. 5, pp. 21-50.

Fam, M., and Santamarina, J. C., (1995). “Study of Geoprocesses with Complementary Mechanical and Electromagnetic Wave Measurements in an Oedometer.” Journal of Geotechnical Engineering, Vol. 18, No. 3, pp. 307-314.

FHWA (2007). “Earth Retaining Structures, Reference Manual.” Publication No. FHWA NHI-07-071. USDOT FHWA, National Highway Institute, December, pp. 2-41.

Finno, R. J., and Kim, T., (2011). “Effects of Stress Path Rotation Angle on Small Strain Responses.” Journal of Geotechnical and Geoenvironmental Engineering, Vol. 138, No. 4, pp. 526-534.

Finno, R.J. and Cho, W., (2011). “Recent Stress-History Effects on Compressible Chicago Glacial Clays.” Journal of Geotechnical and Geoenvironmental Engineering, Vol. 137, No. 3, pp.197-207.

Gasparre, A. and Coop, M., (2006). “Techniques for Performing Small-Strain Probes in the Triaxial Apparatus.” Geotechnique, Vol. 56, No. 7, pp. 491-495.

Gens, A., (1983). “Stress-strain and Strength Characteristics of a Low Plasticity Clay.” Doctoral Dissertation, University of London, London, England.

Hansen, J. B., and Gibson, R. E., (1949). “Undrained Shear Strengths of Anisotropically Consolidated Clays.” Geotechnique, Vol.1, No. 3, pp.189-200.

Hardin, B.O. and Blandford, G.E., (1989). “Elasticity of Particulate Material.” Journal of Geotechnical Engineering, Vol. 115, No. 6, pp.788-805.

Hardin, B.O. and Drnevich, V.P. (1972). “Shear Modulus and Damping in Soils: Measurement and Parameter Effects.” Journal of Soil Mechanics and Foundations Division, ASCE. Vol. 98, No. 6, pp. 603-624.

Hashash, Y., Wotring, D., Yao, J., Lee, J. and Fu, Q. (2002). “Visual Framework for Development and Use of Constitutive Models.” International Journal for Numerical and Analytical Methods in Geomechanics, Vol. 26. No. 15, pp. 1493-1513.

Henkel, D.J. (1956). “The Effect of Overconsolidation on the Behavior of Clays During Shear.” Geotechnique, Vol. 6, No. 4, pp.139-150.

Hirschfield, R. C. (1958). “Factors Influencing the Constant Volume of Clays.” Doctoral dissertation, Howard University, Washington, DC.

Hong, Z. S., Bian, X., Cui, Y. J., Gao, Y. F., Zeng, L. L., (2013). “Effect of Initial Water Content on Undrained Shear Behaviour of Reconstituted Clays.” Geotechnique, Vol. 63, No. 6, pp. 441-450.

Hong, Z. S., Yin, J., Cui, Y. J., (2010). “Compression Behaviour of Reconstituted Soils at High Initial Water Contents.” Geotechnique, Vol. 60, No. 9, pp. 691-700.

Jamiolkowski, M., Lancellotta, R., and Lo Presti, D. C. F., (1995). “Remarks on the Stiffness at Small Strains of Six Italian Clays.” Proceedings of the International Symposium, In Pre-Failure Deformation of Geomaterials, Sapporo, Japan, pp. 817-845.

Jovicic, V., and Coop, M. R., (1998). “The Measurement of Stiffness Anisotropy in Clays with Bender Element Tests in the Triaxial Apparatus.” Geotechnical Testing Journal, ASTM, Vol. 21, No.1, pp. 3-10.

Kang, X., Kang, G.-C., and Bate, B., (2014). “Measurement of Stiffness Anisotropy of Kaolinite Using Bender Element Tests in a Floating Wall Consolidometer”. Geotechnical Testing Journal. ASTM. Vol. 37, No.5, pp. 1-16.

Kulhawy, F. H., and Mayne, P. W., (1990). “Manual on Estimating Soil Properties for Foundation Design.” Electric Power Res. Inst. EL-6800; Prof. 1493-6, Electric Power Research Inst., Palo Alto, CA, pp. 4-5.

Ladd, C.C, and Foott, R., (1974). "New Design Procedure for Stability of Soft Clays." Journal of Geotechnical Engineering Division." Vol. 100, No. 7, pp. 763-768.

Ladd, C.C. (1991). "Stability Evaluation During Staged Construction (22nd Terzaghi Lecture)." Journal of Geotechnical Engineering. Vol. 117 No. 4, pp. 540-615.

Ladd, C.C., Bovee, R.B., Edgers, L. and Rixner, J.J., (1971). "Consolidated-undrained Plane Strain Shear Tests on Boston Blue Clay." Research Report R71-13, No. 273, No. 284, Massachusetts Institute of Technology, Cambridge, pp. 243.

Lade, P. V. (2005). "Overview of Constitutive Models for Soils." Soil constitutive models: Evaluation, selection and calibration, J. A. Yamamuro and V. N. Kaliakin, eds., ASCE, Reston, VA. pp 1-34.

Lade, P. V., and Duncan, J. M., (1999). "Stress-path Independent Behavior of Cohesionless Soil." Journal of the Geotechnical Engineering Division, Vol.102. No. 1, pp. 51-68.

Lambe, T. W. (1967). "Stress Path Method." Journal of Soil Mechanics and Foundations Division,

Lee, C., Lee, J. S., Lee, W., and Cho, H., (2007). "Experiment Setup for Shear Wave and Electrical Resistance Measurements in an Oedometer." Geotechnical Testing Journal, Vol. 31, No. 2, pp. 149-156.

Lings, M. L., Pennington, D. S., and Nash, D. F. T. (2000). "Anisotropic Stiffness Parameters and their Measurement in a Stiff Natural Clay." Geotechnique, Vol. 50, No. 2, pp. 109-125.

Liu, Y. (2004). "The Stress-Strain Behavior of Kaolin Clay in Triaxial." Ph.D. Thesis. University of Delaware. Newark, DE.

Martin, R. T., and Ladd, C. C., (1978). "Fabric of Consolidated Kaolinite." Clays and Clay Minerals, Vol. 23, 17-25.

Mitchell, J.K., and Soga, K., (2005). "Fundamental of Soil Behavior, 3rd Edition." John Wiley and Sons.

Mitchell, R. J., (1972). "Some Deviations from Isotropy in Lightly Overconsolidated Clay." Geotechnique, Vol. 22, No. 3, pp. 459-467.

Moniz, Safia R., (2009). "The Influence of Effective Consolidation Stress on the Normalized Extension Strength Properties of Resedimented Boston Blue Clay." MEng Thesis, MIT, Cambridge, MA.

Nash, D.F.T., Lings, M.L., and Pennington, D.S., (1999). "The Dependence of Anisotropy G_0 Shear Moduli on Void Ratio and Stress State for Reconstituted Gault Clay." Proc., 2nd Int. Symp. on Pre-Failure Deformation Characteristics of Geomaterials, Torino, pp. 229-238.

Olson, R.E., (1962). “The Shear Properties of Calcium Illite.” Geotechnique, Vol.12, No. 1, pp.23-43.

Parry, R. H. G., (2004). “Mohr Circles, Stress Paths and Geotechnics.” Spon Press, London.

Parry, R.H.G. (1960). “Triaxial Compression and Extension Tests on Remolded Clay.” Geotechnique, Vol. 10, No. 4, pp. 160-188.

Parry, R.H.G. and Nadarajah, V., (1974). “Observations on Laboratory Prepared, Lightly Overconsolidated Specimens of Kaolin.” Geotechnique, Vol. 24, No. 4, pp.345-357.

Pennington, D. S., Nash, D. F. T., and Lings, M. L., (1997). “Anisotropy of G_0 Shear Stiffness in Gault Clay.” Geotechnique, Vol. 47, No. 3, pp. 391-398.

Prashant, A. and Penumadu, D., (2005). “A Laboratory Study of Normally Consolidated Kaolin Clay.” Canadian Geotechnical Journal, Vol. 42, No. 1, pp.27-37.

Race, M.L., Coffman, R.A., (2011). “Effects of Piston Uplift, Piston Friction, and Machine Deflection in Reduced Triaxial Extension Testing.” ASCE Geotechnical Special Publication No. 211, Proc. GeoFrontiers 2011: Advances in Geotechnical Engineering, Dallas, Texas, March, pp. 2649-2658.

Richart, F. E., Hall, J. R., and Woods, R. D., (1970). “Vibrations of Soils and Foundations.” Prentice-Hall, Inc., NJ.

Roesler, S. K., (1979). “Anisotropic Shear Modulus due to Stress Anisotropy.” J. Geotech. Eng. Div., Vol. 105, No. 7, pp. 871-880.

Roscoe, K. H., and Burland, J. B. (1968). “On the Generalized Stress-strain Behaviour of “Wet” Clay.” Engineering plasticity, J. Hayman and F. A. A. Leckie, eds., Cambridge Univ. Press, Cambridge, U.K. pp. 535-609.

Roscoe, K. H., Schofield, A., and Wroth, C., P., (1958). “On the Yielding of Soils.” Geotechnique, Vol. 8, No.1, pp. 22-53.

Saada, A.S. and Bianchini, G.F., (1977). “Strength of One Dimensionally Consolidated Clays.” Journal of Geotechnical and Geoenvironmental Engineering, Vol. 103, (HGT-6), pp. 655-660.

Salazar, S. E. and Coffman, R. A., (2014). “Design and Fabrication of End Platens for Acquisition of Small-Strain Piezoelectric Measurements During Large-Strain Triaxial Extension and Triaxial Compression Testing.” Geotechnical Testing Journal, Vol. 37, No. 6, pp. 1-12.

Salazar, Sean E. and Coffman, Richard A. (2015). “Consideration of Internal Board Camera Optics for Triaxial Testing Applications.” Geotechnical Testing Journal, Vol. 38, No. 1, pp. 1–10.

Santagata, M. C. (2008). “Effects of Stress History on the Stiffness of a Soft Clay.” Proceeding Deformational Characteristics of Geomaterials, Keynote Lecture, IOS Press/Millpress.

Scholey, G. K., Frost, J. D., Lo Presti, D. C. E, and Jamiolkowski, M. (1996). “A Review of Instrumentation for Measuring Small Strains During Triaxial Testing of Soil Specimens.” Geotechnical Testing Journal, GTJODJ, Vol. 18, No. 2, pp. 137-156.

Sheahan, T. C. (1991). “An Experimental Study of the Time-dependent Undrained Shear Behavior of Resedimented Clay Using Automated Stress Path Triaxial Equipment.” Doctoral dissertation, Massachusetts Institute of Technology, MA.

Simons, N. E. and Som, N. N. (1970). “Settlement of Structures on Clay: with Particular Emphasis on London Clay.” Construction industry research and information Association, London. Report 22.

Skempton, A. W. (1954) “The Pore-pressure Coefficients A and B.” Geotechnique, Vol. 4, No. 4, pp.143-147.

Skempton, A. W. and Henkel, D. J. (1957). “Test on London Clay from Deep Boarding at Paddington, Victoria and South Bank.” Proceeding of the 4th International Conference on Soil Mechanics and Foundation Engineering, Vol.1, No.100, London, U.K.

Stipho, A. S. A. (1978). “Experimental and Theoretical Investigation of the Behavior of Anisotropically Consolidated Kaolin.” Doctoral Dissertation, University College, Cardiff, U.K.

Tiwari, B., and Ajmera, B., (2011). “New Correlation Equations for Compression Index of Remolded Clays.” Geotechnical and Geoenvironmental Engineering, Vol. 138, No. 6, pp. 757-762.

Viggiani, G. and Atkinson, J. H., (1995). “Stiffness of Fine-grained Soil at Very Small Strains. Geotechnique, Vol. 45, No. 2, pp. 249-265.

Wang, Y. and Ng, C.W., (2005). “Effects of Stress Paths on the Small-strain Stiffness of Completely Decomposed Granite.” Canadian Geotechnical Journal, Vol. 42, No. 4, pp.1200-1211.

Wheeler, S. J., Näätänen, A., Karstunen, M., and Lojander, M., (2003). “An Anisotropic Elastoplastic Model for Soft Clays.” Canadian Geotechnical Journal, Vol. 40. No. 2, pp. 403-418.

Whittle, A.J. and Kavvadas, M.J., (1994). “Formulation of MIT-E3 Constitutive Model for Overconsolidated Clays.” Journal of Geotechnical Engineering, Vol. 120, No.1, pp.173-198.

Woods, R.D. and Partos, A., (1981). “Control of Soil Improvement by Crosshole Testing.” Jn Proceeding to the 10th International Conference on Soil Mechanics and Foundation Engineering, Stockholm, pp. 793-796.

Wroth, C. P., (1984). “The Interpretation of in Situ Soil Tests.” Geotechnique, Vol. 34, No. 4, pp. 449-489.

Wu, W., and Kolymbas, D., (1991). “On Some Issues in Triaxial Extension Tests.” Geotechnical Testing Journal, Vol. 14, No. 3, pp. 276-287.

Yamashita, S., Hori, T., and Suzuki, T., (2005). “Effects of Initial and Induced Anisotropy on Initial Stiffness of Sand by Triaxial and Bender Elements Tests.” Geomechanics, pp. 350-369. doi: 10.1061/40797(172)20.

Yamashita, S., Jamiolkowski, M., and Presti, D.C.F., (2000). “Stiffness Nonlinearity of Three Sands.” Journal of Geotechnical and Geoenvironmental Engineering, Vol. 126, No.10, pp. 929-938.

Yimsiri, S., Soga, K., (2002). “Application of Micromechanics Model to Study Anisotropy of Soils at Small Strain.” Soil and Foundations, Vol. 42, pp. 15-26.

Zdravkovic, L. (1996). “The Stress-strain-strength Anisotropy of a Granular Medium under General Stress Conditions.” Doctoral Dissertation, Imperial College, London, UK.

Zhao, Y., and Coffman, R.A., (2016). “Back-Pressure Saturated Constant-Rate-of-Strain Consolidation Device with Bender Elements: Verification of System Compliance.” Journal of Testing and Evaluation, Vol. 44, No. 6, pp. 1-12.

Zhao, Y., Mahmood, N., and Coffman, R. A., (2017). “Soil Fabric and Anisotropy as Observed Using Bender Elements during Consolidation.” Clays and Clay Minerals, Under Review, Manuscript Number: CCM-1143.

Zhao, Y., Mahmood, N. S., and Coffman, R.A., (2018). “Small-Strain and Large-Strain Modulus Measurements with a Consolidation Device.” Journal of Testing and Evaluation, In Press, Manuscript Number: JTE-2016-0331.

CHAPTER 3: Materials and Testing Procedures

3.1. Chapter Overview

A description of the material properties, equipment, and procedures that were utilized to perform the experimental program are contained within this chapter. Specifically, the properties of the soils that were utilized to prepare the specimens for the experimental program are described in Section 3.2. The methods that were followed to form fully-saturated, reconstituted, specimens are presented in Section 3.3. The advanced triaxial equipment that were used to investigate the stress-strain and strength properties of the reconstituted soils is discussed in Section 3.4. The methods and procedures to perform the triaxial compression and triaxial extension test are described in Section 3.5. Additionally, a description of the bender elements tests along with the procedures to perform the tests are presented in Section 3.6.

3.2. Soil Properties

Kaolinite and illite soils were selected and used for sample preparation throughout the study. Kaolinite was selected 1) due to the high permeability when compared with other cohesive soils and 2) to compare with other available data in the literature (Jafroudi 1983). The high permeability reduced the time required to obtain primary consolidation and also provided a more homogenous distribution of pore water pressure through the specimen. Specifically, KaoWhite-S, a commercially available product that is produced by Thiele Kaolin Company in Sandersville, Georgia, was used. The Kaowhite-S product had G.E. The kaolinite soil had a brightness values between 88 and 90 percent and a pH value from 6.5 to 8.0 (Theile 2016). Illite soil was obtained from the Knight Hawk Coal Company of Percy, Illinois. The illite soil was ground by utilizing a commercially available mechanical grinder. The soil was then sieved using the Number 200 sieve (nominal opening size of 0.075 mm). The portion of the illite soil that passed the sieve was used for the specimens preparation.

Shear strength, consolidation, small-strain modulus, and unsaturated soil information of these two types of the kaolinite and illite soils have been studied at the University of Arkansas to determine the parameters of these soils and to provide the input data for the numerical modeling (Zhao and Coffman 2016, Zhao et al. 2017, Zhao et al. 2018). The index properties of the kaolinite and illite soils are summarized in Table 3.1. The kaolinite and illite soils were classified, according to the Unified Soil Classification System (ASTM D2487, 2011), as Low Plasticity Silt (ML) and Low Plasticity Clay (CL), respectively.

Table 3.1. Properties of kaolinite and illite soils.

Property	Kaolinite	Illite
Liquid limit	31.5	46.7
Plastic limit	28.1	23.6
Clay size fraction (<0.002 mm)	47.2	46.5
Specific gravity, G_s	2.67	2.69

3.3. Specimens Preparation

Laboratory prepared specimens were used throughout the study, instead of naturally deposit soils, to obtain high-quality, fully-saturated soil specimens. The specimens were prepared from slurries in accordance with the procedure that was reported in Zhao and Coffman (2016), Zhao et al. (2017), and Zhao et al. (2018). The kaolinite and illite soils were formed by mixing the powdered soils with de-ionized, de-aired, water. The slurries were prepared at two different water content values. For the slurries that were used to form kaolinite specimens, for the stress path triaxial tests, the slurries were initially mixed at water content of 1.5LL. The slurries that were utilized to form kaolinite and illite specimens to investigate the intrinsic shear strength and intrinsic small-strain behavior were initially mixed at two water content values of 1.5LL and 3LL.

For the kaolinite soil, each slurry was manually mixed with a spatula for three minutes. The slurry was then allowed to settle for one minute, and was then remixed for one additional

minute. For illite soil, the slurry was first mixed with a spatula for two minutes. The slurry was then mixed by utilizing a mechanical dispersion device for five minutes.

Following mixing, the slurry was consolidated in a double drained, 1.5 inch (3.81 centimeter) inside diameter, acrylic, static weight, slurry consolidometer (Figure 3.1). The consolidometer was designed to simulate the K_o-consolidation of natural soils. Before the consolidometer was assembled, a piece of filter paper was placed on the top of the porous stone that was located in the bottom plate. The slurry consolidometer was then assembled by securing the acrylic tube in position between the top and bottom plates. The slurry was poured into the consolidometer through a 0.5-inch aperture plastic funnel. For the illite soil, it was necessary to continuously tap the funnel against the top of the consolidometer to aid in the flow of the slurry into the consolidometer. A piece of filter paper was placed onto the porous stone that was located in the piston. This piece of filter paper was initially moisturized to help keep the filter paper in place after inverting the piston and while pushing the piston into the consolidometer tube. The slurry was allowed to consolidate, in a double drained condition, under a constant overburden pressure of 30 psi (207 kPa). The overburden pressure was achieved by placing sufficient static weight onto the loading piston. The axial deformation of the sample during consolidation was measured by utilizing an electronic dial gauge that was attached to a laboratory stand.

The amount of time required for completion of primary consolidation was calculated using the square root of time procedure, as described by Taylor (1948). After primary consolidation was completed, one specimen was extruded at a time (two total specimens) from each consolidometer. The consolidated specimens were cut using a wire saw to develop a length to diameter ratio of two for each specimen. After extrusion of a given specimen from the consolidometer, the specimen properties: length, diameter, and weight were measured, and

trimmings were collected to obtain the initial water content and the corresponding phase diagram measurements for each of the soil specimens.

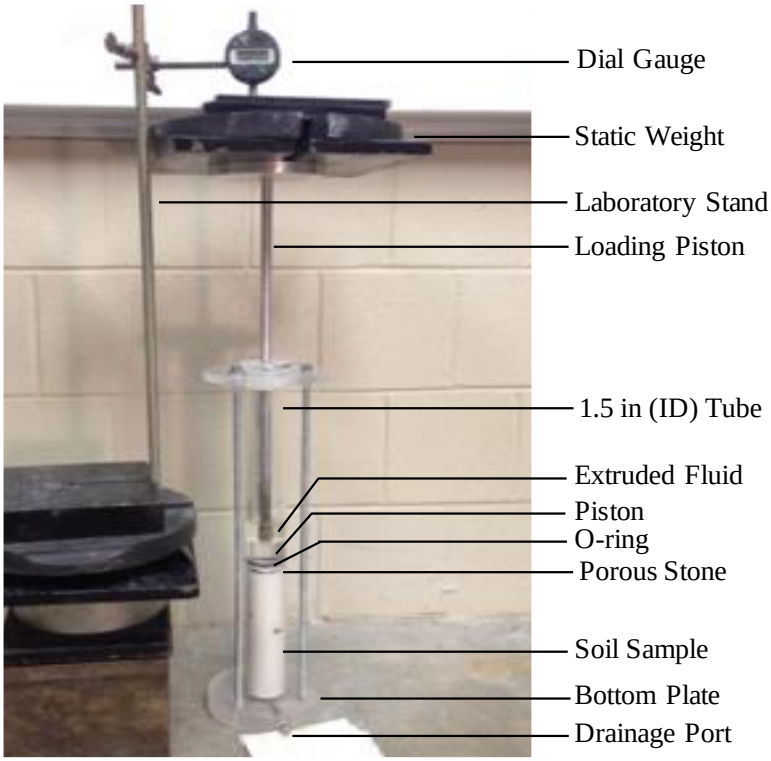

Figure 3.1. Photograph of a slurry consolidometer.

3.4. Triaxial Equipment

Using advanced, automated, triaxial equipment, a series of K_o-consolidated, undrained, triaxial compression ($\overline{CK_oUTC}$) and K_o-consolidated, undrained, triaxial extension ($\overline{CK_oUTE}$) tests with pore water pressure measurements were conducted on the laboratory prepared kaolinite and illite specimens. GEOTAC (Geotechnical Test Acquisition Control) equipment and software were utilized to perform these tests and to record the collected data. The equipment, as illustrated in Figure 3.2, was comprised of 1) a triaxial chamber, 2) an automated load frame with a direct current displacement transducer (DCDT) and a 100 pound (444 N) external load cell, 3) a DigiFlow automated pump (155 ml), filled with silicon oil, to control and measure the cell

pressure, and 4) a DigiFlow automated pump (75 ml), filled with deionized water, to control and measure the backpressure as well as to control the pore water pressure.

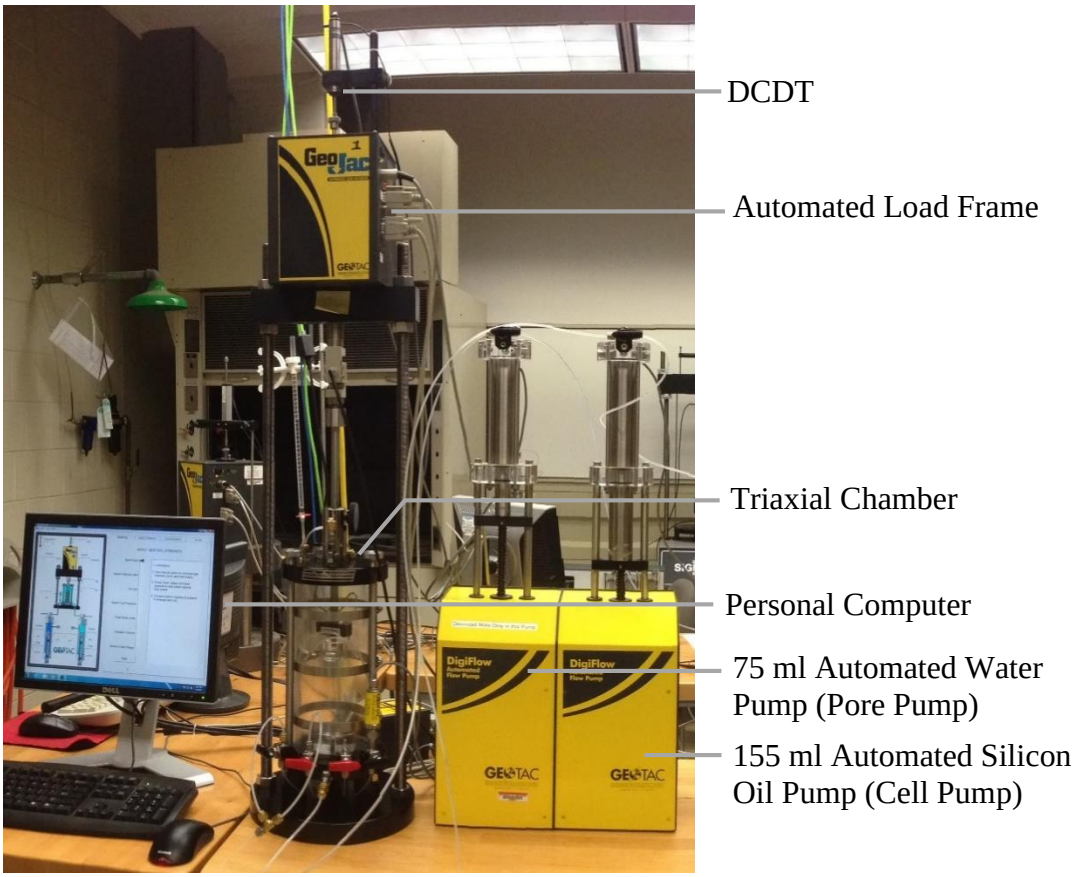

Figure 3.2. The main parts of the triaxial equipment.

The details of the triaxial chamber are illustrated in Figure 3.3. The axial stress was measured inside the triaxial cell with an internal load cell to eliminate the effect of piston friction and piston uplift. By utilizing a vacuum top cap connection (as described in Race and Coffman 2011 and in Salazar and Coffman 2014), the loading piston was connected to the top platten to allow for the application of a downward or upward axial force. To prevent damage to the internal electronics, silicon oil (5cSt) was utilized, instead of water, as the confining fluid. The GEOTAC software named TruePath-SI, Version 1.0.1 was utilized to control the aforementioned equipment and to collect the data from all of the tests. The measured data were recorded and

stored by the associated data acquisition system. The data were then analyzed using spreadsheet tools.

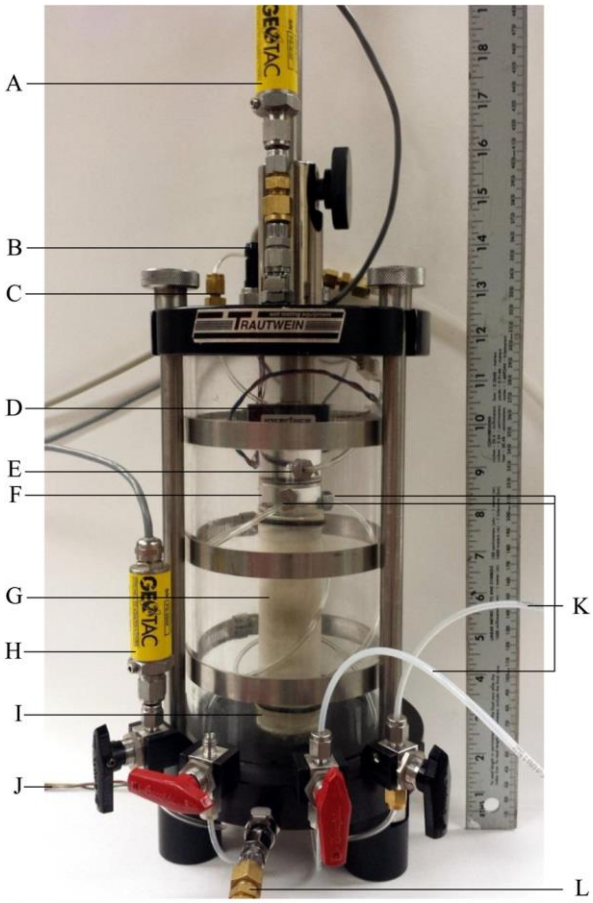

A. Cell pressure transducer.
B. Nine-pin feed-through connector (four pins for the load cell, five pins for the piezoelectric transducers located in the top platen).
C. Throughput vacuum port (for top platen connection).
D. Internal load cell.
E. Vacuum attachment (for top platen connection).
F. Top platen.
G. Soil specimen.
H. Pore pressure transducer.
I. Bottom platen.
J. Wires connecting DAQ system and bottom platen (five wires for the piezoelectric transducers located in the bottom platen).
K. Back-pressure application and pore fluid drainage lines.
L. Cell pressure application line.

Figure 3.3. Photograph of the triaxial chamber (after Salazar and Coffman 2014).

3.5. Triaxial Testing Procedures

The triaxial compression tests were conducted in accordance with ASTM D4767 (2011). Because there is no standard for triaxial extension tests, these tests were conducted following the procedures described by Parry (1960) and Bishop and Henkel (1962). The specimens were mounted into the triaxial chamber using the wet method described in ASTM D4767 (2011). Saturated porous stones were located between the top and the bottom of the specimen and the top and bottom platens. Likewise, pieces of filter paper were placed between the top and bottom surfaces of the specimens and the porous stones. To ensure no fluid connectivity between the cell fluid and the pore fluid, the specimen was encompassed by two latex, non-lubricated membranes (condoms) and two rubber o-rings were used at each end of the specimen to connect the membranes to the top and bottom platens.

A back pressure of at least 40 psi (276 kPa) was used to saturate each specimens and to achieve a pore pressure parameter (B) value greater than 0.95. After the back pressure saturation stage was completed, K_o-strain controlled consolidation, with a strain rate of 0.2 percent per hour, was utilized to consolidate each specimen. To maintain zero lateral strain during the consolidation stage, the GEOTAC software continually adjusted the axial force and cell pressure based on the feedback from the change in volume as measured by the pore water pump. The specimens were initially reconsolidated within the triaxial cell under the K_o conditions to maximum vertical stress levels of 45, 60, and 120 psi (310, 414, and 828 kPa, respectively). As recommended by SHANSEP procedure, the maximum vertical effective stress levels represent 1.5, 2 and 4 times the vertical effective stress that was used to pre-consolidate the soil slurry within the slurry consolidometer. The overconsolidated specimens were then allowed to swell under the K_o conditions to the vertical effective consolidation stresses that was required to achieve the prescribed OCR values, as listed in Table 3.2.

Table 3.2. Stresses associated with the triaxial testing consolidation and overconsolidation processes.

Maximum Vertical Consolidation Stress within the Triaxial Cell ($\sigma'_{v,max}$)*	Pre-shear Vertical Effective Stress (σ'_{vc})			
	OCR=1	OCR=2	OCR=4	OCR=8
[kPa]	[kPa]	[kPa]	[kPa]	[kPa]
310	310	155	78	39
414	414	207	103	52
828	828	414	207	103

* Pre-consolidated to 276 kPa in the slurry consolidometer

To investigate the effect of stress path on the shear strength characteristics, the kaolinite specimens were overconsolidated to four OCR values of 1, 2, 4, and 8. These specimens were then sheared by following one of four stress paths: triaxial compression (TC), reduced triaxial compression (RTC), triaxial extension (TE), or reduced triaxial extension (RTE), as previously presented in Figure 2.1. For the kaolinite and illite specimens that were used to investigate the intrinsic shear strength and intrinsic small-strain behavior, the specimens were overconsolidated to achieve two OCR values of one and eight. These specimens were then sheared by following the prescribed standard procedure of the triaxial compression test.

3.6. Bender Element Tests

To investigate the small-strain properties of the reconstituted soils during triaxial testing, the triaxial apparatus was instrumented with bender elements to measure the shear wave velocity in the specimens. Specifically, vertically-propagated, horizontally-polarized shear waves were passed through the specimens during consolidation and shearing stages of the triaxial tests. The top and bottom platens of the triaxial device, that included bender elements, were developed at the University of Arkansas by Salazar and Coffman (2014). As shown in Figure 3.4, the top and bottom platens were integrated with two types of transducers 1) bender elements to measure shear waves, and 2) bender disks to measure compression waves (the bender disks were not used in this test program). The piezoelectric platens were used by Salazar and Coffman (2014) to

measure shear wave and compression wave velocities in dry Ottawa sand. To measure shear wave velocity in saturated cohesive soils, however, some modifications were made to the top platen to prevent leakage through the platen. These modifications will be discussed in Chapter 6.

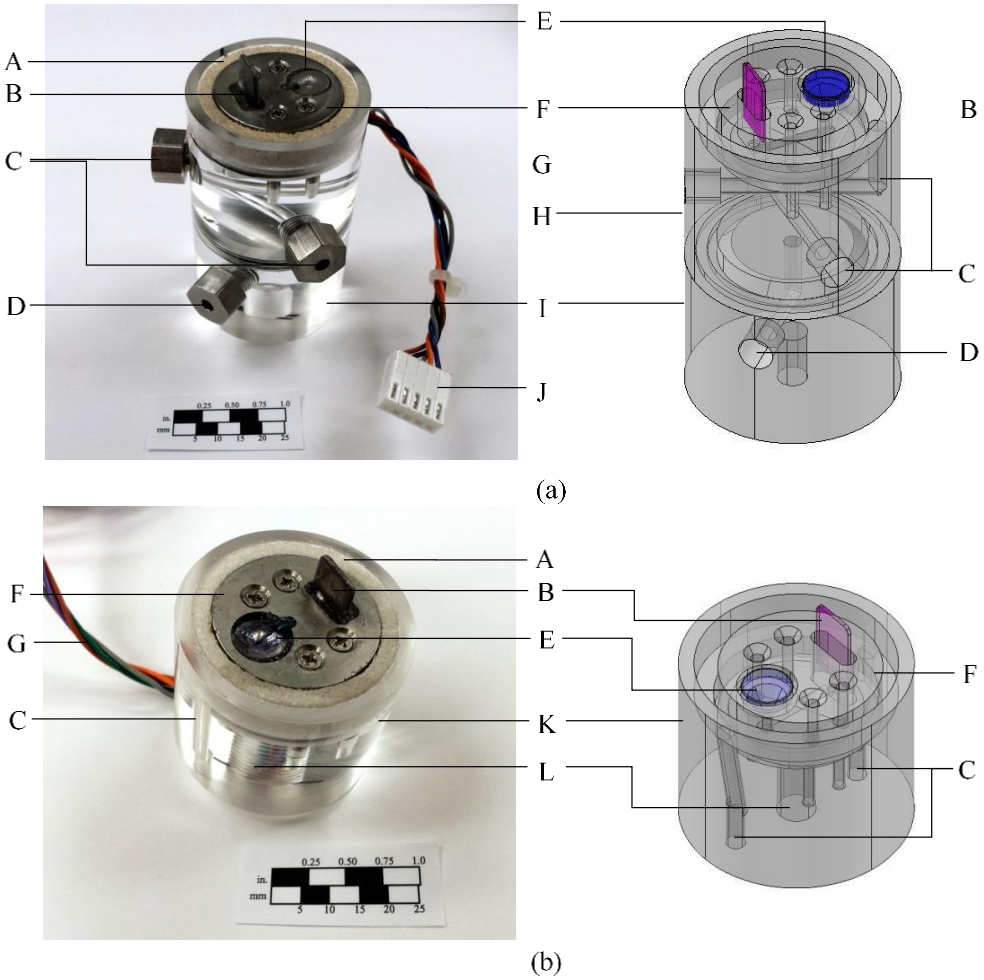

A. Porous ring.
B. Bender element.
C. Drainage ports.
D. Vacuum port (top platen connection).
E. Bender disk.
F. Stainless steel insert (common grounding).
G. Wires (five; +/- bender element, +/- bender disk, and common grounding).
H. Top platen.
I. Vacuum attachment (top platen connection).
J. Five-pin connector.
K. Bottom platen.
L. Wire feed through nylon attachment screw.

Figure 3.4. Photograph and schematics of the (b) piezoelectric-integrated top platen with vacuum and (b) piezoelectric-integrated bottom platen (from Salazar and Coffman 2014).

For each kaolinite and illite soil type, four triaxial tests, with bender elements, were performed on the respective specimens (initially prepared at two w_s values of 1.5LL and 3LL).

Following the same prescribed reconsolidation procedure, the specimens were K_o-reconsolidated to a maximum vertical effective stress of 60 psi (414 kPa). The overconsolidated specimens were then allowed to swell to achieve an OCR value of eight prior to shear. The specimens were then sheared following the standard triaxial compression test stress path.

The velocity of the shear waves that traveled through the specimen was determined following a procedure presented by Brignoli et al. (1996). The transducer at the bottom end was excited, and the developed shear waves were received by the transducer at the top end; the travel time was also recorded. The distance of propagation was calculated by subtracting the embedded length of the bender elements from the total length of the sample at the time of excitation. Axial deformation measurements were used to determine the length of the specimen at any time during the test. Assuming that the specimens represented an infinite, isotropic, and elastic medium, the measured shear wave velocity (V_s), along with the total mass density of the soil (ρ), were then used to calculate the small-strain shear modulus, as previously presented Equation 2.9.

There have been several different interpretation methods to determine the travel time obtained from piezoelectric measurements, as described in Viggiani and Atkinson (1995), Alvarado and Coop (2012), and Salazar and Coffman (2014). The use of time domain or frequency domain have been employed by previous studies to determine the travel time. In this testing program, several excitation frequencies were generated to determine the optimum frequency of the input signal that provided a clear output signal. A frequency of 10 kHz was utilized.

3.7. References

Alvarado, G., and Coop, M. R., (2012). "On the Performance of Bender Elements in Triaxial Tests." Geotechnique, Vol. 62, No. 1, pp 1-17.

American Society for Testing and Materials (2011). "Standard Test Method for Unconsolidated-Undrained Triaxial Compression Test on Cohesive Soils." Annual Book of ASTM Standards, Designation D4767, Vol. 4.08, ASTM, West Conshohocken, PA.

American Society for Testing and Materials (2017). "Standard Practice for Classification of Soils for Engineering Purposes (Unified Soil Classification System)." Annual Book of ASTM Standards, Designation D2487, Vol. 4.08, ASTM, West Conshohocken, PA.

Bishop, A.W., and Henkel, D.J. (1962). "The Measurement of Soil Properties in the Triaxial Test." Edward Arnold LTD, London.

Brignoli, E. G. M., Gotti, M., and Stokoe, K. H., II, (1996). "Measurement of Shear Waves in Laboratory Specimens by Means of Piezoelectric Transducers." Geotechnical Test. J., Vol. 19, No. 4, pp. 384–397.

Jafroudi, S., (1983). "Experimental Verification of Bounding Surface Plasticity Theory for Cohesive Soils." Doctoral dissertation, University of California, Davis, CA.

Parry, R.H.G. (1960). "Triaxial Compression and Extension Tests on Remolded Clay" Geotechnique, Vol. 10, NO. 4, pp. 160-188.

Race, M.L., Coffman, R.A., (2011). "Effects of Piston Uplift, Piston Friction, and Machine Deflection in Reduced Triaxial Extension Testing." ASCE Geotechnical Special Publication No. 211, Proc. GeoFrontiers 2011: Advances in Geotechnical Engineering, Dallas, Texas, March, pp. 2649-2658.

Salazar, S.E., Coffman, R.A., (2014). "Design and Fabrication of End Platens for Acquisition of Small-Strain Piezoelectric Measurements during Large-Strain Triaxial Extension and Triaxial Compression Testing." Geotechnical Testing Journal, Vol. 37, No. 6, pp. 1-12. doi:10.1520/GTJ20140057.

Taylor, D. W. (1948). "Fundamentals of Soil Mechanics." John Wiley and Sons, New York, NY.

Theile (2016). "Product Information for Clay Products." Theile Kaolin Company. https://www.thielekaolin.com/sites/default/files/inline-files/KAOWHITE%20S_0.pdf. Accessed April 2016.

Viggiani, G. and Atkinson, J. H. (1995). "Interpretation of Bender Element Tests." Geotechnique Vol. 45, No. 1, pp.149-154.

Zhao, Y., Mahmood, N., and Coffman, R. A., (2017). "Soil Fabric and Anisotropy as Observed Using Bender Elements during Consolidation." Clays and Clay Minerals, Under Review, Manuscript Number: CCM-1143.

Zhao, Y., Mahmood, N. S., and Coffman, R.A., (2018). "Small-Strain and Large-Strain Modulus Measurements with a Consolidation Device." Journal of Testing and Evaluation, In Press, Manuscript Number: JTE-2016-0331.

CHAPTER 4: The Effects of Stress Path on the Characterization of Reconstituted Low Plasticity Kaolinite

4.1. Chapter Overview

Stress-strain and shear strength characteristics of reconstituted kaolinite specimens were evaluated by conducting undrained triaxial compression and undrained triaxial extension tests with pore pressure measurements. The triaxial tests were conducted on kaolinite specimens that were K_o-reconsolidated to four levels of over-consolidation ratios. The specimens were sheared in the undrained condition by following four different stress paths. The effect of stress path on soil characterizations was thoroughly demonstrated and evaluated. For practical purposes, this evaluation is essential to select adequate soil parameters to characterize the shear strength parameters and to validate constitutive models for a clay soil deposit subjected to different loading conditions.

This chapter contains a research description and a summary (Section 4.1 through Section 4.3), an introduction on the concept and applications of stress path (Section 4.4), a description of the test specimens and procedures (Section 4.5), the findings of this project (Section 4.6), and a description of the implementations and conclusions (Section 4.7 and Section 4.8, respectively). The paper enclosed in this chapter has been submitted to Soils and Foundations Journal. The full reference is: *Mahmood, N. S., and Coffman, R. A., (2017). "The Effects of Stress Path on the Characterization of Reconstituted Low Plasticity Kaolinite." Soils and Foundations, (Under Review, Manuscript Number: SANDF-D-17-00352-R1).*

4.2. The Effects of Stress Path on the Characterization of Reconstituted Low Plasticity Kaolinite

Nabeel S. Mahmood[1], Richard A. Coffman[2]

[1]MSCE, Graduate Research Assistant, Department of Civil Engineering, University of Arkansas, Fayetteville, Arkansas, USA. Instructor, University of Anbar, Ramadi, Iraq.
[2]PhD, PE, PLS, Associate Professor, Department of Civil Engineering, University of Arkansas, Fayetteville, Arkansas, USA.

4.3. Abstract

It is often necessary to apply a stress path, which is representative of the field conditions that a given soil element experiences, to evaluate the deformation and strength characteristics of a soil deposit. A comprehensive triaxial testing program was performed, by utilizing advanced triaxial testing equipment, to explore the effect of the stress path on 1) the stress-strain behavior and 2) the shear strength characteristics of reconstituted low plasticity kaolinite soil. Undrained triaxial compression and triaxial extension tests were conducted on K_o-consolidated specimens at overconsolidation ratios of 1, 2, 4, and 8; one of the four different stress paths was followed during shearing. The testing procedure that was utilized to conduct the stress-controlled triaxial tests is presented herein.

The behavior of the normally consolidated specimens during shear was similar to the typical behavior of overconsolidated clay soils. The stress-strain behavior, as obtained from the triaxial compression and reduced triaxial compression, was almost identical. Likewise, the stress-strain behavior, as obtained from the triaxial extension and reduced triaxial extension stress paths, was almost identical. The behavior of the soil was observed to be highly influenced by the reorientation of the principal stresses (compression and extension values were dissimilar). The values of effective friction angle, as obtained from the extension tests, were from 20 to 35 percent lower than the effective friction angle values that were obtained from the compression tests. The undrained shear strength values, as measured during the compression tests, were 11 to

38 percent greater than the those measured in the extension tests. The axial strain values, at failure, from the extension tests were determined to be 0.3 to 5.0 percent greater than those obtained from the compression tests. As discussed herein, for practical purposes, a testing program that includes triaxial compression tests along with reduced triaxial extension tests is adequate to represent loading or unloading in the field, respectively.

Keywords: Triaxial testing methods; Reconstituted soils; Stress path; Stress-strain behavior; Pore pressure; Site characterization

4.4. Introduction

Triaxial testing is widely used, within the laboratory, to evaluate the strength and strain properties of various soil types. The method of increasing or decreasing the principal stresses on a given sample, commonly referred to as a stress path, has been shown to play a significant role when evaluating the strength and strain properties of clay soils (Lambe 1967). For many geotechnical problems, such as those related to: passive earth pressure, excavation support, and slope stability, the major and minor principal stress states are switched due the field loading conditions. Based on the concept of stress path, many site characterization and design methods have been developed to account for the various orientations of the major, minor, and intermediate principal stress states. For instance, one procedure, identified by the acronym SHANSEP (Stress History and Normalized Soil Engineering Properties), was developed by Ladd and Foott (1974) and later modified by Ladd and DeGroot (2003) to evaluate the undrained shear strength of clay. The SHANSEP procedure was developed because data from triaxial compression test often led to either unsafe or over-conservative designs.

Many other methods have also been used to predict the stress-strain response of a given soil deposit when the soil deposit is subjected to foundation loading or to loading induced by

excavations (e.g., Davis and Poulos 1968, Simons and Som 1970, Davis and Poulos 1972, Coffman et al. 2010). These other methods were developed to account for changes in the stress state within the soil deposit. For these methods, representative soil parameters, as obtained from laboratory stress path tests, were required to determine the field loading conditions. Furthermore, the utilization of stress path tests has received additional attention in recent years. This increased level of attention has been associated with only limited amounts of triaxial compression testing data being available to evaluate the parameters for advanced constitutive models. As discussed in Lade (2005) and Bryson and Salehian (2011), most of the current research related to advanced constitutive modeling has focused on the effect of anisotropy and stress path.

During the shearing stage of triaxial tests, the soil specimen may be sheared in triaxial compression or triaxial extension by increasing or decreasing one or more of the three principal stresses. As described by Lambe (1967) and Ladd and Varallyay (1965), there are four stress paths that represent most of the common field loading conditions: triaxial compression (TC), reduced triaxial compression (RTC), triaxial extension (TE), and reduced triaxial extension (RTE). During the shearing stage of the TC and RTE tests, the cell pressure is maintained while the axial stress is increased for the TC tests or decreased for the RTE tests. For the other two types of tests (RTC and TE), the specimens are sheared by maintaining the axial stress and decreasing the cell pressure for the RTC tests or increasing the cell pressure for the TE tests. The term "R", as used in the prescribed acronyms, has previously been used to describe the tests that were performed by reducing the cell pressure (RTC tests) or reducing the axial stress (RTE tests) during the shearing stage (Salazar and Coffman 2014, Salazar et al. 2017, Zhao et al. 2018). The term "reorientation" of principal stresses was introduced by Duncan and Seed (1966) to describe the change in the state of stress when the orientation of the principal stresses, at the end of

shearing stage, did not coincide with the orientation of the initial principal stresses. During triaxial compression, the orientation of the principal stresses at the end of shearing stage is the same as the orientation of the principal stresses at the beginning of the shearing stage. However, during triaxial extension testing, decreasing the vertical stress or increasing the horizontal stress during the shearing may cause the major principal stress to act in the horizontal direction and the minor principal stress to act in the vertical direction. Therefore, the principal stresses will be reoriented by 90 degrees at the end of shearing stage (Duncan and Seed 1966).

The stress path that a specimen undergoes is one of the major factors that influences both the drained and undrained shear strength parameters for a given soil. Over the past few decades, the relationship between the effective friction angle (ϕ'), as measured from undrained triaxial tests with pore water pressure measurements, and the stress path has been controversial. A few researchers have indicated that the effect of the stress path on the effective shear strength is insignificant. For example, Duncan and Seed (1966) and Gens (1983) reported that the effective angle of internal friction in compression (ϕ'_{comp}) and the effective angle of internal friction in extension (ϕ'_{ext}) are approximately equal. Other researchers (e.g., Parry 1960, Saada and Bianchanini 1977, Rossato et al. 1992) reported that ϕ'_{comp} is less than ϕ'_{ext} by several degrees. Based on the results presented in Atkinson et al. (1990), the critical state lines for the compression and extension tests were symmetrical about the mean effective stress (p') axis; the ϕ'_{comp} values were significantly less than ϕ'_{ext} values. Parry (2004) attributed the difference in the ϕ'_{comp} and ϕ'_{ext} results to the instability of the specimen in extension tests due to the rapid development of necking near failure. Based on the results from other studies (e.g., Ladd and Foott 1974, Parry and Nadarajah 1974, Moniz 2009), the values of undrained strength (s_u) of extension tests were 10 to 25 percent less than those obtained from compression tests. As

discussed by Skempton (1954), the reorientation of the principal stresses influenced the amount of pore water pressure developed during the shearing stage of the triaxial test, thereby affecting the measured strength.

According to Olson (1962), Burland (1990), and Prashant and Penumadu (2007), the arrangement of particles and arrangement of pore space within a given soil, commonly referred to as the microfabric, has also been shown to play an essential role in the engineering behavior of clayey soils. Soil microfabric can vary considerably as a result of using different water content values to "reconstitute" (Burland 1990) clay soils. To form a reconstituted structure, Burland (1990) suggested that the water content of the mixed slurry should be between 1 to 1.5 times the liquid limit of the soil. The term "intrinsic" was introduced by Burland (1990) to describe the properties for specimens that were reconstituted within the aforementioned water content values. Burland (1990) further reported that shear strength and compressibility of reconstituted soils may be utilized to develop a reference framework to correlate obtained properties with those from intact soils.

Olson (1962) indicated that laboratory prepared specimens, at water content less than or slightly above liquid limit, may not represent the natural deposition process. Moreover, Olson (1962) mentioned that these specimens will have dispersed microfabric and exhibit intrinsic properties of overconsolidated clayey soil regardless of the level of overconsolidation within the specimen. To obtain more representative specimens, Olson (1962) reported that the water content of the mixed slurry should be at least two times the liquid limit. However, sedimentation of specimens at such high water content requires an extended period of time. Moreover, it has been shown that these specimens are often difficult to extrude and trim. Therefore, the following researchers: Henkel (1956), Parry (1960), Bryson and Salehian (2011), Tiwari and Ajmera

(2011), Zhao and Coffman (2016), Zhao et al. (2017), and Zhao et al. (2018) have instead prepared reconstituted clay specimens at lower water content values.

To date, data obtained from historic TC tests have been 1) utilized to determine the stress-strain behavior, and then 2) used as inputs for constitutive models. TC tests have specifically been used because of the simplicity and expediency of the TC test as compared with other tests (Bishop and Henkel 1962, Kulhawy and Mayne 1990, Prashant and Penumadu 2004). Relatively few studies (e.g., Ladd and Varallyay 1965, Simons and Som 1970, Wroth 1984) have reported the results from undrained RTC or TE tests. Furthermore, problems associated with previous triaxial extension test results have prevented the use of the results (Wu and Kolymbas 1991, VandenBerge et al. 2015). Specifically, development of necking during shearing in extension tests (Sheahan 1991, Liu 2004), inaccurate determination of the cross-sectional area during shearing (Scholey et al. 1996, Salazar and Coffman 2015), and friction between the loading piston and the bearings within the top cap of the triaxial cell (Bishop and Henkel 1962, Race and Coffman 2011) have all resulted in testing errors within previously obtained triaxial extension test results.

Recent advances in the triaxial testing apparatus, including servo-controlled loading systems to control the stress-strain measurements, have led to a reduction in the amount of testing errors associated with the triaxial extension test. These advances have also led to stress path dependent triaxial tests being easier to conduct. The results from an experimental study on the effects of the change in the magnitudes and/or orientations of the principal stresses on parameters including: shear strength, stress-strain behavior, and excess pore water pressure development in reconstituted low plasticity kaolinite, under undrained triaxial testing conditions, are presented herein. A procedure to perform stress-controlled triaxial testes is also presented. A

total of four series of triaxial compression and triaxial extension tests were conducted on kaolinite specimens that were reconstituted in the laboratory at water content values of 1.5 times the liquid limit of the kaolinite soil. The data obtained from these tests were analyzed and compared to develop an understanding of the testing techniques required to represent certain field conditions. Moreover, these data will be useful to develop or validate kaolinite-based constitutive models.

4.5. Testing Program

The main objective of the testing program, that is presented herein, was to determine the effect of stress path on the shear strength characteristics of saturated, reconstituted, low plasticity kaolinite. A flow chart of the testing program is shown in Figure 4.1. As shown in the flow chart of the testing program, the specimens were K_o- consolidated to various levels of OCR and then sheared by following one of four stress paths: TC, RTC, TE, or RTE. The angle of reorientation of the principal stress between the compression tests and the extension tests was 90 degrees. During the shearing stage, either the axial stress (σ_a) or the cell pressure (σ_c) was changed to produce the required total stress paths (Figure 4.2).

4.5.1. *Test Material and Specimens Preparation*

To obtain high-quality, fully-saturated, reconstituted, soil specimens, laboratory prepared specimens were created and utilized. Kaolinite soil was selected 1) due to the high value of permeability and 2) to compare with other available data in the literature (Jafroudi, 1983, Zhao and Coffman, 2016, Zhao et al., 2018). The high value of permeability of the kaolinite reduced

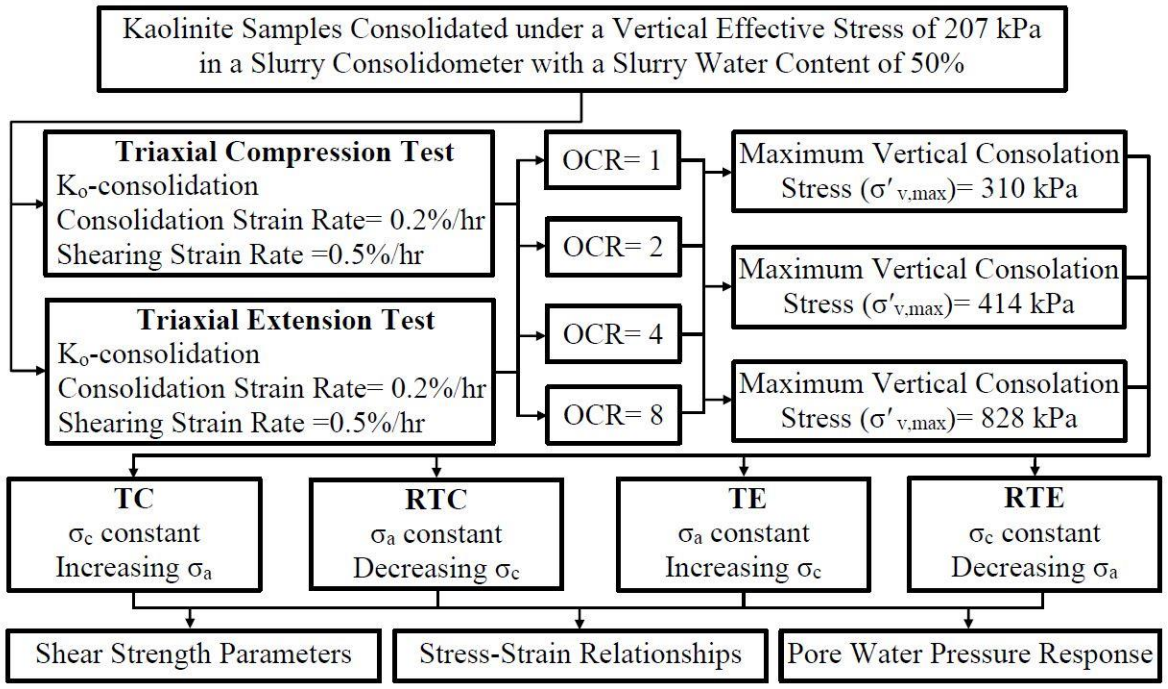

Figure 4.1. Flow chart of the testing program.

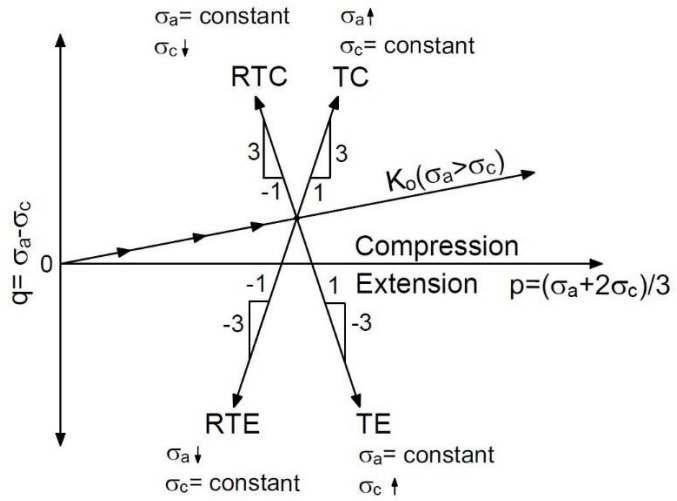

Figure 4.2. Total stress paths that were followed to shear the samples.

the amount of time required to obtain primary consolidation and also provided a more homogenous distribution of pore water pressure through the specimen. Specifically, KaoWhite-S, a commercially available product that is produced by The Thiele Kaolin Company in Sandersville, Georgia, was utilized. This type of kaolinite has been extensively used at the University of Arkansas to study the strength, consolidation, and small-strain stiffness of

laboratory prepared soils (Coffman et al. 2014, Zhao and Coffman 2016, Zhao et al. 2017, Zhao et al. 2018). The kaolinite soil had a liquid limit of 32 percent, a plastic limit of 28 percent, and a clay size fraction (<0.002 mm) of 47 percent.

The specimens were prepared in accordance with the procedure that was reported in Zhao and Coffman (2016), Zhao et al. (2018), and Zhao et al. (2018). Specifically, the kaolinite slurry was prepared at a water content of 1.5 times the liquid limit of the kaolinite by manually mixing dry powdered kaolinite with deaired, deionized, water. The slurry was mixed together with a spatula for three minutes. The slurry was then allowed to settle for one minute, and was then remixed again for one additional minute. Following mixing, the slurry was poured into a 3.81 centimeter inside diameter slurry consolidometer, and was allowed to consolidate, in a double drained condition, under a constant vertical stress of 207 kPa that was applied to the soil by static weight.

The time for primary consolidation was calculated according to the square root of time procedure, as described by Taylor (1948). After primary consolidation was completed, one specimen was extruded at a time (two total specimens) from each consolidometer. The consolidated specimens were cut using a wire saw to develop a length to diameter ratio of two for each specimen. After extrusion of a given specimen from the consolidometer, the specimen: length, diameter, and weight were measured, and trimmings were collected for initial water content and phase diagram measurements for each of the soil specimens.

4.5.2. *Triaxial Testing*

Using advanced, automated, triaxial equipment, a series of K_o-consolidated, undrained, triaxial compression ($\overline{CK_oUTC}$) and K_o-consolidated, undrained, triaxial extension ($\overline{CK_oUTE}$) tests, with pore water pressure measurements, were conducted on the laboratory prepared

kaolinite specimens. GEOTAC (Geotechnical Test Acquisition Control) equipment and software were utilized to perform these tests and to record the data. The equipment was comprised of a triaxial chamber, an automated load frame, and two pumps that were used to control and measure: stresses, strains, cell pressure, and pore pressure within the soil specimen during the tests. The axial stress was measured inside the triaxial cell with an internal load cell to eliminate the effect of piston friction. The triaxial compression tests were conducted in accordance with ASTM D4767 (2011). Because there is no standard for triaxial extension tests, these tests were conducted following the procedures described by Parry (1960) and Bishop and Henkel (1962). The data from all of the tests were recorded and stored by the associated data acquisition system.

The individual specimens were mounted within the triaxial chamber using the wet preparation method as described in ASTM D4767 (2011). Two saturated porous stones were placed at the top and the bottom of the specimen. Filter paper was placed between the top and bottom surfaces of the specimen and the porous stones. To ensure no fluid connectivity between the cell fluid and the pore fluid, the specimen was encompassed by two latex, non-lubricated membranes (condoms) and two rubber o-rings were used at each end of the specimen to clamp the membranes to the top and bottom platens located above and below the specimen, respectively. By utilizing a vacuum top cap connection (as previously described by Race and Coffman, 2011 and in Salazar and Coffman, 2014), the loading piston was connected to the top platten to allow application of a downward or upward axial force. To prevent damage to the internal electronics, silicon oil (5cSt) was utilized, instead of water, as the confining fluid. A back pressure of at least 276 kPa was used to saturate each specimen and to achieve a pore pressure parameter (B) value greater than 0.95.

After the back pressure saturation stage was completed, strain-controlled consolidation, with a strain rate of 0.2 percent per hour, was utilized to consolidate each specimen. The GEOTAC software controlled the axial force and the cell pressure, to maintain zero lateral strain, based on the feedback from the change in the pore water volume. As listed in Table 4.1, for each overconsolidation ratio (1, 2, 4, and 8), the specimens were initially re-consolidated within the triaxial cell under the K_o-conditions to maximum vertical effective stress values of 310, 414, and 828 kPa and then overconsolidated to the respective OCR levels. As recommended by the SHANSEP procedure, the stress levels represented 1.5, 2, and 4 times the vertical effective stress that was used to pre-consolidate the kaolinite slurry within the slurry consolidometer. The K_o values were measured for the specimens during the consolidation and the overconsolidation processes. After consolidating each of the specimens to the required level of vertical effective stress, each specimen was then sheared, under undrained conditions, at an axial strain rate of 0.5 percent per hour. A total of 48 specimens (12 specimens per stress path) were required to develop the four stress paths at the various levels of OCR (as previously presented in Figure 4.1).

Table 4.1. Stresses associated with the triaxial testing consolidation and overconsolidation processes.

Maximum Vertical Consolidation Stress ($\sigma'_{v,max}$), kPa	Pre-shear Vertical Effective Stress (σ'_{vc}), kPa			
	OCR=1	OCR=2	OCR=4	OCR=8
310	310	155	78	39
414	414	207	103	52
828	828	414	207	103

Although, the GEOTAC software controlled all stages of the test: seating, back pressure saturation, consolidation, and shear, inherent shearing procedures were only available within the GEOTAC software for the TC and RTE tests. Following these two stress paths, the cell pressure was maintained and the axial stress was altered by moving the loading piston downward for TC or upward for RTE (strain-controlled) with a constant strain rate of 0.5 percent per hour. To

measure the plastic failure, these tests were continued until 15 percent axial strain was reached. The other two types of tests (RTC and TE) were stress-controlled tests. For these tests, the principal stresses were changed by manually controlling the loading piston and the cell pressure by utilizing the "manual mode" within the GEOTAC software program. For the RTC and TE tests, when the cell pressure was changed by $\Delta\sigma_c$ for each step, the deviatoric stress was also simultaneously changed by $\Delta\sigma_d$ to maintain a constant axial stress (Equation 4.1). The initial change in the cell pressure, for the first step in each of the stress-controlled tests, was estimated based on the maximum deviatoric stress and shearing duration of the corresponding, previously completed, strain-controlled compression and extension tests (i.e. TC and RTE). The rate of strain was monitored every hour and $\Delta\sigma_c$ was adjusted to maintain an axial strain rate of 0.5 percent per hour. However, once the failure was approached and due to the stress softening, excessive levels of strain rate (2.5 to 6 percent per hour) were imposed by the system to maintain the target stresses over the period of the stress increment. Therefore, the stress-controlled tests were stopped at that point and stress-strain data were not considered for these large levels of strain rate. Also, for this reason maximum deviatoric stress was considered as a failure criterion for all the tests. Similar failure criterion for stress-controlled tests was also considered by Parry and Nadarajah (1974).

$$\Delta\sigma_d = \Delta\sigma_c \frac{(A_c - A_p)}{A} \qquad \text{Equation 4.1}$$

where A_c was the area of the specimen top cap; A_p was the area of the piston; A was the corrected area of the specimen at the test step; and $\Delta\sigma_c$ was positive when cell pressure increased and negative when the cell pressure decreased.

4.6. Test Results and Discussion

The behavior of the undrained kaolinite, as obtained from the triaxial tests using the four stress paths, is discussed herein. Specifically, for completeness, four main parts including: 1) shear strength parameters, 2) stress-strain relationships, 3) Young's Modulus, and 4) pore water pressure response are discussed. These parameters are also compared with literature values to gain insight into the measured behavior of the kaolinite soil.

4.6.1. *Shear Strength Parameters*

Effective stress paths, for each series of the tests, in terms of mean effective stress ($p' = \frac{\sigma'_a + 2\sigma'_c}{3}$) and deviatoric stress ($q = \sigma'_a - \sigma'_c$), are shown in Figure 4.3. To determine the effective cohesion (c') and the effective friction angle (ϕ') values, failure envelopes were developed based on the peak principal stress difference (PPSD) that were observed for each stress path. The specimens that were sheared along compression stress paths (TC and RTC) followed identical effective stress paths, however the specimens reached different maximum deviatoric stress values. Similar behavior was also noticed for the specimens sheared along extension stress paths (TE and RTE).

The effective stress paths for the OCR=1 tests initially decreased in p' during shearing (indicating contractive behavior), but before reaching the peak principal stress difference, the stress paths changed direction and began to move to the right (indicating dilative behavior) until the failure envelope was reached. This pattern of behavior, during shearing stage, has typically not been observed for naturally occurring, normally consolidated, clay soil types. However, this behavior was in agreement with prior studies conducted on reconstituted clays (Parry 1960 and Olson 1962). On the other hand, the effective stress paths for the overconsolidated specimens followed the typical behavior of overconsolidated clays. The stress path moved to the right

during shear (dilative behavior) then bent downward or upward for compression and extension, respectively, after reaching the failure envelope.

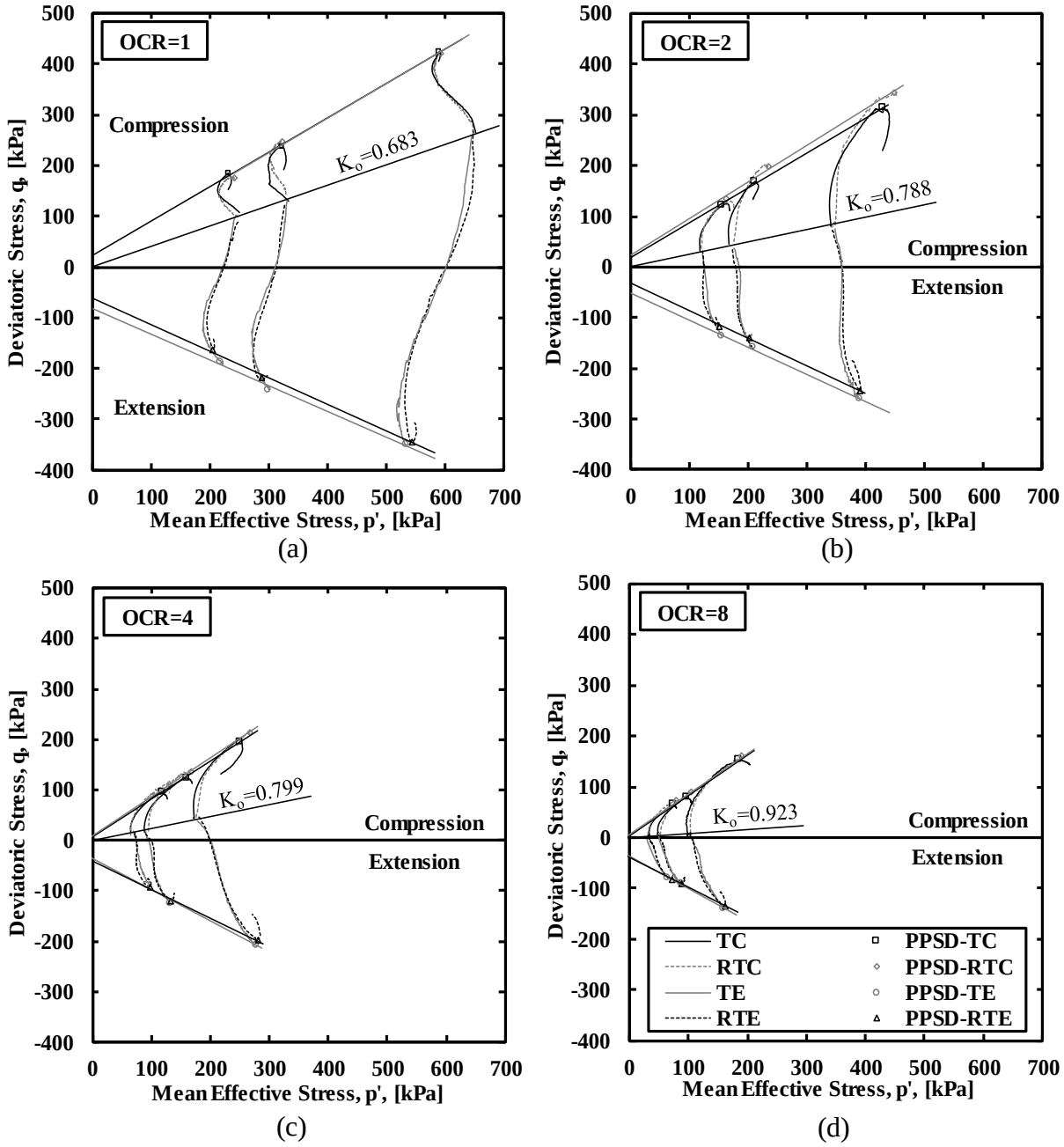

Figure 4.3. Cambridge effective stress paths of the triaxial compression and triaxial extension tests on reconstituted kaolinite: a) OCR= 1, b) OCR= 2, c) OCR= 4, d) OCR= 8.

The variations of the c' and ϕ' values, as a function of the overconsolidation ratio, are shown in Figures 4.4 and 4.5, respectively. It is unusual to have effective cohesion intercept

values for normally consolidated soils (Holtz et al. 2011), however those values may also indicate that the behavior of the normally consolidated reconstituted kaolinite is similar to the behavior of the overconsolidated specimens. It was clear that c' values and ϕ' values obtained from the compression tests (TC and RTC) were similar. Comparable values were also obtained from the extension (TE and RTE) tests; albeit, there was a difference in the cohesion values for the extension tests at low levels of OCR and in the friction angle values for the compression tests at high levels of OCR. Based on these observations, for the specimens that were consolidated to the same vertical effective stress and sheared following the same mode (compression or extension), the effective stress path was independent of the change in the magnitude of the principal stresses. Similar results were reported by Simons and Som (1970) and Wroth (1984).

The change in the stress path, as associated with reorientation of the principal stresses (from compression to extension), had a significant effect on the effective shear strength parameters. As shown in Figure 4.4, the c' values obtained from the extension tests were greater than those obtained from the compression tests by 8 to 34 kPa (almost four times as great for all levels of OCR). However, as indicted by Ladd and Varallyay (1965), the cohesion intercept has been shown to be difficult measure accurately. The relationships between the effective internal friction angle and the OCR, for the different stress paths are shown in Figure 4.5. The values of ϕ' for extension tests were 20 to 35 percent less than those for corresponding compression tests. Similar results and findings regarding the values from extension tests being less than the values obtained from compression tests were reported by Parry (1960) and Saada and Bianchanini (1977).

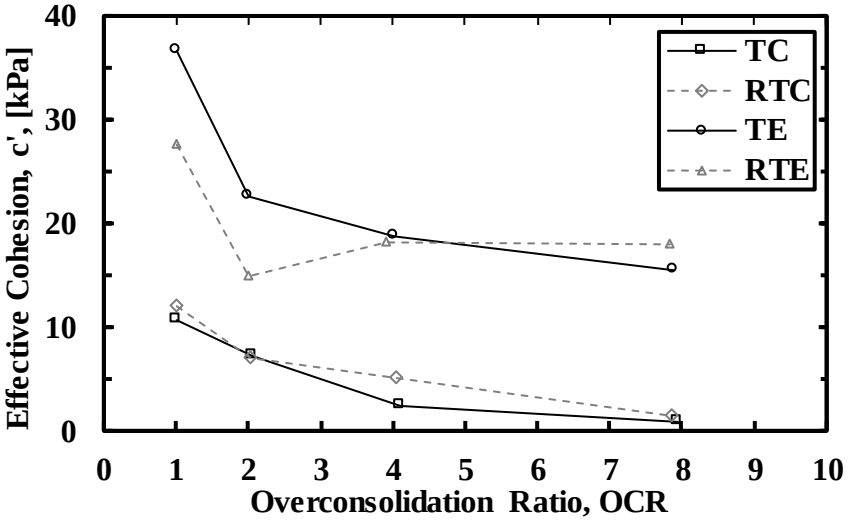

Figure 4.4. Variation of the effective cohesion, as a function of OCR, for the different stress paths.

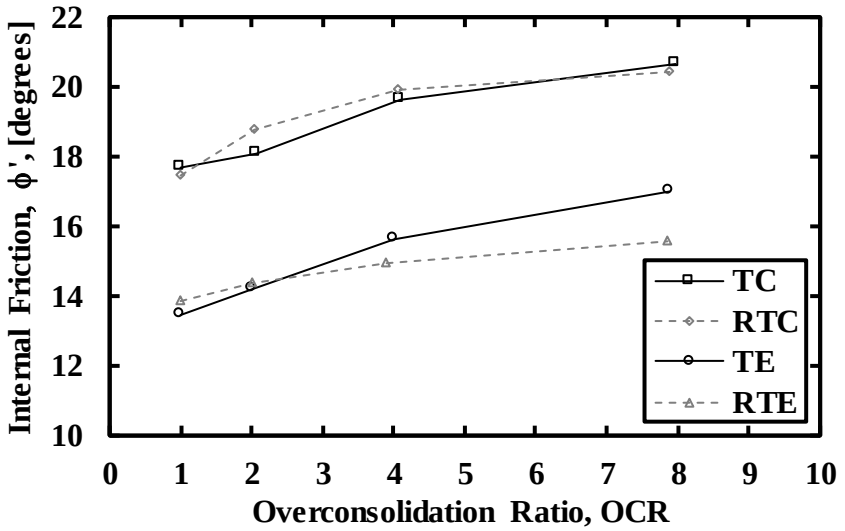

Figure 4.5. Variation of the effective internal friction angle, as a function of OCR, for the different stress paths.

The specimens that were sheared by following the same stress path and at the same overconsolidation ratio (OCR) exhibited similar stress-strain behavior when normalized with respect to the pre-shear vertical effective stress, as shown in Figure 4.6. As prescribed by the SHANSEP procedure, it is useful to estimate the amount of increase in the undrained shear strength, for clays that exhibit normalized behavior, as a function of overconsolidation ratio. The SHANSEP parameters, S (the normalized undrained strength ratio for the respective stress paths

at OCR=1) and m (the slope of the regression line for the respective stress paths), are presented in Figure 4. 7 for the various stress paths. The four stress paths exhibited similar normalized behavior; increased levels of overconsolidation produced increased levels of normalized undrained shear strength. Although the values of m parameter are, typically, larger for extension tests than for compression tests (Ladd and DeGroot 2003), the values of m obtained from the four stress paths were similar. The measured values for the m parameter (0.54 to 0.56) were smaller than the typical value of 0.8 (Ladd 1991, Jamiolkowski et al. 1985) for silt soils. Likewise, with one exception for RTE tests, the measured values for the S parameter (0.26 to 0.28) were larger than the typical value of 0.25 (Ladd 1991) for most silt soils. These findings were in agreement with Ladd (1991), which organic clays and silts had more scattered normalized shear strength than inorganic clays.

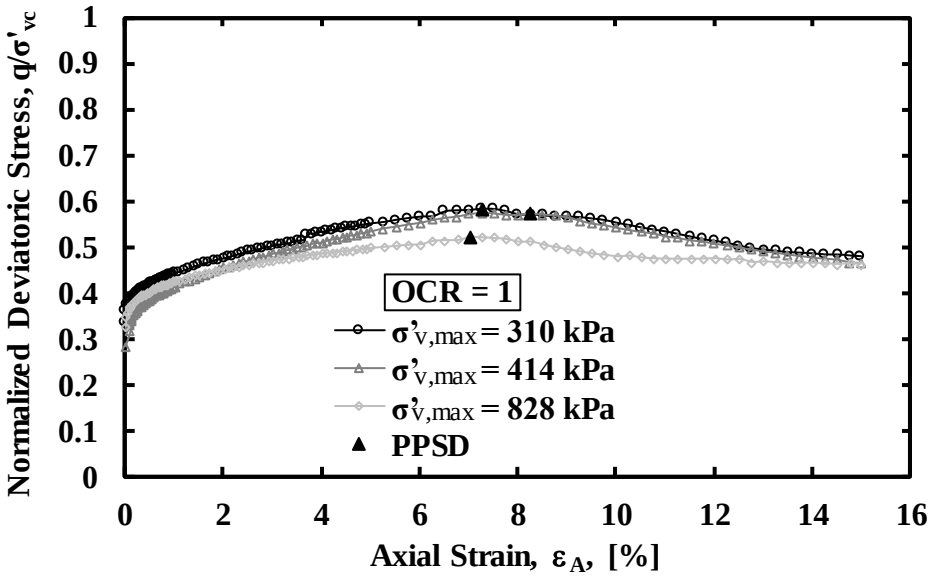

Figure 4.6. Normalized deviatoric stress, as a function of axial strain, for the TC tests at OCR=1.

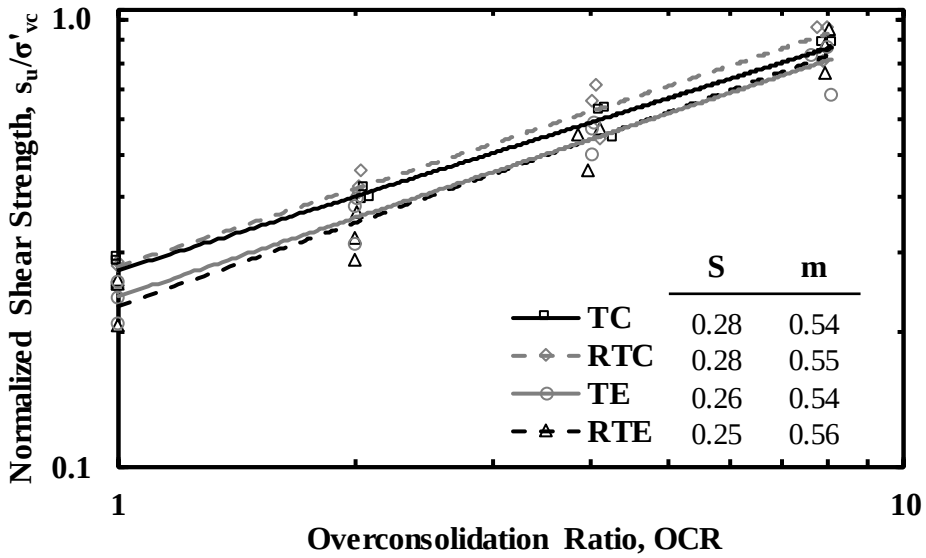

Figure 4.7. Normalized undrained shear strength values from the SHANSEP procedure.

The measured undrained shear strength values obtained from the compression tests were 11 to 38 percent greater than the undrained shear strength values obtained from the extension tests. As described by Bishop (1966), the lower values of the undrained strength that were obtained from the triaxial extension tests may be attributed to the difference in the amount of excess pore water pressure that developed during shearing. Overall, the normalized undrained shear strength values that were measured during the stress-controlled tests (i.e RTC and TE) were higher than those measured in strain-controlled tests (i.e TC and RTE). These higher values that were obtained from the stress-controlled tests may be attributed to the high rate of strain that developed during the shearing stage when the specimens yielded.

4.6.2. *Stress-Strain Relationships*

The deviatoric stress-axial strain curves for all of the tests are shown in Figure 4.8. The points of PPSD are also indicated for completeness. The same general shape of the stress-strain curves was observed for both the normally consolidated and overconsolidated specimens that were tested following the TC and RTE stress paths. The behavior was characterized by a peak deviatoric stress followed by postpeak strain softening. The pattern of failure for the RTC and

TE was similar to the TC and RTE stress paths, respectively, with higher magnitudes of deviatoric stress (q) and higher values of axial strain at failure $(\varepsilon_{A,f})$ being observed for the RTC

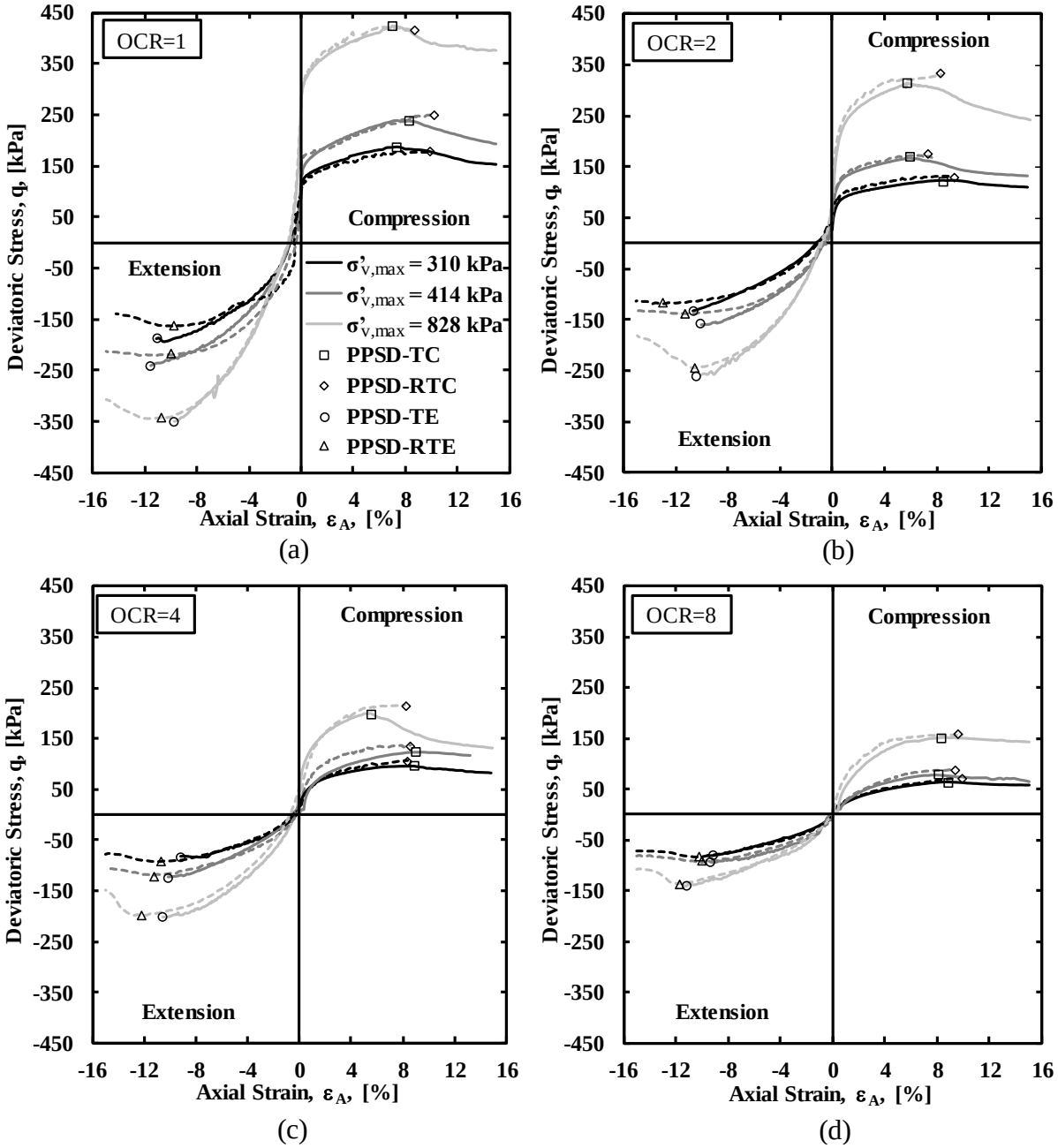

Figure 4.8. Variation of deviatoric stress as a function of axial strain for different stress paths: a) OCR= 1, b) OCR= 2, c) OCR= 4, d) OCR= 8.

tests. Because the RTC and TE tests were stress controlled, no postpeak stress-strain data were observed and no softening was observed. Generally, for each overconsolidation ratio, and each

stress path that was tested, the strain at failure tended to decrease as a function of increasing the amount of maximum consolidation stress. The overconsolidation ratio had an insignificant effect on the amount of axial strain at failure. As shown in the photographs presented in Figure 4. 9, postpeak shear planes were observed for all of the tests regardless of whether the soil was normally consolidated or overconsolidated. As reported by Burland (1990) and Atkinson et al. (1987), shear planes were observed to develop in one-dimensional consolidated kaolinite specimens.

(a) (b) (c) (d)

Figure 4.9. Photographs of the kaolinite samples after triaxial testing showing the failure planes associated with the: a) TC, b) RTC, c) TE, d) RTE stress paths for an OCR=1.

As presented in Figure 4.10, larger axial strain values were required for the extension tests to mobilize the peak resistance and the postpeak strain softening than were required for the mobilization to occur in the compression tests. The average values of the axial strain at failure $(\varepsilon_{A,f})$, for the extension tests, were between 0.3 and 5 percent greater than those for the compression tests. For the compression tests, the $\varepsilon_{A,f}$ values for the RTC tests were between 0.5 and 3.6 percent greater than the axial strain values at failure for the TC tests. For the extension tests, the $\varepsilon_{A,f}$ values for the RTE tests were between 0.1 and 2.4 percent greater than those for the TE tests. As described in the previous section, higher deviatoric stresses and axial strains, which

were obtained from the stress-controlled tests, may be attributed to the high rate of strain of the stress-controlled tests when the specimens yielded. This attribution was also documented in the results from the previous studies on stress rate effects (e.g., Bjerrum 1969, Sheahan 1991, Sheahan et al. 1996). From the aforementioned studies, the deviatoric stress at failure has been shown to decrease with the increasing strain rate.

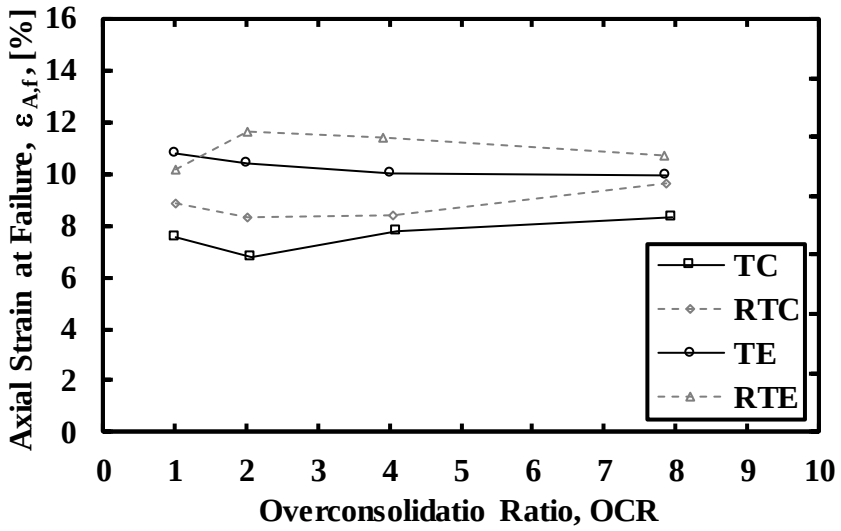

Figure 4.10. Average values of axial strain at failure for different stress paths, as a function of OCR.

4.6.3. *Young's Modulus*

The variations of undrained secant Young's modulus, as normalized to the vertical consolidation stress (E_u / σ'_{vc}), for the different stress paths, are presented in Figure 4.11. In this figure, the modulus relations for the extension tests were also plotted on the positive side of the axial strain axis to facilitate a comparison between the extension and compression test results. Because the axial strain was measured by employing conventional external measurements, the undrained Young's modulus values were only determined for axial strain levels above 0.1 percent. Based on the observed variations of the undrained Young's modulus, as a function of axial strain, 1) the soil exhibited non-linear behavior and 2) the stiffness significantly decreased near failure. Normalizable behavior of the Young's modulus relations was observed for the

normally consolidated specimens. For these specimens, at an axial strain level of 0.1 percent, the values of the normalized undrained Young's modulus for the extension tests were 2 to 2.5 times larger than the values of the normalized undrained Young's modulus for the compression tests. These values were in agreement with Atkinson et al. (1990), where the small strain stiffness was observed to increase as a result of the change in the direction of the stress path (from compression, during consolidation stage, to extension). Furthermore, the Young's modulus values that were obtained from tests conducted on the normally consolidated specimens, as determined from the compression tests, were consistently smaller than the Young's modulus values of the overconsolidated specimens.

For the overconsolidated specimens, the normalized modulus curves did not exhibit a normalized behavior. In addition, there was no clear trend of the modulus variations with the increase in the overconsolidation ratio. As described by Hardin and Blandford (1989) and Jamiolokwski et al. (1994), the initial undrained Young's modulus values were dependent on both the pre-shear effective consolidation stress and the overconsolidation ratio. For the overconsolidated specimens, as the overconsolidation ratio increased, the pre-shear effective consolidation stress decreased. Therefore, it was not a simple task to isolate the effect of the overconsolidation ratio from the effect of the pre-shear effective stress levels.

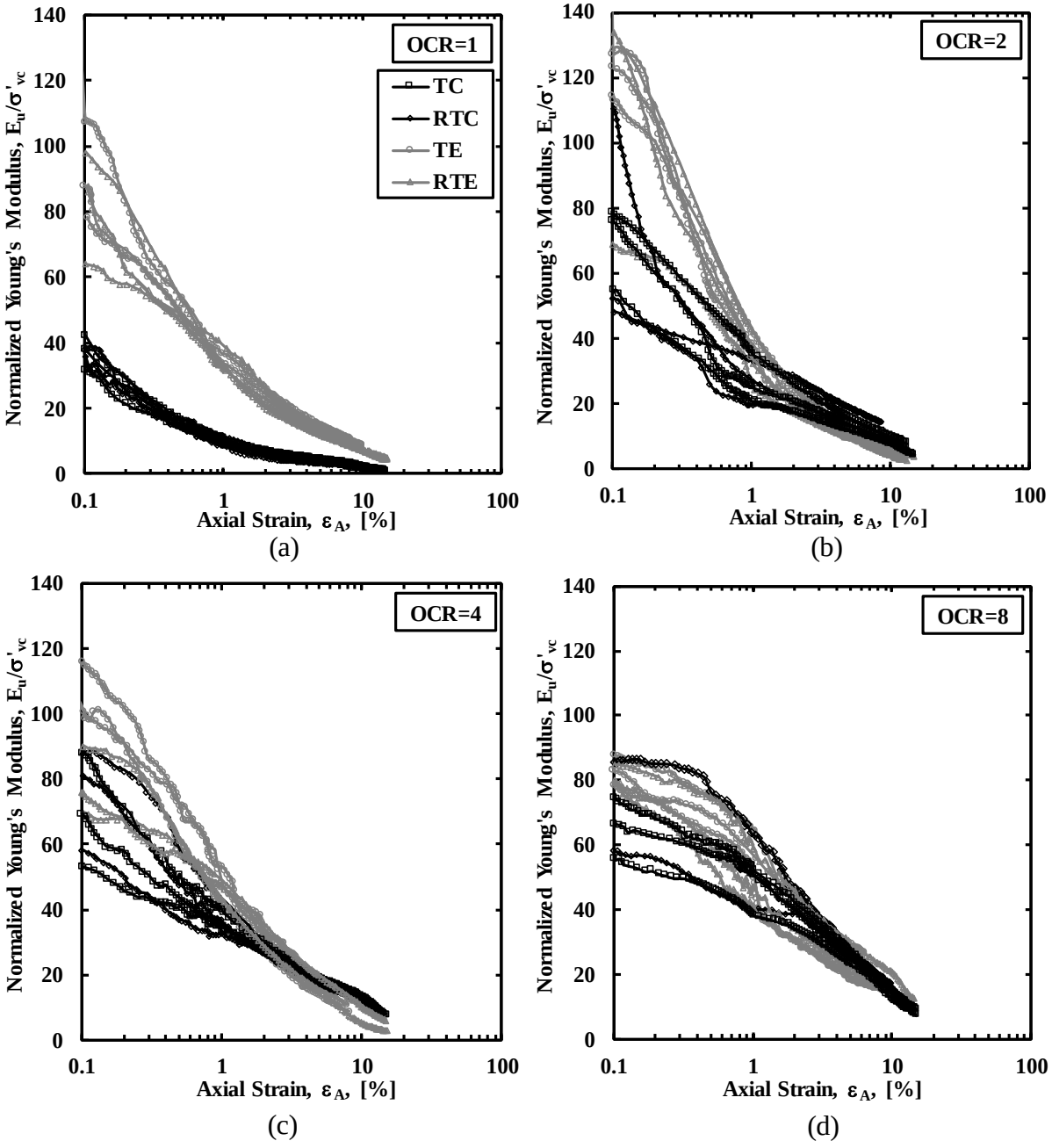

Figure 4.11. Normalized secant Young's modulus relations for: a) OCR= 1, b) OCR= 2, c) OCR= 4, and d) OCR= 8.

4.6.4. *Excess Pore Water Pressure Response*

The variations of excess pore water pressure (u_e), that were developed during shearing, as normalized to the vertical consolidation stress, for the different stress paths, are shown in Figure 4.12. Because the excess pore water pressure was generated by a combination of the

changes in the shearing stress and the changes in the mean total stress, the changes in excess pore water pressure that were developed during shear may not be considered as a unique behavior of the soil, under the applied stress path. The initial portion of the pore pressure response, for all of the stress paths, changed rapidly over small levels of axial strain. This rapid change in the excess pore pressure may also explain the shape of the effective stress paths for the normally consolidated (OCR=1) specimens that were previously presented in Figure 4.3.

For the TC tests that were performed on the normally consolidated specimens, the excess pore water pressure increased during the shearing stage (indicating contractive behavior) until the PPSD was reached and then the values dropped slightly. The excess pore water pressure values, for the TC tests that were conducted on the overconsolidated specimens, showed an initial contractive response and then the pore pressure response changed from a slightly contractive behavior to a slightly dilative behavior. For the stress-controlled RTC tests, where the shearing was associated with a decrease in the cell pressure, a sharp decrease in the amount of excess pore water pressure was observed without an initial contractive response.

An excess pore pressure response that was larger in magnitude than the response obtained from the TC tests was generated during the RTC tests. This difference in pore pressure response was because the shearing during RTC tests was associated with decreasing cell pressure. The general shapes of the variation of the shear induced pore water pressure, that were developed during the triaxial extension tests, were similar regardless of the induced amount of the overconsolidation. As observed by previous researcher, the shear stress-strain and strength characteristics were highly influenced by the shear induced pore water pressure (Skempton,1954, Ladd and DeGroot, 2003). Therefore, difference in the magnitude of the measured excess pore

water pressure during shear may have caused the slight variation of the stress-strain relationships that were obtained from the different stress paths (as shown previously in Figure 4.8).

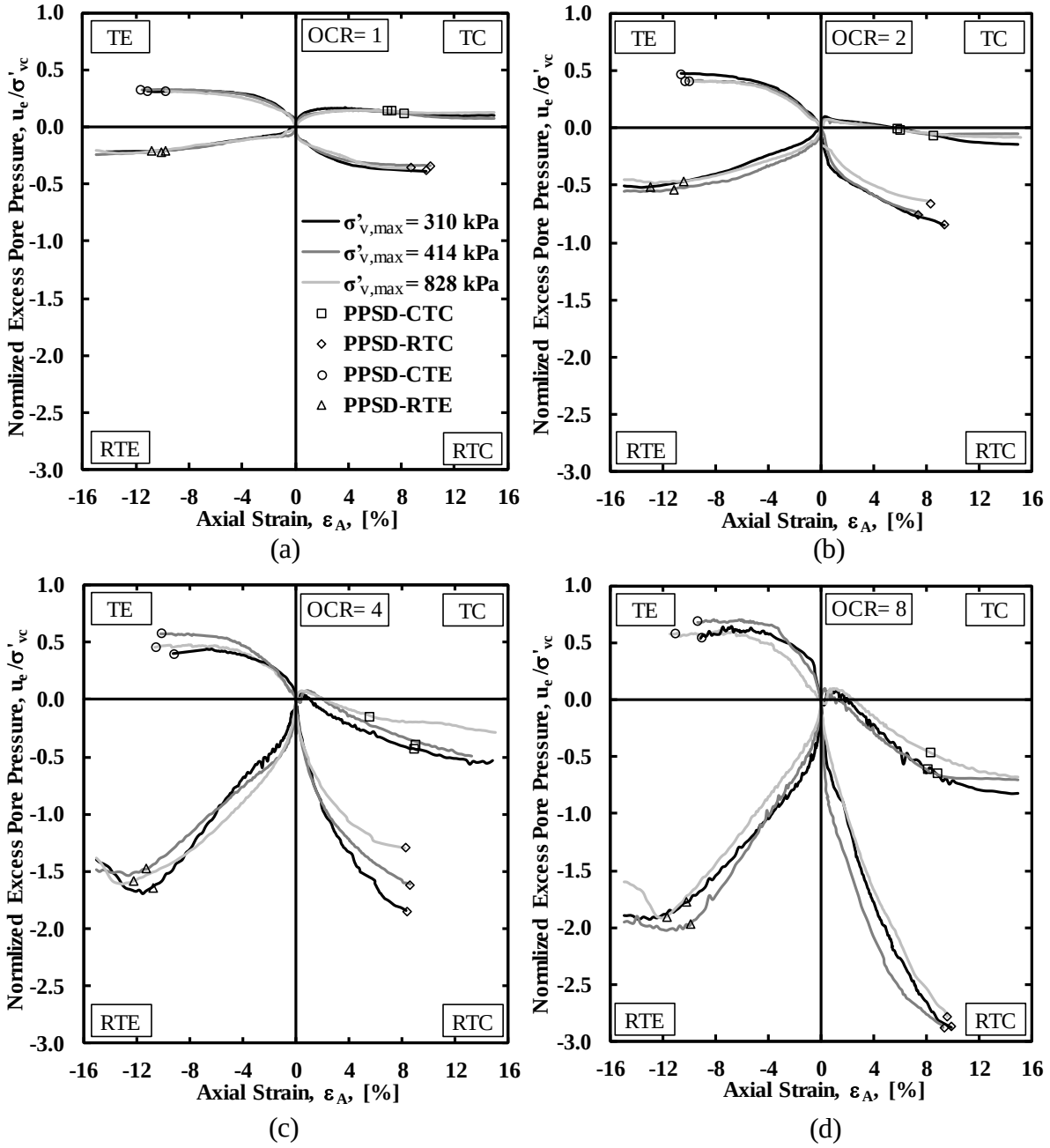

Figure 4.12. Normalized excess pore water pressure relations for: a) OCR= 1, b) OCR= 2, c) OCR= 4, and d) OCR= 8.

4.7. Implementations for Practice

As presented in the previous test results section, for the same orientation of the principal stress, the shear strength properties and failure conditions did not differ greatly regardless of which of the stress paths were utilized to shear the specimens. However, when the orientation of the principal stresses was altered, the corresponding stress paths were different. Even though the observed normalized excess pore pressure profiles were different between TC and RTC tests, geotechnical analyses conducted with shear strength values obtained from TC tests will not differ greatly from analyses based on the values obtained from RTC tests. Likewise, even though the observed normalized excess pore pressure profiles were different between TE and RTE tests, geotechnical analyses conducted with shear strength values obtained from TE tests will not differ greatly from analyses based on the values obtained from RTE tests. Both the effective and the undrained shear strength parameters were affected by the reorientation of the principal stresses. When comparing the results from the compression and extension tests, lower values of shear strain at failure and lower initial stiffness values were measured by the compression tests. Based on these results, if the TC or RTC tests were utilized to obtain shear strength values for a design where the TE or RTE were more representative of the field conditions, then the compression data overestimate the shear strength and lead to an unconservative design. Moreover, TE or RTE tests data will be essential to develop new constitutive models or to validate existing constitutive models that have previously been developed based on only TC or RTC data.

4.8. Conclusions

Undrained triaxial compression and triaxial extension tests were performed on kaolinite specimens to study the influence of the stress path on the corresponding shear strength properties. The specimens were reconstituted at values of water content that were slightly greater than the liquid limit. Based on the findings, similar stress-strain behavior was observed for the

stress paths that had the same orientation of the principal stresses. The stress-strain behavior, however, was found to be different when the orientation of the principal stresses was changed. In general, strength and deformation properties generated from the TC tests corresponded closely to those generated from the RTC tests. The same correspondence was also observed between TE test data and RTE test data. For simplicity and practicality, TC test results may be utilized when compression tests are required, and RTE test results may be utilized when extension tests are required. TC tests data should not be used when extension data are required for design. Likewise, RTE test results should not be used when compression data are required for design. These test types are recommended because strain-controlled testing is much easier to perform than the stress-controlled testing. Regardless of which test is utilized, an internal load cell should be used to measure the axial load to remove the effects of piston uplift and piston friction.

The reorientation of the principal stresses (from compression to extension) had significant effects on the effective and undrained shear strength properties. The measured values of ϕ' were lower for the extension tests than for the compression tests by approximately 20 to 35 percent. The obtained undrained shear strengths values that were collected from the compression tests were greater than those obtained from the extension tests by 11 to 38 percent. The amounts of axial strain at failure, as measured from the extension tests, were 0.3 to 5.0 percent greater than those as measured from the compression tests. The amount of the initial stiffness for normally consolidated specimens, as evaluated from the undrained secant Young's modulus values, were 2 to 2.5 times larger for extension tests than for compression tests. The variation in the undrained Young's modulus values for the overconsolidated specimens showed no obvious trend with the changes in stress path. Moreover, the initial portion of the excess pore water pressure response for all of the stress paths changed rapidly as a function of axial strain until the

yield point was reached. Therefore, any parameters that are utilized to characterize the shear strength of soil or to validate constitutive models should account for the dependence of the reorientation of the principal stress state.

4.9. References

American Society for Testing and Materials (2011). "Standard Test Method for Unconsolidated-Undrained Triaxial Compression Test on Cohesive Soils." Annual Book of ASTM Standards, Designation D4767, Vol. 4.08, ASTM, West Conshohocken, PA.

Atkinson, J. H., Richardson, D., and Robinson, P. J., (1987). "Compression and Extension of K_0 Normally Consolidated Kaolin Clay." Journal of Geotechnical Engineering, Vol.113. No. 12, pp. 1468-1482.

Atkinson, J.H., Richardson, D. and Stallebrass, S.E., (1990). "Effect of Recent Stress History on the Stiffness of Overconsolidated Soil." Geotechnique, Vol.40, No. 4, pp.531-540.

Bishop, A.W., and Henkel, D.J. (1962). "The Measurement of Soil Properties in the Triaxial Test." Edward Arnold LTD, London.

Bishop, A. W., (1966). "The strength of soils as engineering materials." Geotechnique, Vol. 16, pp. 91-130.

Bjerrum, L., Simons, N., and Toblaa, I., (1958). "The Effect of Time on the Shear Strength of a Soft Marine Clay." Proceedings of Conference on Earth Pressure Problems, I, pp.148-158.

Bryson, L. S., and Salehian, A. (2011). "Performance of Constitutive Models in Predicting Behavior of Remolded Clay." Acta Geotechnica, Vol. 6, No. 3, pp.143-154.

Burland, J. B., (1990). "On the Compressibility and Shear Strength of Natural Clays." Geotechnique 40 (3), 329-378.

Coffman, R. A., Bowders, J. J., and Burton, P. M., (2010). "Use of SHANSEP Design Parameters in Landfill Design: A Cost/Benefit Case Study." ASCE Geotechnical Special Publication No. 199, Proceedings GeoFlorida 2010, Advances in Analysis, Modeling and Design, West Palm Beach, FL, Feb 20–24, pp. 2859–2866.

Coffman, R.A., Salazar, S.E., Zhao, Y., (2014). "Discussion of Measurement of Stiffness Anisotropy in Kaolinite Using Bender Element Tests in a Floating Wall Consolidometer by X. Kang, G.-C. Kang, B. Bate." Geotech. Test. J. Vo. 37, No. 6, pp. 1-5.

Davis, E. H., and Poulos, H. G., (1972). "Rate of Settlement Under Two-and Three-dimensional Conditions." Geotechnique, Vol. 22, No. 1.

Davis, E.H. and Poulos, H.G., (1968). "The Use of Elastic Theory for Settlement Prediction under Three-dimensional Conditions." Geotechnique, Vol.18, No. 1, pp.67-91.

Duncan, J. M., and Seed, H. B., (1966). "Anisotropy and Stress Reorientation in Clay." Journal of the Soil Mechanics and Foundations Division, Vol. 92, No. 5, pp. 21-50.

Gens, A., (1983). "Stress-strain and Strength Characteristics of a Low Plasticity Clay." Doctoral dissertation, University of London, London, England.

Hardin, B.O. and Blandford, G.E., (1989). "Elasticity of Particulate Material." Journal of Geotechnical Engineering, Vol. 115, No. 6, pp.788-805.

Henkel, D.J. (1956). "The Effect of Overconsolidation on the Behavior of Clays During Shear." Geotechnique, Vol. 6, No. 4, pp.139-150.

Holtz, R. D., Kovacs, W. D., and Sheahan, T. C., (2011). "An Introduction to Geotechnical Engineering." 2nd Ed. Pearson Education, Upper Saddle River, NJ.

Jafroudi, S., (1983). "Experimental Verification of Bounding Surface Plasticity Theory for Cohesive Soils." Doctoral Dissertation, University of California, Davis, CA.

Jamiolkowski, M., Ladd, C.C., Germaine, J. and Lancellotta, R., (1985). "New Developments in Field and Lab Testing of Soils." Proceedings 11th Intl. Conference on Soil Mechanics and Foundations Engineering, San Francisco, Vol. 2, pp. 57-154.

Jamiolkowski, M., Lancellotta, R., and Lo Presti, D. C. F., (1995). "Remarks on the Stiffness at Small Strains of Six Italian Clays." Proceedings of the International Symposium, In Pre-Failure Deformation of Geomaterials, Sapporo, Japan, pp. 817-845.

Kulhawy, F. H., and Mayne, P. W., (1990). "Manual on Estimating Soil Properties for Foundation Design." Electric Power Res. Inst. EL-6800; Prof. 1493-6, Electric Power Research Inst., Palo Alto, CA, pp. 4-5.

Ladd, C.C, and Foott, R., (1974). "New Design Procedure for Stability of Soft Clays." Journal of Geotechnical Engineering Division." Vol. 100, No. 7, pp. 763-768.

Ladd, C. C., and DeGroot, D. J., (2003). "Recommended Practice for Soft Ground Site Characterization: Arthur Casagrande Lecture." In 12th Panamerican Conference on Soil Mechanics and Geotechnical Engineering Vol. 1, pp. 1-57.

Ladd, C. C., and Varallyay, J., (1965). "The Influence of Stress System on the Behavior of Saturated Clays During Undrained Shear." No. RR-R65-11. Massachusetts Institute of Technology, Cambridge Soil Mechanics Div.

Lade, P. V. (2005). "Overview of Constitutive Models for Soils." Soil constitutive models: Evaluation, selection and calibration, J. A. Yamamuro and V. N. Kaliakin, eds., ASCE, Reston, VA. pp 1-34.

Lambe, T. W. (1967). “Stress Path Method.” Journal of Soil Mechanics and Foundations Division,

Liu, Y. (2004). “The Stress-Strain Behavior of Kaolin Clay in Triaxial.” Ph.D. Thesis. University of Delaware. Newark, DE.

Moniz, Safia R., (2009). “The Influence of Effective Consolidation Stress on the Normalized Extension Strength Properties of Resedimented Boston Blue Clay.” MEng Thesis, MIT, Cambridge, MA.

Olson, R.E., (1962). “The ShearS properties of Calcium Illite.” Geotechnique, Vol.12, No. 1, pp.23-43.

Parry, R. H. G., (2004). “Mohr Circles, Stress Paths and Geotechnics.” Spon Press, London.

Parry, R.H.G. (1960). “Triaxial Compression and Extension Tests on Remolded Clay.” Geotechnique, Vol. 10, No. 4, pp. 160-188.

Parry, R.H.G. and Nadarajah, V., (1974). “Observations on Laboratory Prepared, Lightly Overconsolidated Specimens of Kaolin.” Geotechnique, Vol. 24, No. 4, pp.345-357.

Prashant, A. and Penumadu, D., (2005). “A Laboratory Study of Normally Consolidated Kaolin Clay.” Canadian Geotechnical Journal, Vol. 42, No. 1, pp.27-37.

Prashant, A., and Penumadu, D., (2007). “Effect of Microfabric on Mechanical Behavior of Kaolin Clay Using Cubical True Triaxial Testing.” J. Geotech. Geoenviron. Eng. Vol. 133, No. 4, pp. 433-444.

Race, M.L., Coffman, R.A., (2011). “Effects of Piston Uplift, Piston Friction, and Machine Deflection in Reduced Triaxial Extension Testing.” ASCE Geotechnical Special Publication No. 211, Proc. GeoFrontiers 2011: Advances in Geotechnical Engineering, Dallas, Texas, March, pp. 2649-2658.

Rossato, G., Ninis, N. L., and Jardine, R. J., (1992). “Properties of Some Kaolin-based Model Clay Soils.” Geotech. Test. J., Vol. 15, No. 2, pp.166-179.

Saada, A.S. and Bianchini, G.F., (1977). “Strength of One Dimensionally Consolidated Clays.” Journal of Geotechnical and Geoenvironmental Engineering, Vol. 103, (HGT-6), pp. 655-660.

Salazar, S. E. and Coffman, R. A., (2014). “Design and Fabrication of End Platens for Acquisition of Small-Strain Piezoelectric Measurements During Large-Strain Triaxial Extension and Triaxial Compression Testing.” Geotechnical Testing Journal, Vol. 37, No. 6, pp. 1-12.

Salazar, Sean E. and Coffman, Richard A., (2015). “Consideration of Internal Board Camera Optics for Triaxial Testing Applications.” Geotechnical Testing Journal, Vol. 38, No. 1, pp. 1–10.

Salazar, S.E., Miramontes, L.D., Barnes, A.R., Bernhardt, M.L., Coffman, R.A., (2017). "Verification of an Internal Close-range Photogrammetry Approach for Volume Determination During Undrained Triaxial Testing." Geotech. Test. J. (Under Second Review, Manuscript Number: GTJ-2017-0125-R1).

Scholey, G. K., Frost, J. D., Lo Presti, D. C. E, and Jamiolkowski, M. (1996). "A Review of Instrumentation for Measuring Small Strains During Triaxial Testing of Soil Specimens." Geotechnical Testing Journal, GTJODJ, Vol. 18, No. 2, pp. 137-156.

Sheahan, T. C. (1991). "An Experimental Study of the Time-dependent Undrained Shear Behavior of Resedimented Clay Using Automated Stress Path Triaxial Equipment." Doctoral dissertation, Massachusetts Institute of Technology, MA.

Sheahan, T.C., Ladd, C.C., and Germaine, J.T., (1996). "Rate-dependent Undrained Shear Behavior of Saturated Clay." Journal of Geotechnical Engineering, Vol. 122, No. 2, pp. 99-108.

Simons, N. E. and Som, N. N. (1970). "Settlement of Structures on Clay: with Particular Emphasis on London Clay." Construction industry research and information Association, London. Report 22.

Skempton, A. W. (1954) "The Pore-pressure Coefficients A and B." Geotechnique, Vol. 4, No. 4, pp.143-147.

Taylor, D. W., (1948). "Fundamentals of Soil Mechanics." John Wiley and Sons, New York, NY.

Tiwari, B., and Ajmera, B., (2011). "New Correlation Equations for Compression Index of Remolded Clays." Geotechnical and Geoenvironmental Engineering, Vol. 138, No. 6, pp. 757-762.

Wroth, C. P., (1984). "The Interpretation of in Situ Soil Tests." Geotechnique, Vol. 34, No. 4, pp. 449-489.

Wu, W., and Kolymbas, D., (1991). "On Some Issues in Triaxial Extension Tests." Geotechnical Testing Journal, Vol. 14, No. 3, pp. 276-287.

Zhao, Y., and Coffman, R.A., (2016). "Back-Pressure Saturated Constant-Rate-of-Strain Consolidation Device with Bender Elements: Verification of System Compliance." Journal of Testing and Evaluation, Vol. 44, No. 6, pp. 1-12.

Zhao, Y., Mahmood, N., and Coffman, R. A., (2017). "Soil Fabric and Anisotropy as Observed Using Bender Elements during Consolidation." Clays and Clay Minerals, Under Review, Manuscript Number: CCM-1143.

Zhao, Y., Mahmood, N. S., and Coffman, R.A., (2018). "Small-Strain and Large-Strain Modulus Measurements with a Consolidation Device." Journal of Testing and Evaluation, In Press, Manuscript Number: JTE-2016-0331.

CHAPTER 5: Intrinsic Shear Strength Behavior of Reconstituted Kaolinite and Illite Soils

5.1. Chapter Overview

The effect of slurry water content on the shear strength behavior of reconstituted soils was introduced and discussed. Specifically, undrained triaxial compression tests were performed on kaolinite and illite soil specimens to evaluate the relationship between the slurry water content values and the corresponding shear strength parameters. The influence of the slurry water content on the soil fabric and the compression behavior of the reconstituted soils was also introduced and discussed. A new method was proposed to normalize the undrained shear strength values of overconsolidated soils based on the concept of the intrinsic shear strength line. Using this proposed method, void index values were determined from the intrinsic swelling line rather than from the intrinsic compression line. Better correlation between the undrained shear strength values, for the overconsolidated specimens, and the intrinsic shear strength line was obtained by using the proposed normalization method. It was recommended to prepare soil slurries at water content of three times the corresponding liquid limit of the soil.

An introduction including the research description and summary is included as Section 5.1 through Section 5.3. A literature review of the intrinsic shear strength characteristics is included in Section 5.4. The materials and the experimental program are presented in Section 5.5. The results obtained from the triaxial tests are documented in Section 5.6. The paper enclosed in this chapter has been submitted within Quarterly Journal of Engineering Geology and Hydrogeology. The full reference is: *Mahmood, N. S., and Coffman, R. A., (2018a). "Intrinsic Shear Strength Behavior of Reconstituted Kaolinite and Illite Soils." Quarterly Journal of Engineering Geology and Hydrogeology, (In Review, Manuscript Number: qjegh2018-056-R1).*

5.2. Intrinsic Shear Strength Behavior of Reconstituted Kaolinite and Illite Soils

Nabeel S. Mahmood[1], Richard A. Coffman[2]

[1]MSCE, Graduate Research Assistant, Department of Civil Engineering, University of Arkansas, Fayetteville, Arkansas, USA. Instructor, University of Anbar, Ramadi, Iraq.
[2]PhD, PE, PLS, Associate Professor, Department of Civil Engineering, University of Arkansas, Fayetteville, Arkansas, USA.

5.3. Abstract

The initial water content that is utilized to reconstitute cohesive soils, into a slurry (w_s), may have significant effects on the compression and shear strength behavior of any given soil. The effects are due to the influence of the w_s on the soil fabric. A series of K_o-reconsolidated, undrained, triaxial compression tests were conducted on reconstituted kaolinite and reconstituted illite specimens to explore the relationship between w_s values and the corresponding shear strength characteristics. The soil specimens were created from a slurry mixture at two levels of w_s; w_s values of one and one-half (1.5) and three (3.0) times the corresponding liquid limit of each soil type were investigated. The intrinsic compression, swelling, and shear strength lines were established from the test results. When sheared from the same level of post consolidation vertical stress, the undrained shear strength values of the specimens with w_s values of 3.0 times the liquid limit were from five to 16 percent lower than those of the specimens with w_s of 1.5 times the liquid limit. The effective cohesion tended to increase by increasing the value of w_s. The values of the effective friction angle (ϕ') were found to be independent of the w_s values.

A new method is proposed herein to provide a better correlation between the normalized values of the undrained shear strength for overconsolidated specimens and the "intrinsic shear strength line." Using this proposed method, void index values were determined from the intrinsic swelling line rather than from the intrinsic compression line. As discussed herein, reconstituting a low plasticity kaolinite soil at w_s values of 1.5 times the liquid limit may not be appropriate for

evaluating of the intrinsic shear strength characteristics. However, the illite soil appeared to be less affected than kaolinite soil by an increase in the w_s values. These finding were based on the observed soil fabric and the undrained shear strength behavior.

Keywords: Reconstituted soils; Slurry water content; Intrinsic behavior; Triaxial testing; Stress path; Undrained shear strength

5.4. Background

Laboratory prepared specimens are often utilized to characterize the engineering behavior of natural soils. These prepared specimens basically prepared by mixing natural soil with water to form a slurry of the given soil. The slurry is often consolidated, in a slurry consolidometer, to a certain consolidation stress that is related to the in-site effective stress (Henkel 1956, Olson 1962, Burland 1990, Chandler 2000, Hong et al. 2013, Zhao et al. 2018, Mahmood and Coffman 2017). Previous studies (e.g., Olson 1962, Martin and Ladd 1978, Carrier and Beckman 1984) have shown that using different levels of slurry water content (w_s) to "remold" (Olson 1962) or "reconstitute" (Burland 1990) soil specimens will affect the mechanical behavior of these specimens due to the significant changes in the structure of the soil. This aforementioned soil structure is composed of "fabric", the pattern that is produced from particles shape and arrangement, and "bonding", the interparticle forces in the system. As per Lambe and Whitman (1969), clay partials may have a flocculated (random arrangement) structure or dispersed (parallel arrangement) structure.

The term "intrinsic" was introduced by Burland (1990) to describe specimens that were reconstituted at w_s values between one to one and one-half times the liquid limit (LL) of the given soil. Burland (1990) reported that the intrinsic properties of the reconstituted soils were inherent and independent of the soil structure. Furthermore, the compression curves for different

reconstituted clays prepared with w_s values of one and one-quarter (1.25) times the LL can be normalized by using the void index (I_v), as presented in Equation 5.1.

$$I_v = \frac{e - e^*_{100}}{e^*_{100} - e^*_{1000}} \qquad \text{Burland (1990)} \qquad \text{Equation 5.1}$$

where e^*_{100} and e^*_{1000} are the void ratio of the reconstituted clay that corresponded to vertical effective stress (σ'_v) levels of 100 and 1000 kPa, respectively. As described in Burland (1990), the normalized curves (in the σ'_v-I_v space) were expressed by using one unique curve called the intrinsic compression line (*ICL*). By using the I_v values and the *ICL*, Burland (1990) reported that shear strength and compressibility of reconstituted soils may be utilized as a reference framework for the corresponding intact natural soils.

It has been well documented that the stress-strain behavior of reconstituted soils was significantly affected by w_s values (e.g., Henkel 1962, Burland 1990 Allman and Atkinson 1992, Chandler 2000, Hong et al. 2013). As described by Olson (1962), slurried specimens that were prepared at w_s values less than or slightly above the LL exhibited shear strength characteristics that were similar to the typical characteristics of overconsolidated soils. Therefore, Olson (1962), suggested that slurry water content values of at least two times the LL should be utilized to prepare slurry samples. It has also been reported that the undrained shear strength of reconstituted soils decreased with increased levels of w_s (Chandler 2000, Hong et al. 2013, Al Haj and Standing 2015). Like the *ICL* that was introduced by Burland (1990), Chandler (2000) introduced the concept of intrinsic shear strength behavior to describe the relation between w_s and the undrained shear strength of the reconstituted soils (s^*_u). Specifically, Chandler (2000) followed a normalization procedure that was similar to that of Burland (1990). By using this procedure, the s^*_u values were normalized to I_v values that corresponded to vertical effective

stress values after consolidation and prior to shear (σ'_{vc}). The normalized line (in the s_u^*-I_v space) was defined by Chandler (2000) as the intrinsic strength line (IS_uL). The IS_uL was not unique for a given soil type, but the line was developed based on a single value of the undrained shear strength ratio (R_{su}^*) of 0.33. R_{su}^* was defined by Chandler (2000) as the ratio of the obtained s_u^* value to the corresponding σ'_{vc} value. A similar procedure was successfully utilized by Hong et al. (2013) to normalize the undrained shear strength values, as obtained from isotropically consolidated, undrained, triaxial tests that were conducted on an illitic soil.

Emphasis has been placed on the relationship between the compression properties and the slurry water content of the reconstituted soils (on the *ICL*). A relatively limited number of studies (e.g., Chandler 2000, Hong et al. 2013, Al Haj and Standing 2015) have investigated the correlations between the w_s and s_u^* values (on the IS_uL). Furthermore, based on the literature that was examined, a relationship between I_v and s_u^* values, as obtained from specimens that were overconsolidated during the triaxial test procedure, has not been previously evaluated.

5.5. Materials and Methods

Consolidated-undrained triaxial compression tests were performed on reconstituted kaolinite and illite specimens that were each reconstituted at two different levels of slurry water content (1.5 or 3.0 times the LL). The purpose of this experimental program was to evaluate and compare the intrinsic shear strength properties of the reconstituted kaolinite and illite specimens. Specifically, the triaxial tests were conducted at overconsolidation ratio (*OCR*) values of one and eight to evaluate the effect of the *OCR* on the intrinsic compression and intrinsic shear strength behavior of the reconstituted specimens. The materials and the experimental program are presented herein. Furthermore, the procedures that were followed to normalize the compression, swell, and undrained shear strength values are presented.

5.5.1. *Materials and Specimen Preparation*

A commercially available kaolinite soil (KaoWhite-S) from the Thiele Kaolin Company in Sandersville, Georgia was utilized in this study. Likewise, an illite soil, as obtained from the Knight Hawk Coal Company of Percy, Illinois, was also utilized in this study. The index properties of the kaolinite and illite soils are summarized in Table 5.1. Shear strength, consolidation, and small-strain modulus properties of these two types of soils have been previously studied at the University of Arkansas 1) to determine the parameters of these soils and 2) to provide the input data for numerical modeling purpose (Zhao and Coffman 2016, Zhao et al. 2017, Mahmood and Coffman 2017, Zhao et al. 2018). The kaolinite and illite soils were classified, according to the Unified Soil Classification System (ASTM D2487, 2011), as Low Plasticity Silt (ML) and Low Plasticity Clay (CL), respectively.

Table 5.1. Properties of kaolinite and illite soils.

Property	Kaolinite	Illite
Liquid limit	31.5	46.7
Plastic limit	28.1	23.6
Clay size fraction (<0.002 mm)	47.2	46.5
Specific gravity, G_s	2.67	2.69

The kaolinite and illite slurries were formed by mixing the dry powdered soils with de-ionized, de-aired, water. The slurry preparation procedure followed the laboratory preparation method that was reported in Zhao and Coffman (2016), Zhao et al. (2017), and Zhao et al. (2018). Each soil type was prepared at water content values of one and one-half times the liquid limit (w_s = 1.5LL) and three times the liquid limit (w_s = 3LL) of the corresponding soil type. Each slurry was then preconsolidated in a double drained, 3.81 cm inside diameter slurry consolidometer. The soil slurry inside the consolidometer was subjected to a constant vertical stress of 207 kPa that was applied to the slurry specimens by means of static weight. After primary consolidation was completed in the slurry consolidometer, two specimens, each with a

length to diameter ratio of two, were extruded from each consolidometer and then mounted into the triaxial cells. The length, diameter, and mass of each of the specimens were measured and reported prior to mounting the specimens into the triaxial cell. To examine the influence of the w_s level on the fabric of the prepared specimens, scanning electron microscope images were measured on each type of the specimens extruded from the slurry consolidometer.

5.5.2. *Normalization Procedures*

To evaluate the intrinsic compression behavior of the prepared specimens, the compression curves were normalized by the void index, by using Equation 5.1, as previously presented. The values of e^*_{1000} were estimated by extrapolating the virgin compression line of the compression curves to vertical effective stress values of 1000 kPa. The intrinsic compression lines of the two soils were then compared with the *ICL* proposed by Burland (1990), as presented in Equation 5.2.

$$I_v = 2.45 - 1.285 \log \sigma'_v + 0.015 (\log \sigma'_v)^3 \qquad \text{Burland (1990)} \qquad \text{Equation 5.2}$$

Similar procedure was used to normalize the swell curves. Values of void ratio during swelling were used in Equation 1, as previously presented, to determine the I_v values. The normalized swell curve for each soil (in the σ'_v-I_v space) was referred as the intrinsic swelling line (*ISL*). The propose of the developed *ISL* was to explore a more representative procedure to normalize the undrained shear strength values for specimens that were overconsolidated during the triaxial tests.

To represent the undrained shear strength values of the overconsolidated specimens as a function of I_v, two procedures were followed to determine the I_v values that corresponded to the σ'_{vc} values. In the first procedure, the I_v values were determined by following the same steps that were suggested by Chandler (2000) to develop the IS_uL of normally consolidated specimens. As

presented in Figure 5.1, Chandler (2000) used the void index from the *ICL* (I_{ICL}) at the corresponding level of σ'_{vc}. In the second procedure, the relationship between the undrained shear strength values, for the overconsolidated specimens, and the I_v values were determined by utilizing the *ISL* for each specimen. Specifically, for each specimen, the void index was determined from the *ISL* (I_{ISL}) at the corresponding level of σ'_{vc}.

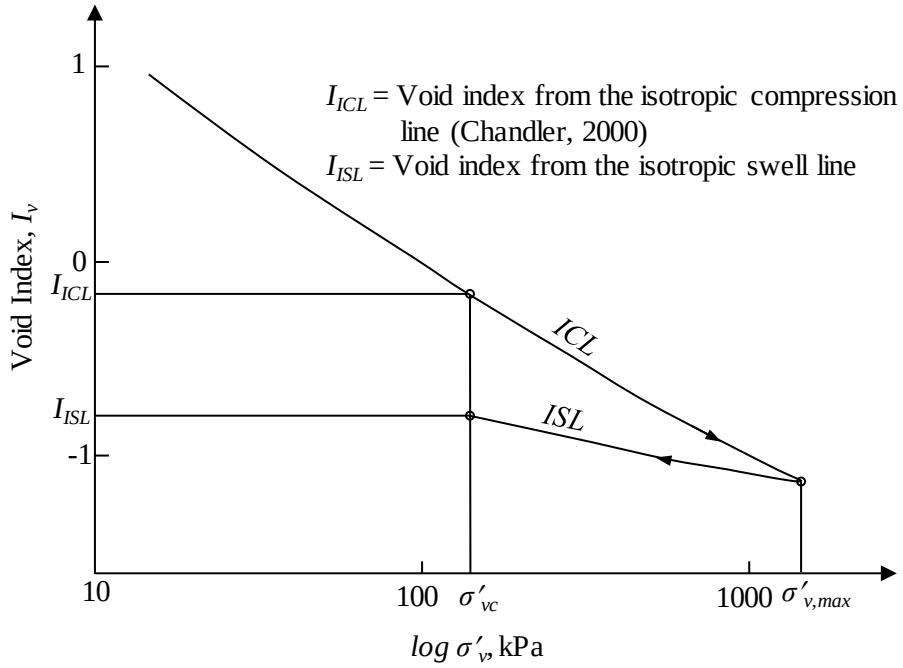

Figure 5.1. A schematic illustration of the determination of I_v values, corresponded to the σ'_{vc} value, from the ICL and from the ISL.

5.5.3. *Testing Methods*

A series of K_o-consolidated, undrained, triaxial compression tests, with pore water pressure measurements ($\overline{CK_oUTC}$), were performed on the aforementioned slurry consolidometer prepared specimens by utilizing advanced triaxial equipment. The triaxial tests were conducted in accordance with ASTM D4767 (2011). The individual specimens were mounted within the triaxial chamber using the wet preparation method, as described in ASTM D4767 (2011). The top and bottom platens of the triaxial device were instrumented with piezoelectric transducers that were

developed at the University of Arkansas (Salazar and Coffman 2014) to investigate the small-strain properties of the specimens (small-strain data are not included within this paper). After the back pressure saturation stage of the test was completed, each specimen was reconsolidated, under the K_o-condition, to the required maximum vertical effective stress.

To investigate the influence of the vertical effective stress on the undrained shear strength, the specimens were reconsolidated and then overconsolidated according to the reconsolidation procedure that was similar to the procedure recommended by Ladd and Foott (1974). Three different levels of maximum vertical effective stress ($\sigma'_{v,max}$), equal to 310, 414, or 828 kPa, were utilized to reconsolidate each of the previously prepared specimens. The aforementioned $\sigma'_{v,max}$ levels represented one and one-half, two, and four times the vertical effective stress value that was used to preconsolidate the slurries within the slurry consolidometer. After the required $\sigma'_{v,max}$ level was reached, the overconsolidated specimens were allowed to swell under K_o-conditions to achieve an *OCR* value of eight prior to shear. The K_o values were measured for the specimens during the consolidation and the over-consolidation processes. After consolidation for the normally consolidated specimens and overconsolidation for the overconsolidated specimens, the specimens were sheared at axial strain rate of 0.5 percent per hour under undrained conditions. A total of 24 triaxial tests were performed (12 tests were performed for each soil type).

5.6. Results and Discussion

The effect of the w_s values on 1) the fabric of laboratory prepared kaolinite and illite soil types and 2) on the engineering behavior of these soils during the performed undrained triaxial compression tests, are discussed herein. Specifically, four main findings are presented and discussed: 1) soil fabric, 2) the characteristics of the compression and swell behavior, 3) the

effective shear strength parameters, and 4) the undrained shear strength behavior. The findings are also compared with information from the literature. For simplicity, the specimens that were prepared from slurries at w_s =1.5LL and w_s =3LL, are hereinafter referred to as K1.5LL and K3LL for kaolinite, respectively, and as I1.5LL and I3LL for illite, respectively. Likewise, the NC and OC terms were added to indicate if the triaxial test was performed on normally consolidated or overconsolidated soil, respectively. A summary of the measured initial soil properties and the triaxial test results is presented in Table 5.2. As is common, and as was previously presented in this manuscript, the asterisk was used, throughout the paper, to identify the intrinsic parameters for the reconstituted soils.

5.6.1. *Soil Fabric*

The typical soil fabric of the reconstituted kaolinite and illite soils, as observed using the scanning electron microscope images, is presented in Figure 5.2. Visual examination of these images indicated that the fabric of the kaolinite specimens was affected by an increased level of w_s. The fabric of the kaolinite specimens at w_s = 3LL was more homogenous than the fabric of the kaolinite specimens at w_s =1.5LL. The fabric of the kaolinite specimens with lower w_s was characterized by more open and randomly aggregated areas. For the kaolinite specimens at w_s=3LL and for the illite specimens at both values of w_s (1.5LL and 3LL), the observed fabrics were well-oriented; these fabrics were similar to the typical fabric observed for one-dimensional, normally consolidated, flocculated, clays that were reported in Cotecchia and Chandler (1997) and Fearon and Coop (2000).

Table 5.2. Summary of initial physical soil properties and triaxial tests values.

Soil	*Specimen*	$\frac{w_s}{LL}$	*OCR*	$\sigma'_{v,max}$ *[KPa]*	w_o *[%]*	γ_T *[kN/m^3]*	e_o	R^*_{su}	s^*_u *[kPa]*
Kaolinite	K1.5LL-NC	1.5	1	310	31.4	18.0	0.89	0.299	92.7
				414	31.4	18.0	0.90	0.286	118.3
				828	30.6	18.1	0.88	0.256	212.1
Kaolinite	K3LL-NC	3	1	310	38.7	17.4	1.07	0.277	85.8
				414	38.3	17.4	1.06	0.238	98.6
				828	39.0	18.0	1.00	0.241	199.7
Kaolinite	K1.5LL-OC	1.5	8	310	31.3	17.6	0.93	0.871	31.7
				414	31.2	18.0	0.89	0.782	39.1
				828	31.7	18.0	0.90	0.756	75.8
Kaolinite	K3LL-OC	3	8	310	37.5	17.6	1.01	0.782	30.4
				414	38.4	17.9	1.00	0.671	37.3
				828	39.0	18.1	0.99	0.763	73.7
Illite	I1.5LL-NC	1.5	1	310	37.7	17.9	1.00	0.253	78.5
				414	35.2	17.6	0.99	0.312	128.9
				828	35.8	17.4	1.03	0.285	235.4
Illite	I3LL-NC	3	1	310	42.6	17.0	1.17	0.225	69.9
				414	42.1	17.0	1.16	0.286	118.5
				828	42.6	17.0	1.18	0.270	223.3
Illite	I1.5LL-OC	1.5	8	310	37.0	16.9	1.11	1.663	64.2
				414	36.6	17.5	1.02	1.752	90.6
				828	35.9	17.7	0.99	1.570	131.9
Illite	I3LL-OC	3	8	310	40.1	17.0	1.13	1.592	61.5
				414	39.8	17.1	1.12	1.654	85.5
				828	42.6	17.0	1.18	1.580	133.1

w_o, γ_T, e_o are initial water content, total unit weight, and initial void ratio of the specimens after being removed from the slurry consolidometer following preconsolidation, respectively.

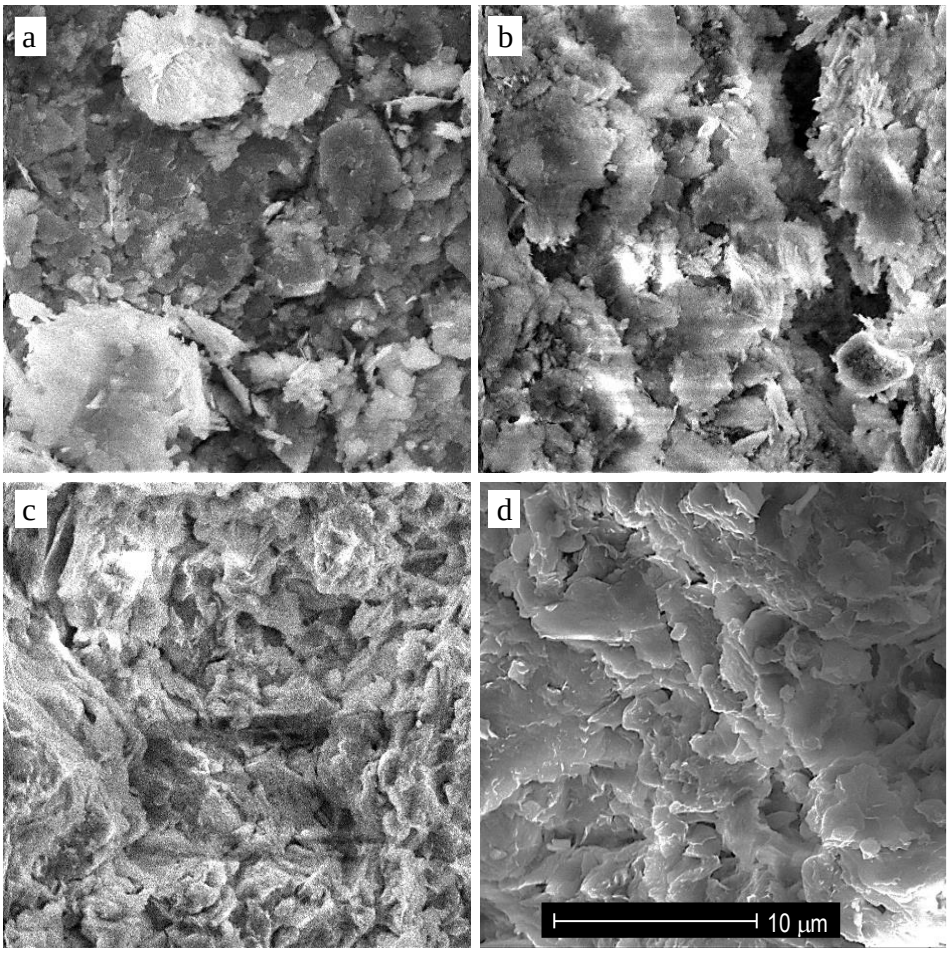

Figure 5.2. Scanning electron microscope images of the reconstituted soils: a) kaolinite, w_s=1.5LL, b) kaolinite, w_s=3LL, c) illite, w_s=1.5LL, d) illite, w_s= 3LL.

5.6.2. *Characteristics of the Compression and Swell Behavior*

The typical compression and swelling curves for the kaolinite and illite specimens are shown in Figure 5.3. The two soils followed similar patterns during the compression and swelling stages. The shape of the compression curves was similar to the typical shape of other compression curves for medium to stiff natural clays (Cotecchia and Chandler, 1997). However, the shape of the observed curves was in disagreement with the generally observed shape from oedometer obtained curves from reconstituted soils (Burland 1990, Hong et al. 2010, Tiwari and Ajmera 2011, Yin and Miao 2013, Al Haj and Standing 2015). The shape of the compression curves that was observed by these aforementioned previous studies on reconstituted soils tended

to be slightly concave upward, in a pattern similar to that for soft clay soils. There were marked differences in the size of the specimens, the loading rate, and the lateral confinement between the triaxial tests in this study and the oedometer tests from the previous studies. The measured curves from the triaxial tests in this study matched those obtained from the constant rate-of-strain consolidation test performed by Zhao and Coffman (2016). Similar to the observations that were documented by Zhao and Coffman (2016), both the initial void ratio and the compression behavior were highly affected by the water content of the slurry. The compression curves of the specimens with a higher slurry water content (w_s =3LL) lied above the compression curves of the specimens with a lower slurry water content (w_s =1.5LL). This observation also matched the observations from other previous studies (e.g. Carrier and Beckman 1984, Cerato and Lutenegger 2004, Hong et al. 2010) in which it was determined that increasing the water content of the slurry tended to increase the initial void ratio and to increase the compressibility of the reconstituted clays for a given change in the vertical effective stress values.

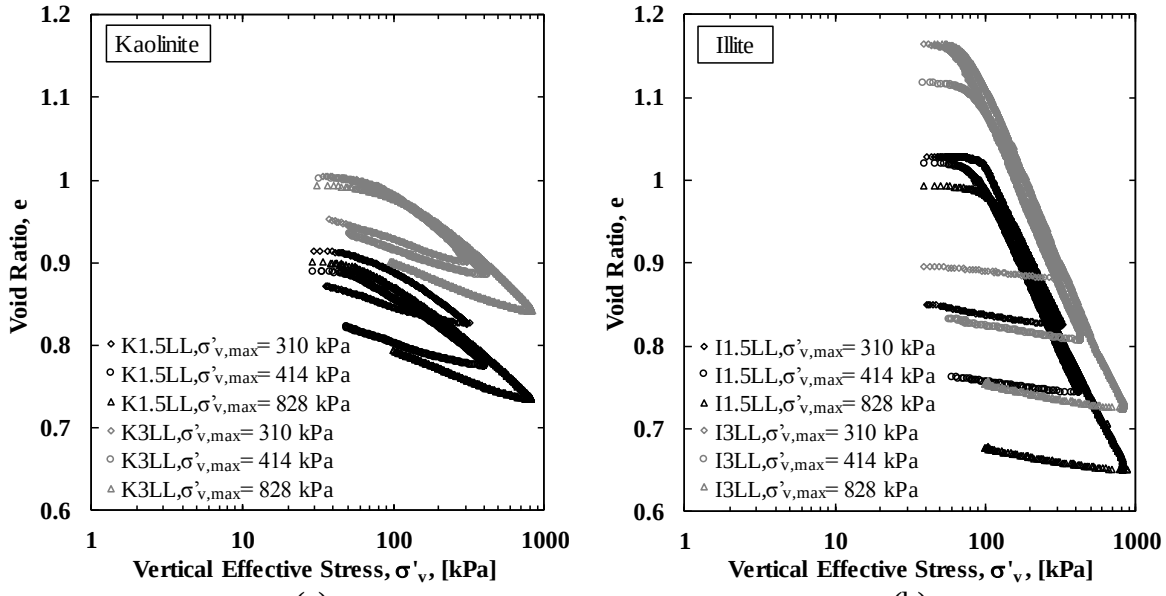

(a) (b)

Figure 5.3. Typical compression and swelling curves for: a) kaolinite, and b) illite soil specimens.

In general, the illite specimens were more compressible than the kaolinite specimens, as shown by higher measured values of intrinsic compression index, C_c^* (the slope of the linear portion of the loading curves). The average measured value of the C_c^* parameter was 0.15 for kaolinite and 0.40 for illite. The average measured value of the intrinsic swelling index, C_s^* (the slope of the linear portions of the unloading curves) was higher for kaolinite (0.032) than for illite (0.011). This observation, of the C_s^* value being greater for kaolinite than for illite, may imply that the illite specimens were more structured than the kaolinite specimens and, therefore, the bonding reduced the amount of swelling (Gasparre and Coop 2008). Furthermore, the difference between the void ratio of the compression curves for the illite soil tended to decrease with increased levels of the applied vertical effective stress. As described by Cerato and Lutenegger (2004) and Hong et al. (2013), the difference in the compression behavior between kaolinite and illite may be attributed to the difference in the mineralogical compositions.

As shown in Figure 5.4, the intrinsic compression lines that were obtained for the two soils exhibited similar behavior as the *ICL* that was obtained by using Equation 5.2, as previously presented. Based on a comparison of the results that are shown in Figure 5.4, the *ICL* that was proposed by Burland (1990) may be applicable for specimens that are reconstituted at w_s values of up to three times the liquid limit of the soil. Moreover, based on a comparison of the intrinsic compression lines of the kaolinite soil to the Burland (1990) *ICL*, the Burland (1990) *ICL* equation may be applicable for low plasticity silts. The swell curves that were normalized by using the parameter I_v are also presented in Figure 5.4. The swell curves seem to be more of a function of soil type; the slope of the normalized swelling curves was steeper for kaolinite soil type than for illite soil type.

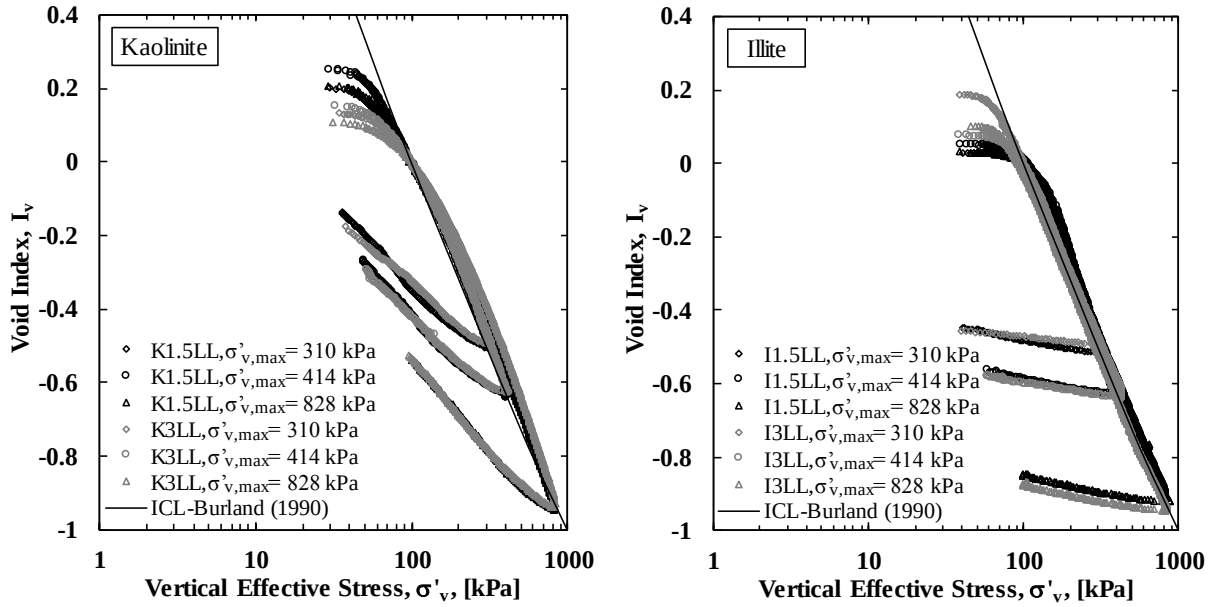

Figure 5.4. Variation void index, as a function of vertical effective stress, for the laboratory prepared: a) kaolinite, and b) illite soil specimens.

5.6.3. *Effective Shear Strength Parameters*

Effective stress paths, for the normally consolidated and for the overconsolidated specimens, are shown in Figure 5.5. The effective stress paths were represented in terms of Cambridge mean effective stress (p') and deviatoric stress (q), as presented in Equations 5.3 and 5.4, respectively.

$$p' = \frac{\sigma'_a + 2\sigma'_c}{3} \qquad \text{Equation 5.3}$$

$$q = \sigma'_a - \sigma'_c \qquad \text{Equation 5.4}$$

Within Equations 5.3 and 5.4, σ'_a and σ'_c were the effective axial stress and the effective confining pressure, respectively. For the same types of specimens that were sheared at different levels of vertical effective stress, the effective cohesion (c') and the effective friction angle (ϕ') values were determined from the failure envelopes that were plotted through the peak principal stress difference (PPSD) value that was observed for each stress path.

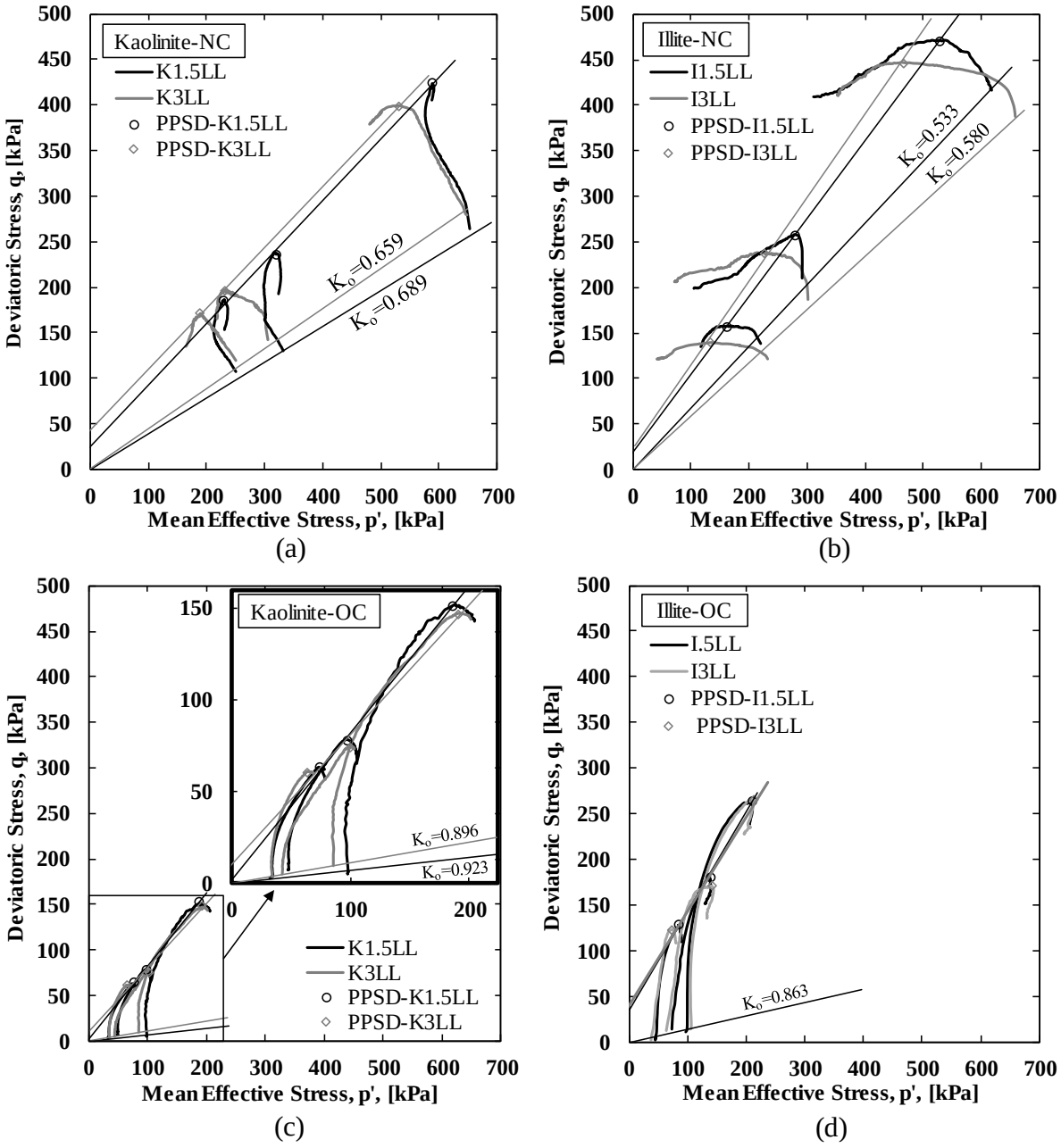

Figure 5.5. Cambridge effective stress paths for the triaxial compression tests performed on the reconstituted kaolinite and illite specimens: a) kaolinite-NC, b) illite-NC, c) kaolinite-OC, d) illite-OC.

For the normally consolidated K1.5LL specimens, the effective stress paths initially decreased in p' (indicating contractive behavior), but before reaching the failure envelope, the p' values began to increase and the stress paths changed directions (dilative behavior) until the PPSD was reached. All of the other normally consolidated specimens (K3LL, I1.5LL, and I3LL)

followed stress paths that were characterized by contractive behavior from the beginning of the shearing stage. The contractive behavior was observed to be greater for the illite specimens.

The effective stress paths for the kaolinite and illite overconsolidated specimens followed the typical behavior of overconsolidated soils during the shearing stage. The stress paths increased in p' (indicating dilative behavior) then bent downward after reaching the PPSD. The pattern of behavior, during shearing of the normally consolidated K1.5LL, was different from the typical behavior that has been observed for normally consolidated soils (Mitchell and Soga 2005). However, similar behavior has been previously reported for the reconstituted soils (e.g., Parry 1960, Olson 1962, Mahmood and Coffman 2017).

The deviatoric stress-axial strain curves for all the triaxial tests are presented in Figure 5.6. Except for the overconsolidated K3LL, the same general shape of deviatoric stress-axial strain curves was observed for all the specimens during the shearing stage. The behavior was characterized by an increase in the deviatoric stress until a peak, followed by strain softening behavior. This behavior was similar to the typical behavior of overconsolidated clays, as described by Mitchell and Soga (2005). Furthermore, at high levels of axial strain, the stress-strain curves of the specimens with lower values of w_s tended to converge with the curves for the specimens with higher values of w_s. Postpeak shear planes were observed to develop during shearing within both the normal consolidated specimens and the overconsolidated specimens, regardless of the w_s values. These planes may explain the peak deviatoric stress values that were observed for the normally consolidated specimens, which might not otherwise be expected for the normally consolidated specimens. Similar findings regarding the stress-strain behavior of one-dimensionally, normally consolidated, reconstituted clays were reported by Atkinson et al. (1987) and Burland (1990).

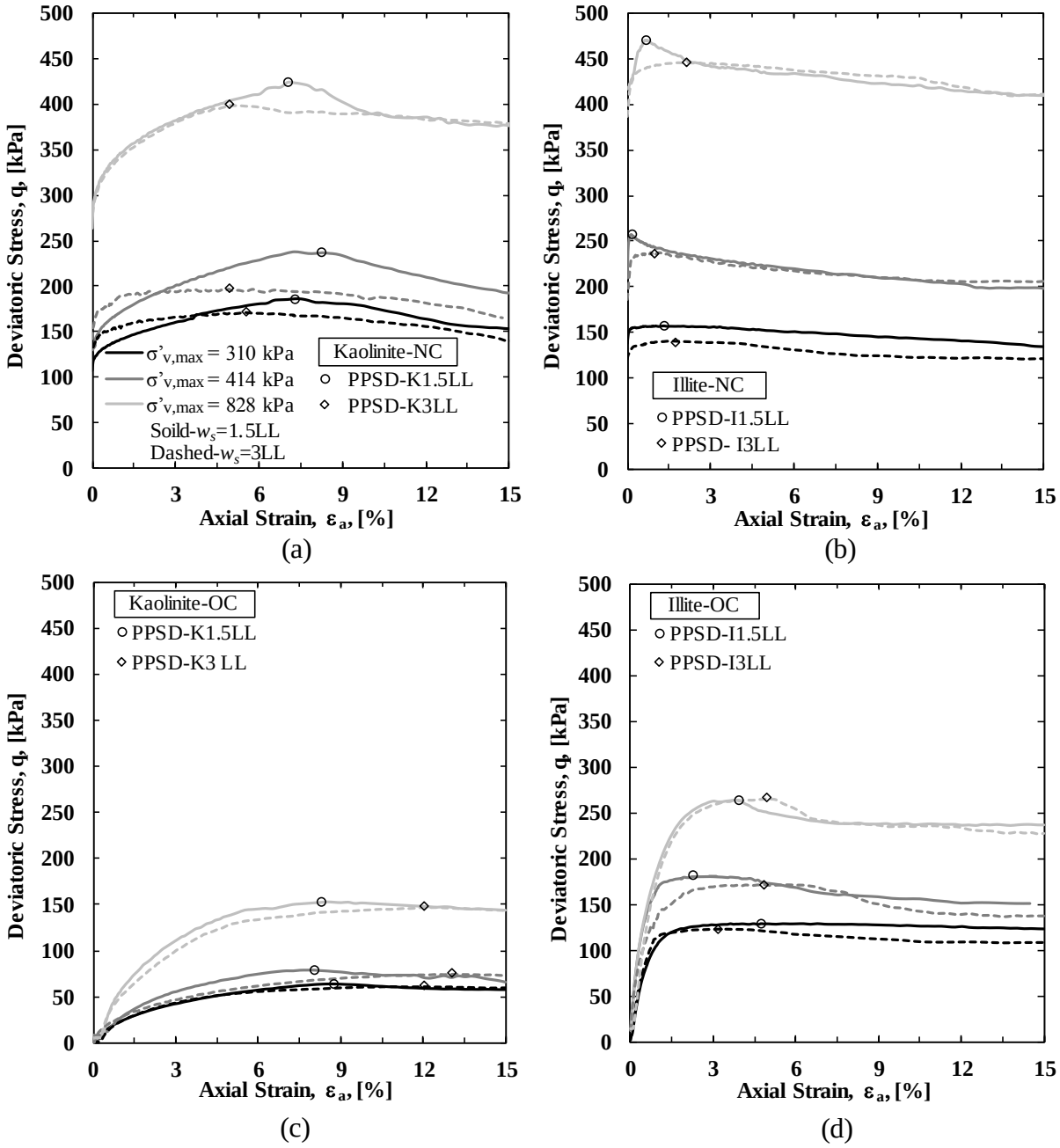

Figure 5.6. Variation of deviatoric stress, as a function of axial strain, for the reconstituted kaolinite and illite specimens: a) kaolinite-NC, b) illite-NC, c) kaolinite-OC, d) illite-OC.

The illite specimens reached failure at lower levels of the axial strain when compared to the levels of the axial strain at which the kaolinite specimens reached failure. For specimens prepared at w_s =1.5LL, the values axial strain at failure $(\varepsilon_{a,f})$ were from 0.2 to 4.7 percent for the illite specimens and from 7.1 to 8.7 percent for the kaolinite specimens. Likewise, for the

specimens with w_s =1.5LL, the $\varepsilon_{a,f}$ values were from 0.9 to 4.8 percent for the illite specimens and from 4.9 to 13.0 percent for the kaolinite specimens. The low levels of the axial strain at failure for the illite specimens may support the claim that the illite specimens were more "structured" than the kaolinite specimens. This was in agreement with a description of the typical behavior of structured soils that has been presented in the literature (e.g., Coop et al. 1995, Kavvadas and Amorosi 2000). Larger values of $\varepsilon_{a,f}$ were observed for the overconsolidated specimens, which may be attributed to the lower level of vertical effective stress that was applied to these specimens as compared to the level of the vertical effective stress that was maintained on the normally consolidated specimens.

Variations within the measured excess pore water pressure (u_e), as normalized by the vertical consolidation stress for the different stress paths, are presented in Figure 5.7. For the triaxial tests that were conducted on the NC specimens, the shear induced excess pore water pressure values of the K1.5LL and I1.5LL specimens were consistently smaller than the shear induced excess pore water pressure values of the K3LL and I3LL specimens, respectively. For the NC specimens, the excess pore water pressure continued to increase (contractive behavior) during the shearing stage, with the exception of the K1.5LL specimens. For the K1.5LL specimens, the excess pore water pressure values initially increased, in the same manner as the other NC specimens, and then the values decreased slightly before the PPSD was reached. The observed "strong" contractive behavior for the NC I3LL specimens, as observed from the pore water pressure response that was also observed from the shape of the stress path, may be attributed to the "rigid body sliding" following the formation of the shear planes (Burland 1990). An initial contractive behavior was observed, from the excess pore water pressure response, for all of the overconsolidated specimens then the excess pore pressure response changed to that of a

dilative behavior. The differences in the magnitude of the shear induced excess pore water pressure values that were observed during shearing may explain the variation in the shape of the effective stress paths that were previously described and presented in Figure 5.5.

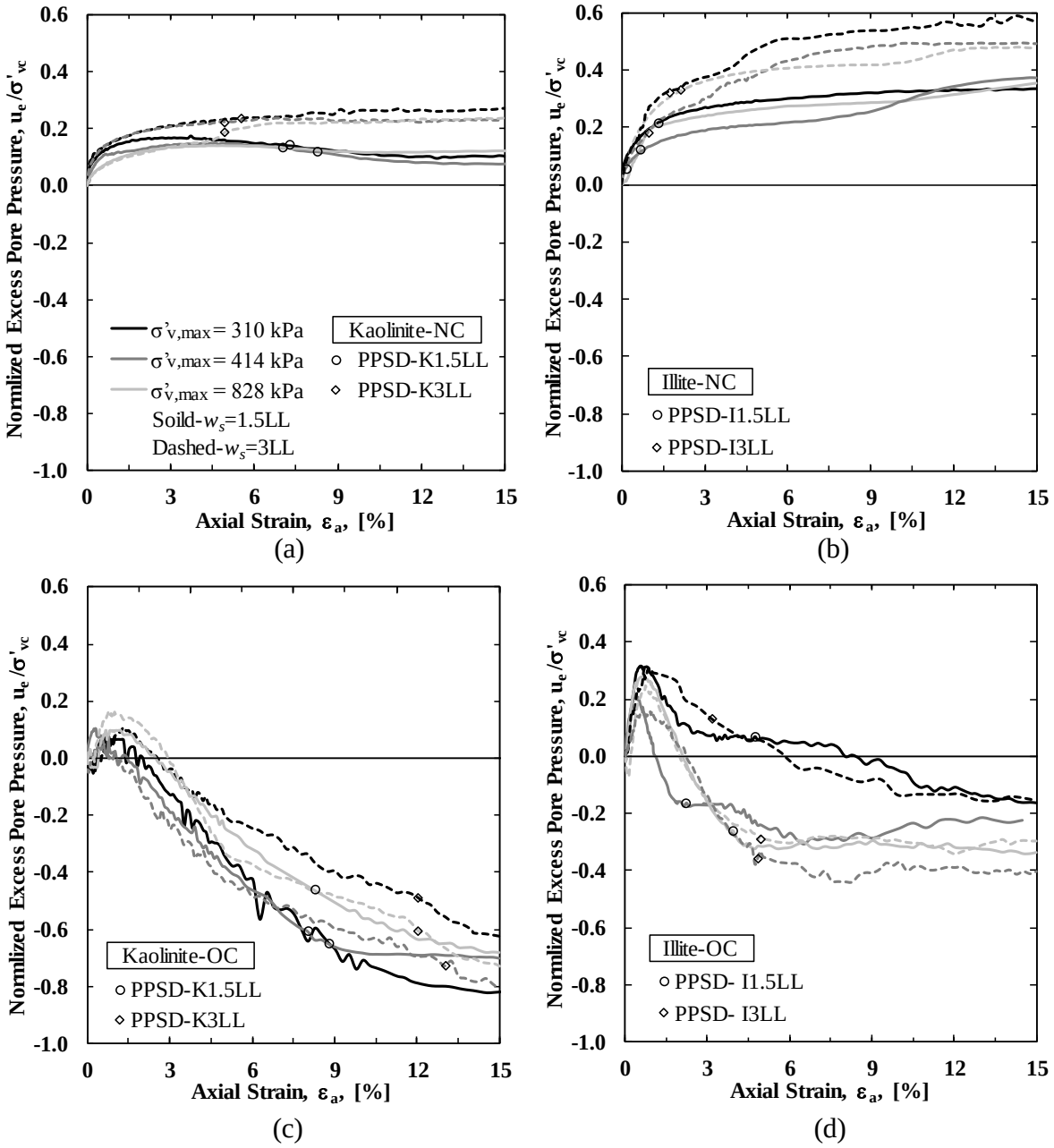

Figure 5.7. Normalized excess pore water pressure relationships for: a) kaolinite-NC, b) illite-NC, c) kaolinite-OC, d) illite-OC.

The variations of the c' and ϕ' values, as a function of the slurry water content, are shown in Figure 5.8. The measured values of c' ranged from 1.5 to 18.3 kPa; the values tended to

increase as a function of an increase in the amount of the w_s. Effective cohesion intercept values are typically not measured for naturally occurring, normally consolidated, soils (Holtz et al. 2011). Moreover, values for cohesion intercept have been shown to be difficult measure accurately from undrained triaxial testing (Ladd and Varallyay 1965). Cohesion intercept values were measured and reported in this study because the behavior of the reconstituted normally consolidated kaolinite specimens were similar to the typical behavior of overconsolidated specimens. In addition to the observed values of cohesion intercept, the observed change in the values of ϕ', due to an increase in the values of w_s, was from -6 to +11 percent. Unlike the cohesion intercept being dependent upon w_s, the ϕ' values were independent of w_s (Figure 5.8b).

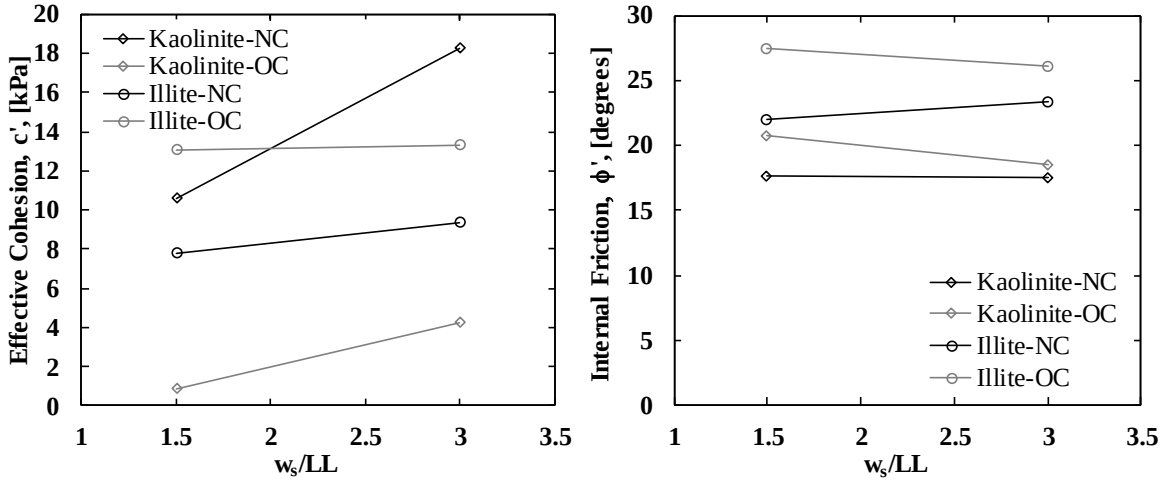

Figure 5.8. Variation of a) effective cohesion, c', and b) effective internal friction angle, ϕ', as a function of the normalized slurry water content.

5.6.4. *Undrained Shear Strength Behavior*

The values of the undrained shear strength that were measured at different levels of σ'_{vc} and w_s, are presented in Figure 5.9. The undrained shear strength values increased proportionately with the values of applied post consolidation/preshear vertical effective stress. For the normally consolidated specimens, the s_u^* values of the specimens, with higher values of

w_s (K3LL-NC and I3LL-NC), were from 5.0 to 16.0 percent lower than those of the specimens with lower values of w_s (K1.5LL-NC and I1.5LL-NC). For the overconsolidated specimens, the s_u^* values of the K3LL-OC and I3LL-OC specimens were from 0.5 to 5.5 percent less than the s_u^* values for the K1.5LL-OC and I1.5LL-OC. Following the preconsolidation process in the slurry consolidometer, the increased levels of w_s produced specimens with higher void ratio values and higher initial water content (w_o), which led to the decrease in the s_u^* values.

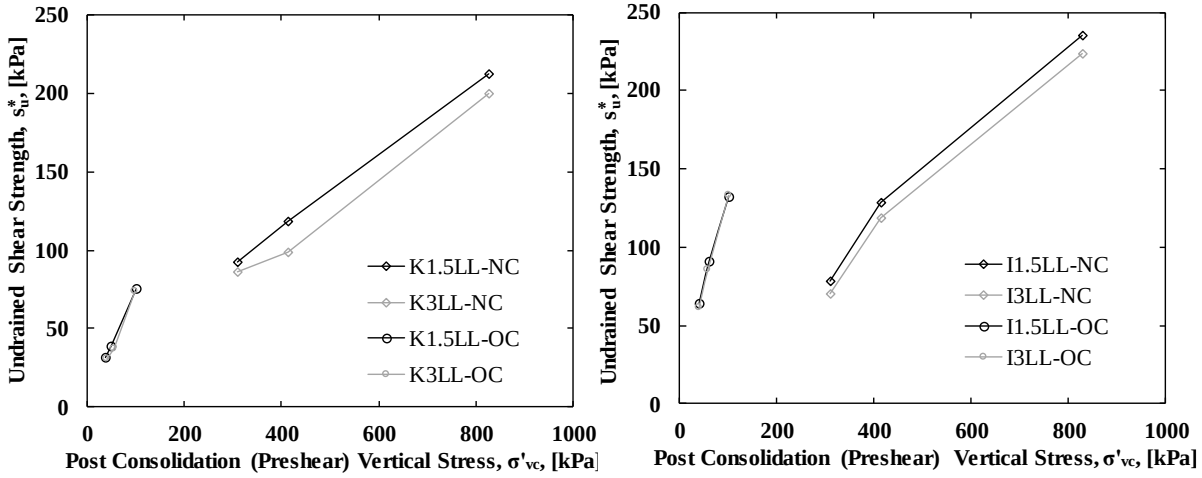

(a) (b)

Figure 5.9. Undrained shear strength values for: a) kaolinite, b) illite.

As shown in Figure 5.10, the undrained shear strength values were represented as a function of the I_v values that were determined from the *ICL* at the corresponding levels of σ'_{vc}. The IS_uL that was proposed by Chandler (2000) is also shown in Figure 5.10. The prescribed method of normalization of the s_u^* values, based on the values of I_v from the *ICL*, was unable to accurately represent the overconsolidated specimens (Figure 5.10). The value of the coefficient of determination (R^2) for the regression line of the s_u^*-I_v values was 0.62. The new normalization procedure, that was described in the Materials and Methods section, was utilized to determine the I_v values for the overconsolidated specimens, as presented in Figure 5.11. The aforementioned

normalization procedure was also applied to s_u^* values that were obtained from K_o-consolidated undrained triaxial tests that were conducted on K1.5LL specimens (Figure 5.11), at two other *OCR* levels (*OCR*= 2 and *OCR*= 4); the data from these *OCR* levels were obtained from Mahmood and Coffman (2017). The new normalized data, for the overconsolidated specimens, were in a better agreement with the IS_uL. Furthermore, by utilizing this procedure the R^2 value for the all of the normalized data increased to 0.90.

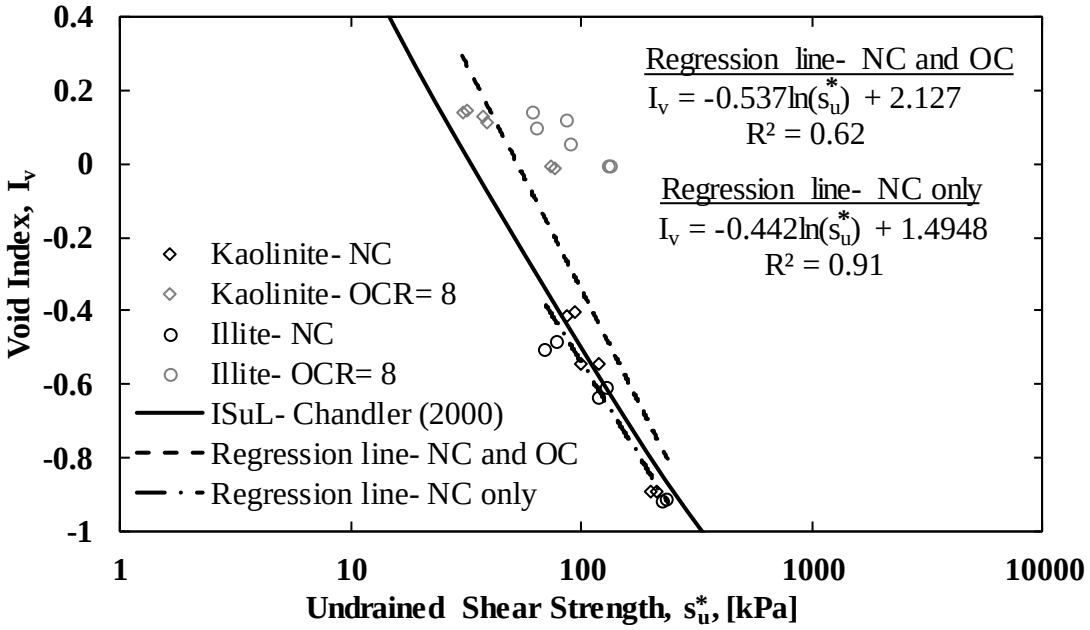

Figure 5.10. The relationship between void index, as obtained from ICL, and undrained shear strength values.

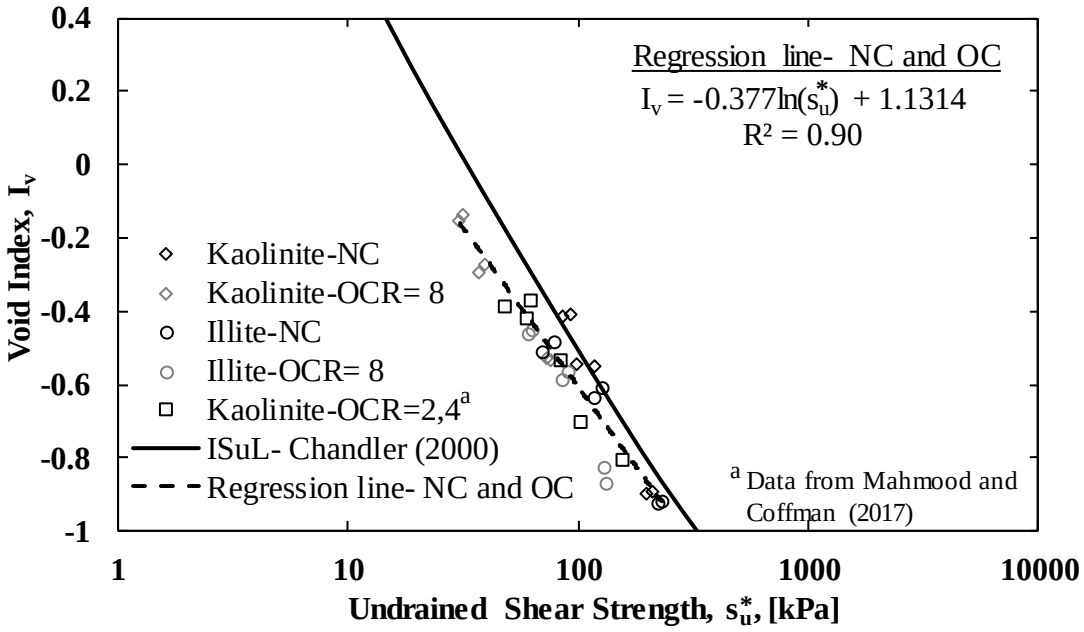

Figure 5.11. The relationship between void index, as obtained from intrinsic swelling lines for the OC specimens, and undrained shear strength values.

The relationship between the values of I_v and the undrained shear strength ratio (R_{su}^*) is presented in Figure 5.12. The deviation of the s_u^* values for the OC specimens from the *IS$_u$L* may be attributed to the higher values of the R_{su}^* of these specimens as compared to the R_{su}^* of 0.33 that was used by Chandler (2000) to develop the IS_uL. This observation indicated that different IS_uL could be found for the different values of R_{su}^* rather than a single IS_uL. More data are required to confirm this finding.

Based on the aforementioned results, the influence of the slurry water content on the 1) stress-strain and 2) strength characteristics of the kaolinite soil was much more than the influence on the same characteristics of the illite soil. The increased level of slurry water content of the kaolin slurry led to a more homogenous fabric that produced the stress-strain behavior and excess pore water pressure response that were like the typical behavior of the naturally occurring, normally consolidated, soils. Based on these observations, the slurry water content of

1 to 1.5LL, that was recommended by Burland (1990) may not be appropriate to reconstitute low plasticity kaolinite soils. The difference in the magnitude of the shear induced excess pore water pressure between the kaolinite specimens that were prepared at different w_s values may have caused the observed variations of the stress-strain and strength characteristics behavior of these different specimens. As discussed by Cerato and Lutenegger (2004), the diffuse double layer may have not completely been developed around the particles of the flocculated soils that were reconstituted at low slurry water content values. Therefore, the particles may have absorbed additional water during shear, depending on the initial water content of the specimens. The low values of the w_o for the K1.5LL specimens, as compared to those for the other specimens, as previously listed in Table 2, confirms this assumption.

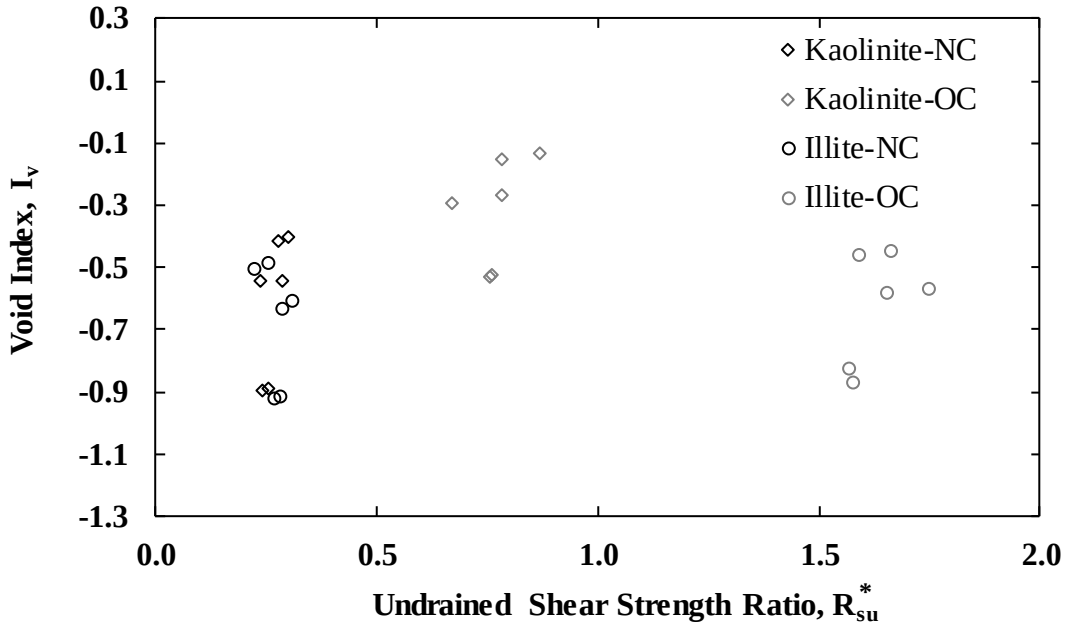

Figure 5.12. The relation between void index, as obtained from intrinsic swelling lines for the OC specimens, and undrained shear strength ratio.

5.7. Conclusions

Undrained triaxial compression tests were performed on reconstituted kaolinite and illite specimens to study the influence of the slurry water content on the corresponding intrinsic shear strength properties. The slurry water content was observed to affect the compression behavior, effective shear strength parameters, and undrained shear strength for the reconstituted soils. The intrinsic compression lines of both reconstituted soil type were established and found to be the same as the *ICL* that was proposed by Burland (1990). Following the same procedure used to establish the *ICL*, *ISL* was successfully established for each soil. The *ISL* was identical for each soil that was reconstituted at different w_s and unloaded from the same level of the maximum effective stress.

The kaolinite soil that was reconstituted at w_s of 1.5LL may not represent the intrinsic behavior because the fabric of the soil and the shear strength characteristics were different than those observed for kaolinite soil that was reconstituted at a w_s value of 3LL. Based on these observations, a low plasticity soil that was reconstructed at w_s value from 1 to 1.5LL, as recommended by Burland (1990), may not exhibit the intrinsic properties that were described by Burland (1990). While the effective cohesion tended to increase with increasing values of the w_s, the values of ϕ' were determined to be independent of the levels of w_s. The s_u^* values for the specimens with w_s of 3LL were from 5 to 16 percent lower than the s_u^* values for the specimens with w_s of 1.5LL. A better correlation between the normalized values of s_u^* and the IS_uL for the overconsolidated specimens was obtained by using the values of the I_v from the *ISL* instead of the values of the I_v from *ICL*. The differences in the shear strength behavior was determined to be caused by the differences in the shear induced excess pore water pressure response.

5.8. References

Al Haj, K. M. A., and Standing, J. R., (2015). "Mechanical Properties of Two Expansive Clay Soils from Sudan." Geotechnique, Vol. 65, No.4, pp. 258-273.

Allman, M. A., and Atkinson, J. H., (1992). "Mechanical Properties of Reconstituted Bothkennar Soil." Geotechnique, Vol. 42, No.2, pp. 289-301.

ASTM D2487, (2011). "Standard Practice for Classification of Soils for Engineering Purposes (Unified Soil Classification System)." ASTM International, West Conshohocken, PA, USA.

ASTM D4767, (2011). "Standard Test Method for Consolidated Undrained Triaxial Compression Test for Cohesive Soils." ASTM International, West Conshohocken, PA, USA.

Atkinson, J.H., Richardson, D., and Robinson, P.J., (1987). "Compression and Extension of K_o Normally Consolidated Kaolin Clay." Journal of Geotechnical Engineering, Vol. 113, No.12, pp.1468-1482.

Burland, J.B., (1990). "On the Compressibility and Shear Strength of Natural Clays." Geotechnique, Vol.40, No. 3, pp. 329-378.

Carrier, W. D., and Beckman, J. F., (1984). "Correlations Between Index Tests and the Properties of Remolded Clays." Geotechnique, Vol. 34, No. 2, pp. 211-228.

Cerato, A.B., and Lutenegger, A.J., (2004). Determining Intrinsic Compressibility of Fine Grained Soils." Journal of Geotechnical and Geoenvironmental Engineering, Vol. 130, No. 8, pp. 872-877.

Chandler, R.J., (2000). "Clay Sediments in Depositional Basins: The Geotechnical Cycle." Quarterly J. of Eng. Geology and Hydrogeology, Vol. 33, No. 1, pp.7-39.

Coop, M. R., Atkinson, J. H., and Taylor. R. N., (1995). "Strength, yielding and Stiffness of Structured and Unstructured Soils." Proceedings of the 11th European Conference on Soil Mechanics and Foundation Engineering, Copenhagen, Denmark, Vol. 28.

Cotecchia, F., and Chandler, R.J., (1997). "The Influence of Structure on the Pre-Failure Behaviour of a Natural Clay." Geotechnique, Vol. 47, No. 3, pp. 523-544.

Fearon, R.E., and Coop, M.R., (2000). "Reconstitution: What Makes an Appropriate Reference Material?." Geotechnique, Vol. 50, No. 4, pp. 471-477.

Gasparre, A., and Coop, M.R., (2008). "Quantification of the Effects of Structure on the Compression of a Stiff Clay." Canadian Geotechnical Journal, Vol 45, No. 9, pp. 1324-1334.

Henkel, D.J., (1956). "The Effect of Overconsolidation on the Behavior of Clays During Shear." Geotechnique, Vol. 6, No. 4, pp. 139-150.

Holtz, R. D., Kovacs, W. D., and Sheahan, T. C., (2011). "An Introduction to Geotechnical Engineering, 2nd Edition." Pearson Education, Upper Saddle River, New Jersey.

Hong, Z. S., Yin, J., and Cui, Y. J, (2010). "Compression Behaviour of Reconstituted Soils at High Initial Water Contents." Geotechnique, Vol. 60, No. 9, pp. 691-700.

Hong, Z.S., Bian, X., Cui, Y.J., Gao, Y.F., and Zeng, L.L., (2013). "Effect of Initial Water Content on Undrained Shear Behaviour of Reconstituted Clays." Geotechnique, Vol. 63, No. 6, pp. 441-450.

Kavvadas, M., and Amorosi, A., (2000). "A constitutive Model for Structured Soils." Geotechnique, Vol. 50, No. 3, pp. 263-273.

Ladd, C. C., and Foott, R., (1974). "New Design Procedure for Stability of Soft Clays." Journal of Geotechnical Engineering Division, Vol. 100, No. 7, pp. 763-768.

Ladd, C. C., and Varallyay, J., (1965). "The Influence of Stress System on the Behavior of Saturated Clays during Undrained Shear." No. RR-R65-11. Massachusetts Institute of Technology, Cambridge Soil Mechanics Div.

Lambe, T. W., and Whitman, R. V., (1969). "Soil Mechanics." John Wiley and Sons, New York.

Mahmood, N. S., and Coffman, R.A., 2017. The Effects of Stress Path on the Characterization of Reconstituted Low Plasticity Kaolinite." Soils and Foundations, (Under Review, Manuscript Number: SANDF-D-17-00352-R1).

Martin, R. T., and Ladd, C. C., (1978). "Fabric of consolidated kaolinite." Clays and Clay Minerals, Vol. (23), pp. 17-25.

Mitchell, J.K., and Soga, K., (2005). "Fundamental of Soil Behavior, 3rd Edition." John Wiley and Sons, New York.

Olson, R. E., (1962). "The Shear Strength Properties of Calcium Illite." Geotechnique, Vol. 12, No. 1, pp. 23-43.

Parry, R. H. G., (1960). "Triaxial Compression and Extension Tests on Remolded Clay." Geotechnique, Vol. 10, No. 4, pp. 160-188.

Salazar, S. E., and Coffman, R. A., (2014). "Design and Fabrication of End Platens for Acquisition of Small-Strain Piezoelectric Measurements During Large-Strain Triaxial Extension and Triaxial Compression Testing." Geotech. Test. J., Vol. 37, No. 6, pp. 1-12.

Tiwari, B., and Ajmera, B., (2011). "New Correlation Equations for Compression Index of Remolded Clays." J. Geotech. Geoenviron. Eng., Vol. 138, No. 6, pp. 757-762.

Yin, J., and Miao, Y., (2013). "Intrinsic Compression Behavior of Remolded and Reconstituted Clays-Reappraisal." Open Journal of Civil Engineering, Vol.3, No. 3, pp. 8-12.

Zhao, Y., and Coffman, R.A., (2016). "Back-Pressure Saturated Constant-Rate-of-Strain Consolidation Device with Bender Elements: Verification of System Compliance." Journal of Testing and Evaluation, Vol. 44, No. 6, pp.1-12.

Zhao, Y., Mahmood, N. S., and Coffman, R.A., (2017). "Soil Fabric and Anisotropy as Observed Using Bender Elements during Consolidation." Clays and Clay Minerals, (Under Review, Manuscript Number: CCM-1143-R1).

Zhao, Y., Mahmood, N. S., and Coffman, R.A., (2018). "Small-Strain and Large-Strain Modulus Measurements with a Consolidation Device." Journal of Testing and Evaluation, (In Press).

CHAPTER 6: Small-strain of Reconstituted Soils: The Effect of Slurry Water Content

6.1. Chapter Overview

The influence of the slurry water content on the small-strain properties of reconstituted kaolinite and illite soils were investigated by performing shear wave velocity measurements. Vertically-propagated, horizontally-polarized shear wave velocity measurements were obtained by utilizing bender elements within triaxial testing equipment. To quantify the amount of fabric anisotropy, the triaxial shear wave velocity measurements were compared to horizontally-propagated, vertically-polarized, shear wave velocity measurements that were obtained by utilizing bender elements within a consolidation device. The values of the shear wave velocity and shear modulus were normalized to the void index to examine the intrinsic small-strain properties. The values of both shear wave velocity and shear modulus did not normalize with respect to the void index procedure. It was recommended to utilize a water content of the slurry of at least three times the liquid limit of the soil to obtain small-strain characteristics for reconstituted soils that are in better agreement with those for natural soils.

This chapter contains a research description, additional results, and a summary (Section 6.1 through Section 6.4), an introduction on small-strain characteristics (Section 6.5), a description of the test specimens and procedures (Section 6.6 and Section 6.7, respectively), the findings of this project (Section 6.8), and a description of the conclusions and recommendations (Section 6.9). The paper enclosed in this chapter has been submitted within the Geotechnical Testing Journal. The full citation of this document is: *Mahmood, N. S. and Coffman, R. A., (2018b). "Small-strain of reconstituted soils: The effect of slurry water content." Geotechnical Testing Journal, (Under Review, Manuscript Number: GTJ-2018-0098-R1).*

6.2. Additional Results not Included in the Aforementioned Manuscript

The measured values of shear wave velocity and shear modulus, for the two soils during the shearing stage, are presented in Figure 6.1. Because external axial strain measurements were utilized to measure the axial strain values, modulus degradation at small axial strain levels could not be measured. There was no clear trend of the variation of shear wave velocity with the vertical effective stress. The increase and decrease in the vertical effective stress levels during shear may have caused the variable trend of the measured shear wave velocity values. However, the values of the shear modulus tended to decrease, during shearing, before failure was reached. As previously observed during the reconsolidation stage, the values of the shear modulus for the specimens with w_s of 3LL were less than those for the specimens with w_s of 1.5LL. The decrease in shear modulus with the increasing w_s values may be attributed to the same factors (grater e_o and w_o values for the specimens with w_s of 3LL) that were believed to have affected the shear wave velocity as a result of increasing w_s during reconsolidation, as previously presented.

The shear modulus values that were obtained from tests conducted on the normally consolidated specimens, as determined from the bender element measurements, were 1.4 to 2.5 times the values of the shear modulus for the overconsolidated specimens. However, the difference in the shear modulus values between the normally and overconsolidated specimens cannot be solely explained by the change in the OCR values because it was not possible to isolate the effect of the overconsolidation ratio from the effect of the vertical effective stress prior to shear. As the overconsolidation ratio increased from 1 to 8, the pre-shear effective vertical stress decreased from 414 to 51.75 kPa.

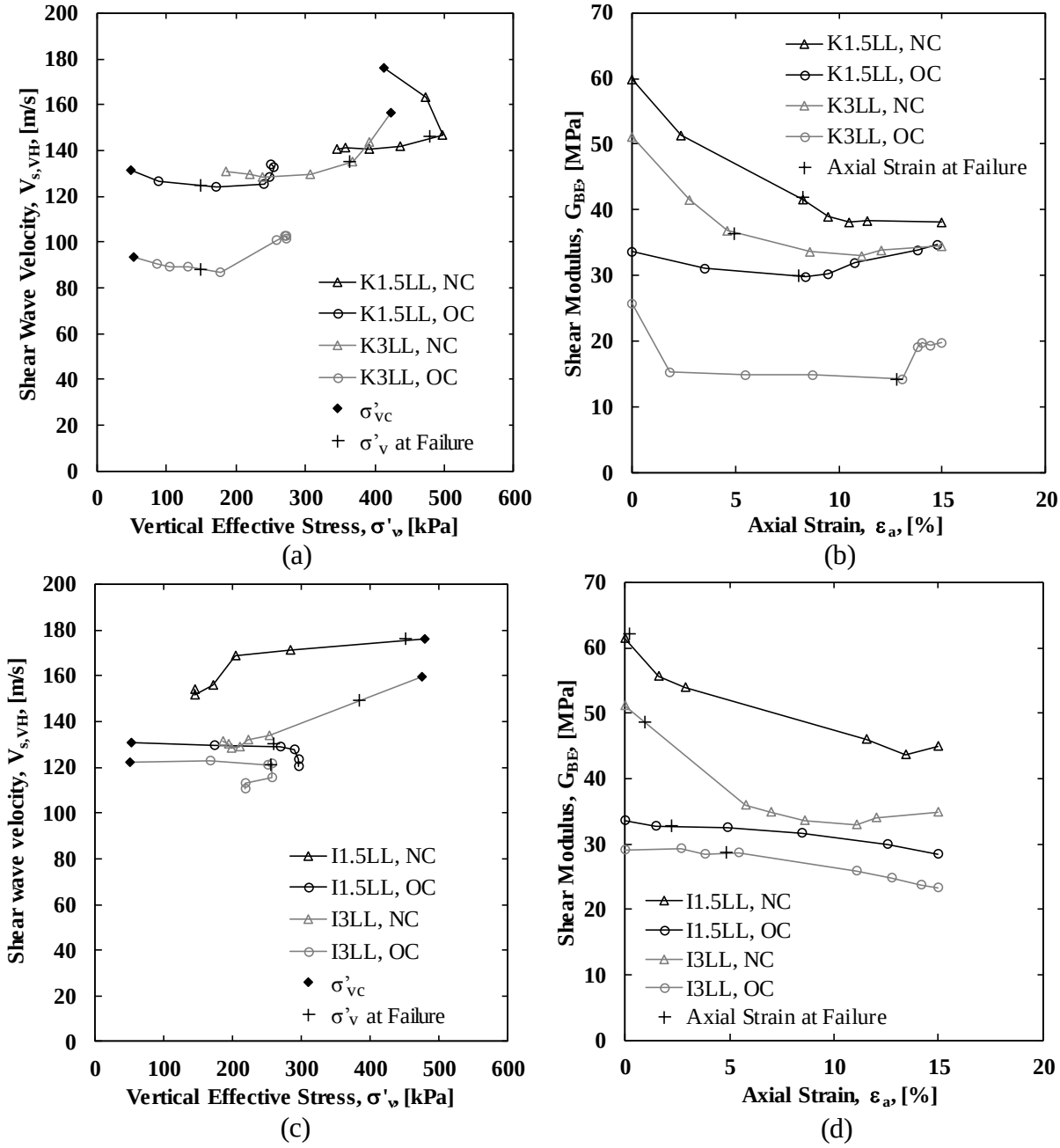

Figure 6.1. The results of small-strain values during the shearing stage: (a) shear wave velocity- vertical effective stress relationships for kaolinite, (b) shear modulus- axial strain relationships for kaolinite, (c) shear wave velocity- vertical effective stress relationships for illite, and (d) shear modulus- axial strain relationships for illite.

Two main phenomena that may have led to the inconsistent and, therefore, not reliable shear modulus-axial strain relationships. First, as observed by Mahmood and Coffman (2018a) postpeak shear planes were developed in all of the normally and overconsolidated specimens.

These planes caused non-uniformity of the specimens and discontinuity in the travel paths of the shear wave, thereby affecting the shear modulus. Second, alignment errors may have resulted from tilting of both the specimen and the top platen during shear.

6.3. Small-strain Characteristics of Reconstituted Soils: The Effect of Slurry Water Content

Nabeel S. Mahmood[1], Sean E. Salazar[2], Richard A. Coffman[3]

[1]MSCE, Graduate Research Assistant, Department of Civil Engineering, University of Arkansas, Fayetteville, Arkansas, USA. Instructor, University of Anbar, Ramadi, Iraq.
[2]MSCE, Graduate Research Assistant, Department of Civil Engineering, University of Arkansas, Fayetteville, Arkansas, USA.
[3]PhD, PE, PLS, Associate Professor, Department of Civil Engineering, University of Arkansas, Fayetteville, Arkansas, USA.

6.4. Abstract

The influences of slurry water content (w_s) and fabric anisotropy, on the small-strain behavior of reconstituted kaolinite and illite specimens were investigated. Bender elements were employed, within triaxial testing equipment, to obtain vertically-propagated, horizontally-polarized, shear wave velocity measurements, and corresponding shear modulus, during the consolidation of eight triaxial tests. The soils were initially prepared at water content values of one and one-half (1.5x) and three (3x) times the respective liquid limit for each soil type. At the same level of overconsolidation ratio and vertical effective stress, the specimens with lower w_s values were from 1.1 to 2.1 times stiffer than those with higher w_s values. The shear wave velocity and shear modulus data were normalized to the void index by following a procedure that was similar to procedures that have previously been used to normalize compression and undrained shear strength data. Unique “intrinsic” relationships for shear wave velocity or shear modulus, independent of soil fabric, were not observed during this study.

Inherent fabric anisotropy was also assessed by comparing the aforementioned triaxial shear wave velocity data to measurements of horizontally-propagated, vertically-polarized, shear

wave velocity that were obtained by utilizing bender elements within a consolidation device. The amount of fabric anisotropy was dissimilar and the characteristics of the cross-anisotropic fabric was not observed for the specimens. The amount of inherent fabric anisotropy ranged from 0.63 to 0.97 for the kaolinite and illite specimens with w_s values of 1.5x the liquid limit, and ranged from 1.13 to 1.21 for kaolinite specimens with w_s values of 3x the liquid limit. During the shearing stage, inconsistent and unreliable relationships were obtained for the shear wave velocity-vertical effective stress behavior and shear modulus-axial strain behavior. As discussed herein, the w_s level should be considered when reconstituting specimens of cohesive soils for small-strain determination.

Keywords: Shear Wave Velocity, Shear Modulus, Bender Elements, Reconstituted Soils, Slurry Water Content, Intrinsic Behavior, Fabric Anisotropy

6.5. Introduction

Accurate measurements of soil moduli are essential for geotechnical analyses when computing deformations and stress distributions in a soil mass by utilizing numerical methods and advanced constitutive models. Various field and laboratory testing methods have been employed to determine elastic shear modulus, at small strains, based on the measurements of shear wave velocity through the soil. During the last few decades, bender elements have been used extensively within odometer (e.g., Jamiolkowski et al. 1995; Fam and Santamarina 1995; Kang et al. 2014; Zhao and Coffman 2016) and triaxial devices (e.g., Viggiani and Atkinson 1995; Jovicic and Coop 1998; Gasparre and Coop 2006; Choo et al. 2013; Salazar and Coffman 2014) to measure shear wave velocities. This technique has proven to be an inexpensive and reliable means of studying dynamic soil properties (Clayton 2011).

The effect of 1) void ratio and 2) fabric of cohesive soils on the small-strain stiffness has been well documented in previous studies. As reported by Atkinson et al. (1990), Lings et al. (2000), Clayton (2011), and Finno and Cho (2011), small-strain stiffness was observed to increase with decreasing values of void ratio. The importance of soil fabric, as a factor influencing the small-strain stiffness, has also been discussed and illustrated (e.g., Hardin and Brandford 1989; Jovicic and Coop 1998; Kang et al. 2014; Zhao et al. 2017). Based on the results from many studies (e.g., Olson 1962; Martin and Ladd 1978; Carrier and Beckman 1984; Burland 1990; Cerato and Lutenegger 2004; Mahmood and Coffman 2018a), the use of different levels of slurry water content (w_s) to "reconstitute" (Burland 1990) cohesive soils will affect the initial void ratio, soil fabric, and initial water content (w_o) of the prepared specimens. As described by Olson (1962), specimens reconstituted at w_s values less than or slightly above the liquid limit (LL), will have dispersed fabric and the particles will be well-orientated in directions perpendicular to the direction of deposition. Olson (1962) also indicated that sedimentation of specimens from slurries with w_s values higher than two times (2x) the liquid limit will produce specimens with a flocculated fabric.

The "void index (I_v)" concept was introduced by Burland (1990) to normalize compression curves of reconstituted soils that have been prepared from soil slurries at w_s values between 1x and 1.5x the liquid limit of the soil. Burland (1990) also introduced the intrinsic compression line (*ICL*) to describe the "intrinsic" compression behavior that was independent of the initial structure of the reconstituted soils. Based on the described concept, several studies have attempted to correlate the I_v concept to different engineering related soil properties to obtain properties of intact soils. In particular, normalized relationships have been successfully established between void index and undrained shear strength (Chandler 2000; Hong et al. 2013;

Mahmood and Coffman 2018a), between void index and swelling curves (Mahmood and Coffman 2018a), and unsuccessfully established between void index and hydraulic conductivity (Zeng et al. 2011).

Previously, reconstituted specimens have been used to characterize the small-strain behavior of cohesive soils (e.g., Viggiani and Atkinson 1995; Jung et al. 2012; Trhlikova 2012; Choo 2013; Zhao and Coffman 2016). The values of w_s that have been used in the aforementioned studies ranged from 0.7x to 2x the corresponding liquid limit of the soil. The majority of these studies focused on the effects of overconsolidation ratio, stress path, void ratio, and fabric anisotropy on the small-strain behavior of the reconstituted soils. The previous studies also focused on the difference in the small-strain stiffness behavior between reconstituted and intact soils. Except for the research that was performed by Zhao et al. (2017), the effect of w_s levels on small-strain stiffness and stiffness anisotropy of reconstituted soils was not previously addressed in the literature.

Based on past studies related to soil anisotropy (Duncan and Seed 1966; Mitchell 1972; Martin and Ladd 1978; Jovicic and Coop 1998), anisotropy of the soil fabric occurs during deposition of soil particles (inherent anisotropy) or as a result of changes in the stress conditions (stress-induced anisotropy). Different shear wave velocity values have been measured from different waves propagation directions depending on the installation position of the bender elements within the specimen, and as a result of fabric anisotropy (Jovicic and Coop 1998; Yamashita et al. 2005; Kang et al. 2014; Zhao et al. 2017). Moreover, different shear modulus values have been calculated from the corresponding shear wave velocity measurements. According to Roesler (1979), Jamiolkowski et al. (1995), Lings et al. (2000), Kang et al. (2014), and Zhao et al. (2017), the values of bender elements acquired stiffness anisotropy, as referred to

as the ratio of shear modulus in the horizontal direction to the shear modulus in the vertical direction, ranged from 1.2 to 1.7 for normally and lightly overconsolidated soils. For overconsolidated soils, the stiffness anisotropy was greater than 2.0. Furthermore, as reported by Jovicic and Coop (1998) and Zhao et al. (2017), during the K_o-reconsolidation process, the effect of stress-induced fabric anisotropy on small-strain stiffness was insignificant when compared with the effect of inherent fabric anisotropy.

A comprehensive understanding of the influence of 1) the slurry water content and 2) the fabric anisotropy of reconstituted soils on the small-strain characteristics has not been demonstrated in the reviewed literature. Furthermore, the relationships between the shear wave velocity and the corresponding shear modulus of reconstituted soils and the void index concept has not been evaluated. To evaluate these concepts, a series of undrained triaxial compression tests, with measurements of vertically-propagated, horizontally-polarized shear wave velocity, were performed on reconstituted kaolinite and illite specimens. The soils were initially mixed at respective water content values of 1.5x and 3x the liquid limit of the respective soil type. The values of shear wave velocity and shear modulus of these specimens were measured during the K_o-reconsolidation and shearing stages. The relationships between the void index and 1) the shear wave velocity measurements and 2) the shear modulus measurements are discussed. The values of the vertically-propagated shear wave velocity are also compared with the horizontally-propagated shear wave velocities that were previously measured by Zhao et al. (2017) to evaluate the fabric anisotropy of the reconstituted soils.

6.6. Test Specimens

Kaolinite and illite soil types were used to determine the effect of the slurry water content on the small-strain properties of these soils. KaoWhite-S, a commercially available kaolinite soil,

and illite soil obtained from the Knight Hawk Coal Company of Percy, Illinois were utilized in this experimental program. These types of kaolinite and illite soils have been used previously at the University of Arkansas to evaluate shear strength, compression, and small-strain stiffness of reconstituted soils (Coffman et al. 2014; Zhao and Coffman 2016; Mahmood and Coffman 2017; Zhao et al. 2017, Zhao et al. 2018; Mahmood and Coffman 2018a). The index properties of the utilized soils are presented in Table 6.1. The kaolinite and illite soils were classified as Low Plasticity Silt (ML) and Low Plasticity Clay (CL), respectively, according to the Unified Soil Classification System (ASTM D2487-2017).

Table 6.1. Properties of kaolinite and illite soils (from Mahmood and Coffman, 2018a).

Property	Kaolinite	Illite
Liquid limit	31.5	46.7
Plastic limit	28.1	23.6
Clay size fraction (<0.002 mm)	47.2	46.5
Specific gravity, G_s	2.67	2.69

The specimens were prepared according to the method that was described by Zhao and Coffman (2016). Each powdered form of the kaolinite and illite soil was mixed with de-ionized, de-aired water to form a slurry at two different levels of water content (1.5x and 3x the corresponding liquid limit of the soil). The slurries were then pre-consolidated in a double drained, 3.81 cm, inside diameter, acrylic, static weight, slurry consolidometer under a constant vertical stress of 207kPa. After primary consolidation was completed for the pre-consolidation process, two specimens were extruded from each consolidometer. Each extruded specimen was trimmed to develop a specimen with a length to diameter ratio of two and then placed into the triaxial device.

6.7. Testing Apparatus and Methods

Advanced, automated, triaxial equipment, with pore water pressure measurements, were utilized to perform K_o-consolidated, undrained, triaxial compression tests ($\overline{CK_oUTC}$) on the prepared specimens, in accordance with ASTM D4767-2011. Each specimen was reconsolidated,

under the K_o-condition, to a maximum vertical effective stress ($\sigma'_{v,max}$) of 414 kPa, which represented two times the pre-consolidation stress of the slurry within the slurry consolidometer. The overconsolidated specimens were allowed to swell, under the K_o-conditions, to achieve an overconsolidation ratio (OCR) of eight (8) prior to shear. After reconsolidating the specimens to the required levels of vertical effective stress and OCR, the specimens were sheared in an undrained condition at an axial strain rate of 0.5 percent per hour. A total number of eight triaxial tests were performed on the prepared specimens (four tests were performed for each soil type).

The top and bottom platens of the triaxial device were instrumented with piezoelectric transducers that were developed at the University of Arkansas (Salazar and Coffman 2014). As shown in Figure 6.2, the top and bottom platens were integrated with two types of transducers: 1) bender elements to measure shear waves, and 2) bender disks to measure compression waves (bender disks were not used in this testing program). Similar piezoelectric platens were previously used by Salazar and Coffman (2014) to measure shear wave and compression wave velocities in dry Ottawa sand. Modifications were made to the Salazar and Coffman (2014) top platen to prevent leaking through the top platen that was observed during earlier triaxial tests. It was determined that the leak occurred due to the drainage ports and the wire feed port. The leak from the drainage ports was eliminated by utilizing a pair of O-rings, a metal tube, and a union to connect each drainage port to the corresponding drainage tube (Figure 6.2). To eliminate the leak through the wire feed port, high vacuum grease was injected into the cavity between the stainless steel insert and the acrylic platen.

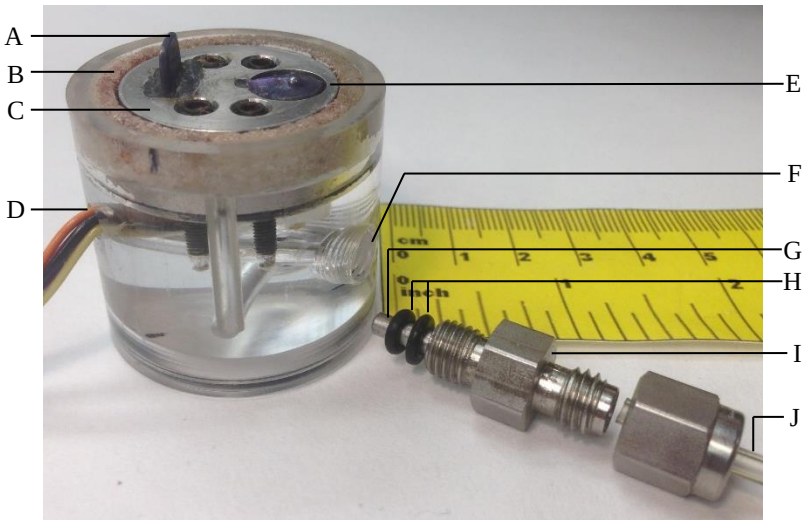

A. Bender element
B. Porous ring
C. Stainless steel insert
D. Wire feed port
E. Bender disk
F. Drainage port
G. Steel tube (1/8 inch) placed into (F)
H. O-ring
I. Union (1/8 inch pipe taper threads to 1/8 inch single ferrule threads)
J. Drainage tube

Figure 6.2. Photograph of inverted top platen with the details of the drainage tube attachment.

The velocity of the shear waves that traveled through the specimen was determined following the procedure presented by Brignoli et al. (1996). The bender element located in the bottom platen was excited, and the developed shear waves were received by the bender element located in the top platen. The travel time during sending and receiving was recorded. The distance of propagation was calculated by subtracting the embedded length of the bender elements from the total length of the specimen at the time of excitation. Axial deformation measurements were used to determine the length of the specimen at any time during the test. Assuming that the specimens represented an infinite, isotropic, and elastic medium, the measured shear wave velocity (V_s), along with the total mass density of the soil (ρ), were then used to calculate the small-strain shear modulus (G_{BE}), as presented in Equation 6.1 (Richart et al. 1970).

$$G_{BE} = \rho V_s^2 \qquad \text{Richart et al. (1970)} \qquad \text{(Equation 6.1)}$$

Because there have been several different interpretation methods to determine the travel time, as obtained from piezoelectric measurements (for example, by using the time or frequency domains of the signals, as described in Atkinson 1995, Alvarado and Coop 2012, and Salazar and Coffman 2014), several excitation frequencies were used to determine the optimum frequency of the input signal (10kHz) that provided a clear output signal.

6.8. Test Results and Discussion

The small-strain stiffness values that were determined for the laboratory prepared kaolinite and illite specimens, as obtained from shear wave velocity measurements are discussed herein. Specifically, three main items: 1) intrinsic compression and swelling behavior; 2) shear wave velocity measurements and shear modulus determination during reconsolidation; and 3) fabric anisotropy are discussed and compared with literature values. For simplicity, the specimens that were prepared from slurries at w_s values of 1.5x and 3x the corresponding liquid limit of the soil, are hereinafter referred to as K1.5LL and K3LL for kaolinite, respectively, and as I1.5LL and I3LL for illite, respectively. A summary of the initial values for the specimens is presented in Table 6.2.

Table 6.2. Summary of initial physical soil properties.

Soil	*Specimen*	$\frac{w_s}{LL}$	*OCR*	$\sigma'_{v,max}$ *[kPa]*	w_o *[%]*	γ_T *[kN/m^3]*	e_o	C_c
Kaolinite	K1.5LL-NC	1.5	1	414	31.4	18.0	0.90	0.124
Kaolinite	K3LL-NC	3	1	414	38.3	17.4	1.06	0.132
Kaolinite	K1.5LL-OC	1.5	8	414	31.2	18.0	0.89	0.122
Kaolinite	K3LL-OC	3	8	414	38.4	17.9	1.00	0.135
Illite	I1.5LL-NC	1.5	1	414	35.2	17.6	0.99	0.402
Illite	I3LL-NC	3	1	414	42.1	17.0	1.16	0.433
Illite	I1.5LL-OC	1.5	8	414	36.6	17.5	1.02	0.400
Illite	I3LL-OC	3	8	414	39.8	17.1	1.12	0.432

w_o, γ_T, e_o are initial water content, total unit weight, and initial void ratio of the specimens after being removed from the slurry consolidometer following pre-consolidation, respectively.

6.8.1. *Intrinsic Compression and Swelling Behavior*

Typical compression and swelling curves for the kaolinite and illite specimens, as obtained from the K_o-reconsolidation stage during the triaxial tests, are presented in Figure 6.3. The values of the initial void ratio and the compression index were affected by the increase in w_s values. The values of the initial void ratio for the specimens that were reconstituted at w_s values of 3LL were between 10 and 18 percent greater than those for the specimens that were reconstituted at w_s values of 1.5LL. Similarly, the values of the compression index (C_c) for the specimens with w_s equal to 3LL were between eight and 18 percent greater than the C_c values for the specimens with w_s equal to 1.5LL. Similar observations regarding the variation of e_o and C_c values at different w_s values were reported by Carrier and Beckman (1984), Burland (1990), Cerato and Lutenegger (2004), and Hong et al. (2010).

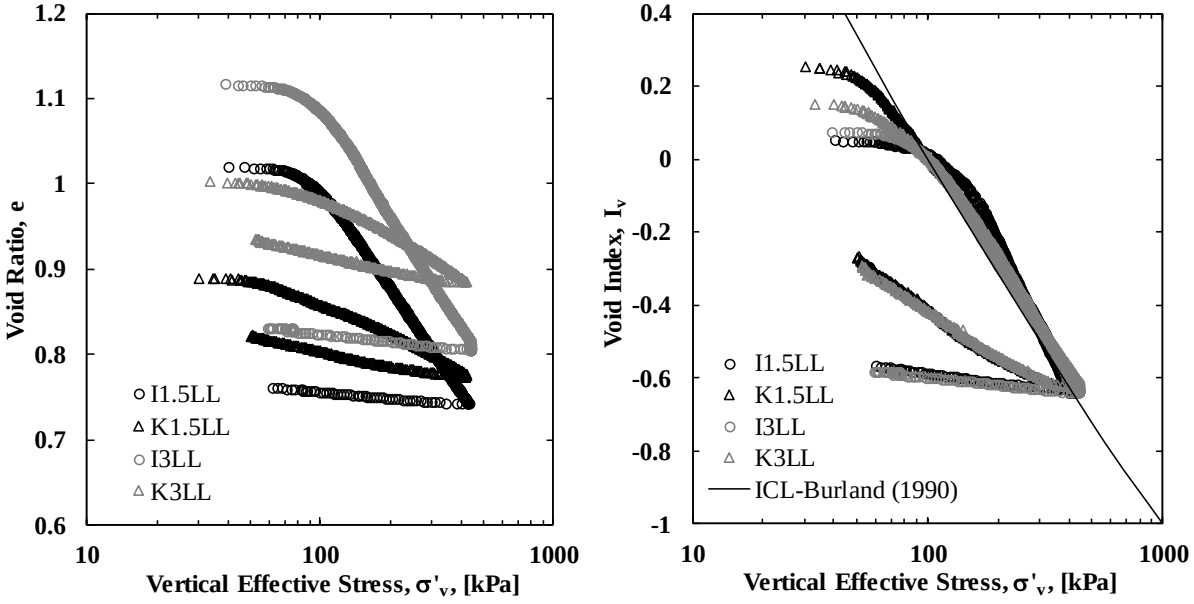

Figure 6.3. Compression relationships for the reconstituted soils: (a) typical compression and swelling curves, (b) void index as a function of vertical effective stress.

To evaluate the intrinsic compression behavior of the reconstituted specimens, the compression curves were normalized using the void index (I_v) concept that was proposed by Burland (1990), as is presented as Equation 6.2.

$$I_v = \frac{e - e^*_{100}}{e^*_{100} - e^*_{1000}} \qquad \text{Burland (1990)} \qquad \text{(Equation 6.2)}$$

In Equation 6.2, e^*_{100} and e^*_{1000} corresponded to the void ratio of the reconstituted soil at vertical effective stress (σ'_v) levels of 100 and 1000 kPa, respectively. The e^*_{1000} values were determined by extrapolating the straight line portions of the version compression curves in Figure 6.3a to an effective stress of 1000 kPa. The void index was also utilized to normalize the swelling curves, as described in Mahmood and Coffman (2018a). Using Equation 3, as proposed by Burland (1990), the intrinsic compression curves of the two soils exhibited almost identical relationships with respect to the Burland (1990) *ICL*.

$$I_v = 2.45 - 1.285 \log \sigma'_v + 0.015 (\log \sigma'_v)^3 \qquad \text{Burland (1990)} \qquad \text{(Equation 6.3)}$$

The well-normalized compression curves for the specimens with w_s values of 3LL may indicate that the use of the *ICL* is applicable to normalize the compression curves for the specimens that are reconstituted at w_s levels above the 1.25LL level that was recommended by Burland (1990). The shape of the intrinsic compression lines for the kaolinite specimens, which was identical to the *ICL*, may also indicated that the use of the *ICL* is applicable for normalization of the compression behavior of low plasticity silts.

6.8.2. *Shear Wave Velocity and Shear Modulus during Reconsolidation*

The values of the shear wave velocity and shear modulus, during the reconsolidation stage of the triaxial tests, are presented in Figure 6.4. The same general shape of the shear wave velocity-vertical effective stress curves was observed for the kaolinite and illite soils, regardless of the w_s

values. The behavior was characterized by increasing shear wave velocity with increasing vertical effective stress during loading, followed by decreasing shear wave velocity with decreasing vertical effective stress during unloading. The change of the shear wave velocity during loading and unloading was associated with the change in the void ratio values from consolidation of the soil.

At similar levels of effective stress, during reconsolidation, the specimens that were reconstituted from w_s values of 1.5LL had higher values of shear wave velocity than the specimens that were reconstituted from w_s values of 3LL. The shear wave velocity values for the K1.5LL specimens were between 20 and 41 percent higher than those for the K3LL specimens. Similarly, the shear wave velocity values for the I1.5LL specimens were between seven and 14 percent higher than those for the I3LL specimens. The slower shear wave velocities that were measured for the specimens that were reconstituted at higher w_s were attributed to the 1) higher initial void ratio and 2) higher initial water content (w_o) of these specimens prior to reconsolidation in the triaxial testing device. Increasing level of w_s led to slower measured values of shear wave velocity because shear waves do not propagate through water. The additional water that was present occupied the void space and separated the particles, thereby slowing the measured shear wave velocity. Moreover, the influence of w_s on the shear wave velocity was greater for kaolinite soil than for illite soil. As reported by Mahmood and Coffman (2018a), more changes in the fabric were observed for kaolinite soil than for illite soil as a result of increased w_s values. As also indicated by Zhao et al. (2017) and Mahmood and Coffman (2018a), the influence of the w_s on the shear wave velocity, stress-strain behavior, and strength characteristics of the kaolinite soil was more significant than the influence of w_s on the same characteristics of the illite soil.

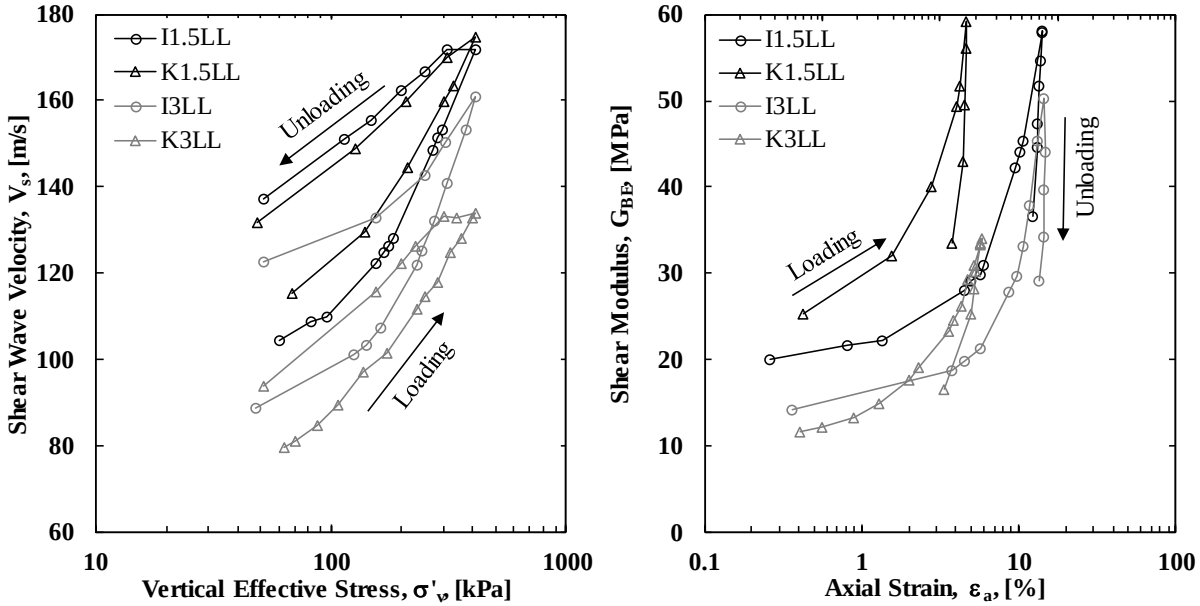

Figure 6.4. Small strain results obtained from bender elements during reconsolidation and overconsolidation: (a) shear wave velocity-vertical effective stress relationships, (b) shear wave velocity-axial strain relationships.

The shear modulus-axial strain relations followed the same trend of the shear wave velocity-effective stress relations during loading and unloading. The shear modulus within the shear modulus-axial strain curves was observed to increase with increasing axial strain during loading, then a sharp decrease was observed in the shear modulus during unloading. The G_{BE} values for K1.5LL specimens were from 1.7 to 2.1 higher than the G_{BE} values for the K3LL specimens. Likewise, the I1.5LL specimens were from 1.1 to 1.4 higher than the I3LL specimens. The observation that the specimens with lower w_s values were stiffer than those with higher w_s values was in agreement with the results of the observed undrained shear strength that were obtained by Mahmood and Coffman (2018a).

As shown in Figure 6.5, the values of shear wave velocity and shear modulus were normalized as a function of I_v. The values of I_v that were used to normalize these curves were determined from the *ICL* of each specimen, as previously presented in Figure 6.3, at the

corresponding vertical effective stress. The same general shape of the V_s-I_v curves and G_{BE}-I_v curves was observed for the two soils during the re-consolidation and swelling stages. However, unlike the historic ability of the void index normalization procedure to produce a unique relationship between I_v and compression or undrained shear strength, the void index normalization procedure was unable to produce a unique relationship between the V_s and I_v values. Likewise, the shear modulus data did not appear to normalize within the shear modulus-void index space. As previously described, there were other factors affecting shear wave velocity and small-strain stiffness beside the void ratio that was accounted for in the void index value in Equation 6.2. The difference in the initial water content of the specimens, as well as the difference in the fabric between the specimens, that were initially prepared at different levels of slurry water content, appeared to dominate the values of shear wave velocity. This difference in fabric was not completely captured in the void ratio values that were used to calculate the void index values.

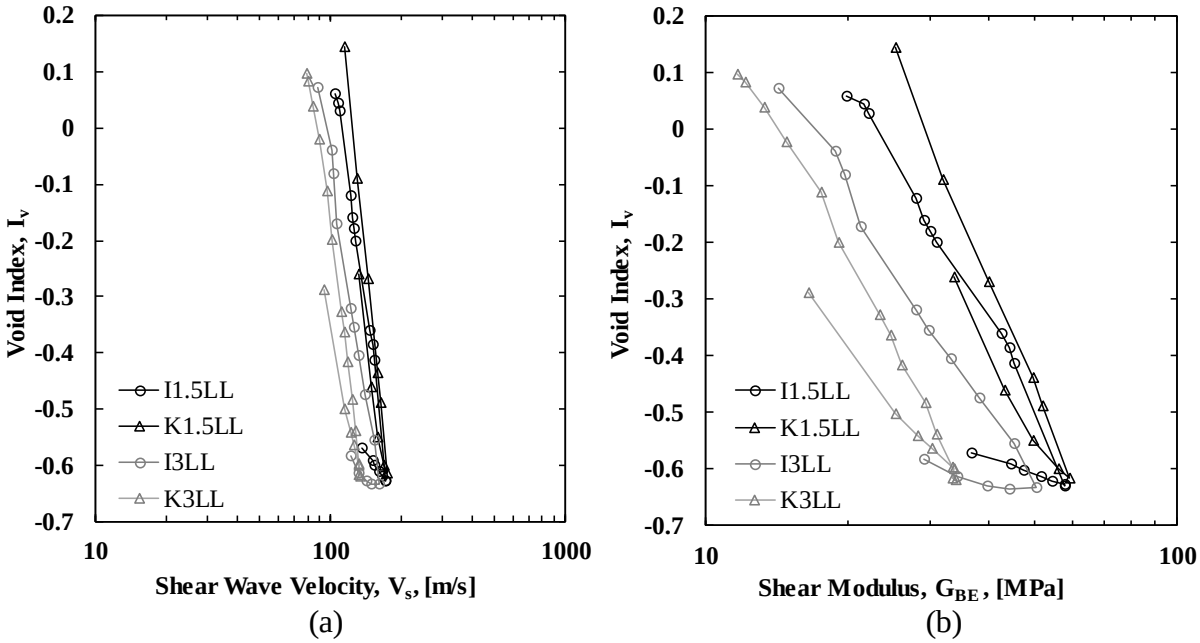

Figure 6.5. Normalized small-strain results: (a) shear wave velocity as a function of void index, (b) shear modulus as a function of void index.

6.8.3. *Fabric Anisotropy*

The values of the shear wave velocity during the reconsolidation stage were compared with the values of shear wave velocity that were obtained from a back-pressure saturated, constant rate-of-strain, consolidation device, with bender elements (BP-CRS-BE) that were measured by Zhao and Coffman (2016). As shown in Figure 6.6, the values of horizontally propagated-vertically polarized shear wave velocity $(V_{s,HV})$, as obtained by utilizing the BP-CRS-BE device, were compared with the values of vertically propagated-horizontally polarized shear wave velocity $(V_{s,VH})$ that were measured in this study.

The difference in the velocity between the vertically-propagated shear waves and the horizontally-propagated shear waves indicated that the reconstituted specimens from both soils had inherent fabric anisotropy. However, the amount of the inherent anisotropy was dissimilar. For the K1.5LL specimens, the amount of fabric anisotropy $(V_{s,HV}/V_{s,VH})$ ranged from 0.89 to 0.97 at the corresponding levels of applied vertical effective stress. Likewise, for the I1.5LL specimens, the $(V_{s,HV}/V_{s,VH})$ ratio ranged from 0.63 to 0.74. The observation that the K1.5LL and I1.5LL specimens had higher values of vertically-propagated shear wave velocity than horizontally-propagated shear wave velocity was in direct contrast with that of Yamashita et al. (2005), Choo et al. (2013), and Kang et al. (2014). The higher values of $V_{s,VH}$ may be attributed to the dispersed fabric of the 1.5LL specimens that was created within the slurry consolidometer. Within the dispersed fabric, the contact areas between the faces of the particles along the vertical direction were much greater than the contact areas between the edges of the particles along the direction of prefered orientation. Therefore, the shear waves propagated faster in the vertical direction.

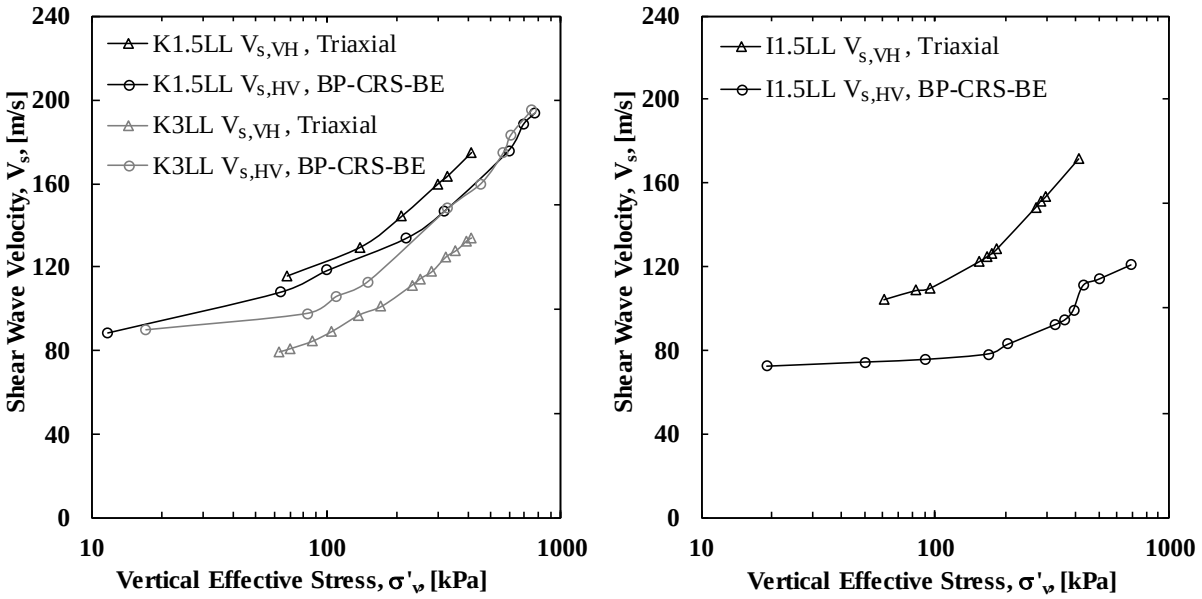

Figure 6.6. Comparison of the values of shear wave velocity values obtained from bender elements in the triaxial apparatus and BP-CRS-BE device, during Ko-reconsolidation, for: (a) kaolinite, and (b) illite.

When comparing the values of $V_{s,HV}$ to the values of $V_{s,VH}$ for the K3LL specimens, the amount of fabric anisotropy ($V_{s,HV}/V_{s,VH}$) ranged from 1.13 to 1.21. Although previous studies (e.g., Jovicic and Coop 1998; Lings et al. 2000; Yimsiri and Soga 2000; Cho and Finno 2010) have indicated that one-dimensionally deposited soils will essentially experience cross anisotropy ($V_{s,HV} \approx V_{s,VH}$), perfect cross anisotropic fabric was not observed for the specimens that were reconstituted from a slurry, at high slurry water content values. The fabric anisotropy of natural clays that have been observed by Pennington et al. (1997) and Lee et al. (2008) have led to the indication that the values of $V_{s,HV}$ were greater than the values $V_{s,VH}$. Similar observations being obtained for the K3LL samples ($V_{s,HV} > V_{s,VH}$) implies that reconstitution of soils at water content levels of at least 3LL may produce a soil fabric that is similar to the fabric of naturally sedimented soils.

6.9. Conclusions

Based on the results of triaxial compression tests, with shear wave velocity measurements, the w_s was determined to be a significant parameter that influenced the compression behavior, shear wave velocity, shear modulus, and fabric anisotropy of the reconstituted soils. During K_o-reconsolidation, the values of the shear wave velocity of the specimens, that were initially reconstituted with lower slurry water content, were from 7 to 41 percent higher than those that were reconstituted at higher slurry water content. The decrease in shear wave velocity, as a function of increasing w_s, was believed to be caused by the higher initial void ratio and higher initial water content of the specimens. Furthermore, the specimens with lower w_s values were from 1.1 to 2.1 stiffer than those with higher w_s values. Following the same procedures that were used by Mahmood and Coffman (2018a) to normalize the compression and undrained shear strength values, the values of shear wave velocity and shear modulus were normalized by utilizing the corresponding values of the void index. The normalized curves did not appear to normalize with respect to the I_v procedure.

The amount of inherent fabric anisotropy for specimens prepared at w_s of 1.5LL ranged from 0.89 to 0.97 for the kaolinite and from 0.63 to 0.74 for illite. However, the amount of inherent fabric anisotropy was between 1.13 and 1.21 for kaolinite specimens prepared at w_s of 3LL. These observations indicated that the fabric anisotropy characteristics of the natural soils could not be reproduced by reconsidering kaolinite and illite soils prepared at w_s of 1.5 LL. As documented herein, the w_s levels should be considered when reconstituting specimens of cohesive soils for small-strain measurements. Furthermore, the small-strain behavior of reconstituted kaolinite and illite soils cannot be simply quantified by reconstituting the soils at slurry water content values that range from 1 to 1.5 times the liquid limit of the soil, as suggested by Burland (1990).

Therefore, a water content of the slurry of at least 3LL is recommended to obtain small-strain characteristics of reconstituted soils that are more representative of the small-strain characteristics of natural soils.

6.10. References

Alvarado, G., and Coop, M. R., (2012). "On The Performance of Bender Elements in Triaxial Tests." Geotechnique, Vol. 62, No. 3, pp. 1–17.

ASTM Standard D2487 (2011). Unified Soil Classification System. ASTM International, West Conshohocken, PA, www.astm.org

ASTM Standard D4767 (2011). Standard Test Method for Consolidated Undrained Triaxial Compression Test for Cohesive Soils. ASTM International, West Conshohocken, PA, www.astm.org

Atkinson, J. H., Richardson, D. and Stallebrass, S.E., (1990). "Effect of Recent Stress History on the Stiffness of Overconsolidated Soil." Geotechnique, Vol. 40, No. 4, pp. 531-540.

Brignoli, E. G. M., Gotti, M., and Stokoe, K. H., II, (1996). "Measurement of Shear Waves in Laboratory Specimens by Means of Piezoelectric Transducers." Geotech. Test. J., Vol. 19, No. 4, pp. 384-397.

Burland, J. B., (1990). "On the Compressibility and Shear Strength of Natural Clays." Geotechnique, Vol. 40, No. 3, pp. 329-378.

Carrier, W. D., and Beckman, J. F., (1984). "Correlations Between Index Tests and the Properties of Remolded Clays." Geotechnique, Vol. 34, No. 2, pp. 211–228.

Cerato, A. B., and Lutenegger, A.J., (2004). "Determining Intrinsic Compressibility of Fine Grained Soils." Journal of Geotechnical and Geoenvironmental Engineering, Vol. 130, No. 8, pp. 872–877.

Chandler, R. J., (2000). "Clay Sediments in Depositional Basins: The Geotechnical Cycle." Quarterly J. of Eng. Geology and Hydrogeology, Vol. 33, No. 1, pp.7–39.

Cho, W., and Finno, R.J., (2010). "Stress-strain Responses of Block Samples of Compressible Chicago Glacial Clays." Journal of Geotechnical and Geoenvironmental Engineering, Vol. 136, No. 1, pp.178-188.

Choo, J., Jung, Y.H., Cho, W. and Chung, C.K., (2013). "Effect of Pre-Shear Stress Path on Nonlinear Shear Stiffness Degradation of Cohesive Soils." Geotech. Test. J., Vol. 36, No. 2. pp. 198-205.

Clayton, C. R. I., (2011). "Stiffness at Small Strain: Research and Practice." Geotechnique, Vol. 61, No1, pp. 5-37.

Coffman, R.A., Salazar, S.E., and Zhao, Y., (2014). "Discussion of measurement of stiffness anisotropy in kaolinite using bender element tests in a floating wall consolidometer by X. Kang, G.-C. Kang, B. Bate." Geotech. Test. J., Vol. 37, No. 6, pp. 1-5.

Duncan, J. M., and Seed, H. B., (1966). "Anisotropy and Stress Reorientation in Clay." Journal of the Soil Mechanics and Foundations Division, Vol. 92, No. 5, pp. 21-50.

Fam, M. and Santamarina, J. C., (1995). "Study of Geoprocesses with Complementary Mechanical and Electromagnetic Wave Measurements in an Oedometer." Geotech. Test. J., Vol. 18, No. 3, pp. 307–314.

Finno, R. J. and Cho, W., (2011). "Recent Stress-History Effects on Compressible Chicago Glacial Clays." Journal of Geotechnical and Geoenvironmental Engineering, Vol.137, No. 3, pp. 197-207.

Gasparre, A. and Coop, M., (2006). "Techniques for Performing Small-Strain Probes in the Triaxial Apparatus." Geotechnique, Vol. 56, No. 7, pp. 491–495.

Hardin, B. O. and Blandford, G. E., (1989). "Elasticity of Particulate Materials." Journal of Geotechnical Engineering, Vol. 115, No. 6, pp. 788-805.

Hong, Z. S., Bian, X., Cui, Y. J., Gao, Y. F., and Zeng, L. L., (2013). "Effect of Initial Water Content on Undrained Shear Behaviour of Reconstituted Clays." Geotechnique, Vol. 63, No. 6, pp. 441–450.

Jamiolkowski, M., Lancellotta, R., and Lo Presti, D. C. F., (1995). "Remarks on the Stiffness at Small Strains of Six Italian Clays." Proceedings of the International Symposium, In Pre-Failure Deformation of Geomaterials, Sapporo, Japan, pp. 817-845.

Jovicic, V. and Coop, M. R., (1998). "The Measurement of Stiffness Anisotropy in Clays with Bender Element Tests in the Triaxial Apparatus." Geotech. Test. J., Vol. 21, No. 1, pp. 3-10.

Kang, X., Kang, G.-C., and Bate, B., (2014). "Measurement of Stiffness Anisotropy in Kaolinite Using Bender Element Tests in A Floating Wall Consolidometer." Geotech. Test. J., Vol. 37, No. 5, pp. 869–883.

Ladd, C. C., and Foott, R., (1974). "New Design Procedure for Stability of Soft Clays." Journal of Geotechnical Engineering Division, Vol.100, No.7, pp. 763-768.

Lee, C., Lee, J. S., Lee, W., and Cho, H., (2007). "Experiment Setup for Shear wave and Electrical Resistance Measurements in an Oedometer." Geotech. Test. J., Vol. 31, No. 2, pp. 149-156.

Lings, M. L., Pennington, D. S., and Nash, D. F. T., (2000). "Anisotropic Stiffness Parameters and Their Measurement in a Stiff Natural Clay." Geotechnique, Vol. 50, No. 2, pp. 109–125.

Mahmood, N. S. and Coffman, R. A., (2017). "The Effects of Stress Path on the Characterization of Reconstituted Low Plasticity Kaolinite." Soils and Foundations (In Review, Manuscript Number: SANDF-D-17-00352-R1).

Mahmood, N. S. and Coffman, R. A., (2018a). "Intrinsic Shear Strength Behavior of Reconstituted Kaolinite and Illite Soils." Quarterly Journal of Engineering Geology and Hydrogeology, (In Review, Manuscript Number: qjegh2018-056-R1).

Martin, R. T. and Ladd, C. C. (1978). "Fabric of Consolidated Kaolinite." Clays and Clay Minerals J., Vol. 23, pp. 17-25

Mitchell, R. J., (1972). "Some Deviations from Isotropy in Lightly Overconsolidated Clay." Geotechnique, Vol. 22, No. 3, pp. 459-467.

Olson, R. E., (1962). "The Shear Strength Properties of Calcium Illite." Geotechnique, Vol.12, No. 1, pp. 23-43.

Richart, F. E., Hall, J. R., and Woods, R. D., (1970). "Vibrations of Soils and Foundations." Prentice-Hall, Inc., NJ.

Roesler, S. K., (1979). "Anisotropic Shear Modulus Due to Stress Anisotropy." Journal of the Geotechnical Engineering Division, Vol. 105, pp. 871-880.

Salazar, S. E. and Coffman, R. A., (2014). "Design and Fabrication of End Platens for Acquisition of Small-Strain Piezoelectric Measurements During Large-Strain Triaxial Extension and Triaxial Compression Testing." Geotech. Test. J., Vol. 37, No. 6, pp. 1-12.

Trhlikova, J., Masin, D., and Bohac, J., (2012). "Small-strain Behaviour of Cemented Soils." Geotechnique, Vo. 62, No. 10, pp. 943-947.

Viggiani, G. and Atkinson, J. H., (1995). "Stiffness of Fine-grained Soil at Very Small Strains. Geotechnique, Vol. 45, No. 2, pp. 249-265.

Yamashita, S., Hori, T., and Suzuki, T., (2003). "Effects of Initial and Induced Anisotropy on Initial Stiffness of Sand by Triaxial and Bender Elements Tests." Geomechanics: Testing, modeling, and simulation (GSP 143), A. J.Yamamuro and J.Koseki, eds., ASCE, Reston, Va., pp. 350–369.

Yimsiri, S. and Soga, K., (2000). "Micromechanics-based Stress- Strain Behaviour of Soils at Small Strains." Geotechnique, Vol. 50, No. 5, pp. 559–571.

Zeng, L. L., Hong, Z. S., Cai, Y. Q., and Han, J., (2011). "Change of Hydraulic Conductivity During Compression of Undisturbed and Remolded Clays." Applied Clay Science, Vol. 51, No. 1, pp. 86-93.

Zhao, Y. and Coffman, R.A., (2016). "Back-Pressure Saturated Constant-Rate-of-Strain Consolidation Device with Bender Elements: Verification of System Compliance." Journal of Testing and Evaluation, Vol.44, No.6, pp. 1-12.

Zhao, Y., Mahmood, N. S., Coffman, R.A., (2017). “Soil Fabric and Anisotropy as Observed Using Bender Elements During Consolidation.” Clays and Clay Minerals, (In Review, Manuscript Number: CCM-1143-R1).

Zhao, Y., Mahmood, N. S., Coffman, R.A., (2018). “Small-Strain and Large-Strain Modulus Measurements with a Consolidation Device.” Journal of Testing and Evaluation, (In Press).

CHAPTER 7: Conclusions and Recommendations

7.1. Chapter Overview

A description of the conclusions drawn from the findings of the research project, and recommendations for further research on reconstituted soils are contained in this chapter. Specifically, the contributions from the research project, as discussed in this document, are presented in Section 7.2. The conclusions drawn from the results obtained from this testing program, as described previously in Chapters 4 through 6, are provided in Section 7.3. Recommendations for additional work are presented in Section 7.4.

7.2. Selected Contributions from this Research Project

The purpose of this research project was to evaluate the compression, shear strength, and small-strain properties of reconstituted kaolinite and illite. The primary contributions of the research project are described briefly in this section. The stress path testing program consisted of utilizing advanced triaxial testing equipment to evaluate stress-strain and strength characteristics of reconstituted soils subject to different loading conditions. The need for advanced testing was associated with data from conventional triaxial testing being used for site characterization. The use of conventional triaxial data has often led to either unsafe or over-conservative designs. The primary contribution of this scope of the research was the development of an understanding of the testing techniques that are required to represent certain loading conditions in the field. Furthermore, the collected stress path testing data will be useful in the development or validation of advanced constitutive models. Using the new data, models that account for the various orientations of the principal stresses can be developed.

Historically, reconstituted specimens have been conveniently utilized to evaluate shear strength and small-strain behavior of cohesive soils. However, few studies have investigated the relationship between the slurry water content and 1) the intrinsic shear strength and 2) the

intrinsic small-strain behavior of the created soil specimens. Through the work described herein, a new method to normalize the intrinsic undrained shear strength values, using the void index concept, was introduced for overconsolidated specimens. Recommended values of slurry water content that should be used to prepare slurries of cohesive soils for triaxial testing and bender element measurements were also developed. These recommended levels of water content will produce reconstituted specimens with shear strength and small-strain soil properties that are in better agreement with shear strength and small-strain properties for natural soil specimens.

7.3. Conclusions of Intrinsic Properties of Reconstituted Soils

The conclusions drawn from the observations of the reconstituted soil properties are contained in this section. Conclusions related to the effect of stress path on 1) the stress-strain behavior and 2) the shear strength characteristics of reconstituted low plasticity kaolinite soil are documented in Section 7.3.1. The conclusions drawn from the triaxial testing program that was performed to evaluate the intrinsic shear strength behavior of reconstituted illite and kaolinite soils, are discussed in Section 7.3.2. Conclusions related to the 1) small-strain stiffness, and 2) fabric anisotropy of reconstituted illite and kaolinite soils are described in Section 7.3.

7.3.1. *Conclusions Regarding the Effects of Stress Path*

A triaxial testing program was performed on reconstituted low plasticity kaolinite soil to determine the effects of the magnitudes and orientations of the principal stresses on parameters including: shear strength, stress-strain behavior, and excess pore water pressure development. The stress-strain behavior, as obtained from the TC and RTC stress paths, was found to be almost identical as shown previously in Figure 4.8 on page 77. Likewise, the stress-strain behavior, as obtained from the TE and RTE stress paths, was found to be almost identical. As presented in Table 7.1, the effective friction angle (ϕ') values, as obtained from the extension

tests, were from 20 to 35 percent lower than the ϕ' values that were obtained from the compression tests. Likewise, the measured undrained shear strength values (s_u), as obtained from the extension tests, were from 11 to 38 percent lower than the s_u values that were obtained from the compression tests.

Table 7.1. Effective shear strength parameters for the different stress paths.

	TC		RTC		TE		RTE	
	c'	ϕ'	c'	ϕ'	c'	ϕ'	c'	ϕ'
OCR	[kPa]	[degree]	[kPa]	[degree]	[kPa]	[degree]	[kPa]	[degree]
1	10.6	17.7	12.1	17.5	36.8	13.5	27.6	13.9
2	7.2	18.1	7.1	18.8	22.7	14.2	14.9	14.4
4	2.4	19.6	5.0	19.9	18.8	15.6	18.1	14.9
8	0.8	20.7	1.4	20.4	15.5	17.0	18.1	15.6

The axial strain values, at failure, that were obtained from the extension tests were determined to be 0.3 to 5.0 percent greater than the axial strain values, at failure, that were obtained from the compression tests. For normally consolidated specimens, the values of undrained secant Young's modulus obtained from the compression tests were from two to two and one-half times greater than the values obtained from the extension tests. For overconsolidated specimens, there was no clear relationship between the undrained secant Young's modulus and the axial strain. Additionally, for all of the stress paths, the excess pore water pressure changed rapidly, as a function of axial stress, until the peak principle stress level was reached. For practical purposes, a series of TC tests along with a series of RTE tests are adequate to characterize the strength properties for cohesive soils when only the magnitude of the principal stresses is changed without a change in the orientation of the principal stresses. Furthermore, shear strength parameters, as obtained from these stress path tests, should be utilized to develop or validate soil constitutive models.

7.3.2. *Conclusions Regarding Intrinsic Shear Strength*

The intrinsic shear strength properties of reconstituted soils were evaluated by performing a series of triaxial compression tests on reconstituted kaolinite and illite specimens that were each reconstituted at two different levels of slurry water content (1.5 or 3.0 times the LL). A new method was proposed to normalize the undrained shear strength values for the overconsolidated specimens based on the void index concept. It was observed that compression behavior and undrained shear strength behavior for the reconstituted specimens were highly dependent on the level of the slurry water content. The *ICL* for each soil type was identical to the *ICL* that was proposed by Burland (1990). For each soil type, the intrinsic swell lines for all of the specimens were similar when the specimens were unloaded from the same level of the maximum stress, regardless of the slurry water content value that was used.

The undrained shear strength values of the specimens with w_s= 1.5LL were from 5 to 16 percent lower than the undrained shear strength values of the specimens with w_s = 3LL. The effective cohesion tended to increase as a function of increasing amount of w_s while the values of the effective friction angle values were independent of the w_s values. By utilizing the proposed normalization method, the normalized undrained shear strength values for the overconsolidated specimens were in a better agreement with the IS_uL. The kaolinite soil was more affected than the illite soil by an increase in the w_s values. Based on the observed soil fabric and the undrained shear strength values, reconstituting a low plasticity kaolinite soil at w_s =1.5 LL is not appropriate to evaluate the intrinsic shear strength behavior of this soil. Soil slurries should be prepared at water content values of at least three times the corresponding liquid limit of the soil to obtain undrained shear strength characteristics that are in better agreement with undrained shear strength characteristics for natural soils.

7.3.3. *Conclusions Regarding Small-Strain Measurements of Reconstituted Soils*

The effects of the slurry water content and the soil fabric on the small-strain properties of reconstituted kaolinite and illite soils were investigated by performing triaxial tests with bender element measurements. Values of shear wave velocity and shear modulus were normalized by utilizing the concept of void index. The major observations are summarized below.

1) At the same level of overconsolidation ratio and vertical effective stress, the V_s values for the kaolinite and illite specimens with w_s=1.5LL were from 7 to 41 percent greater than the V_s values for the specimens with w_s=3LL. Accordingly, the shear modulus values for the kaolinite and illite specimens prepared at w_s=1.5LL were from 1.1 to 2.1 times greater than the shear modulus values for the kaolinite and illite specimens prepared at w_s=3LL.
2) Unique intrinsic relationships for V_s-I_v or G_{BE}-I_v were not observed for the normalized values because the small-strain properties were highly dependent on the soil fabric.
3) Cross anisotropic characteristics of the fabric ($V_{s,HV} \approx V_{s,VH}$) were not observed for the kaolinite specimens that were prepared at w_s values of 3LL. When comparing the values of $V_{s,HV}$, as obtained by utilizing the BP-CRS-BE device, to the values of $V_{s,VH}$, the amount of fabric anisotropy ($V_{s,HV}/V_{s,VH}$) ranged from 1.13 to 1.21.
4) The inherent fabric anisotropy ranged from 0.63 to 0.97 for the kaolinite and illite specimens with w_s=1.5 LL, and ranged from 1.13 to 1.21 for the kaolinite specimens with w_s=3LL.
5) The w_s level should be considered when reconstituting cohesive soil specimens for small-strain measurements. Soil slurries should be prepared at water content values of at least three times the corresponding liquid limit of the soil to obtain small-strain characteristics that are in better agreement with small-strain characteristics for natural soils.

7.4. Recommendations for Future Work

Recommendations for further research, related to the intrinsic properties of the reconstituted soils, are summarized below.

1. Preparation and testing of reconstituted soils with various values of slurry water content is recommended for further examination of the findings of this research. The recommended slurry water content levels are one, two, and four times the liquid limit of the soil. By utilizing these levels of slurry water content, compression and shear strength characteristics different than those obtained from this research project are expected.
2. Preparation and testing of other soil types should be performed to examine the effect of mineralogy and plasticity index on the intrinsic soil properties that were investigated in this research project. The recommended soil types including, but not limited to, montmorillonite and high plasticity kaolinite.
3. The obtained experimental data should be utilized to review and assess previous empirical equations to calculate the coefficient of lateral earth pressure at rest (K_o). Specifically, the effect of 1) slurry water content, 2) OCR, and 3) shear strength parameters should be investigated when evaluating the ability of these empirical equations to predict the K_o values of reconstituted soils.
4. A comprehensive image analysis of the scanning electron microscope images should be performed to quantify the influence of the w_s level on the fabric of the reconstituted soils. Examples of image analyses to quantify soil fabric are described in Frost and Wright (1993).
5. Local strain measurements, such as LDVT, should be incorporated within the triaxial device to measure axial strain and radial strain at small-strain range (from 0.001 to 0.1 percent) during the consolidation and shearing stages of the triaxial tests.

6. Two additional sets of bender elements should be incorporated within the triaxial device. The first set should include two horizontally oriented bender elements to measure horizontally-propagated, vertically polarized shear wave velocity. The second set should include two vertically oriented bender elements to measure horizontally-propagated, horizontally polarized shear wave velocity. The propose of these sets is to evaluate fabric anisotropy within the same soil specimen.
7. The obtained experimental data may be utilized to developed new constitutive models to predict the behavior of reconstituted soils when subjected to different loading conditions. The developed models should account for the dependence of the compression and shear strength parameters on the soil structure and on the applied stress path.
8. The parameters that were obtained from this research project may be utilized to investigate the validity of selected constitutive models. The selected constitutive models to be validated may include, but are not limited to, 1) Modified Cam Clay (MCC) that was developed by Roscoe and Burland (1968), 2) MIT-E3 (Whittle and Kavvadas 1994), and 3) S-CLAY1 (Wheeler et al. 2003). The MCC model has been widely used with numerical and analytical methods in geotechnical engineering (Lade 2005). The MIT-E3 model and S-CLAY1 model were developed to account for soil anisotropy and soil structure (Whittle and Kavvadas 1994; Wheeler et al. 2003).

7.5. References

Burland, J.B., (1990). "On the Compressibility and Shear Strength of Natural Clays." Geotechnique, Vol.40, No. 3, pp. 329-378.

Frost, J. D., and Wright, J. R. (1993). "Digital Image Processing; Techniques and Applications in Civil Engineering." Proceedings, ASCE, New York.

Lade, P. V. (2005). "Overview of Constitutive Models for Soils." Soil Constitutive Models: Evaluation, selection and calibration, J. A. Yamamuro and V. N. Kaliakin, eds., ASCE, Reston, VA. pp 1-34.

Roscoe, K. H., and Burland, J. B. (1968). “On the Generalized Stress-strain Behaviour of “Wet” Clay.” Engineering Plasticity, J. Hayman and F. A. A. Leckie, eds., Cambridge Univ. Press, Cambridge, U.K. pp. 535-609.

Wheeler, S. J., Näätänen, A., Karstunen, M., and Lojander, M., (2003). “An Anisotropic Elastoplastic Model for Soft Clays.” Canadian Geotechnical Journal, Vol. 40, No. 2, pp. 403-418.

Whittle, A. J., and Kavvadas, M. J., (1994). “Formulation of MIT-E3 Constitutive Model for Overconsolidated Clays.” Journal of Geotechnical Engineering, Vol. 120, No. 1, pp. 173-198.

CHAPTER 8: References

Al Haj, K. M. A., and Standing, J. R., (2015). "Mechanical Properties of Two Expansive Clay Soils from Sudan." Geotechnique, Vol. 65, No.4, pp. 258-273.

Allman, M. A., and Atkinson, J. H., (1992). "Mechanical Properties of Reconstituted Bothkennar Soil." Geotechnique, Vol. 42, No.2, pp. 289-301.

Alvarado, G., and Coop, M. R., (2012). "On The Performance of Bender Elements in Triaxial Tests." Geotechnique, Vol. 62, No. 3, pp. 1–17.

American Society for Testing and Materials (2011). "Standard Practice for Classification of Soils for Engineering Purposes (Unified Soil Classification System)." Annual Book of ASTM Standards, Designation D2487, Vol. 4.08, ASTM, West Conshohocken, PA.

American Society for Testing and Materials (2011). "Standard Test Method for Unconsolidated-Undrained Triaxial Compression Test on Cohesive Soils." Annual Book of ASTM Standards, Designation D4767, Vol. 4.08, ASTM, West Conshohocken, PA.

Amorosi, A., Callisto, L., and Rampello, S., (1999). "Observed Behavior of Reconstituted Clay Along Stress Paths Typical of Excavations." Proceedings of the Second International Symposium on Pre-Failure Deformation Characteristics of Geomaterials, Torino, Italy, pp. 28-30. CRC Press.

Atkinson, J. H., (2000). "Non-linear Soil Stiffness in Routine Design." Geotechnique, Vol.50, No. 5, pp 487-508.

Atkinson, J. H., Richardson, D. and Stallebrass, S.E., (1990). "Effect of Recent Stress History on the Stiffness of Overconsolidated Soil." Geotechnique, Vol. 40, No. 4, pp. 531-540.

Atkinson, J. H., Richardson, D., and Robinson, P. J., (1987). "Compression and Extension of K_0 Normally Consolidated Kaolin Clay." Journal of Geotechnical Engineering, Vol.113. No. 12, pp. 1468-1482.

Atkinson, J.H., Richardson, D. and Stallebrass, S.E., (1990). "Effect of Recent Stress History on the Stiffness of Overconsolidated Soil." Geotechnique, Vol.40, No. 4, pp.531-540.

Atkinson, J.H., Richardson, D., and Robinson, P.J., (1987). "Compression and Extension of K_o Normally Consolidated Kaolin Clay." Journal of Geotechnical Engineering, Vol. 113, No.12, pp.1468-1482.

Baldi, G., Hight, D. W., and Thomas, G. E. (1988). "A Reevaluation of Conventional Triaxial Test Methods." Advanced triaxial testing of soil and rock." ASTM STP, 977, 219-263.

Bayoumi, A., (2006). "New Laboratory Test Procedure for the Enhanced Calibration of Constitutive Models." Doctoral dissertation, Georgia Institute of Technology, GA.

Bishop, A. W., (1966). “The strength of soils as engineering materials.” Geotechnique, Vol. 16, pp. 91-130.

Bishop, A.W., and Henkel, D.J. (1962). “The Measurement of Soil Properties in the Triaxial Test.” Edward Arnold LTD, London.

Bjerrum, L., (1973). “Problems of Soil Mechanics and Construction on Soft Clays and Structurally Unstable Soils (Collapsible, Expansive and others).” In Proceeding of 8th International Conference on SMFE ,Vol. 3, pp. 111-159.

Bjerrum, L., Frimann, L.J., Has, M. and Duncan, J.M., (1972). “Earth Pressures on Flexible Structures.” A State-of-the-Art-Report; Procedding of the 5th European Conference on Soil Mechanics and Foundations Engineering, Madrid, Vol 2, pp. pp.169 - 196.

Bjerrum, L., Simons, N., and Toblaa, I., (1958). “The Effect of Time on the Shear Strength of a Soft Marine Clay.” Proceedings of Conference on Earth Pressure Problems, I, pp.148-158.

Brignoli, E. G. M., Gotti, M., and Stokoe, K. H., II, (1996). “Measurement of Shear Waves in Laboratory Specimens by Means of Piezoelectric Transducers.” Geotech. Test. J., Vol. 19, No. 4, pp. 384-397.

Bryson, L. S., and Salehian, A. (2011). “Performance of Constitutive Models in Predicting Behavior of Remolded Clay.” Acta Geotechnica, Vol. 6, No. 3, pp.143-154.

Burland, J. B., (1990). “On the Compressibility and Shear Strength of Natural Clays.” Geotechnique, Vol. 40, No. 3, pp. 329-378.

Carrier, W. D., and Beckman, J. F., (1984). “Correlations Between Index Tests and the Properties of Remolded Clays.” Geotechnique, Vol. 34, No. 2, pp. 211–228.

Cerato, A. B., and Lutenegger, A. J., (2004). “Determining Intrinsic Compressibility of Fine Grained Soils.” Journal of Geotechnical and Geoenvironmental Engineering, Vol. 130, No. 8, pp. 872–877.

Chandler, R. J., (2000). “Clay Sediments in Depositional Basins: The Geotechnical Cycle.” Quarterly J. of Eng. Geology and Hydrogeology, Vol. 33, No. 1, pp.7–39.

Cho, W., and Finno, R.J., (2010). “Stress-strain Responses of Block Samples of Compressible Chicago Glacial Clays.” Journal of Geotechnical and Geoenvironmental Engineering, Vol. 136, No. 1, pp.178-188.

Choo, J., Jung, Y.H., Cho, W. and Chung, C.K., (2013). “Effect of Pre-Shear Stress Path on Nonlinear Shear Stiffness Degradation of Cohesive Soils.” Geotech. Test. J., Vol. 36, No. 2. pp. 198-205.

Clayton, C. R. I., (2011). “Stiffness at Small Strain: Research and Practice.” Geotechnique, Vol. 61, No1, pp. 5-37.

Clayton, C.R.I., and Heymann, G., (2001). “Stiffness of Geomaterials at Very Small Strains.” Geotechnique, Vol. 51, No. 3, pp 245–255.

Coffman, R. A., Bowders, J. J., and Burton, P. M., (2010). “Use of SHANSEP Design Parameters in Landfill Design: A Cost/Benefit Case Study.” ASCE Geotechnical Special Publication No. 199, Proceedings GeoFlorida 2010, Advances in Analysis, Modeling and Design, West Palm Beach, FL, Feb 20–24, pp. 2859–2866.

Coffman, R. A., Bowders, J. J., and Burton, P. M., (2010). “Use of SHANSEP Design Parameters in Landfill Design: A Cost/Benefit Case Study.” ASCE Geotechnical Special Publication No. 199, Proceedings GeoFlorida 2010, Advances in Analysis, Modeling and Design, West Palm Beach, FL, Feb 20–24, pp. 2859–2866.

Coffman, R.A., Salazar, S.E., and Zhao, Y., (2014). “Discussion of measurement of stiffness anisotropy in kaolinite using bender element tests in a floating wall consolidometer by X. Kang, G.-C. Kang, B. Bate.” Geotech. Test. J., Vol. 37, No. 6, pp. 1-5.

Coop, M. R., Atkinson, J. H., and Taylor. R. N., (1995). “Strength, yielding and Stiffness of Structured and Unstructured Soils.” Proceedings of the 11th European Conference on Soil Mechanics and Foundation Engineering, Copenhagen, Denmark, Vol. 28.

Cotecchia, F., and Chandler, R.J., (1997). “The Influence of Structure on the Pre-Failure Behaviour of a Natural Clay.” Geotechnique, Vol. 47, No. 3, pp. 523-544.

Davis, E. H., and Poulos, H. G., (1972). “Rate of Settlement Under Two-and Three-dimensional Conditions.” Geotechnique, Vol. 22, No. 1.

Davis, E.H. and Poulos, H.G., (1968). “The Use of Elastic Theory for Settlement Prediction under Three-dimensional Conditions.” Geotechnique, Vol.18, No. 1, pp.67-91.

Duncan, J. M., and Seed, H. B., (1966). “Anisotropy and Stress Reorientation in Clay.” Journal of the Soil Mechanics and Foundations Division, Vol. 92, No. 5, pp. 21-50.

Fam, M. and Santamarina, J. C., (1995). “Study of Geoprocesses with Complementary Mechanical and Electromagnetic Wave Measurements in an Oedometer.” Geotech. Test. J., Vol. 18, No. 3, pp. 307–314.

Fearon, R.E., and Coop, M.R., (2000). “Reconstitution: What Makes an Appropriate Reference Material?.” Geotechnique, Vol. 50, No. 4, pp. 471-477.

FHWA (2007). “Earth Retaining Structures, Reference Manual.” Publication No. FHWA NHI-07-071. USDOT FHWA, National Highway Institute, December, pp. 2-41.

Finno, R. J. and Cho, W., (2011). “Recent Stress-History Effects on Compressible Chicago Glacial Clays.” Journal of Geotechnical and Geoenvironmental Engineering, Vol.137, No. 3, pp. 197-207.

Frost, J. D., and Wright, J. R. (1993). “Digital Image Processing; Techniques and Applications in Civil Engineering.” Proceedings, ASCE, New York.

Gasparre, A. and Coop, M., (2006). “Techniques for Performing Small-Strain Probes in the Triaxial Apparatus.” Geotechnique, Vol. 56, No. 7, pp. 491–495.

Gens, A., (1983). “Stress-strain and Strength Characteristics of a Low Plasticity Clay.” Doctoral dissertation, University of London, London, England.

Hansen, J. B., and Gibson, R. E., (1949). “Undrained Shear Strengths of Anisotropically Consolidated Clays.” Geotechnique, Vol.1, No. 3, pp.189-200.

Hardin, B. O. and Blandford, G. E., (1989). “Elasticity of Particulate Materials.” Journal of Geotechnical Engineering, Vol. 115, No. 6, pp. 788-805.

Hardin, B.O. and Blandford, G.E., (1989). “Elasticity of Particulate Material.” Journal of Geotechnical Engineering, Vol. 115, No. 6, pp.788-805.

Hardin, B.O. and Drnevich, V.P. (1972). “Shear Modulus and Damping in Soils: Measurement and Parameter Effects.” Journal of Soil Mechanics and Foundations Division, ASCE. Vol. 98, No. 6, pp. 603-624.

Hashash, Y., Wotring, D., Yao, J., Lee, J. and Fu, Q. (2002). “Visual Framework for Development and Use of Constitutive Models.” International Journal for Numerical and Analytical Methods in Geomechanics, Vol. 26. No. 15, pp. 1493-1513.

Henkel, D.J. (1956). “The Effect of Overconsolidation on the Behavior of Clays During Shear.” Geotechnique, Vol. 6, No. 4, pp.139-150.

Hirschfield, R. C. (1958). “Factors Influencing the Constant Volume of Clays.” Doctoral dissertation, Howard University, Washington, DC.

Holtz, R. D., Kovacs, W. D., and Sheahan, T. C., (2011). “An Introduction to Geotechnical Engineering.” 2nd Ed. Pearson Education, Upper Saddle River, NJ.

Hong, Z. S., Bian, X., Cui, Y. J., Gao, Y. F., and Zeng, L. L., (2013). “Effect of Initial Water Content on Undrained Shear Behaviour of Reconstituted Clays.” Geotechnique, Vol. 63, No. 6, pp. 441–450.

Hong, Z. S., Yin, J., Cui, Y. J., (2010). “Compression Behaviour of Reconstituted Soils at High Initial Water Contents.” Geotechnique, Vol. 60, No. 9, pp. 691-700.

Hong, Z.S., Bian, X., Cui, Y.J., Gao, Y.F., and Zeng, L.L., (2013). “Effect of Initial Water Content on Undrained Shear Behaviour of Reconstituted Clays.” Geotechnique, Vol. 63, No. 6, pp. 441-450.

Jafroudi, S., (1983). “Experimental Verification of Bounding Surface Plasticity Theory for Cohesive Soils.” Doctoral dissertation, University of California, Davis, CA.

Jamiolkowski, M., Ladd, C.C., Germaine, J. and Lancellotta, R., (1985). "New Developments in Field and Lab Testing of Soils." Proceedings 11th Intl. Conference on Soil Mechanics and Foundations Engineering, San Francisco, Vol. 2, pp. 57-154.

Jamiolkowski, M., Lancellotta, R., and Lo Presti, D. C. F., (1995). "Remarks on the Stiffness at Small Strains of Six Italian Clays." Proceedings of the International Symposium, In Pre-Failure Deformation of Geomaterials, Sapporo, Japan, pp. 817-845.

Jovicic, V. and Coop, M. R., (1998). "The Measurement of Stiffness Anisotropy in Clays with Bender Element Tests in the Triaxial Apparatus." Geotech. Test. J., Vol. 21, No. 1, pp. 3-10.

Kang, X., Kang, G.-C., and Bate, B., (2014). "Measurement of Stiffness Anisotropy in Kaolinite Using Bender Element Tests in A Floating Wall Consolidometer." Geotech. Test. J., Vol. 37, No. 5, pp. 869–883.

Kavvadas, M., and Amorosi, A., (2000). "A constitutive Model for Structured Soils." Geotechnique, Vol. 50, No. 3, pp. 263-273.

Kulhawy, F. H., and Mayne, P. W., (1990). "Manual on Estimating Soil Properties for Foundation Design." Electric Power Res. Inst. EL-6800; Prof. 1493-6, Electric Power Research Inst., Palo Alto, CA, pp. 4-5.

Ladd, C. C., and DeGroot, D. J., (2003). "Recommended Practice for Soft Ground Site Characterization: Arthur Casagrande Lecture." In 12th Panamerican Conference on Soil Mechanics and Geotechnical Engineering Vol. 1, pp. 1-57.

Ladd, C. C., and Foott, R., (1974). "New Design Procedure for Stability of Soft Clays." Journal of Geotechnical Engineering Division, Vol.100, No.7, pp. 763-768.

Ladd, C. C., and Varallyay, J., (1965). "The Influence of Stress System on the Behavior of Saturated Clays During Undrained Shear." No. RR-R65-11. Massachusetts Institute of Technology, Cambridge Soil Mechanics Div.

Ladd, C.C. (1991). "Stability Evaluation During Staged Construction (22nd Terzaghi Lecture)." Journal of Geotechnical Engineering. Vol. 117 No. 4, pp. 540-615.

Ladd, C.C., Bovee, R.B., Edgers, L. and Rixner, J.J., (1971). "Consolidated-undrained Plane Strain Shear Tests on Boston Blue Clay." Research Report R71-13, No. 273, No. 284, Massachusetts Institute of Technology, Cambridge, pp. 243.

Lade, P. V. (2005). "Overview of Constitutive Models for Soils." Soil constitutive models: Evaluation, selection and calibration, J. A. Yamamuro and V. N. Kaliakin, eds., ASCE, Reston, VA. pp 1-34.

Lade, P. V., and Duncan, J. M., (1999). "Stress-path Independent Behavior of Cohesionless Soil." Journal of the Geotechnical Engineering Division, Vol.102. No. 1, pp. 51-68.

Lambe, T. W. (1967). “Stress Path Method.” Journal of Soil Mechanics and Foundations Division,

Lambe, T. W., and Whitman, R. V., (1969). “Soil Mechanics.” John Wiley and Sons, New York.

Lee, C., Lee, J. S., Lee, W., and Cho, H., (2007). “Experiment Setup for Shear wave and Electrical Resistance Measurements in an Oedometer.” Geotech. Test. J., Vol. 31, No. 2, pp. 149-156.

Lings, M. L., Pennington, D. S., and Nash, D. F. T. (2000). “Anisotropic Stiffness Parameters and their Measurement in a Stiff Natural Clay.” Geotechnique, Vol. 50, No. 2, pp. 109-125.

Liu, Y. (2004). “The Stress-Strain Behavior of Kaolin Clay in Triaxial.” Ph.D. Thesis. University of Delaware. Newark, DE.

Mahmood, N. S. and Coffman, R. A., (2017). “The Effects of Stress Path on the Characterization of Reconstituted Low Plasticity Kaolinite.” Soils and Foundations (In Review, Manuscript Number: SANDF-D-17-00352-R1).

Mahmood, N. S. and Coffman, R. A., (2018a). “Intrinsic Shear Strength Behavior of Reconstituted Kaolinite and Illite Soils.” Quarterly Journal of Engineering Geology and Hydrogeology, (In Review, Manuscript Number: qjegh2018-056-R1).

Mahmood, N. S., and Coffman, R. A., (2018b). “Small-strain of Reconstituted Soils: The Effect of Slurry Water Content.” Geotechnical Testing Journal, (Under Review, Manuscript Number: GTJ-2018-0098-R1).

Martin, R. T. and Ladd, C. C. (1978). “Fabric of Consolidated Kaolinite.” Clays and Clay Minerals J., Vol. 23, pp. 17-25

Mitchell, J.K., and Soga, K., (2005). “Fundamental of Soil Behavior, 3rd Edition.” John Wiley and Sons, New York.

Mitchell, R. J., (1972). “Some Deviations from Isotropy in Lightly Overconsolidated Clay.” Geotechnique, Vol. 22, No. 3, pp. 459-467.

Moniz, Safia R., (2009). “The Influence of Effective Consolidation Stress on the Normalized Extension Strength Properties of Resedimented Boston Blue Clay.” MEng Thesis, MIT, Cambridge, MA.

Nash, D.F.T., Lings, M.L., and Pennington, D.S., (1999). “The Dependence of Anisotropy G_0 Shear Moduli on Void Ratio and Stress State for Reconstituted Gault Clay.” Proc., 2nd Int. Symp. on Pre-Failure Deformation Characteristics of Geomaterials, Torino, pp. 229-238.

Olson, R. E., (1962). “The Shear Strength Properties of Calcium Illite.” Geotechnique, Vol.12, No. 1, pp. 23-43.

Parry, R. H. G., (1960). "Triaxial Compression and Extension Tests on Remolded Clay." Geotechnique, Vol. 10, No. 4, pp. 160-188.

Parry, R. H. G., (2004). "Mohr Circles, Stress Paths and Geotechnics." Spon Press, London.

Parry, R.H.G. and Nadarajah, V., (1974). "Observations on Laboratory Prepared, Lightly Overconsolidated Specimens of Kaolin." Geotechnique, Vol. 24, No. 4, pp.345-357.

Pennington, D. S., Nash, D. F. T., and Lings, M. L., (1997). "Anisotropy of G_0 Shear Stiffness in Gault Clay." Geotechnique, Vol. 47, No. 3, pp. 391-398.

Prashant, A. and Penumadu, D., (2005). "A Laboratory Study of Normally Consolidated Kaolin Clay." Canadian Geotechnical Journal, Vol. 42, No. 1, pp.27-37.

Prashant, A., and Penumadu, D., (2007). "Effect of Microfabric on Mechanical Behavior of Kaolin Clay Using Cubical True Triaxial Testing." J. Geotech. Geoenviron. Eng. Vol. 133, No. 4, pp. 433-444.

Race, M.L., Coffman, R.A., (2011). "Effects of Piston Uplift, Piston Friction, and Machine Deflection in Reduced Triaxial Extension Testing." ASCE Geotechnical Special Publication No. 211, Proc. GeoFrontiers 2011: Advances in Geotechnical Engineering, Dallas, Texas, March, pp. 2649-2658.

Richart, F. E., Hall, J. R., and Woods, R. D., (1970). "Vibrations of Soils and Foundations." Prentice-Hall, Inc., NJ.

Roesler, S. K., (1979). "Anisotropic Shear Modulus Due to Stress Anisotropy." Journal of the Geotechnical Engineering Division, Vol. 105, pp. 871-880.

Roesler, S. K., (1979). "Anisotropic Shear Modulus due to Stress Anisotropy." J. Geotech. Eng. Div., Vol. 105, No. 7, pp. 871-880.

Roscoe, K. H., and Burland, J. B. (1968). "On the Generalized Stress-strain Behaviour of "Wet" Clay." Engineering plasticity, J. Hayman and F. A. A. Leckie, eds., Cambridge Univ. Press, Cambridge, U.K. pp. 535-609.

Roscoe, K. H., Schofield, A., and Wroth, C., P., (1958). "On the Yielding of Soils." Geotechnique, Vol. 8, No.1, pp. 22-53.

Rossato, G., Ninis, N. L., and Jardine, R. J., (1992). "Properties of Some Kaolin-based Model Clay Soils." Geotech. Test. J., Vol. 15, No. 2, pp.166-179.

Saada, A.S. and Bianchini, G.F., (1977). "Strength of One Dimensionally Consolidated Clays." Journal of Geotechnical and Geoenvironmental Engineering, Vol. 103, (HGT-6), pp. 655-660.

Salazar, S. E. and Coffman, R. A., (2014). "Design and Fabrication of End Platens for Acquisition of Small-Strain Piezoelectric Measurements During Large-Strain Triaxial

Extension and Triaxial Compression Testing." Geotechnical Testing Journal, Vol. 37, No. 6, pp. 1-12.

Salazar, S. E., Miramontes, L. D., Barnes, A.R., Bernhardt, M.L., Coffman, R.A., (2017). "Verification of an Internal Close-range Photogrammetry Approach for Volume Determination During Undrained Triaxial Testing." Geotech. Test. J. (Under Second Review, Manuscript Number: GTJ-2017-0125-R1).

Salazar, Sean E. and Coffman, Richard A. (2015). "Consideration of Internal Board Camera Optics for Triaxial Testing Applications." Geotechnical Testing Journal, Vol. 38, No. 1, pp. 1–10.

Santagata, M. C. (2008). "Effects of Stress History on the Stiffness of a Soft Clay." Proceeding Deformational Characteristics of Geomaterials, Keynote Lecture, IOS Press/Millpress.

Scholey, G. K., Frost, J. D., Lo Presti, D. C. E, and Jamiolkowski, M. (1996). "A Review of Instrumentation for Measuring Small Strains During Triaxial Testing of Soil Specimens." Geotechnical Testing Journal, GTJODJ, Vol. 18, No. 2, pp. 137-156.

Sheahan, T. C. (1991). "An Experimental Study of the Time-dependent Undrained Shear Behavior of Resedimented Clay Using Automated Stress Path Triaxial Equipment." Doctoral dissertation, Massachusetts Institute of Technology, MA.

Sheahan, T.C., Ladd, C.C., and Germaine, J.T., (1996). "Rate-dependent Undrained Shear Behavior of Saturated Clay." Journal of Geotechnical Engineering, Vol. 122, No. 2, pp. 99-108.

Simons, N. E. and Som, N. N. (1970). "Settlement of Structures on Clay: with Particular Emphasis on London Clay." Construction industry research and information Association, London. Report 22.

Skempton, A. W. (1954) "The Pore-pressure Coefficients A and B." Geotechnique, Vol. 4, No. 4, pp.143-147.

Skempton, A. W. and Henkel, D. J. (1957). "Test on London Clay from Deep Boarding at Paddington, Victoria and South Bank." Proceeding of the 4th International Conference on Soil Mechanics and Foundation Engineering, Vol.1, No.100, London, U.K.

Stipho, A. S. A. (1978). "Experimental and Theoretical Investigation of the Behavior of Anisotropically Consolidated Kaolin." Doctoral Dissertation, University College, Cardiff, U.K.

Taylor, D. W. (1948). "Fundamentals of Soil Mechanics." John Wiley and Sons, New York, NY.

Theile (2016). "Product Information for Clay Products." Theile Kaolin Company. https://www.thielekaolin.com/sites/default/files/inline-files/KAOWHITE%20S_0.pdf. Accessed April 2016.

Tiwari, B., and Ajmera, B., (2011). "New Correlation Equations for Compression Index of Remolded Clays." Geotechnical and Geoenvironmental Engineering, Vol. 138, No. 6, pp. 757-762.

Trhlikova, J., Masin, D., and Bohac, J., (2012). "Small-strain Behaviour of Cemented Soils." Geotechnique, Vo. 62, No. 10, pp. 943-947.

VandenBerge, D. R., Duncan, J. M., and Brandon, T. L., (2015). "Undrained Strength of Compacted Clay Under Principal Stress Reorientation." J. Geotech. Geoenviron. Eng., Vol. 141, No. 8, pp.1-11.

Viggiani, G. and Atkinson, J. H. (1995). "Interpretation of Bender Element Tests." Geotechnique Vol. 45, No. 1, pp.149-154.

Wang, Y. and Ng, C.W., (2005). "Effects of Stress Paths on the Small-strain Stiffness of Completely Decomposed Granite." Canadian geotechnical journal, Vol. 42, No. 4, pp.1200-1211.

Wheeler, S. J., Näätänen, A., Karstunen, M., and Lojander, M., (2003). "An Anisotropic Elastoplastic Model for Soft Clays." Canadian Geotechnical Journal, Vol. 40. No. 2, pp. 403-418.

Whittle, A. J., and Kavvadas, M. J., (1994). "Formulation of MIT-E3 Constitutive Model for Overconsolidated Clays." Journal of Geotechnical Engineering, Vol. 120, No. 1, pp. 173-198.

Woods, R.D. and Partos, A., (1981). "Control of Soil Improvement by Crosshole Testing." Jn Proceeding to the 10th International Conference on Soil Mechanics and Foundation Engineering, Stockholm, pp. 793-796.

Wroth, C. P., (1984). "The Interpretation of in Situ Soil Tests." Geotechnique, Vol. 34, No. 4, pp. 449-489.

Wroth, C. P., (1984). "The Interpretation of in Situ Soil Tests." Geotechnique, Vol. 34, No. 4, pp. 449-489.

Wu, W., and Kolymbas, D., (1991). "On Some Issues in Triaxial Extension Tests." Geotechnical Testing Journal, Vol. 14, No. 3, pp. 276-287.

Yamashita, S., Hori, T., and Suzuki, T., (2003). "Effects of Initial and Induced Anisotropy on Initial Stiffness of Sand by Triaxial and Bender Elements Tests." Geomechanics: Testing, modeling, and simulation (GSP 143), A. J.Yamamuro and J.Koseki, eds., ASCE, Reston, Va., pp. 350–369.

Yamashita, S., Jamiolkowski, M., and Presti, D.C.F., (2000). "Stiffness Nonlinearity of Three Sands." Journal of Geotechnical and Geoenvironmental Engineering, Vol. 126, No.10, pp. 929-938.

Yimsiri, S. and Soga, K., (2000). “Micromechanics-based Stress- Strain Behaviour of Soils at Small Strains.” Geotechnique, Vol. 50, No. 5, pp. 559–571.

Yimsiri, S., Soga, K., (2002). “Application of Micromechanics Model to Study Anisotropy of Soils at Small Strain.” Soil and Foundations, Vol. 42, pp. 15-26.

Yin, J., and Miao, Y., (2013). “Intrinsic Compression Behavior of Remolded and Reconstituted Clays-Reappraisal.” Open Journal of Civil Engineering, Vol.3, No. 3, pp. 8-12.

Zdravkovic, L. (1996). “The Stress-strain-strength Anisotropy of a Granular Medium under General Stress Conditions.” Doctoral Dissertation, Imperial College, London, UK.

Zeng, L. L., Hong, Z. S., Cai, Y. Q., and Han, J., (2011). “Change of Hydraulic Conductivity During Compression of Undisturbed and Remolded Clays.” Applied Clay Science, Vol. 51, No. 1, pp. 86-93.

Zhao, Y. and Coffman, R.A., (2016). “Back-Pressure Saturated Constant-Rate-of-Strain Consolidation Device with Bender Elements: Verification of System Compliance.” Journal of Testing and Evaluation, Vol.44, No.6, pp. 1-12.

Zhao, Y., and Coffman, R.A., (2016). “Back-Pressure Saturated Constant-Rate-of-Strain Consolidation Device with Bender Elements: Verification of System Compliance.” Journal of Testing and Evaluation, Vol. 44, No. 6, pp. 1-12.

Zhao, Y., Mahmood, N. S., and Coffman, R. A., (2017). “Soil Fabric and Anisotropy as Observed Using Bender Elements during Consolidation.” Clays and Clay Minerals, (Under Review, Manuscript Number: CCM-1143-R1).

Zhao, Y., Mahmood, N. S., and Coffman, R.A., (2018). “Small-Strain and Large-Strain Modulus Measurements with a Consolidation Device.” Journal of Testing and Evaluation, In Press, Manuscript Number: JTE-2016-0331.

APPENDIX A: Triaxial Testing Data

A.1. Chapter Overview

Continued in this appendix are 1) the initial values and the physical properties of the specimens and 2) the triaxial tests values, and 3) the bender elements measurements, as obtained from the laboratory testing program.

A.2. Specimen Properties

Contained in this section are 1) data collected during specimen preparation within the slurry consolidometer, and 2) initial physical properties of the specimens. The specimens were pre-consolidated by utilizing a slurry consolidometer. The time-consolidation curves for the prepared slurries were developed from the data collected during the pre-consolidation process. The time-consolidation curves for the kaolinite specimens that were used for the controlled stress path triaxial tests are presented in Figure A.1. The time-consolidation curves for the kaolinite and illite specimens that were used for the triaxial tests with bender element measurements are presented in Figure A.2.

The initial properties of the specimens were measured after the specimens were removed from the slurry consolidometer following the pre-consolidation process. A summary of the initial properties of the specimen, that were used for the controlled stress path triaxial tests, is presented in Table A.1. The initial properties of the specimens that were used for the triaxial tests with bender element measurements are presented in Table A.2.

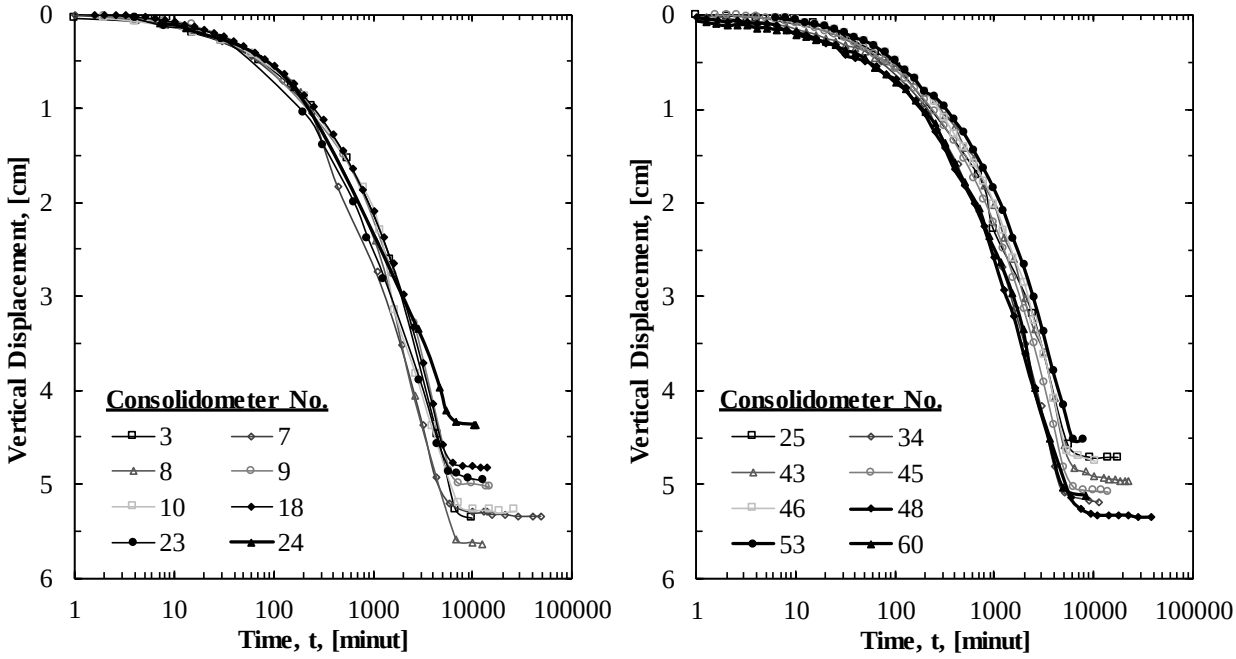

Figure A.1. Time-consolidation curves for the kaolinite specimens that were used for the stress path tests.

Table A.1. The initial properties of the specimen used for the stress path triaxial tests.

			Consolidometer		Specimen				
Test	OCR	$\sigma'_{v,max}$ [kPa]	No.	Slurry Height, [cm]	Length [cm]	w [%]	γ_T [kN/m^3]	S [%]	e
TC	1	310	3	26.9	7.67	31.4	18.0	94.20	0.89
		414	3	26.9	7.87	31.4	18.0	93.15	0.90
		828	7	27.1	7.84	30.6	18.0	92.84	0.88
TC	2	310	7	27.1	7.65	31.5	18.0	93.45	0.90
		414	8	27.4	7.85	31.8	18.2	91.30	0.93
		828	8	27.4	7.90	31.2	18.0	92.56	0.90
TC	4	310	9	22.5	7.59	31.6	18.1	90.72	0.93
		414	9	22.5	7.62	31.3	18.2	94.97	0.88
		828	13	22.1	7.82	31.5	18.1	94.50	0.89
TC	8	310	10	22.8	7.86	31.3	18.1	89.86	0.93
		414	13	22.1	7.65	31.2	18.0	93.60	0.89
		828	10	22.8	7.98	31.7	18.0	94.04	0.90
RTC	1	310	34	22.5	7.52	31.6	18.2	95.88	0.88
		414	39	22.1	7.92	31.3	17.9	91.84	0.91
		828	39	22.1	7.59	30.5	18.0	92.54	0.88
RTC	2	310	34	22.5	7.65	31.5	17.9	92.42	0.91
		414	43	22.9	7.80	31.4	18.1	94.20	0.89
		828	41	22.2	7.98	32.0	18.0	94.93	0.90
RTC	4	310	43	22.9	7.92	31.2	18.1	94.66	0.88
		414	44	22.8	7.34	32.2	18.0	94.48	0.91
		828	45	22.1	7.75	31.7	18.1	95.10	0.89
RTC	8	310	45	22.1	7.87	31.7	17.9	93.01	0.91
		414	60	22.6	7.89	31.7	18.2	96.18	0.88
		828	60	22.6	7.82	30.5	18.3	95.81	0.85
TE	1	310	46	23.4	7.98	30.6	18.1	93.91	0.87
		414	48	21.9	7.98	31.8	18.0	94.34	0.90
		828	48	21.9	7.80	31.3	18.1	94.97	0.88
TE	2	310	54	22.5	7.62	31.5	18.0	94.50	0.89
		414	49	23.1	7.90	30.1	18.2	93.45	0.86
		828	55	22.1	7.80	31.7	18.2	96.18	0.88
TE	4	310	54	22.5	7.54	30.1	18.2	94.55	0.85
		414	53	21.2	7.82	31.4	18.0	94.20	0.89
		828	53	21.2	7.82	30.1	18.2	94.55	0.85
TE	8	310	55	22.1	8.03	31.2	18.0	93.60	0.89
		414	46	23.4	7.72	31.9	18.2	95.70	0.89
		828	47	22.7	7.98	30.6	18.0	92.84	0.88
RTE	1	310	21	22.5	7.72	30.6	18.0	92.84	0.88
		414	23	22.5	7.98	31.1	18.1	94.36	0.88
		828	18	22.8	7.62	31.3	18.0	93.90	0.89
RTE	2	310	18	22.8	7.85	30.7	18.1	94.22	0.87
		414	23	22.5	7.73	31.4	18.2	95.27	0.88
		828	19	22.2	7.80	30.4	17.8	90.19	0.90
RTE	4	310	21	22.5	7.65	30.9	18.1	93.75	0.88
		414	24	20.8	7.80	31.5	17.8	91.42	0.92
		828	22	22.7	7.44	31.5	17.9	92.42	0.91
RTE	8	310	24	20.8	7.76	31.5	18.0	93.45	0.90
		414	25	22.4	7.67	31.3	18.0	88.91	0.94
		828	25	22.4	7.98	31.3	17.9	92.86	0.90

w, γ_T, S, e are water content, total unit weight, degree of saturation, and void ratio of the specimens respectively.

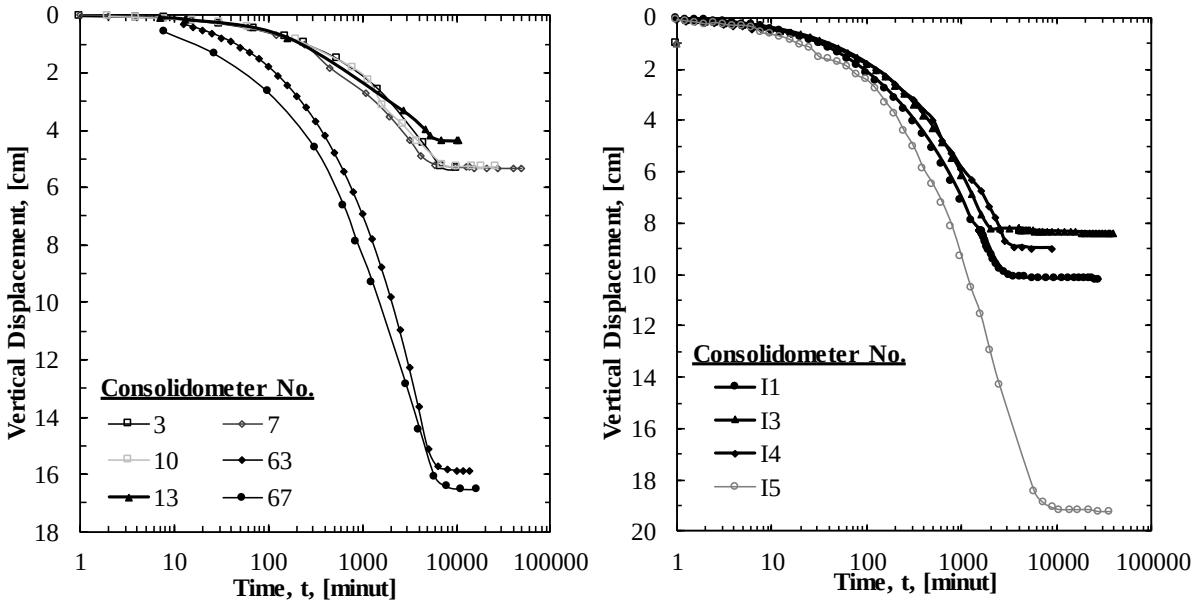

Figure A.2. Time-consolidation curves for the a) kaolinite and b) illite specimens that were utilized for the triaxial tests with bender element measurements.

Table A.2. The initial properties of the specimen used for the triaxial tests with bender elements.

			Consolidometer		Specimen				
Test	OCR	$\sigma'_{v,max}$ [kPa]	No.	Slurry Height, [cm]	Length [cm]	w [%]	γ_T [kN/m^3]	S [%]	e
K1.5LL-NC	1	310	3	26.9	7.67	31.4	18.0	94.20	0.89
		414	3	26.9	7.87	31.4	18.0	93.15	0.90
		828	7	27.1	7.84	30.6	18.0	92.84	0.88
K3LL-NC	1	310	59	32.1	7.98	38.7	17.4	96.6	1.07
		414	63	33.4	8.01	38.3	17.4	96.5	1.06
		828	59	32.1	7.72	37.7	18.0	100.0	1.00
K1.5LL-OC	8	310	10	22.8	7.86	31.3	18.1	89.86	0.93
		414	13	22.1	7.65	31.2	18.0	93.60	0.89
		828	10	22.8	7.98	31.7	18.0	94.04	0.90
K3LL-OC	8	310	63	33.4	7.62	37.5	17.6	99.1	1.01
		414	67	31.7	7.80	37.4	17.9	99.9	1.00
		828	67	31.7	7.90	37.4	18.1	100.0	0.99
I1.5LL-NC	1	310	I1	34.5	7.80	37.7	17.9	100.0	1.00
		414	I1	34.5	7.59	35.2	17.6	95.6	0.99
		828	I2	33.4	7.66	37.8	17.4	98.7	1.03
I3LL-NC	1	310	I5	41.5	7.87	42.6	17.0	97.9	1.17
		414	I5	41.5	7.62	42.1	17.0	97.6	1.16
		828	I7	38.4	7.84	42.6	17.0	97.1	1.18
I1.5LL-OC	8	310	I2	33.4	7.55	38.9	16.9	94.3	1.11
		414	I3	34.3	7.61	36.6	17.5	96.5	1.02
		828	I4	32.6	7.92	35.9	17.7	97.5	0.99
I3LL-OC	8	310	I7	38.4	8.10	40.1	17.0	95.5	1.13
		414	I8	43.2	7.62	39.8	17.1	95.6	1.12
		828	I9	42.8	7.72	42.6	17.0	97.1	1.18

w, γ_T, S, e are water content, total unit weight, degree of saturation, and void ratio of the specimens respectively.

A.3. Triaxial Tests Data

Included in this section are the results obtained from the triaxial tests that were performed on the kaolinite and illite specimens. The triaxial tests data, for the specimens that were used for the controlled stress path triaxial tests are summarized in Table A.3 and Table A.4. The results of the triaxial tests with bender element measurements that were conducted on kaolinite and illite specimens are summarized in Tables A.5 and Table A.6. The triaxial test data are also presented as 1) deviatoric stress as a function of axial strain, 2) excess pore water pressure as a function of axial strain, 3) Mohr circle, and 4) Cambridge p-q stress path, as recommended by ASTM D4767 (2011).

Table A.3. Summary of triaxial test values as obtained from the stress path testing program.

				Triaxial Tests Values at Failure					Specimen Values (after shearing)			
Test	*OCR*	$\sigma'_{v,max}$ [kPa]	K_o	$\sigma'_{v,f}$ [kPa]	$\sigma'_{c,f}$ [kPa]	$\sigma'_{d,f}$ [kPa]	$\varepsilon_{,f}$ [%]	$u_{e,f}$ [kPa]	w [%]	γ_T [kN/m^3]	S [%]	e
		310	0.715	354.50	169.10	185.40	7.28	44.90	29.8	18.6	98.2	0.81
TC	1	414	0.714	479.85	243.15	236.70	8.27	49.21	27.8	18.5	92.8	0.80
		828	0.681	871.25	447.02	424.23	7.03	110.82	27.1	19.1	100.0	0.72
		310	0.785	235.76	114.71	121.06	8.52	-9.32	29.5	18.5	96.1	0.82
TC	2	414	0.761	322.90	155.22	167.68	6.02	-2.60	29.3	18.4	94.3	0.83
		828	0.785	638.19	324.58	313.61	5.73	-2.36	28.1	19.1	100	0.74
		310	0.777	181.10	84.95	96.14	8.88	-32.74	30.1	17.1	82.0	0.98
TC	4	414	0.872	242.61	118.49	124.12	9.00	-37.79	29.9	18.6	97.4	0.82
		828	0.773	382.91	183.91	199.00	5.52	-27.19	29.1	19.1	100	0.75
		310	0.912	116.74	53.31	63.42	8.77	-23.25	31.0	17.8	91.0	0.91
TC	8	414	0.856	149.96	71.69	78.27	8.03	-29.57	29.9	18.2	93.9	0.85
		828	0.914	287.25	135.58	151.67	8.28	-42.10	28.7	18.8	98.2	0.78
		310	0.700	358.14	180.82	177.32	9.92	120.26	28.8	18.8	98.6	0.78
RTC	1	414	0.729	487.72	238.45	249.27	10.22	157.76	27.8	18.6	95.2	0.78
		828	0.698	868.45	453.37	415.08	8.76	300.70	27.3	19.3	100	0.71
		310	0.889	248.13	119.13	129.00	9.35	134.89	30.3	18.7	100	0.80
RTC	2	414	0.892	349.43	176.03	173.40	7.36	162.78	28.6	18.7	96.7	0.79
		828	0.844	668.73	337.42	331.31	8.33	274.65	30.0	19.4	100.0	0.74
		310	1.043	200.17	93.43	106.73	8.34	142.94	29.8	18.4	95.9	0.83
RTC	4	414	0.874	257.19	121.03	136.16	8.59	167.28	29.5	18.5	96.1	0.82
		828	0.876	409.60	194.22	215.38	8.20	256.84	28.0	18.8	98.4	0.76
		310	1.060	126.81	55.51	71.30	9.90	117.81	30.3	18.3	95.2	0.85
RTC	8	414	1.000	163.12	75.62	87.50	9.30	148.08	30.1	18.7	99.2	0.81
		828	0.952	296.38	138.38	158.00	9.60	290.58	29.5	19.0	99.9	0.77
		310	0.683	92.37	280.46	-188.08	-11.09	95.70	29.4	18.9	99.87	0.78
TE	1	414	0.662	138.65	379.84	-241.19	-11.59	133.43	29.1	18.9	100.0	0.77
		828	0.667	298.40	649.51	-351.11	-9.76	261.17	28.8	19.4	99.87	0.72
		310	0.831	65.28	198.17	-132.89	-10.66	77.05	29.9	19.3	106.4	0.75
TE	2	414	0.980	102.02	261.32	-159.30	-10.12	85.32	30.1	19.0	103.0	0.78
		828	0.902	215.20	476.57	-261.37	-10.40	168.84	30.2	19.3	107.5	0.75
		310	1.024	37.05	120.05	-83.00	-9.22	31.33	29.7	18.7	99.1	0.80
TE	4	414	0.963	48.33	172.38	-124.05	-10.18	59.83	30.8	18.9	99.8	0.80
		828	0.975	143.20	344.37	-201.17	-10.60	94.17	29.8	19.3	98.4	0.75
		310	0.906	13.04	93.86	-80.82	-9.18	22.85	30.2	18.4	97.1	0.83
TE	8	414	0.985	28.24	120.12	-91.88	-9.41	35.31	29.8	18.4	95.9	0.83
		828	1.107	67.77	208.01	-140.24	-11.18	59.06	29.5	19.2	98.7	0.75
		310	0.675	94.57	257.78	-163.21	-9.77	-65.73	29.5	19.2	105.0	0.75
RTE	1	414	0.686	141.33	358.49	-217.16	-10.02	-93.85	28.1	18.8	97.4	0.77
		828	0.676	313.92	657.24	-343.33	-10.78	176.23	26.8	19.1	99.4	0.72
		310	0.630	70.74	187.99	-117.26	-13.04	-81.11	29.1	18.7	98.4	0.79
RTE	2	414	0.877	108.11	246.09	-137.98	-11.26	114.54	28.8	18.7	97.3	0.79
		828	0.844	225.73	470.84	-245.11	-10.52	195.15	27.2	19.0	98.1	0.74
		310	0.725	35.64	127.37	-91.73	-10.77	131.34	29.9	18.5	96.2	0.83
RTE	4	414	0.879	51.63	171.91	-120.28	-11.27	160.82	30.0	18.7	100.0	0.80
		828	0.919	147.36	344.90	-197.54	-12.27	340.73	28.3	18.5	94.5	0.80
		310	0.977	17.43	100.78	-83.35	-10.28	-70.98	30.0	18.2	94.2	0.85
RTE	8	414	1.040	28.24	119.25	-91.01	-10.02	102.05	29.6	17.2	97.6	0.81
		828	0.980	71.91	208.07	-136.17	-11.77	201.10	28.7	18.6	95.8	0.80

Table A.4. The effective shear strength parameters as obtained from the controlled stress path triaxial tests.

	TC		RTC		TE		RTE	
OCR	c' [kPa]	ϕ' [degree]	c' [kPa]	ϕ' [degree]	c' [kPa]	ϕ' [degree]	c' [kPa]	ϕ' [degree]
1	10.6	17.7	12.1	17.5	36.8	13.5	27.6	13.9
2	7.2	18.1	7.1	18.8	22.7	14.2	14.9	14.4
4	2.4	19.6	5.0	19.9	18.8	15.6	18.1	14.9
8	0.8	20.7	1.4	20.4	15.5	17.0	18.1	15.6

Table A.5. Summary of the triaxial test values as obtained from the triaxial tests with bender element measurements.

			Triaxial Tests Values at Failure					Specimen Values (after shearing)			
Test	*OCR*	$\sigma'_{v,max}$ [kPa]	$\sigma'_{v,f}$ [kPa]	$\sigma'_{c,f}$ [kPa]	$\sigma'_{d,f}$ [kPa]	$\varepsilon_{,f}$ [%]	$u_{e,f}$ [kPa]	w [%]	γ_T [kN/m^3]	S [%]	e
K1.5LL-NC	1	310	354.50	169.10	185.40	7.28	44.90	29.8	18.6	98.2	0.81
		414	479.85	243.15	236.70	8.27	49.21	27.8	18.5	92.8	0.80
		828	871.25	447.02	424.23	7.03	110.82	27.1	19.1	100.0	0.72
K3LL-NC	1	310	169.63	41.19	128.44	4.73	2.66	28.1	16.9	77.9	0.96
		414	258.87	77.67	181.20	2.23	-8.51	29.5	18.2	89.3	0.88
		828	384.70	120.93	263.78	3.93	-26.98	27.4	17.9	86.8	0.84
K1.5LL-OC	8	310	116.74	53.31	63.42	8.77	-23.25	31.0	17.8	91.0	0.91
		414	149.96	71.69	78.27	8.03	-29.57	29.9	18.2	93.9	0.85
		828	287.25	135.58	151.67	8.28	-42.10	28.7	18.8	98.2	0.78
K3LL-OC	8	310	154.73	31.83	122.90	3.18	4.98	35.5	18.0	99.8	0.95
		414	254.81	83.75	171.06	4.83	-18.46	34.8	18.5	99.8	0.93
		828	389.50	123.27	266.23	4.93	-29.99	28.9	17.5	85.1	0.91
I1.5LL-NC	1	310	265.99	108.91	157.08	1.32	67.63	31.0	18.5	99.1	0.84
		414	450.66	192.89	257.77	0.15	23.16	29.0	19.9	99.5	0.78
		828	841.87	371.07	470.80	0.68	103.41	25.1	20.5	99.4	0.68
I3LL-NC	1	310	169.63	41.19	128.44	4.73	2.66	28.7	18.2	98.7	0.78
		414	258.87	77.67	181.20	2.23	-8.51	29.3	18.5	97.1	0.81
		828	384.70	120.93	263.78	3.93	-26.98	25.0	18.9	93.7	0.72
I1.5LL-OC	8	310	226.40	86.60	139.80	1.71	100.51	31.3	18.5	100.0	0.84
		414	383.00	146.00	237.00	0.95	74.95	29.5	19.1	99.7	0.80
		828	762.73	316.14	446.59	2.13	274.66	26.1	19.4	98.0	0.72
I3LL-OC	8	310	154.73	31.83	122.90	3.18	4.98	31.9	18.1	97.4	0.88
		414	254.81	83.75	171.06	4.83	-18.46	30.3	18.7	99.3	0.82
		828	389.50	123.27	266.23	4.93	-29.99	25.0	18.9	93.7	0.72

Table A.6. Shear strength parameters for kaolinite and illite soils as obtained from the triaxial tests with bender element measurements.

Test	*OCR*	$\sigma'_{v,max}$ [kPa]	c' [kPa]	ϕ' [degree]	R^*_{su}	s^*_u *[kPa]*
K1.5LL-NC	1	310	10.62	17.69	0.299	92.7
		414			0.286	118.3
		828			0.256	212.1
K3LL-NC	1	310	18.31	17.55	0.277	85.8
		414			0.238	98.6
		828			0.241	199.7
K1.5LL-OC	8	310	0.85	20.70	0.871	31.7
		414			0.782	39.1
		828			0.756	75.8
K3LL-OC	8	310	4.26	18.47	0.782	30.4
		414			0.671	37.3
		828			0.763	73.7
I1.5LL-NC	1	310	7.79	21.98	0.253	78.5
		414			0.312	128.9
		828			0.285	235.4
I3LL-NC	1	310	9.40	23.38	0.225	69.9
		414			0.286	118.5
		828			0.270	223.3
I1.5LL-OC	8	310	13.07	27.43	1.663	64.2
		414			1.752	90.6
		828			1.570	131.9
I3LL-OC	8	310	13.34	26.09	1.592	61.5
		414			1.654	85.5
		828			1.580	133.1

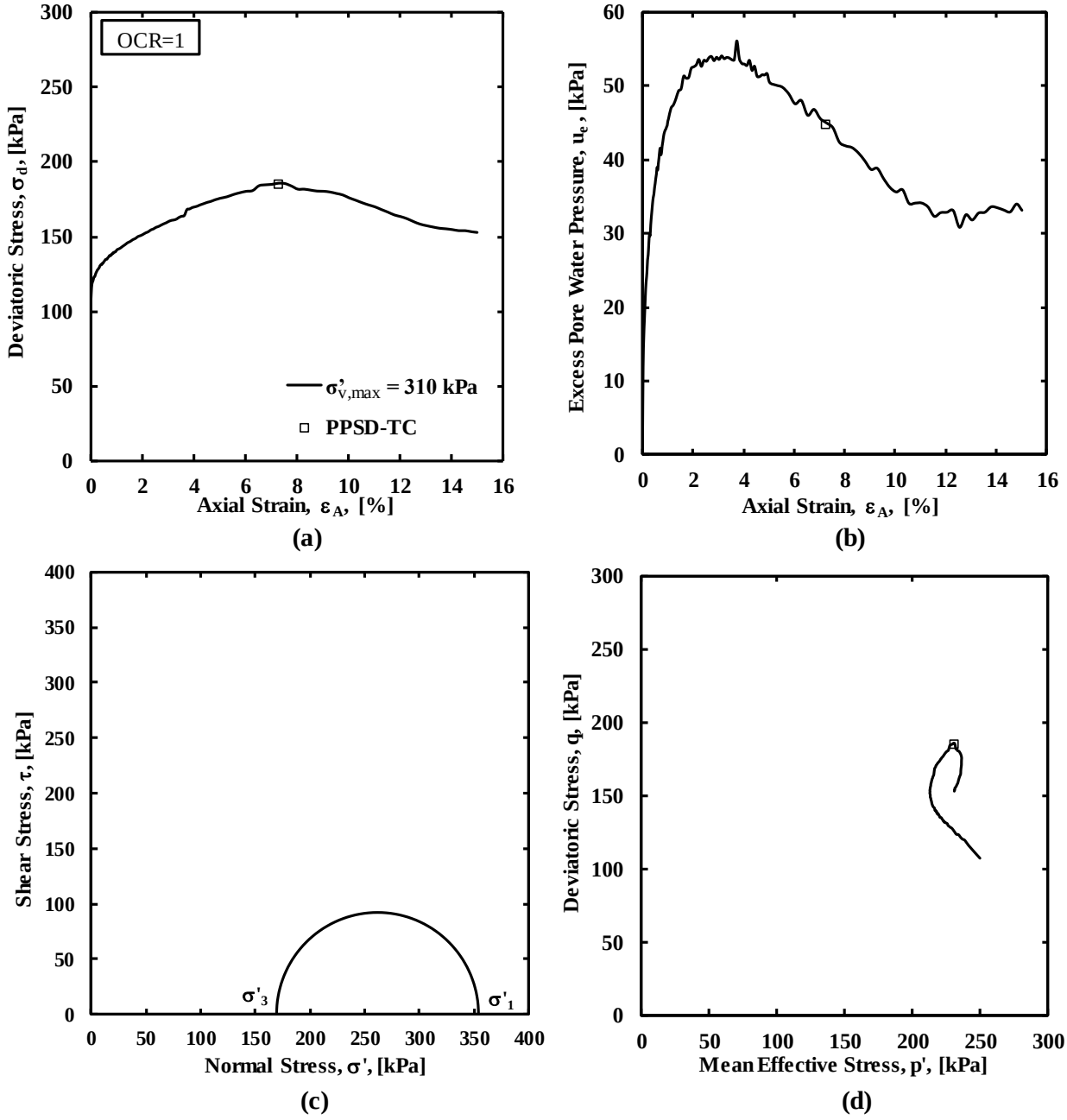

Figure A.3. a) Deviatoric stress as a function of axial strain, b) excess pore water pressure as a function of axial strain, c) Mohr circle, and d) Cambridge p-q stress path for the TC test at OCR=1 and σ'$_{v,max}$=310 kPa.

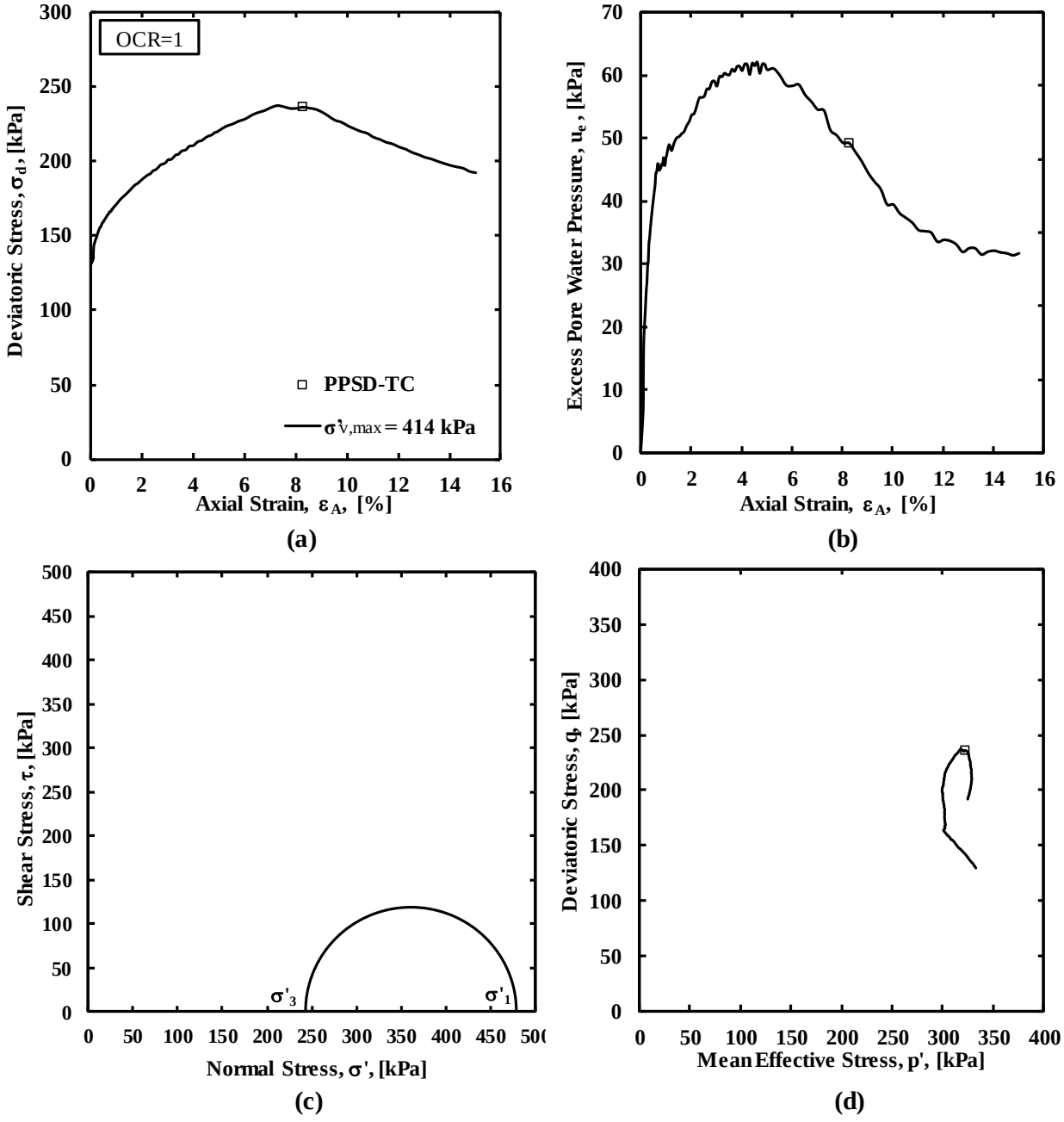

Figure A.4. a) Deviatoric stress as a function of axial strain, b) excess pore water pressure as a function of axial strain, c) Mohr circle, and d) Cambridge p-q stress path for the TC test at OCR=1 and $\sigma'_{v,max}$=414 kPa.

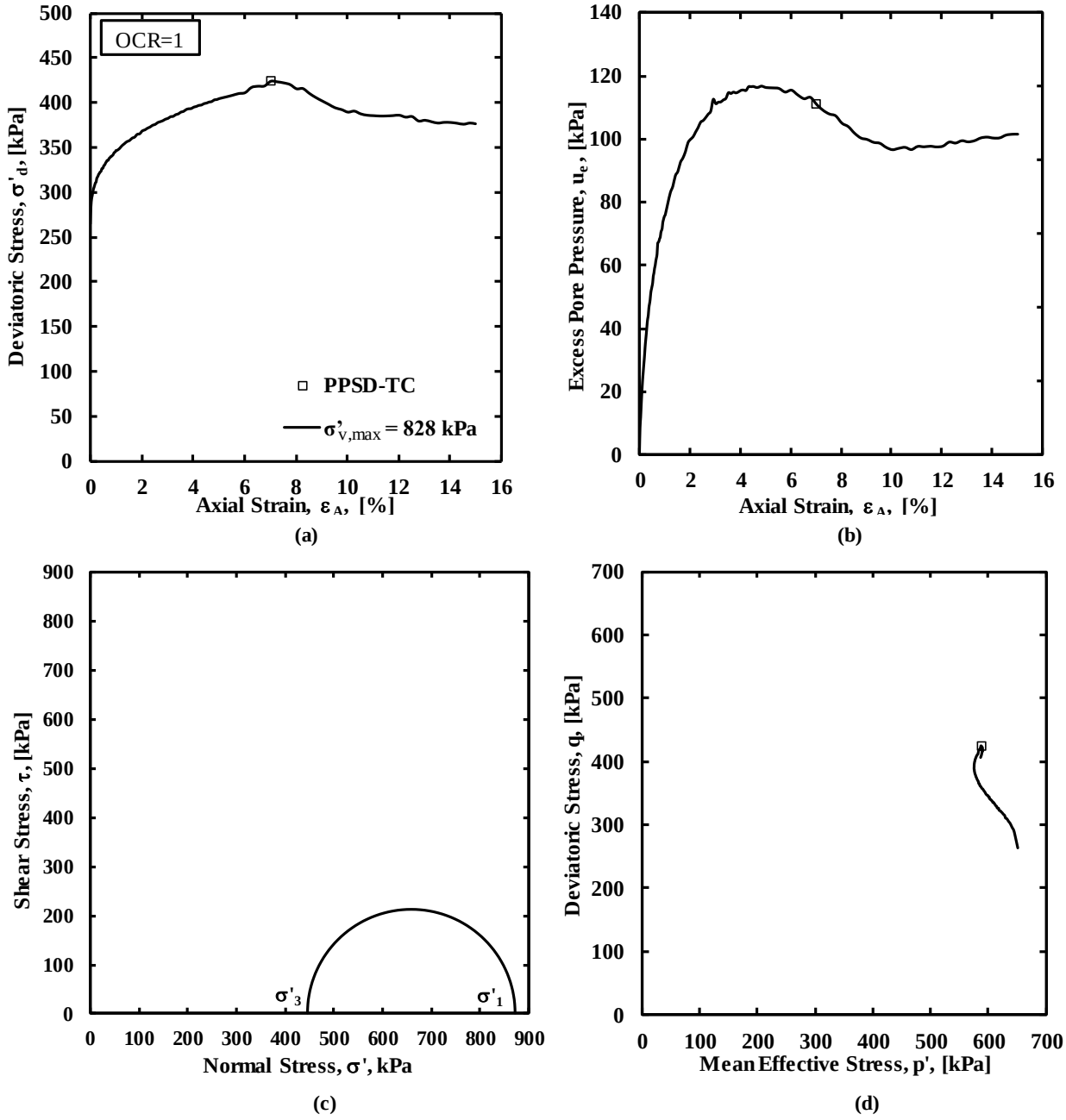

Figure A.5. a) Deviatoric stress as a function of axial strain, b) excess pore water pressure as a function of axial strain, c) Mohr circle, and d) Cambridge p-q stress path for the TC test at OCR=1 and $\sigma'_{v,max}$=828 kPa.

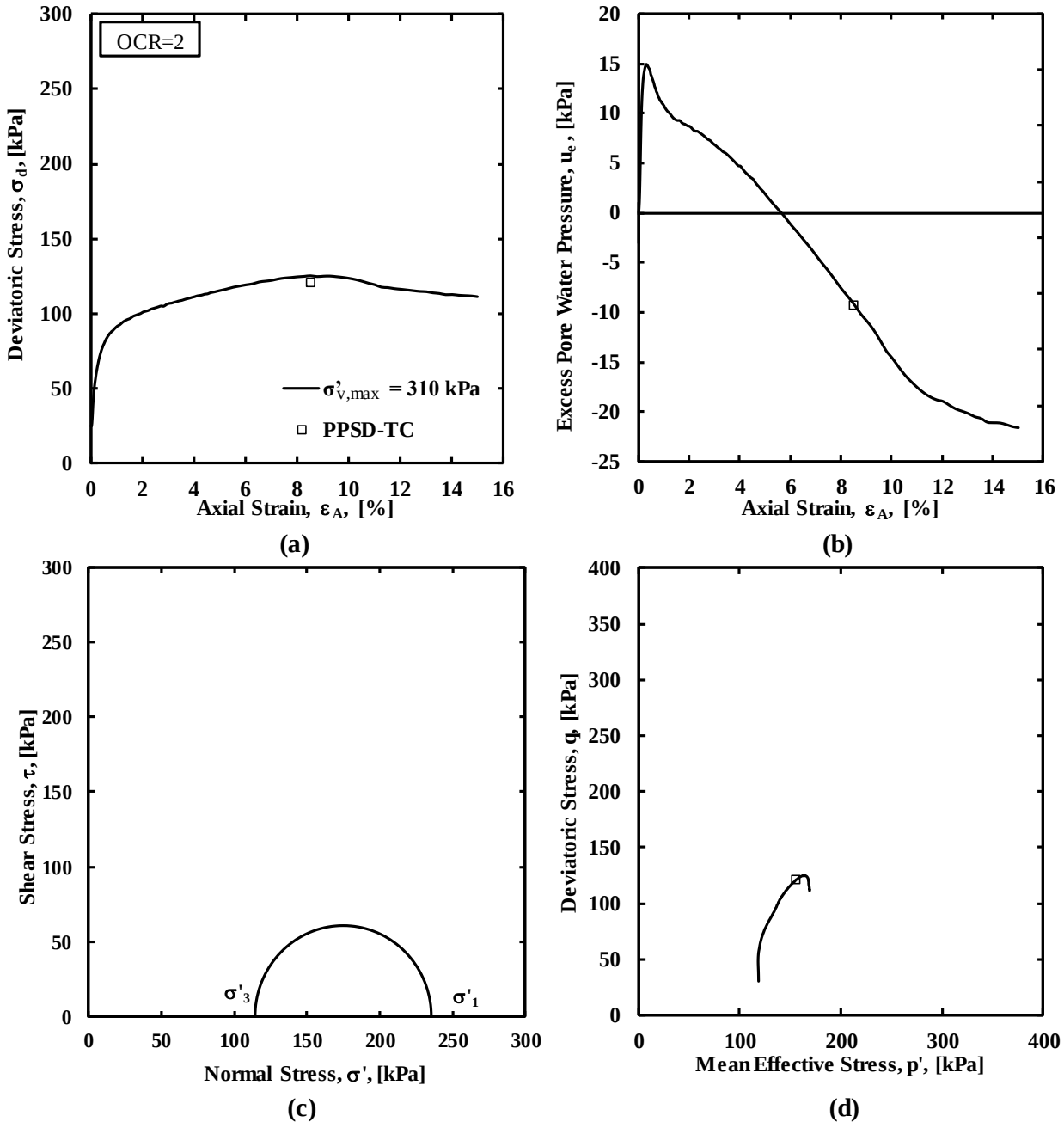

Figure A.6. a) Deviatoric stress as a function of axial strain, b) excess pore water pressure as a function of axial strain, c) Mohr circle, and d) Cambridge p-q stress path for the TC test at OCR=2 and $\sigma'_{v,max}$=310 kPa.

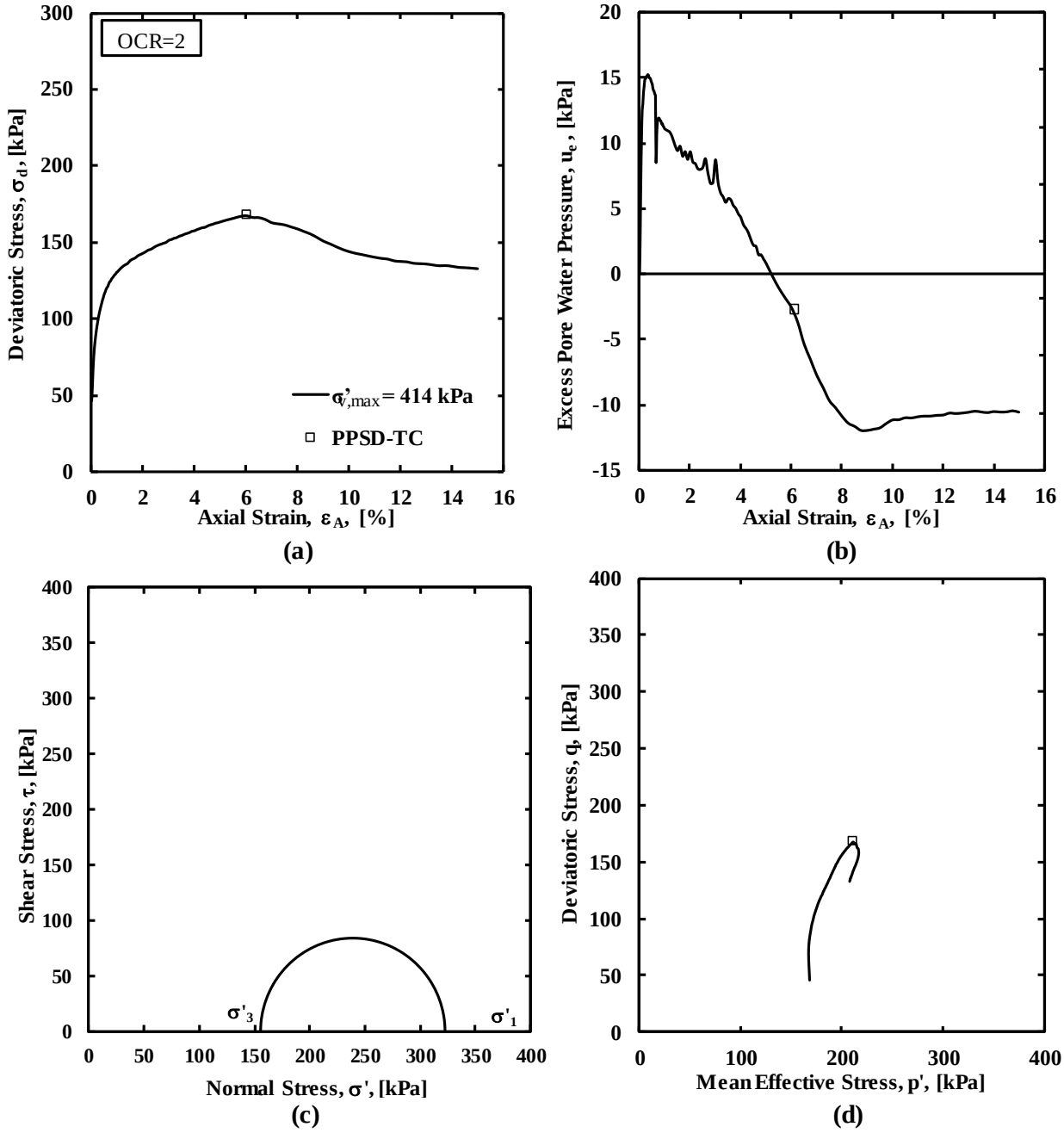

Figure A.7. a) Deviatoric stress as a function of axial strain, b) excess pore water pressure as a function of axial strain, c) Mohr circle, and d) Cambridge p-q stress path for the TC test at OCR=2 and σ'$_{v,max}$=414 kPa.

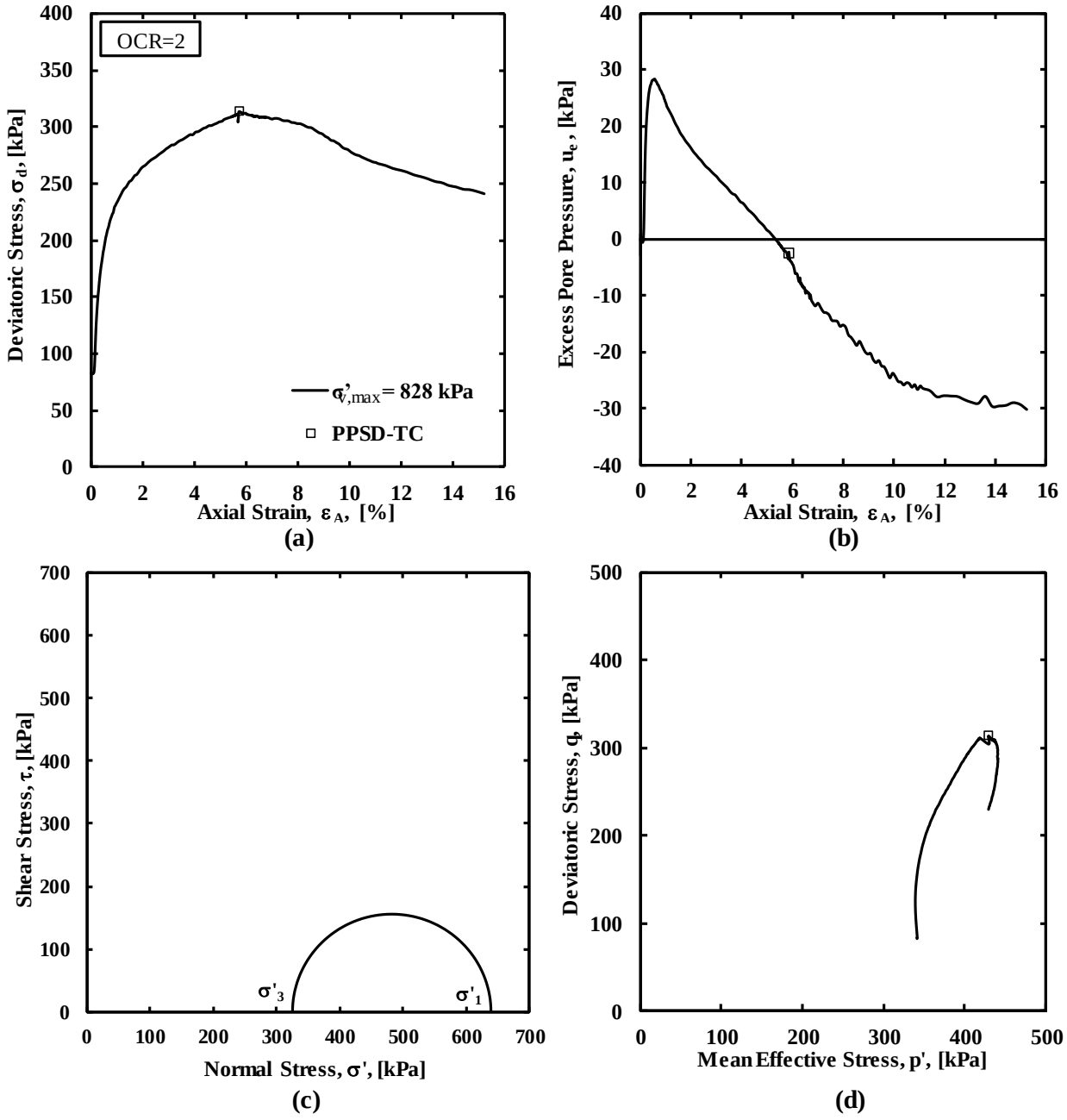

Figure A.8. a) Deviatoric stress as a function of axial strain, b) excess pore water pressure as a function of axial strain, c) Mohr circle, and d) Cambridge p-q stress path for the TC test at OCR=2 and $\sigma'_{v,max}$=828 kPa.

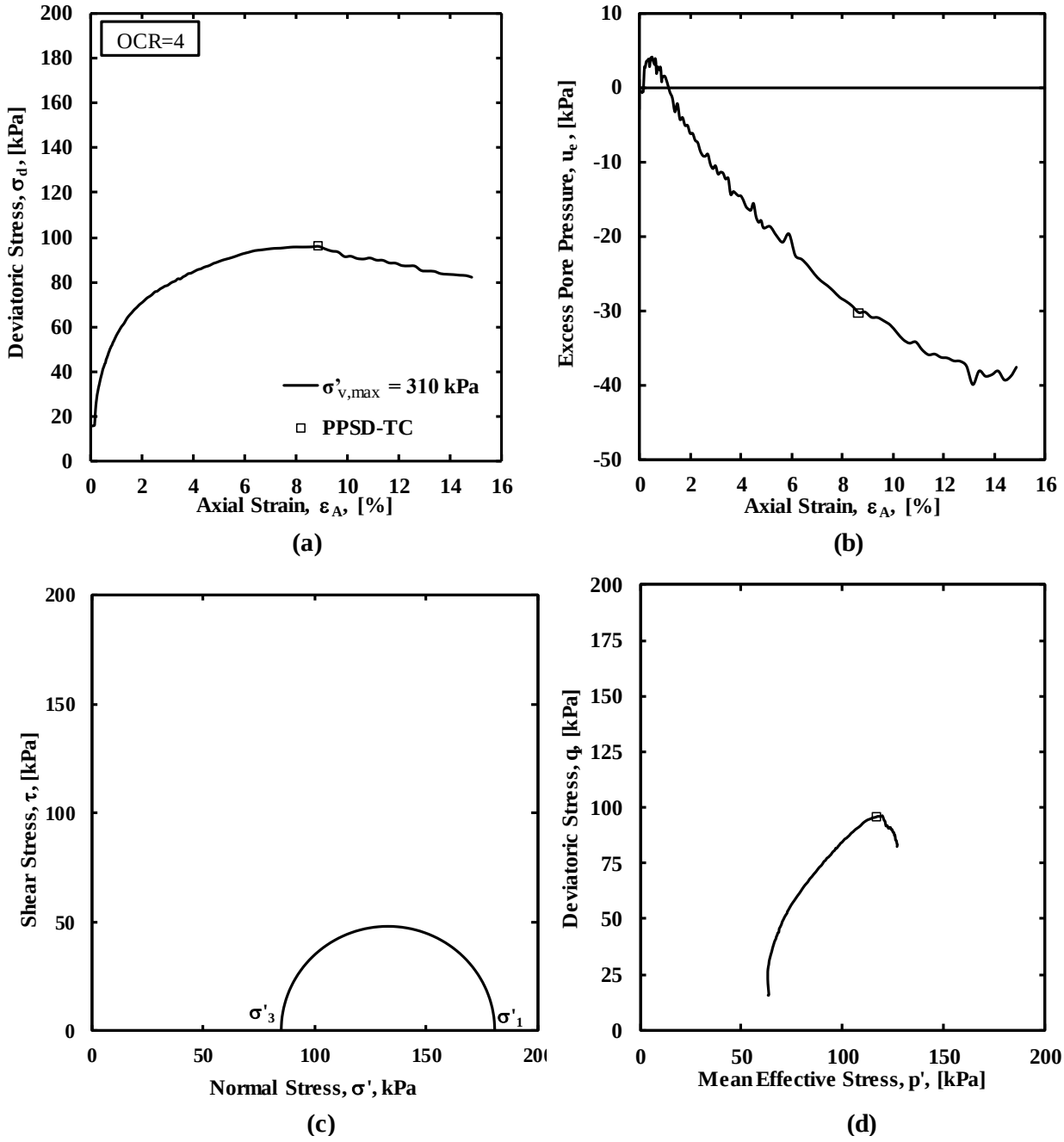

Figure A.9. a) Deviatoric stress as a function of axial strain, b) excess pore water pressure as a function of axial strain, c) Mohr circle, and d) Cambridge p-q stress path for the TC test at OCR=4 and $\sigma'_{v,max}$=310 kPa.

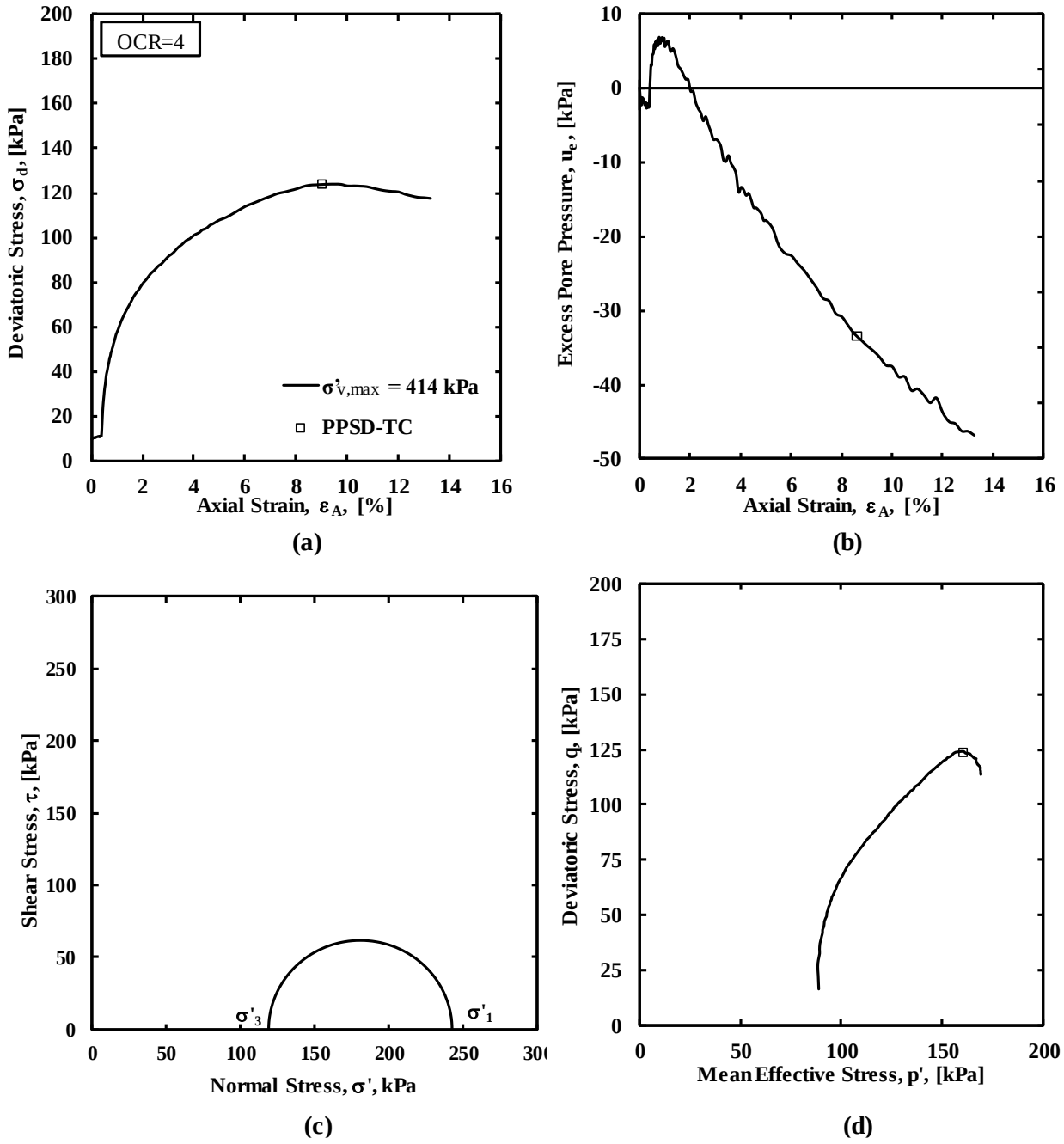

Figure A.10. a) Deviatoric stress as a function of axial strain, b) excess pore water pressure as a function of axial strain, c) Mohr circle, and d) Cambridge p-q stress path for the TC test at OCR=4 and $\sigma'_{v,max}$=414 kPa.

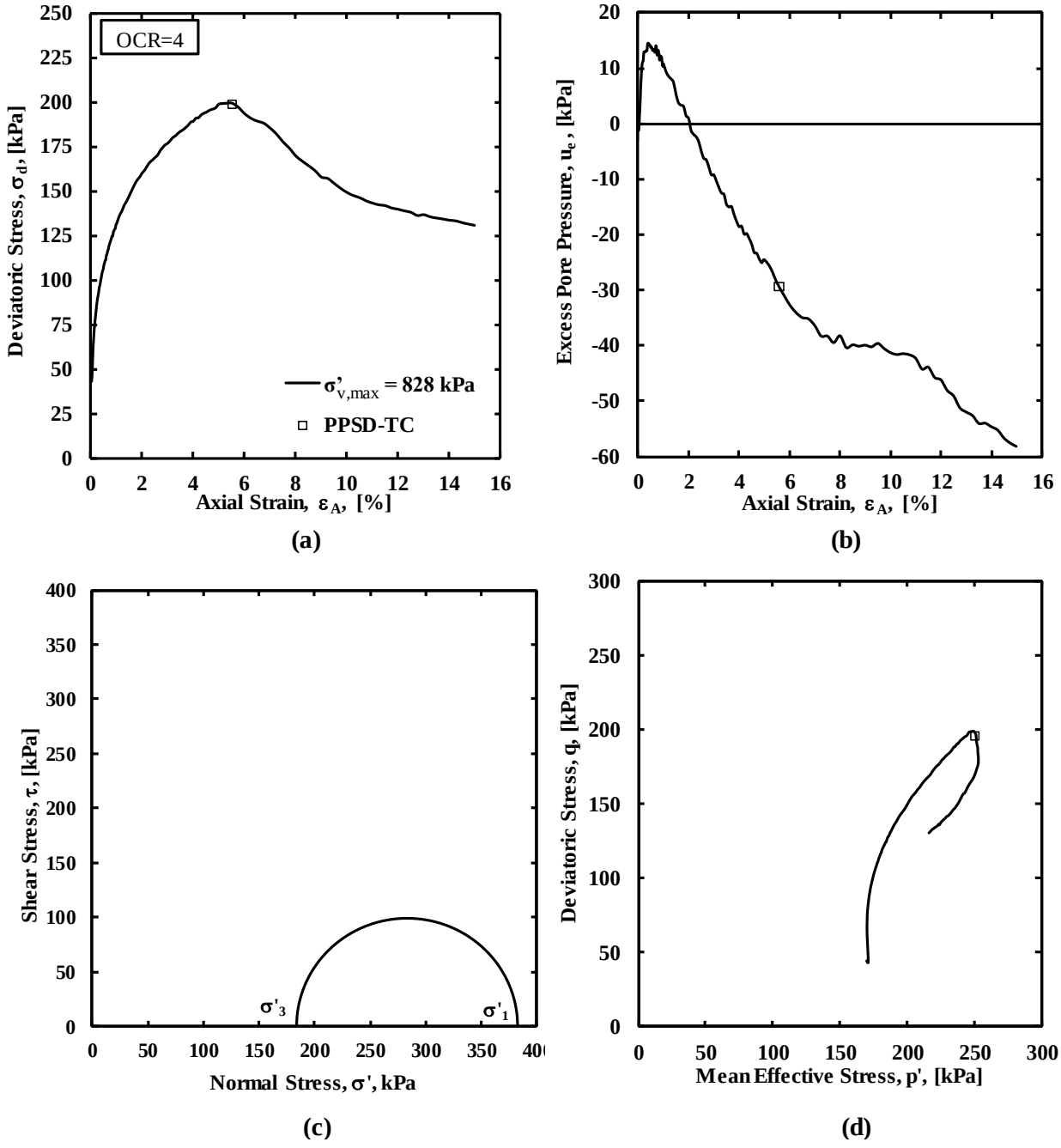

Figure A.11. a) Deviatoric stress as a function of axial strain, b) excess pore water pressure as a function of axial strain, c) Mohr circle, and d) Cambridge p-q stress path for the TC test at OCR=4 and $\sigma'_{v,max}$=828 kPa.

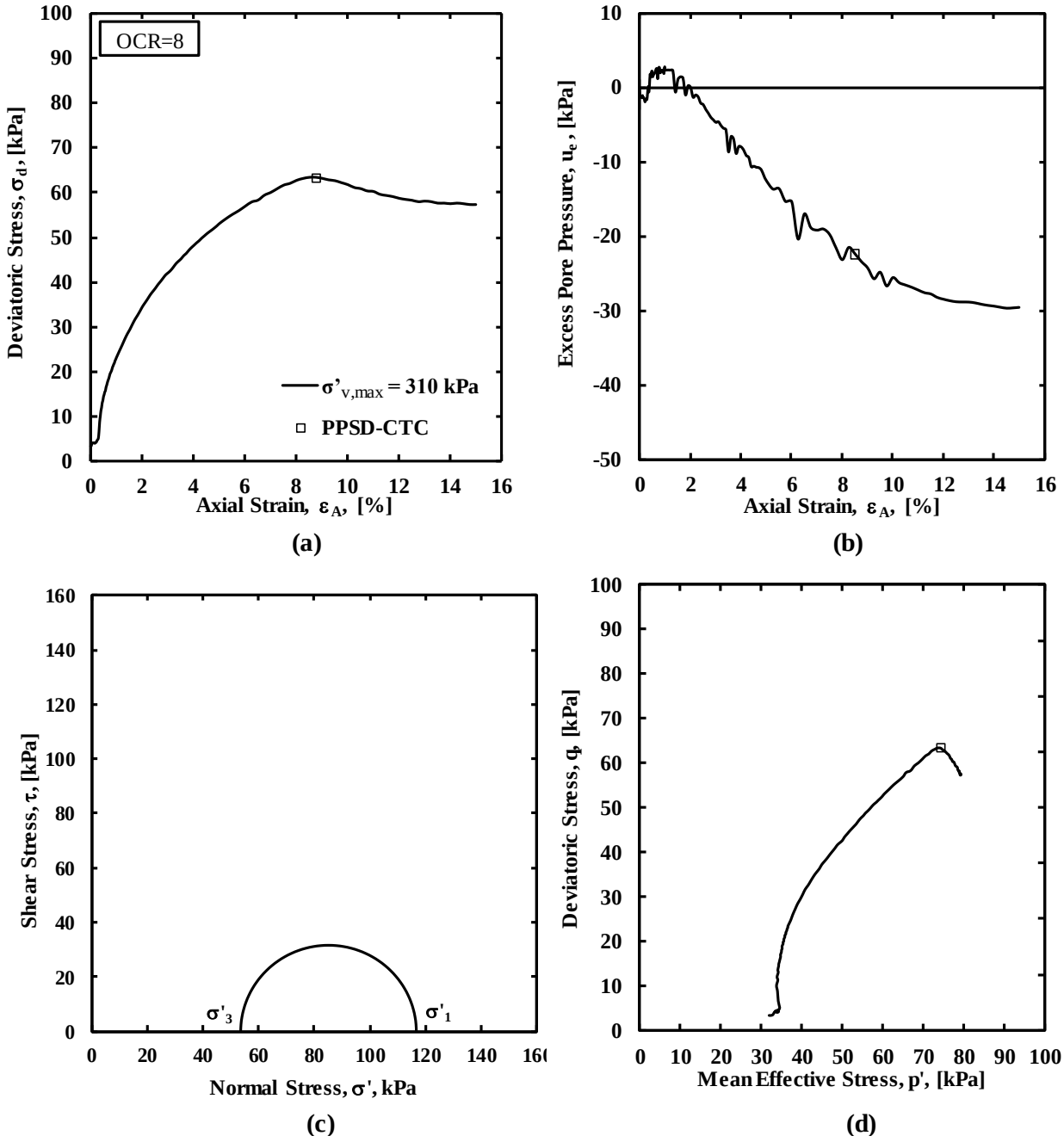

Figure A.12. a) Deviatoric stress as a function of axial strain, b) excess pore water pressure as a function of axial strain, c) Mohr circle, and d) Cambridge p-q stress path for the TC test at OCR=8 and $\sigma'_{v,max}$=310 kPa.

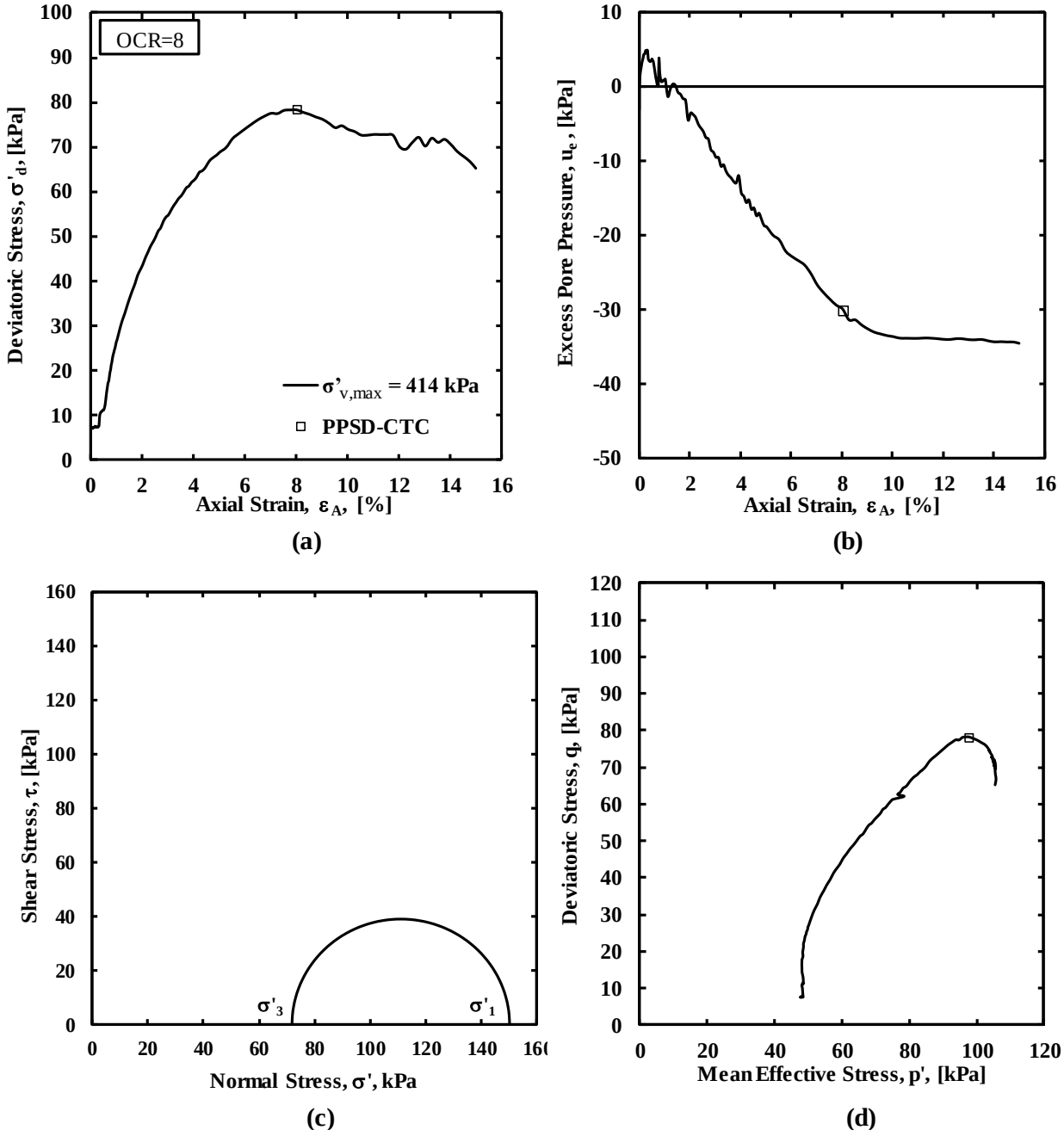

Figure A.13. a) Deviatoric stress as a function of axial strain, b) excess pore water pressure as a function of axial strain, c) Mohr circle, and d) Cambridge p-q stress path for the TC test at OCR=8 and σ'$_{v,max}$=414 kPa.

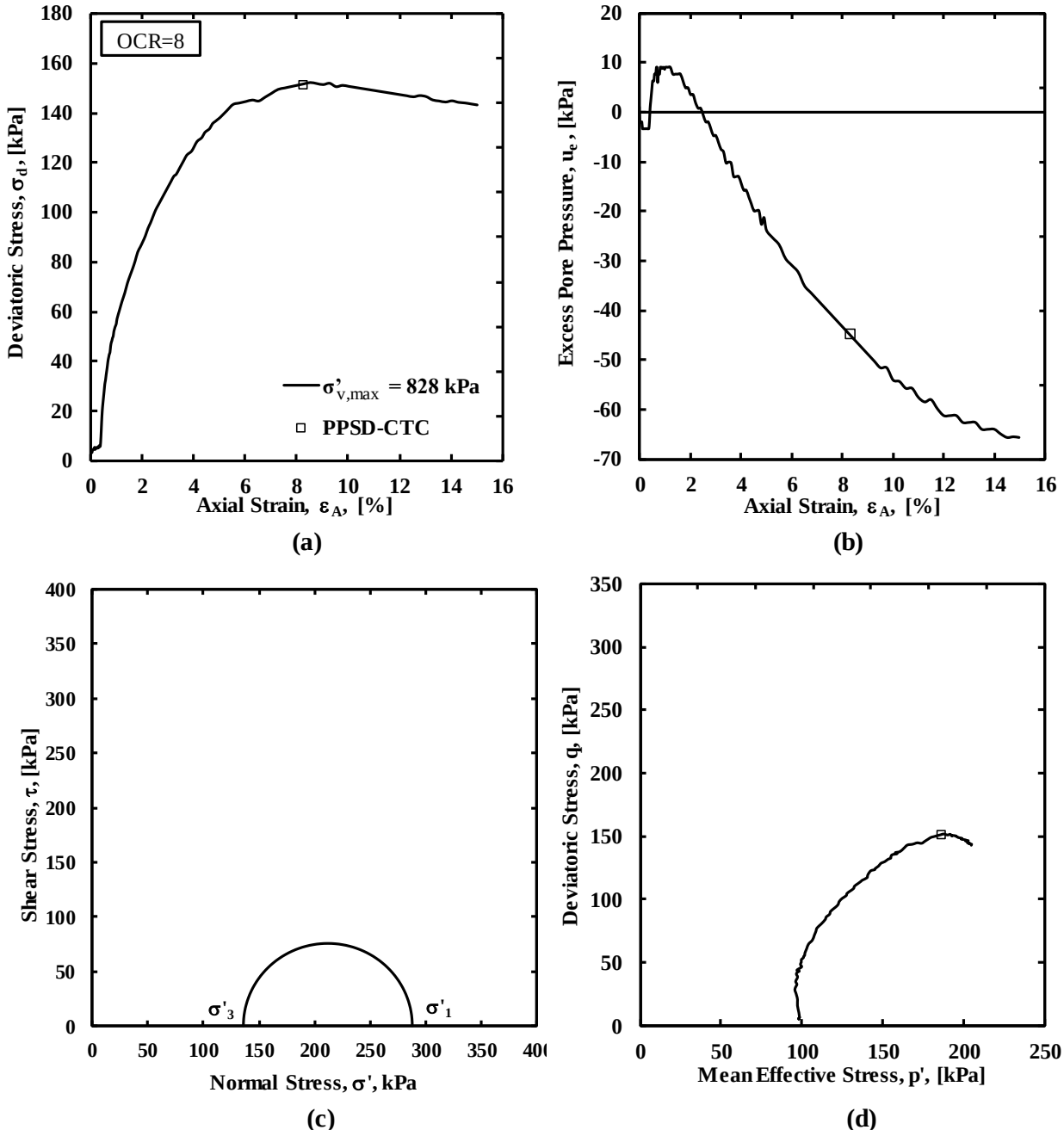

Figure A.14. a) Deviatoric stress as a function of axial strain, b) excess pore water pressure as a function of axial strain, c) Mohr circle, and d) Cambridge p-q stress path for the TC test at OCR=8 and $\sigma'_{v,max}$=828 kPa.

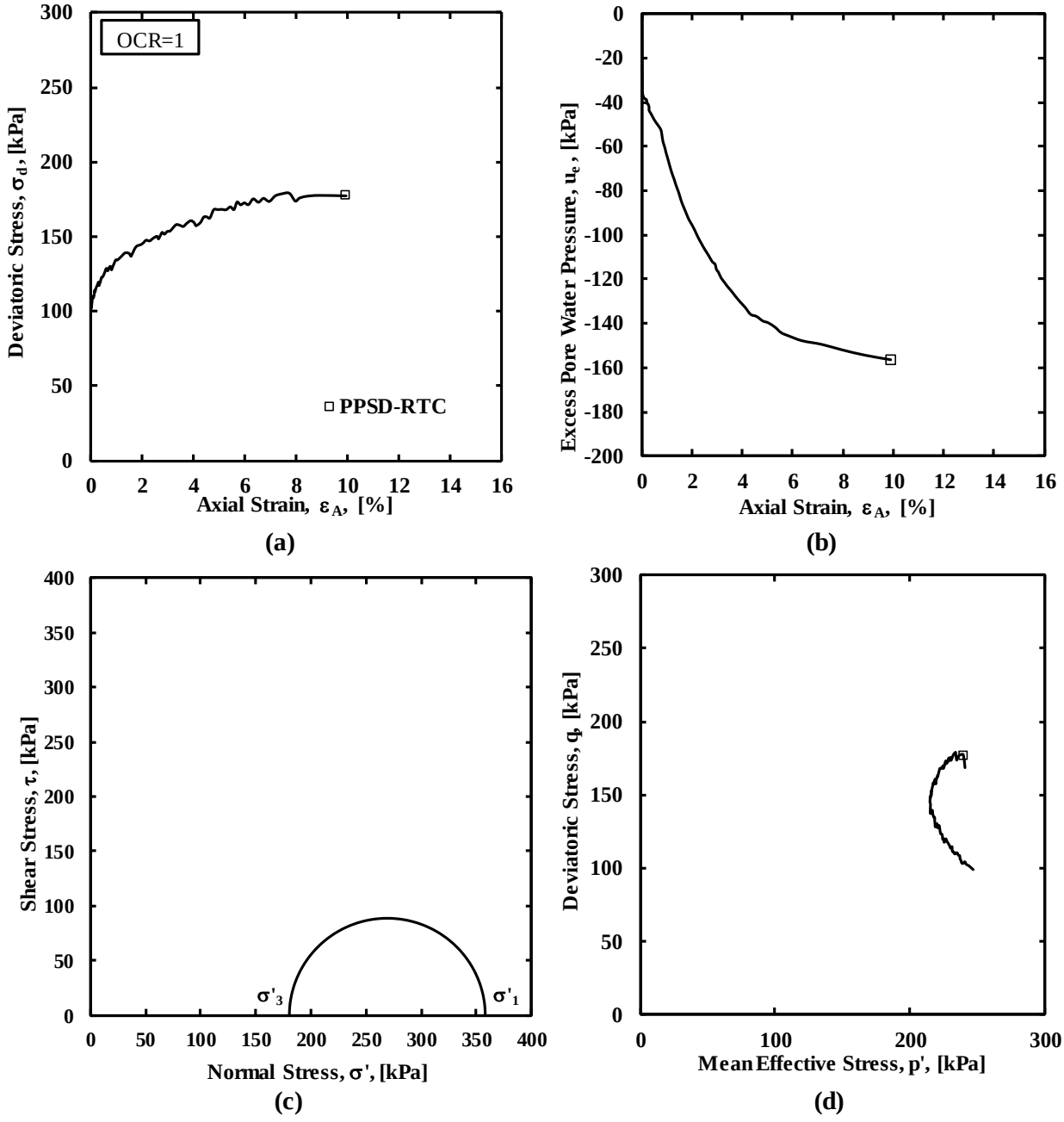

Figure A.15. a) Deviatoric stress as a function of axial strain, b) excess pore water pressure as a function of axial strain, c) Mohr circle, and d) Cambridge p-q stress path for the RTC test at OCR=1 and $\sigma'_{v,max}$=310 kPa.

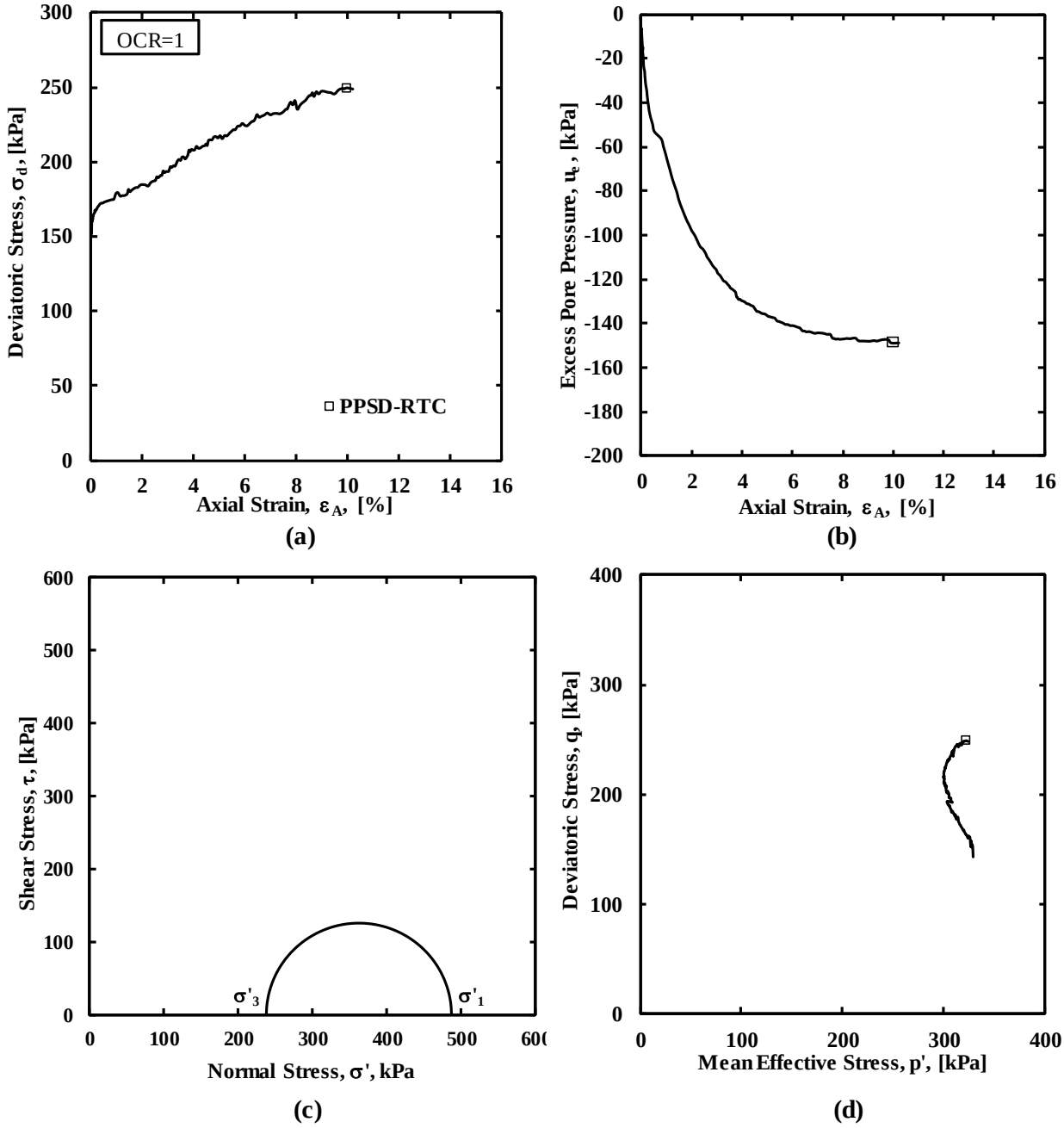

Figure A.16. a) Deviatoric stress as a function of axial strain, b) excess pore water pressure as a function of axial strain, c) Mohr circle, and d) Cambridge p-q stress path for the RTC test at OCR=1 and $\sigma'_{v,max}$=414 kPa.

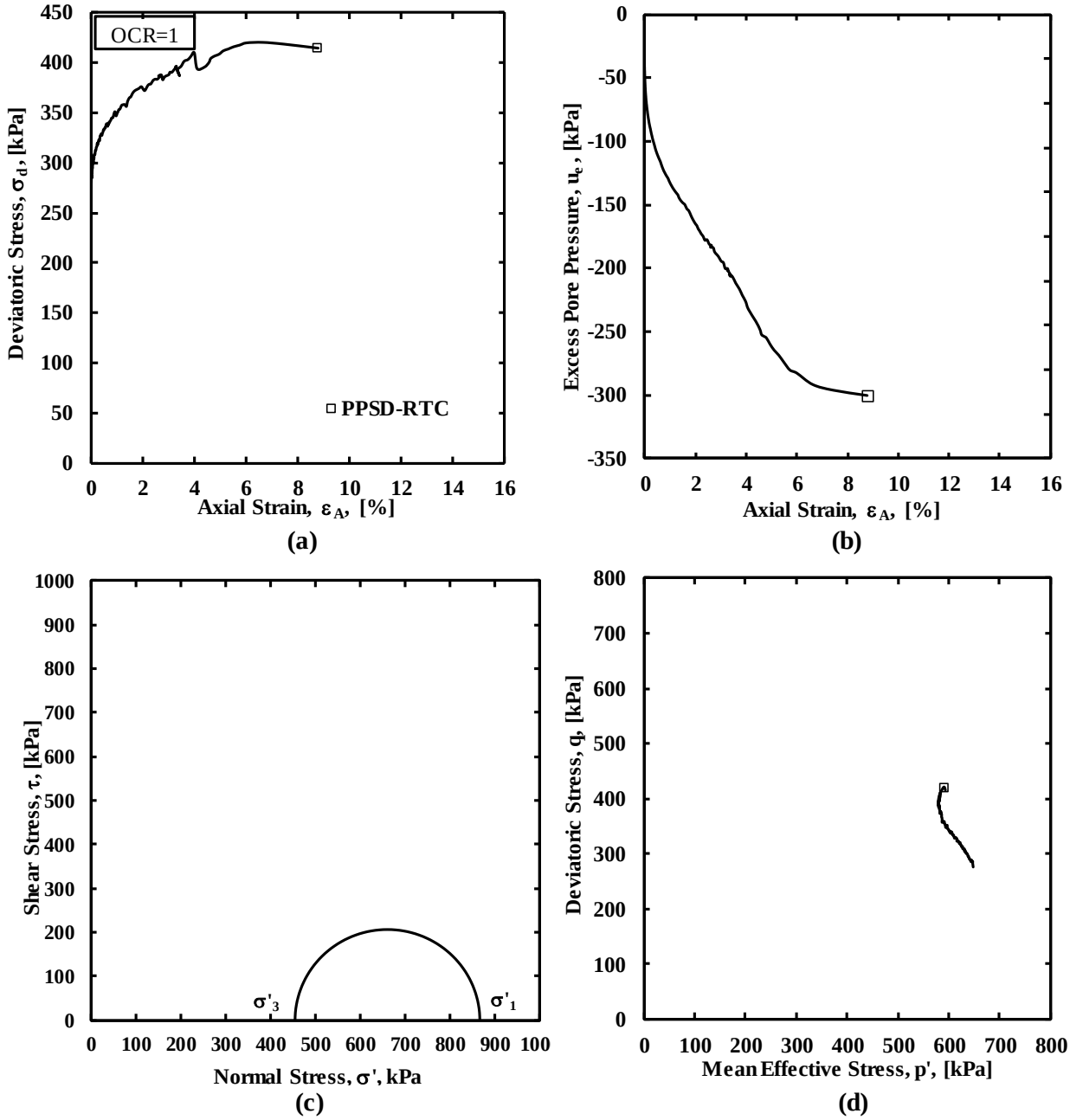

Figure A.17. a) Deviatoric stress as a function of axial strain, b) excess pore water pressure as a function of axial strain, c) Mohr circle, and d) Cambridge p-q stress path for the RTC test at OCR=1 and $\sigma'_{v,max}$=828 kPa.

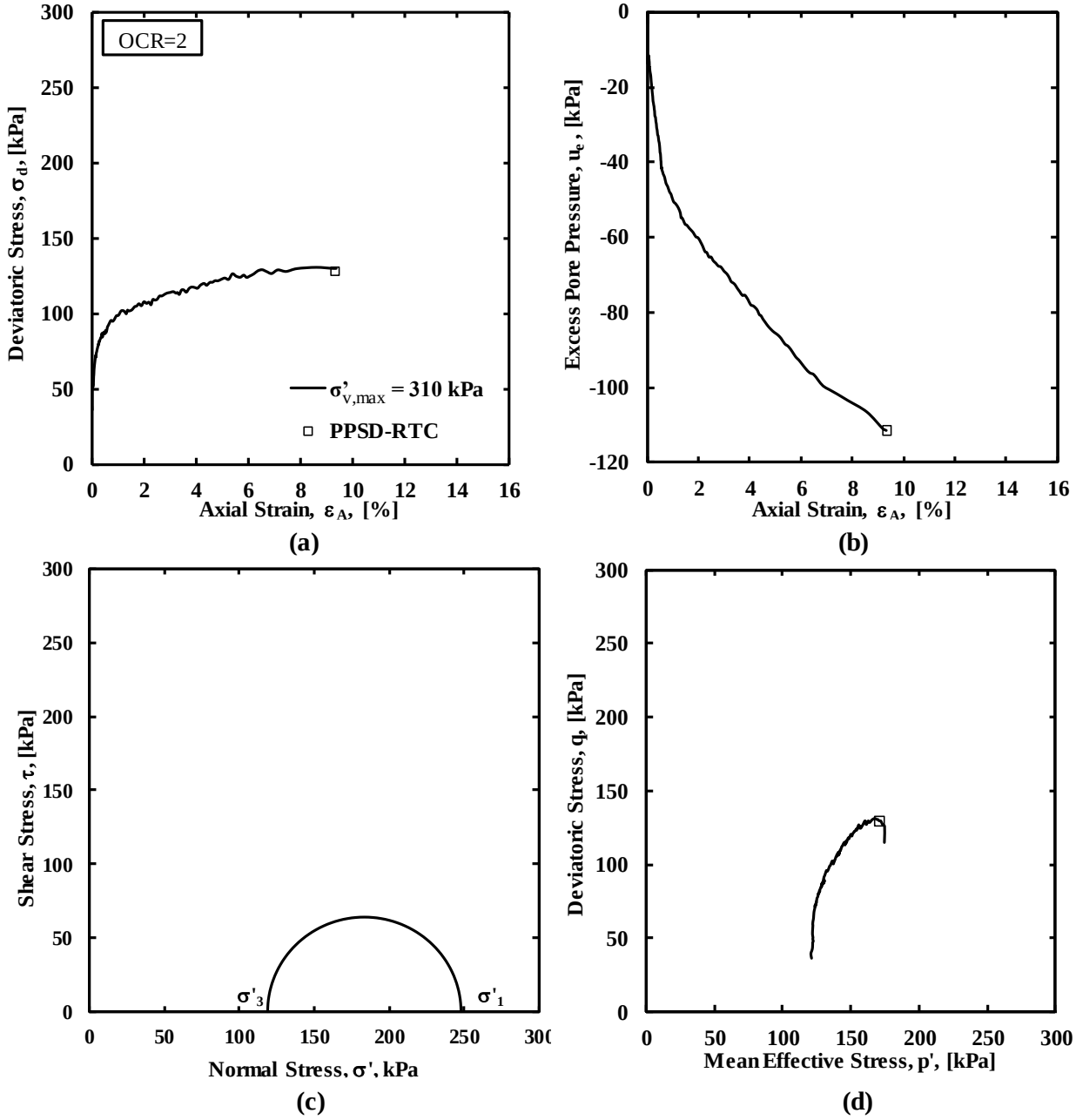

Figure A.18. a) Deviatoric stress as a function of axial strain, b) excess pore water pressure as a function of axial strain, c) Mohr circle, and d) Cambridge p-q stress path for the RTC test at OCR=2 and $\sigma'_{v,max}$=310 kPa.

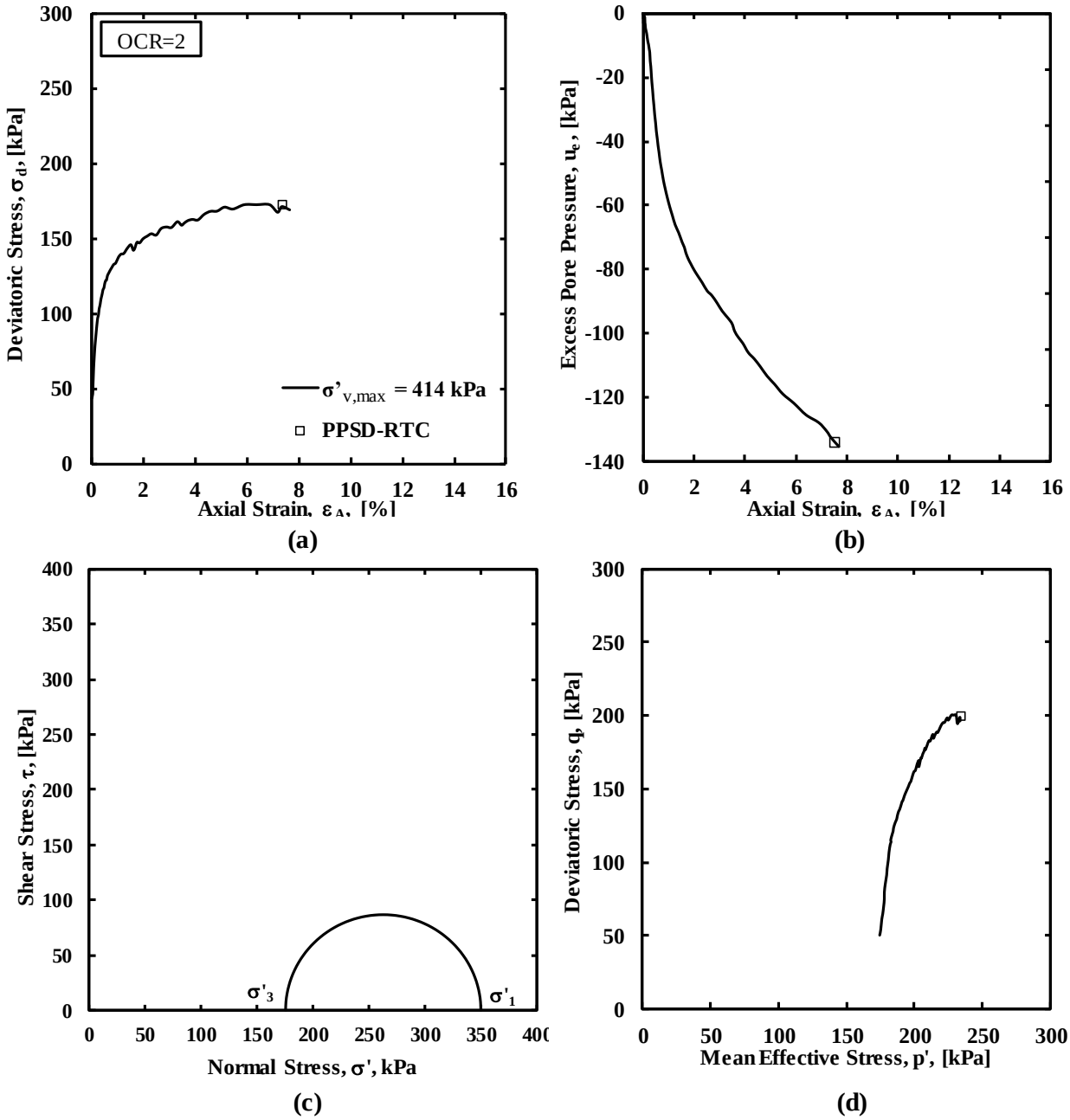

Figure A.19. a) Deviatoric stress as a function of axial strain, b) excess pore water pressure as a function of axial strain, c) Mohr circle, and d) Cambridge p-q stress path for the RTC test at OCR=2 and $\sigma'_{v,max}$=414 kPa.

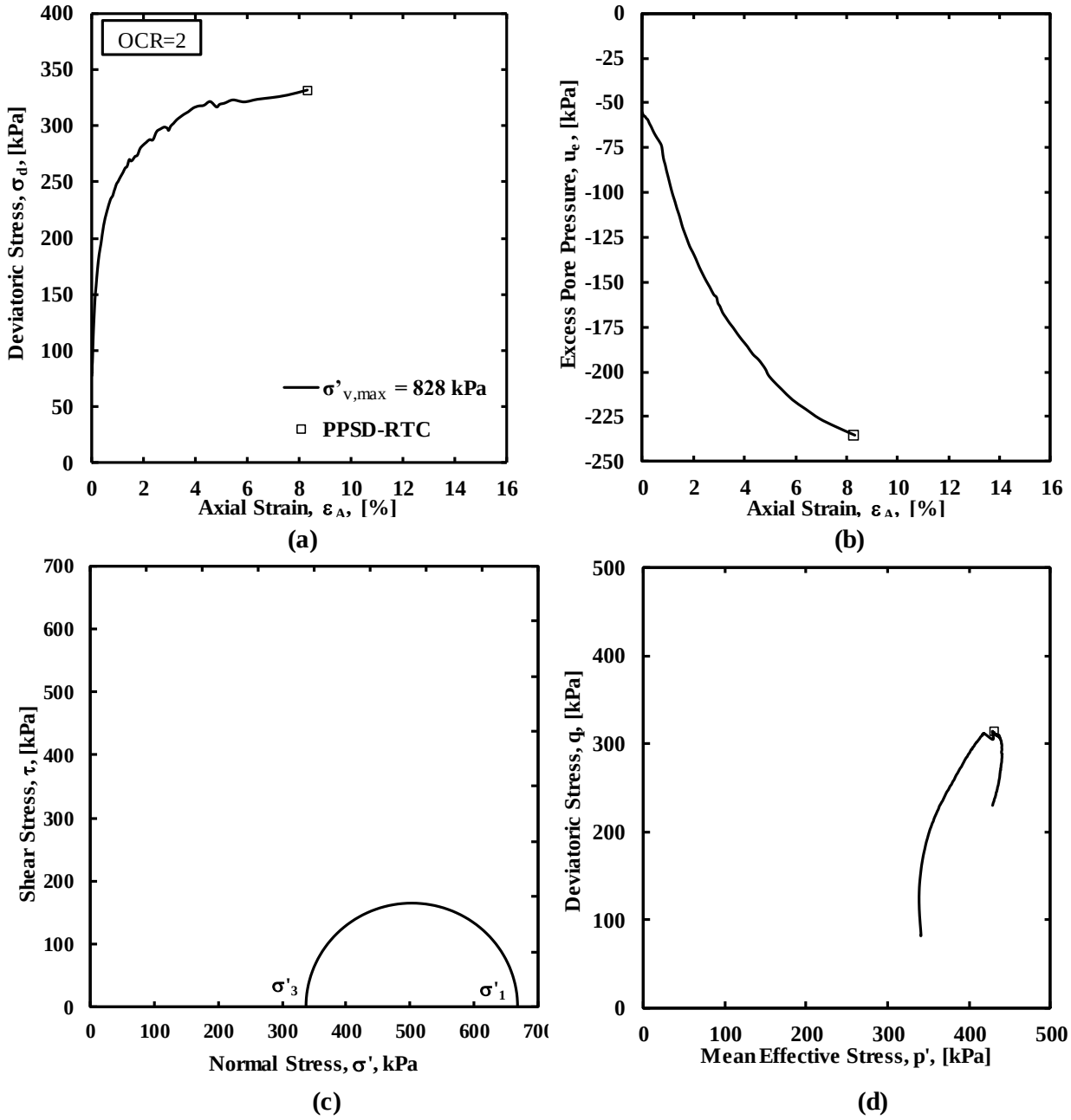

Figure A.20. a) Deviatoric stress as a function of axial strain, b) excess pore water pressure as a function of axial strain, c) Mohr circle, and d) Cambridge p-q stress path for the RTC test at OCR=2 and $\sigma'_{v,max}$=828 kPa.

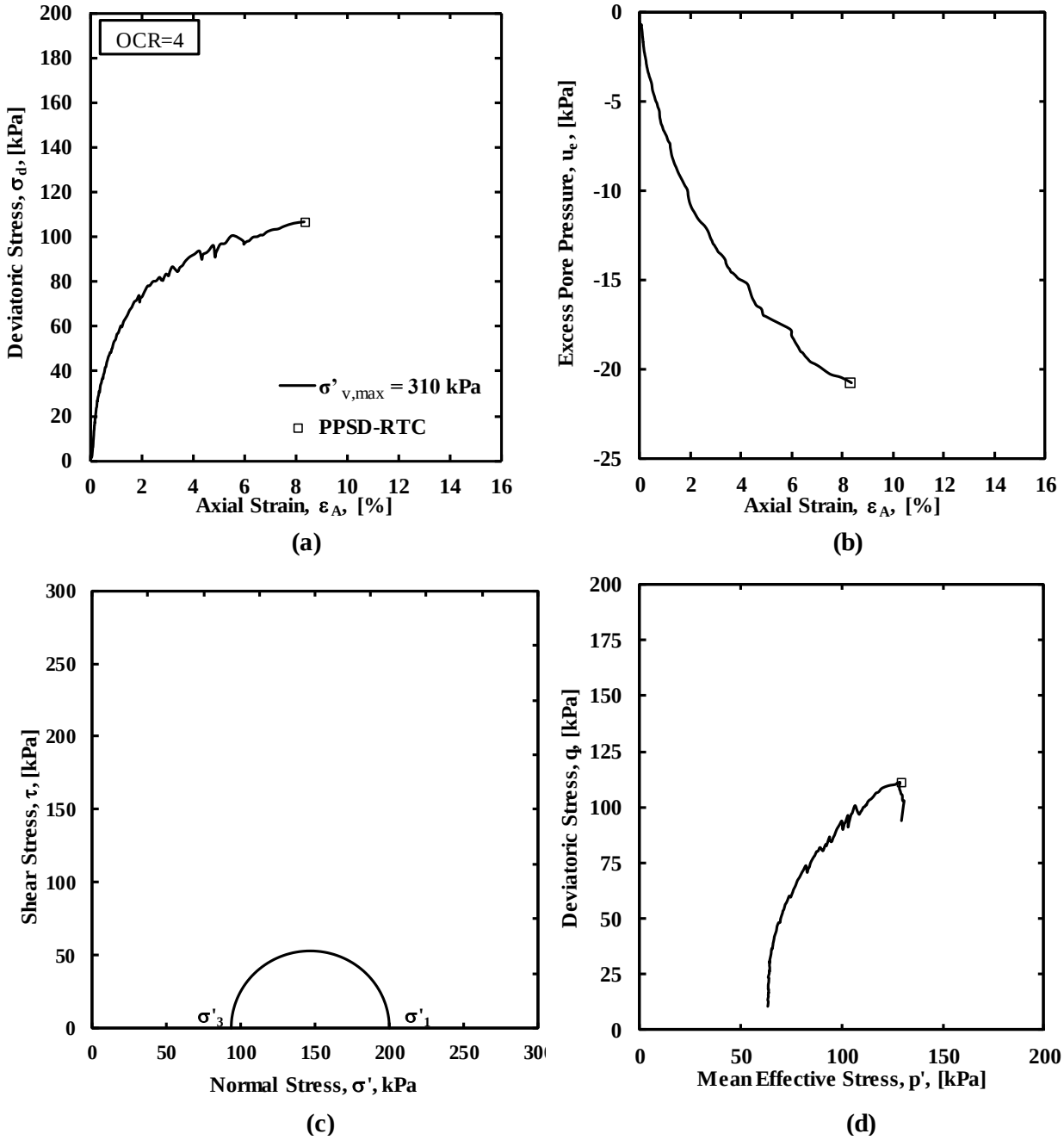

Figure A.21. a) Deviatoric stress as a function of axial strain, b) excess pore water pressure as a function of axial strain, c) Mohr circle, and d) Cambridge p-q stress path for the RTC test at OCR=4 and $\sigma'_{v,max}$=310 kPa.

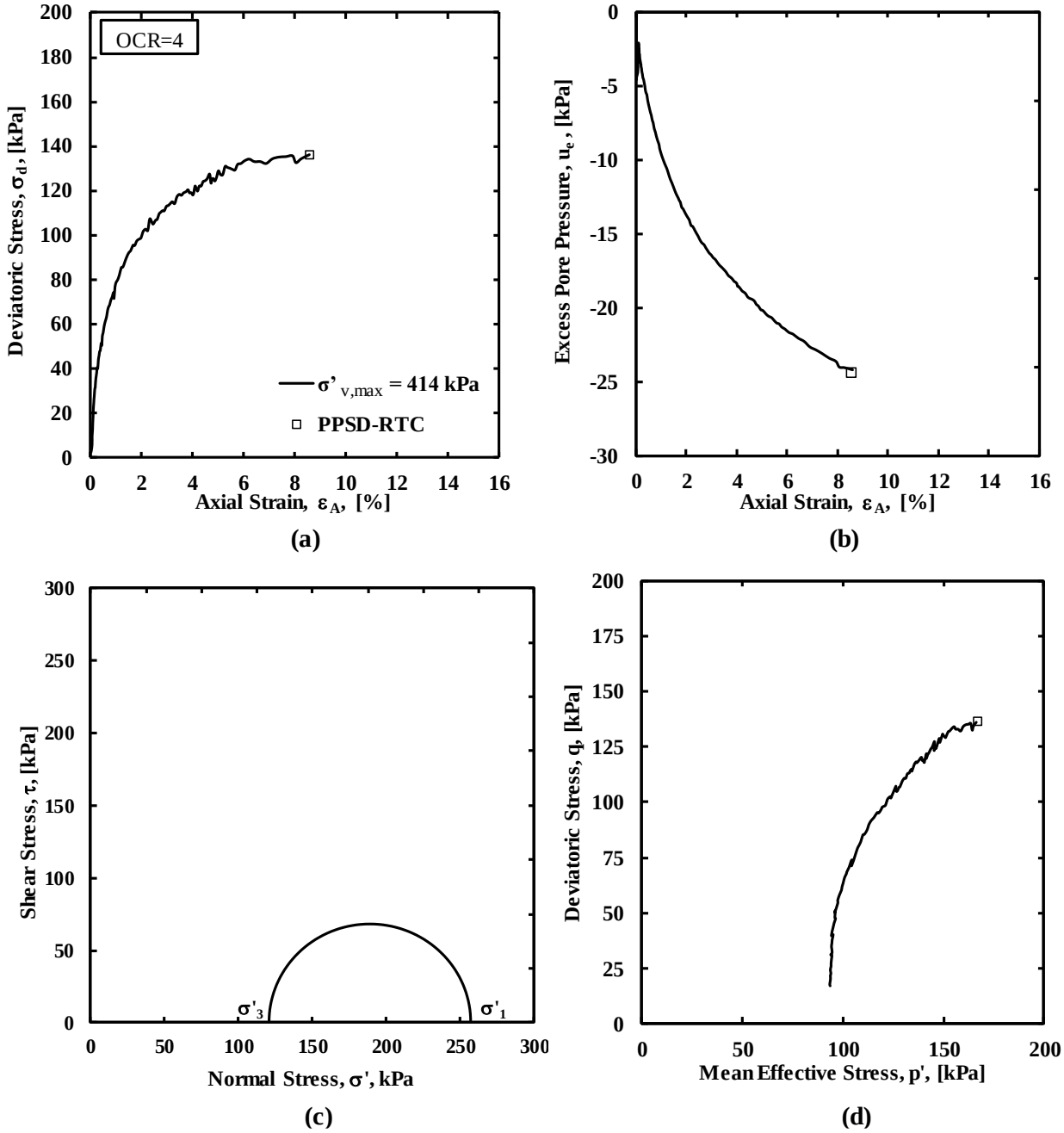

Figure A.22. a) Deviatoric stress as a function of axial strain, b) excess pore water pressure as a function of axial strain, c) Mohr circle, and d) Cambridge p-q stress path for the RTC test at OCR=4 and σ'$_{v,max}$=414 kPa.

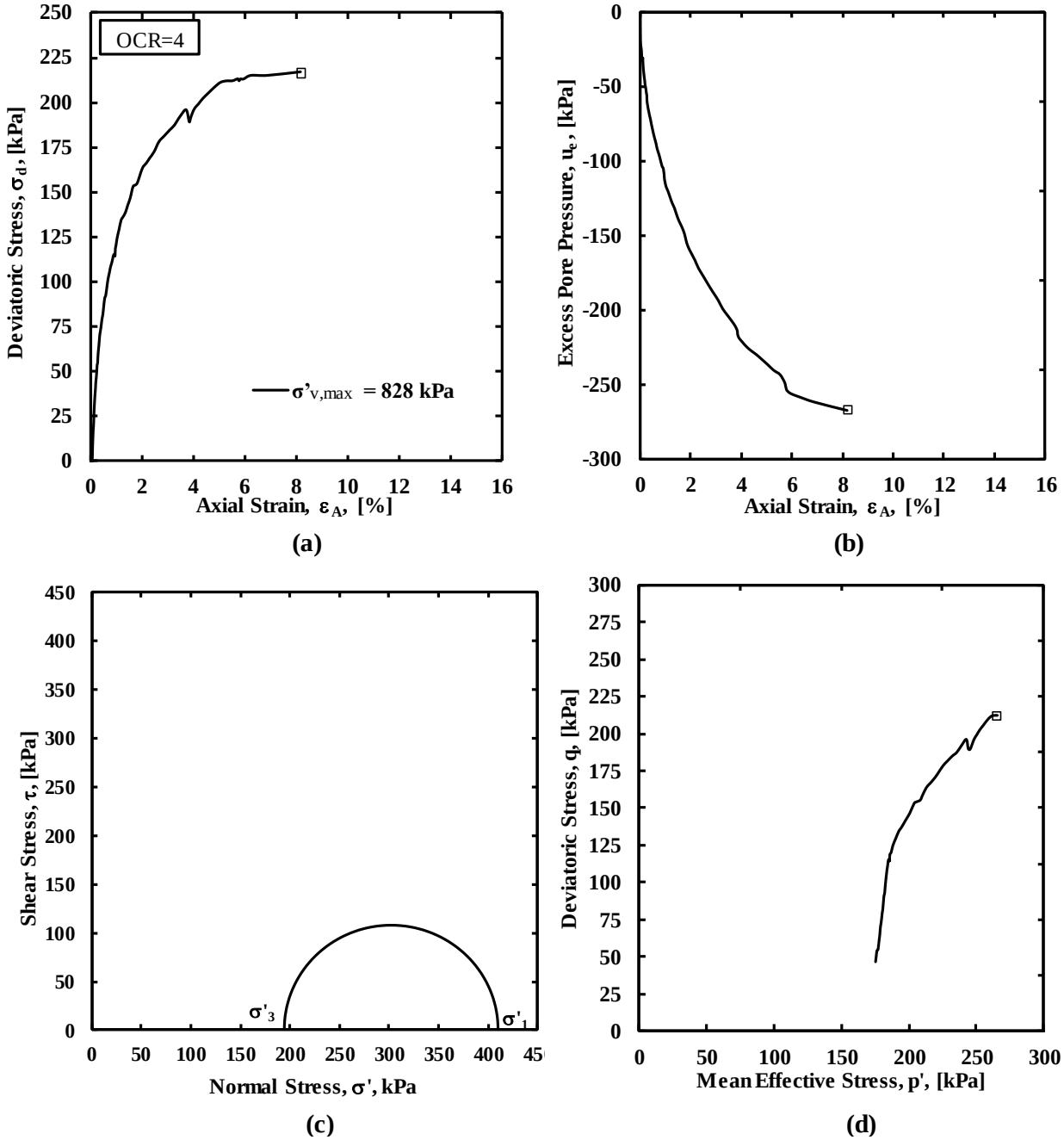

Figure A.23. a) Deviatoric stress as a function of axial strain, b) excess pore water pressure as a function of axial strain, c) Mohr circle, and d) Cambridge p-q stress path for the RTC test at OCR=4 and $\sigma'_{v,max}$=828 kPa.

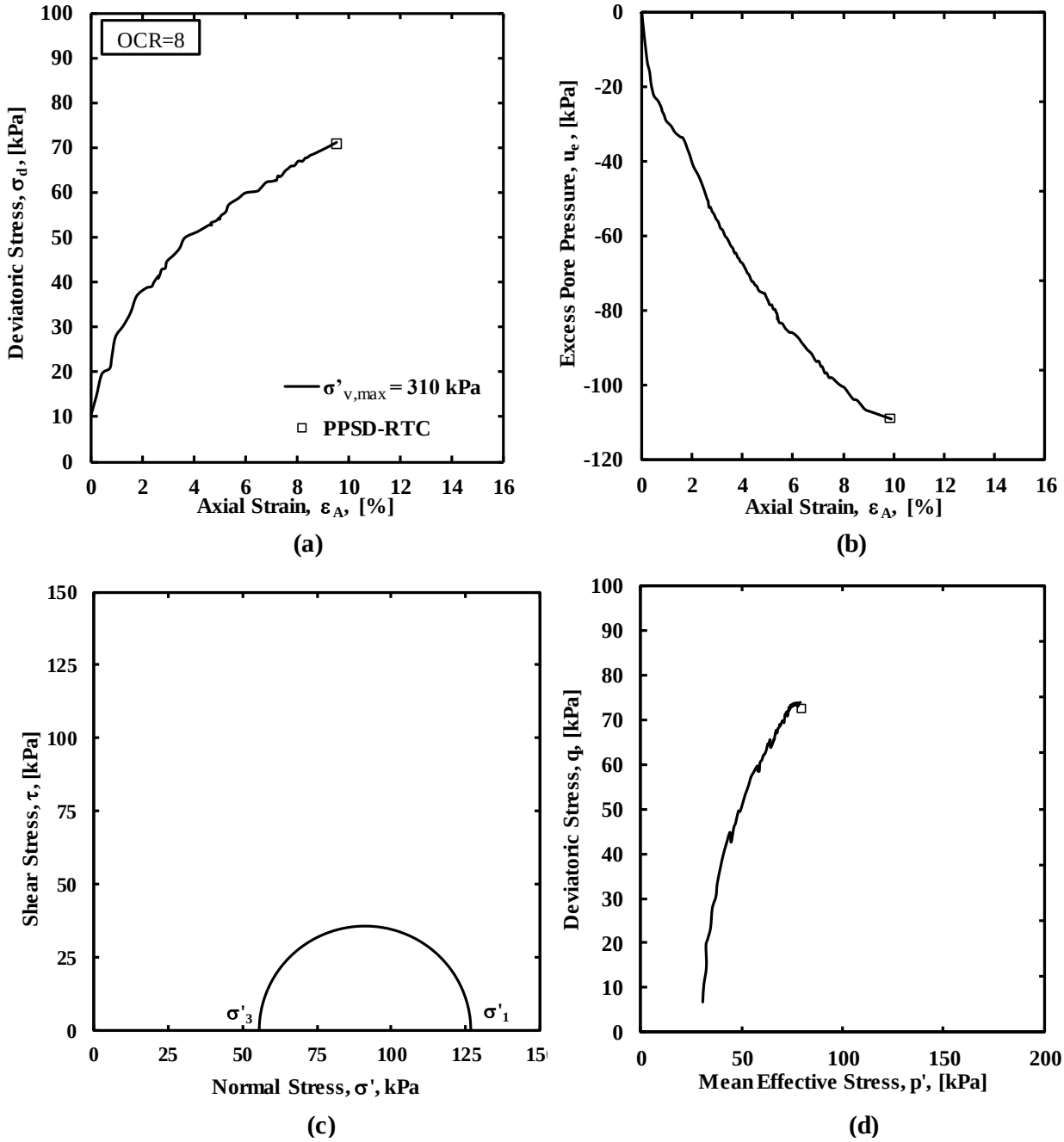

Figure A.24. a) Deviatoric stress as a function of axial strain, b) excess pore water pressure as a function of axial strain, c) Mohr circle, and d) Cambridge p-q stress path for the RTC test at OCR=8 and $\sigma'_{v,max}$=310 kPa.

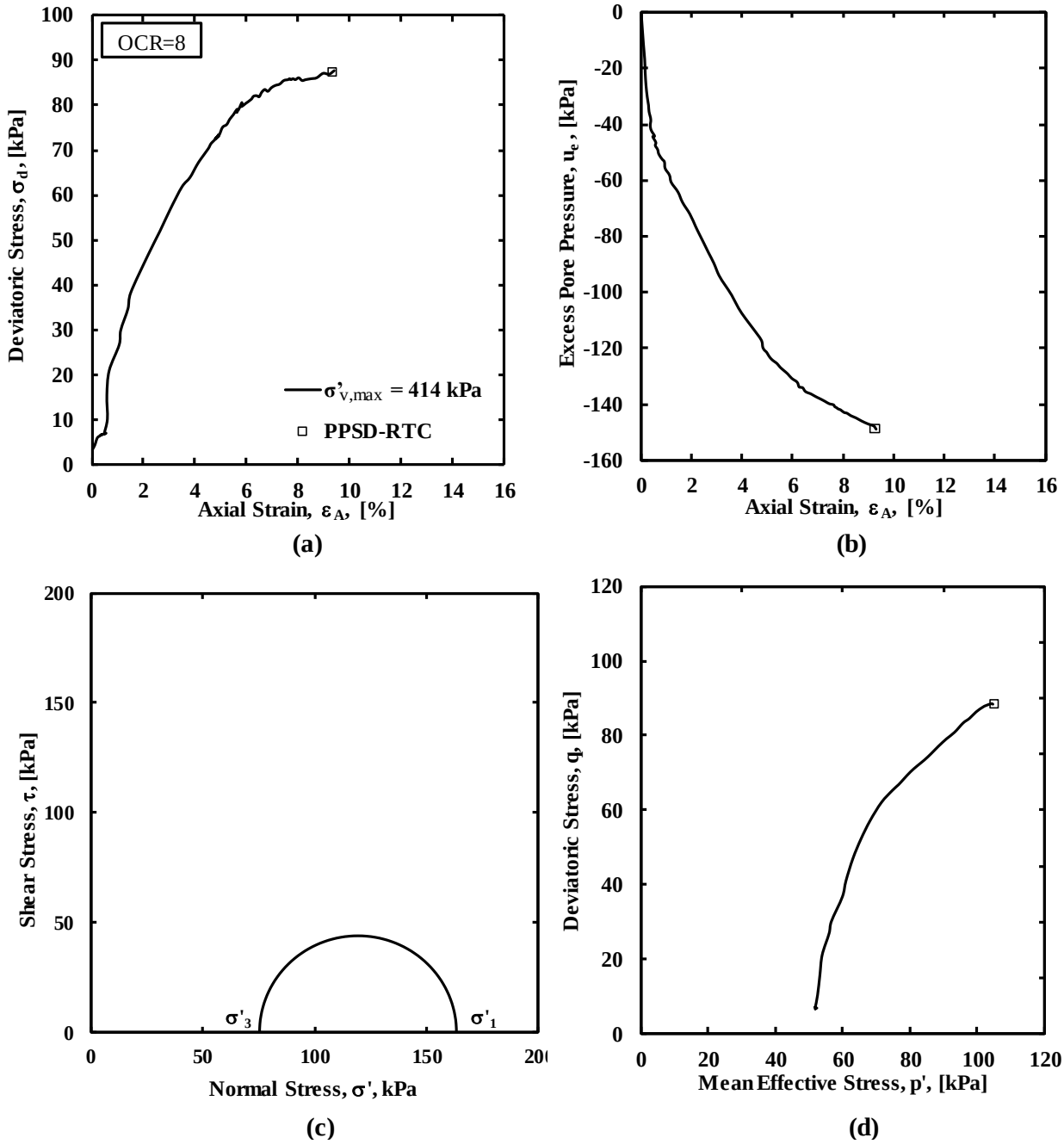

Figure A.25. a) Deviatoric stress as a function of axial strain, b) excess pore water pressure as a function of axial strain, c) Mohr circle, and d) Cambridge p-q stress path for the RTC test at OCR=8 and $\sigma'_{v,max}$=414 kPa.

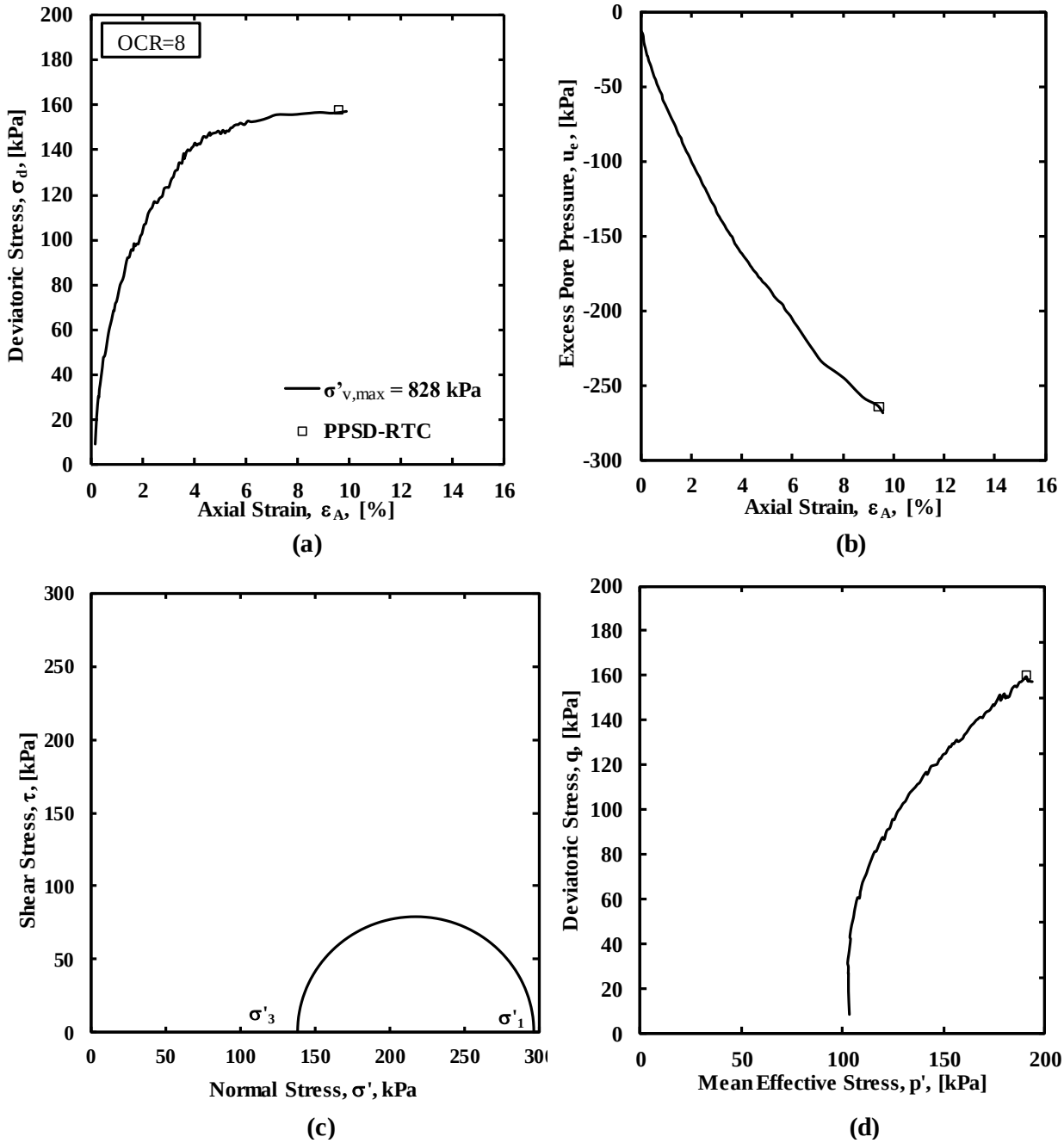

Figure A.26. a) Deviatoric stress as a function of axial strain, b) excess pore water pressure as a function of axial strain, c) Mohr circle, and d) Cambridge p-q stress path for the RTC test at OCR=8 and $\sigma'_{v,max}$=828 kPa.

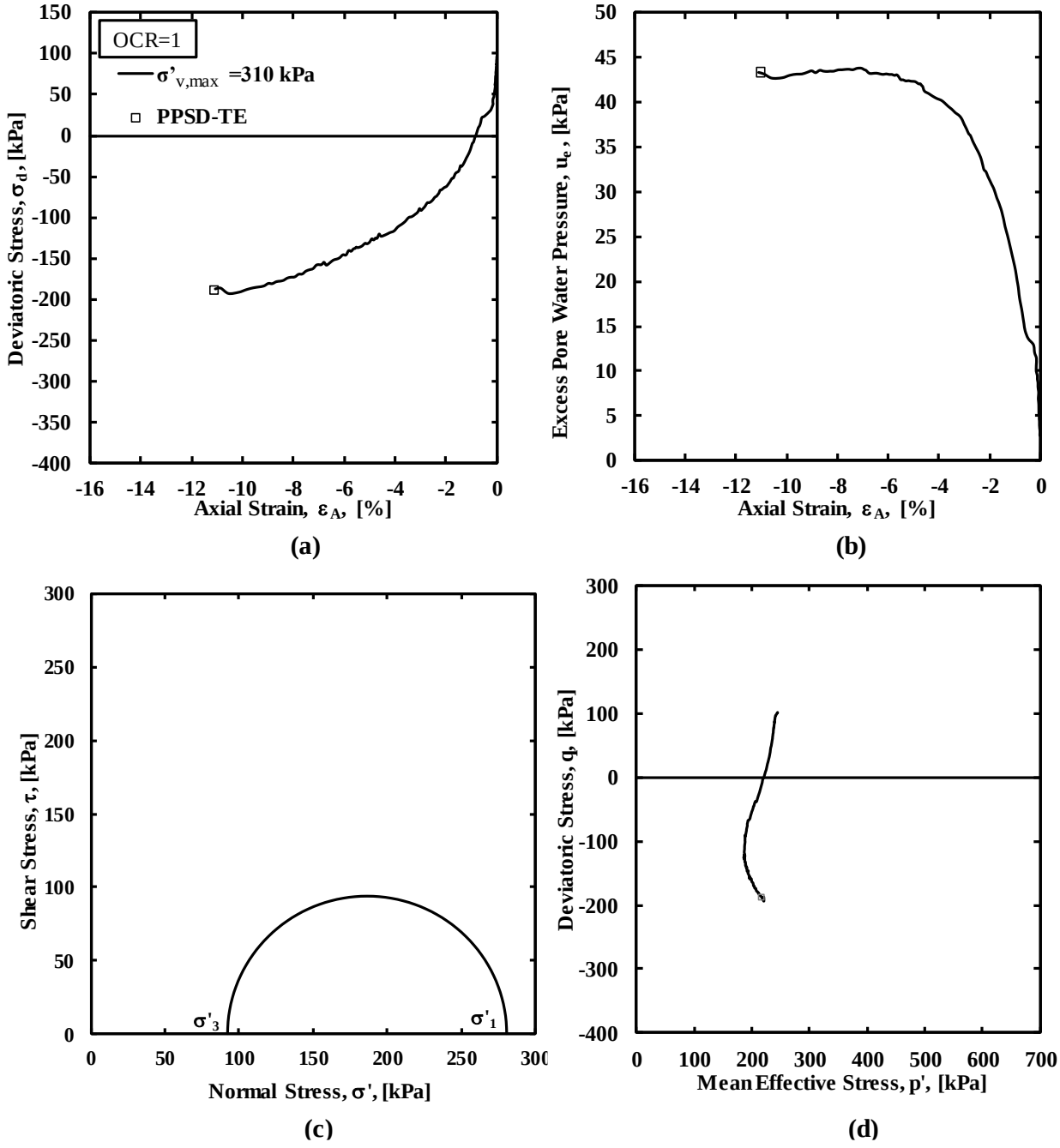

Figure A.27. a) Deviatoric stress as a function of axial strain, b) excess pore water pressure as a function of axial strain, c) Mohr circle, and d) Cambridge p-q stress path for the TE test at OCR=1 and $\sigma'_{v,max}$ =310 kPa.

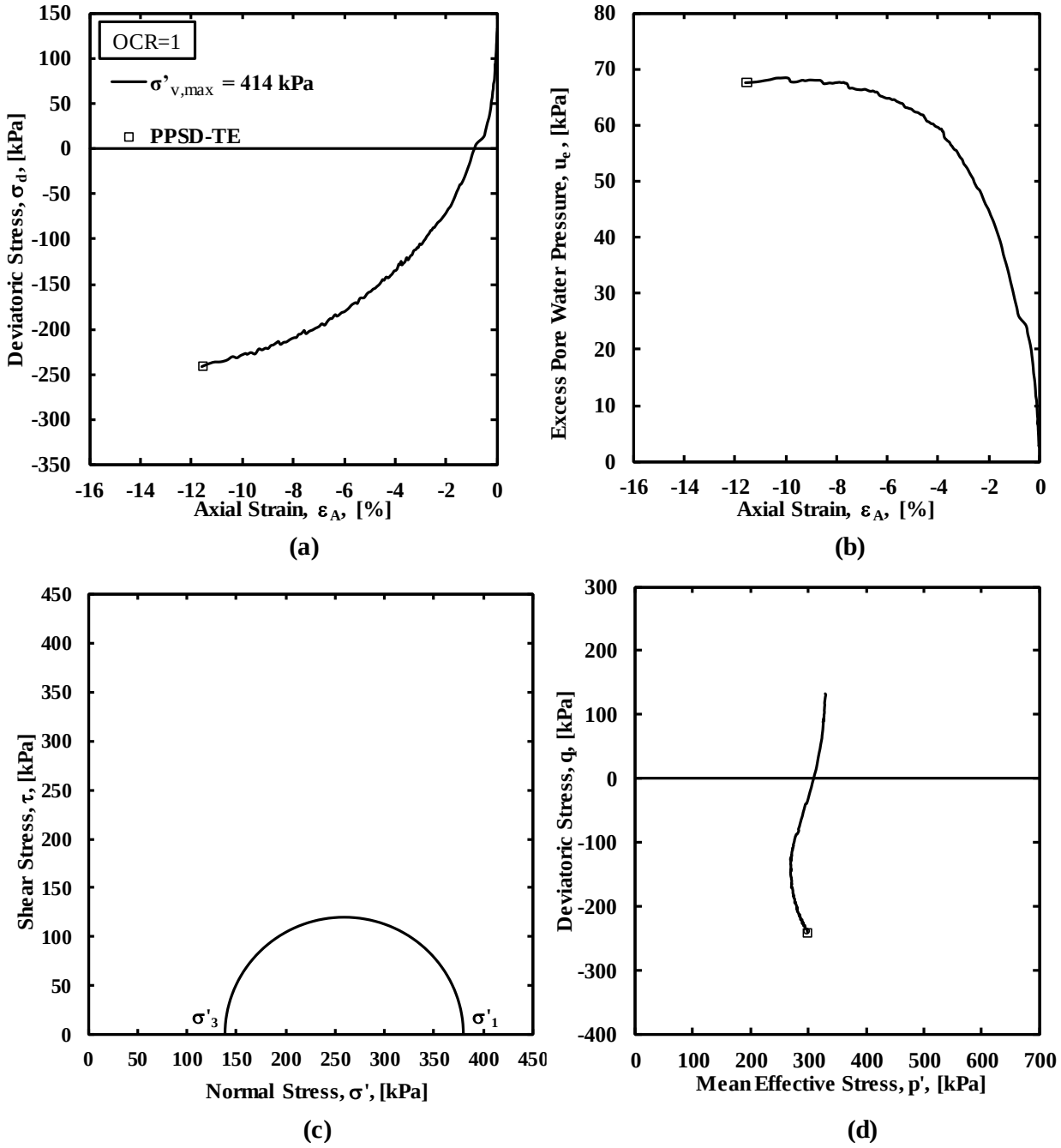

Figure A.28. a) Deviatoric stress as a function of axial strain, b) excess pore water pressure as a function of axial strain, c) Mohr circle, and d) Cambridge p-q stress path for the TE test at OCR=1 and $\sigma'_{v,max}$ =414 kPa.

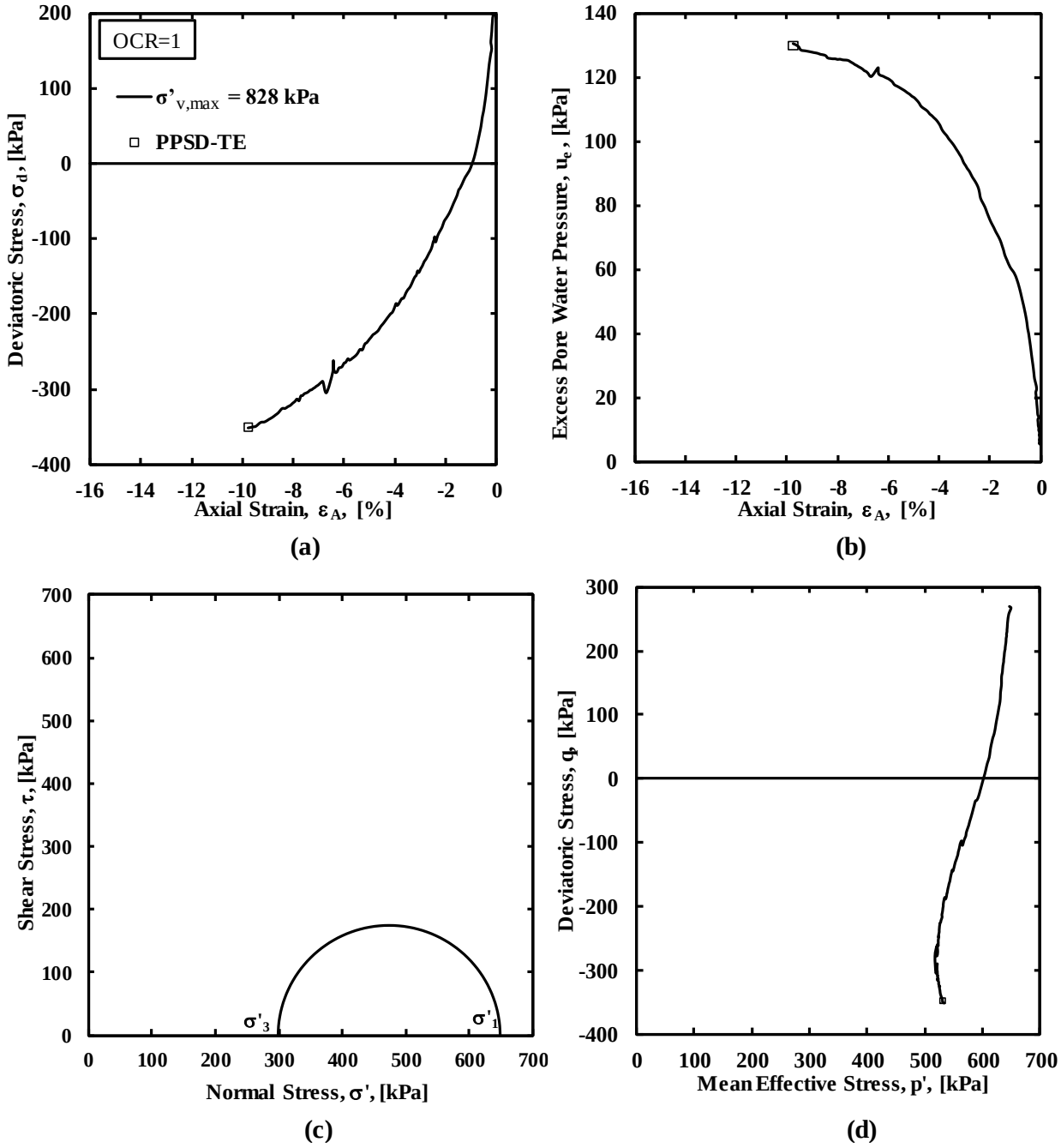

Figure A.29. a) Deviatoric stress as a function of axial strain, b) excess pore water pressure as a function of axial strain, c) Mohr circle, and d) Cambridge p-q stress path for the TE test at OCR=1 and $\sigma'_{v,max}$=828 kPa.

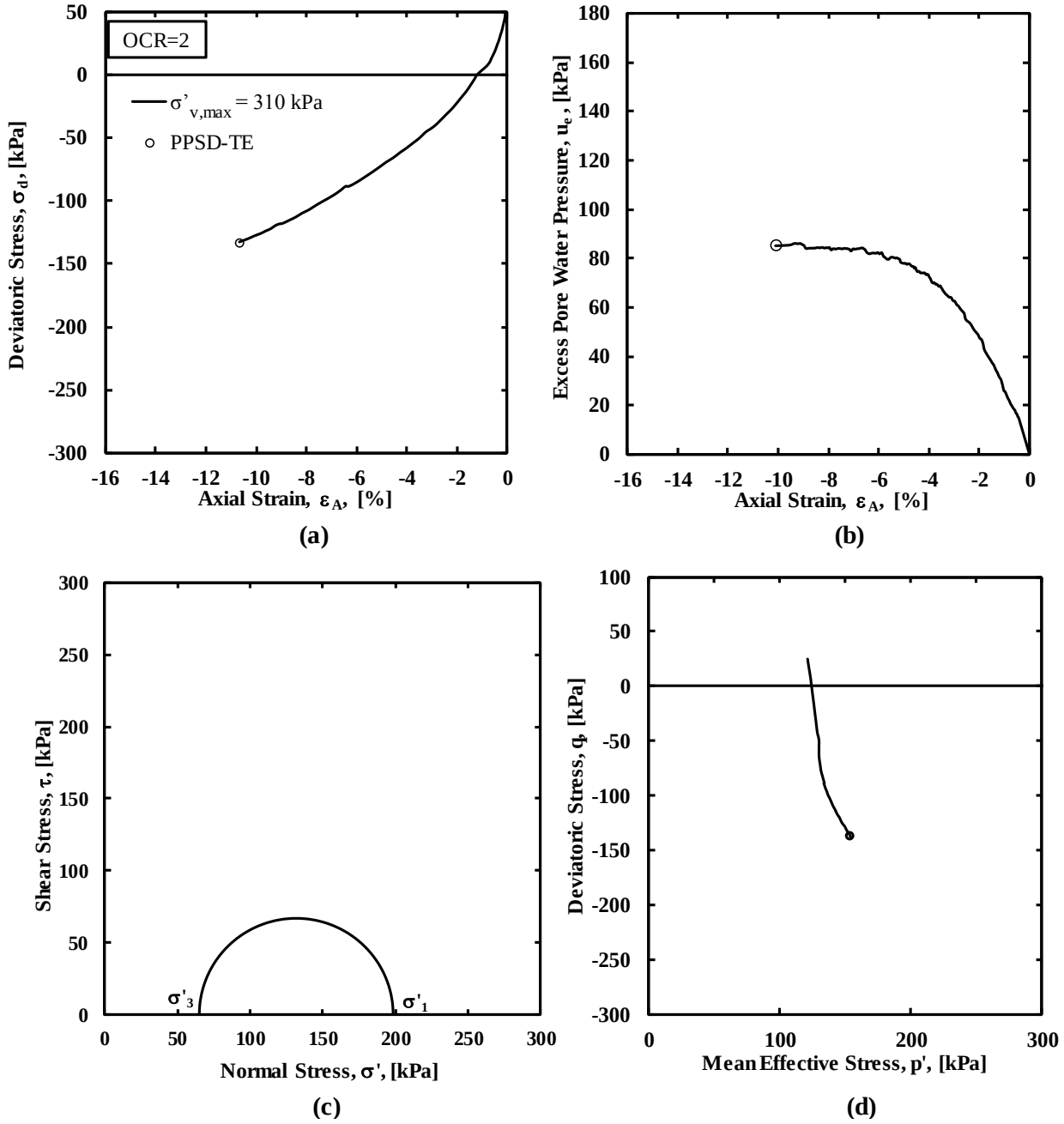

Figure A.30. a) Deviatoric stress as a function of axial strain, b) excess pore water pressure as a function of axial strain, c) Mohr circle, and d) Cambridge p-q stress path for the TE test at OCR=2 and $\sigma'_{v,max}$=310 kPa.

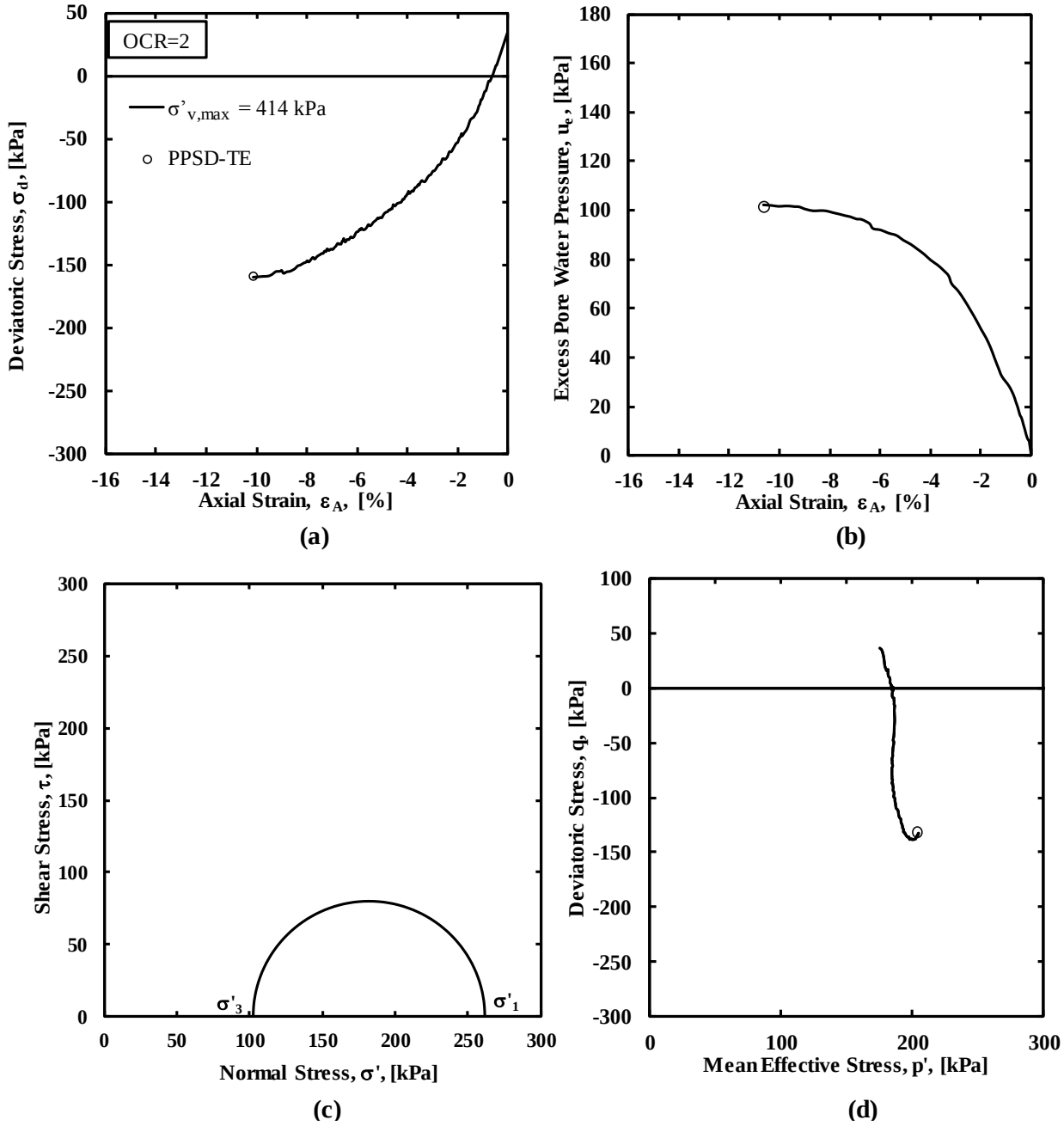

Figure A.31. a) Deviatoric stress as a function of axial strain, b) excess pore water pressure as a function of axial strain, c) Mohr circle, and d) Cambridge p-q stress path for the TE test at OCR=2 and $\sigma'_{v,max}$=414 kPa.

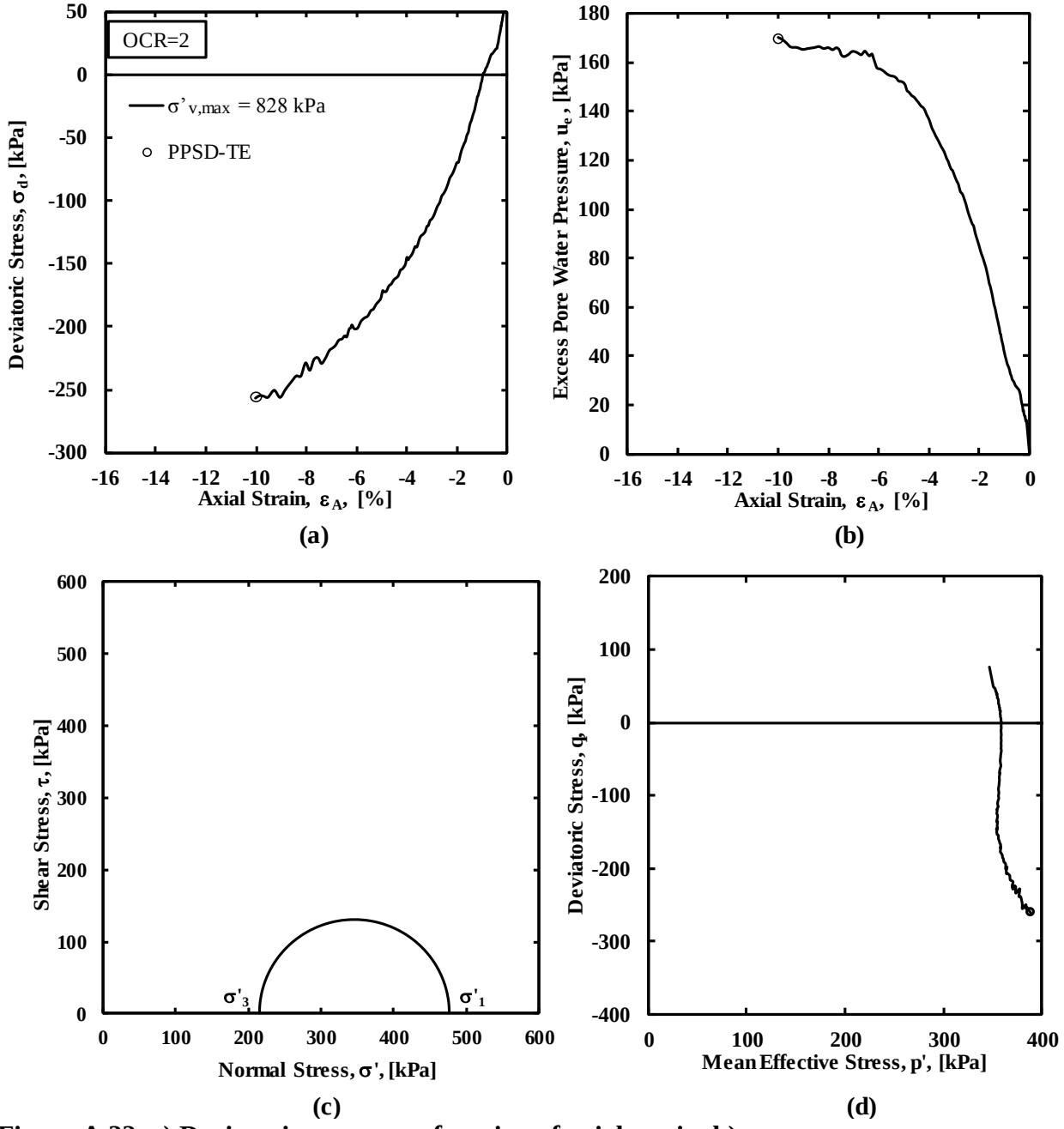

Figure A.32. a) Deviatoric stress as a function of axial strain, b) excess pore water pressure as a function of axial strain, c) Mohr circle, and d) Cambridge p-q stress path for the TE test at OCR=2 and $\sigma'_{v,max}$=828 kPa.

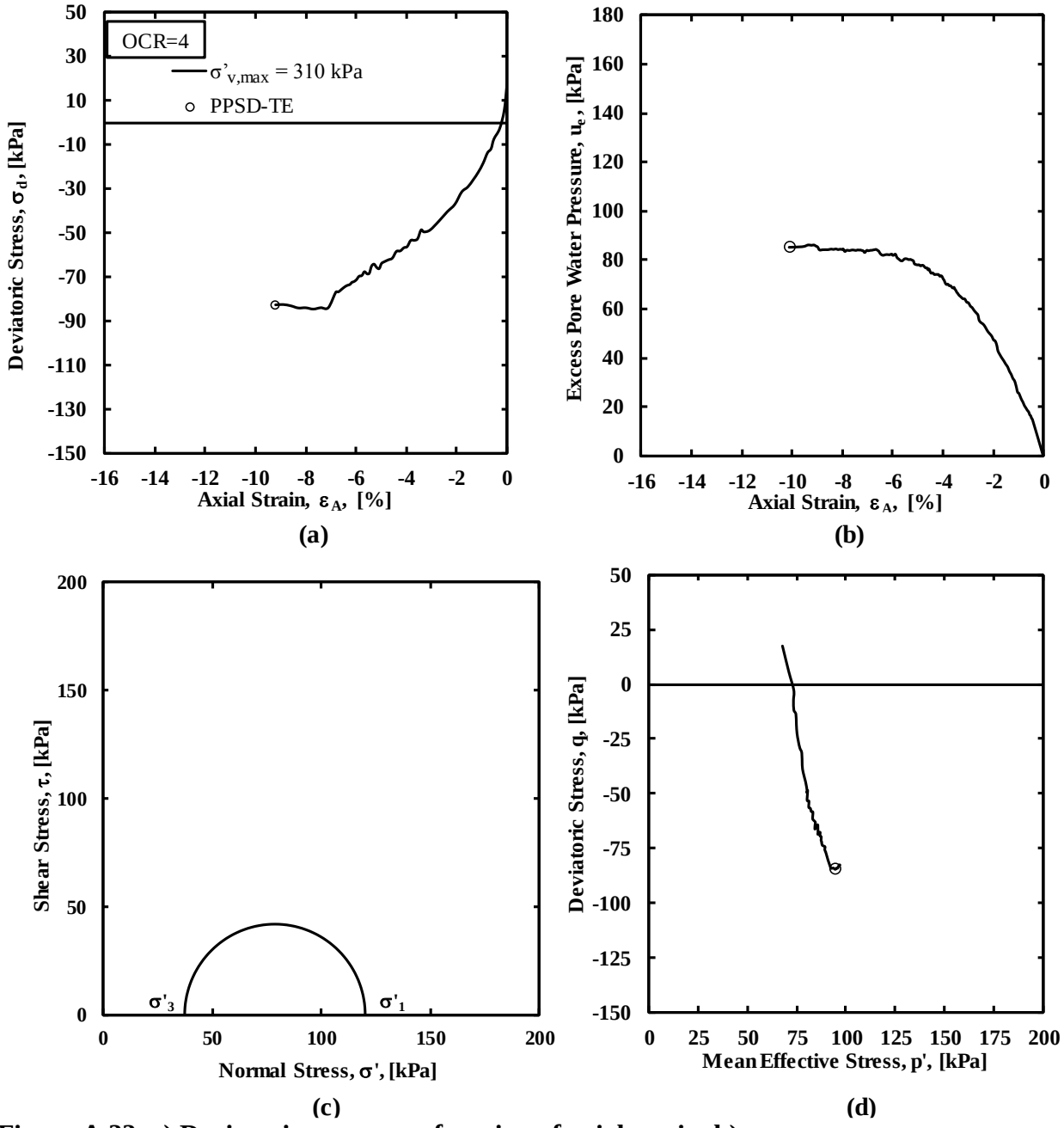

Figure A.33. a) Deviatoric stress as a function of axial strain, b) excess pore water pressure as a function of axial strain, c) Mohr circle, and d) Cambridge p-q stress path for the TE test at OCR=4 and $\sigma'_{v,max}$=310 kPa.

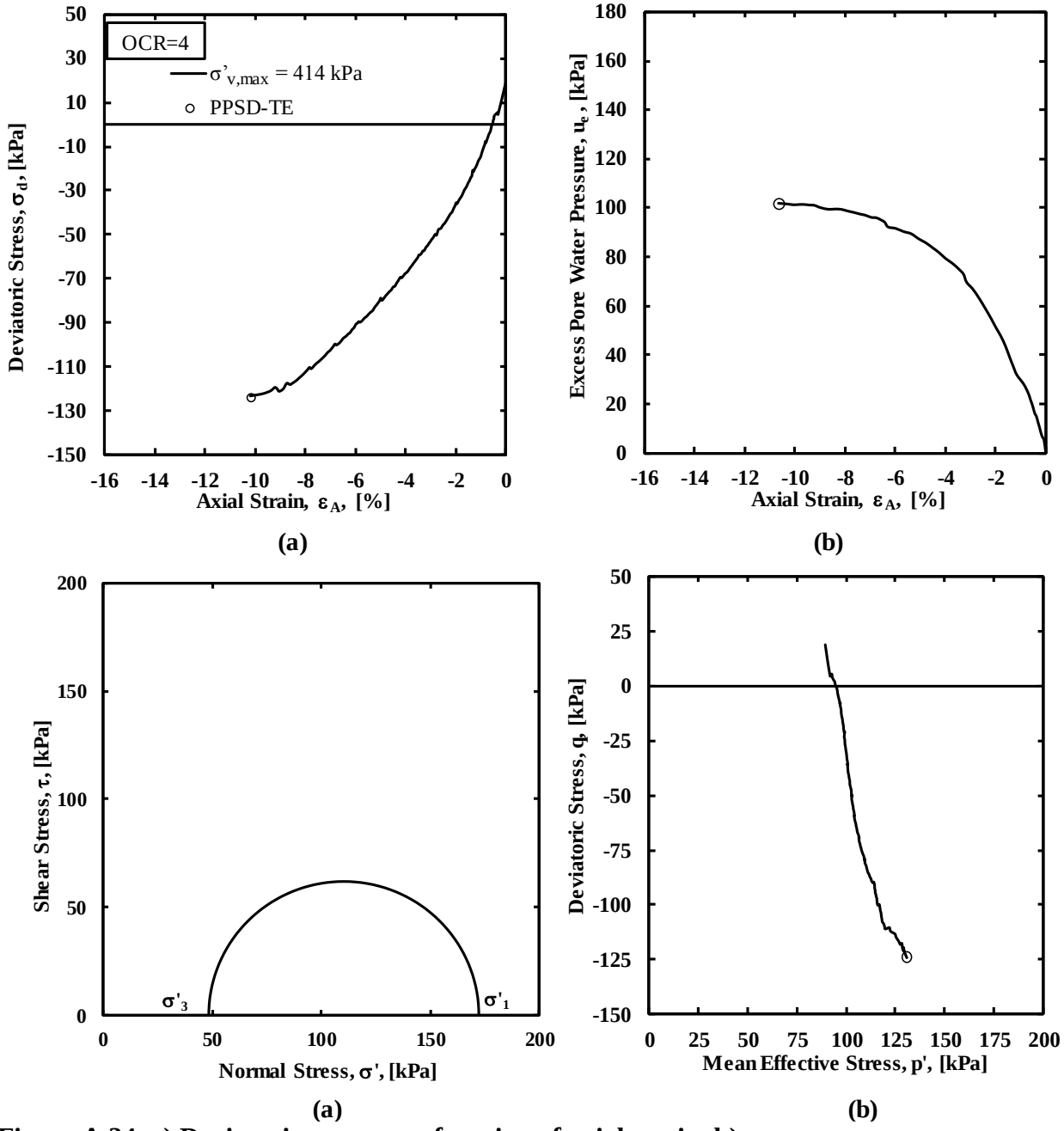

Figure A.34. a) Deviatoric stress as a function of axial strain, b) excess pore water pressure as a function of axial strain, c) Mohr circle, and d) Cambridge p-q stress path for the TE test at OCR=4 and $\sigma'_{v,max}$=414 kPa.

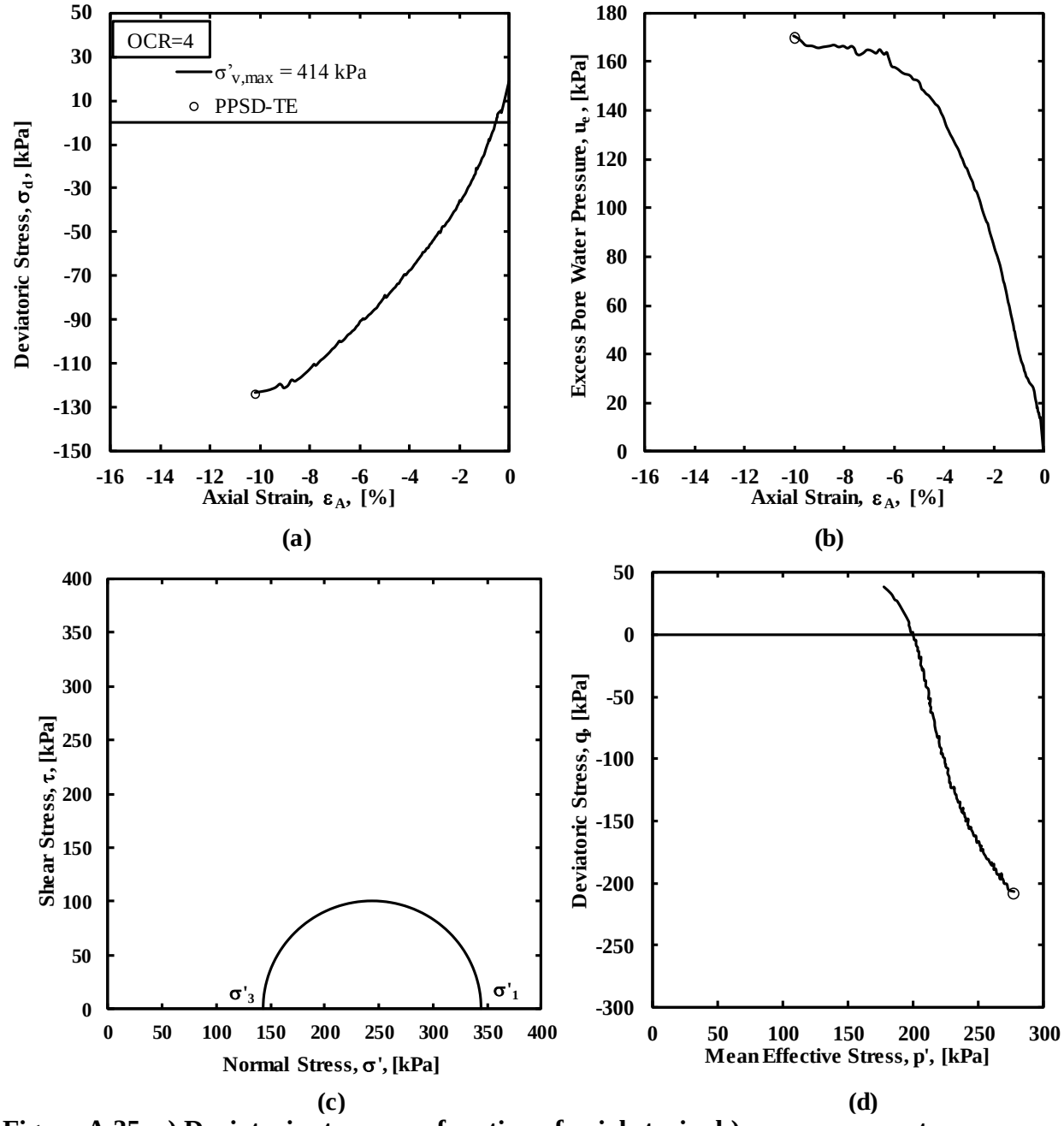

Figure A.35. a) Deviatoric stress as a function of axial strain, b) excess pore water pressure as a function of axial strain, c) Mohr circle, and d) Cambridge p-q stress path for the TE test at OCR=4 and $\sigma'_{v,max}$=828 kPa.

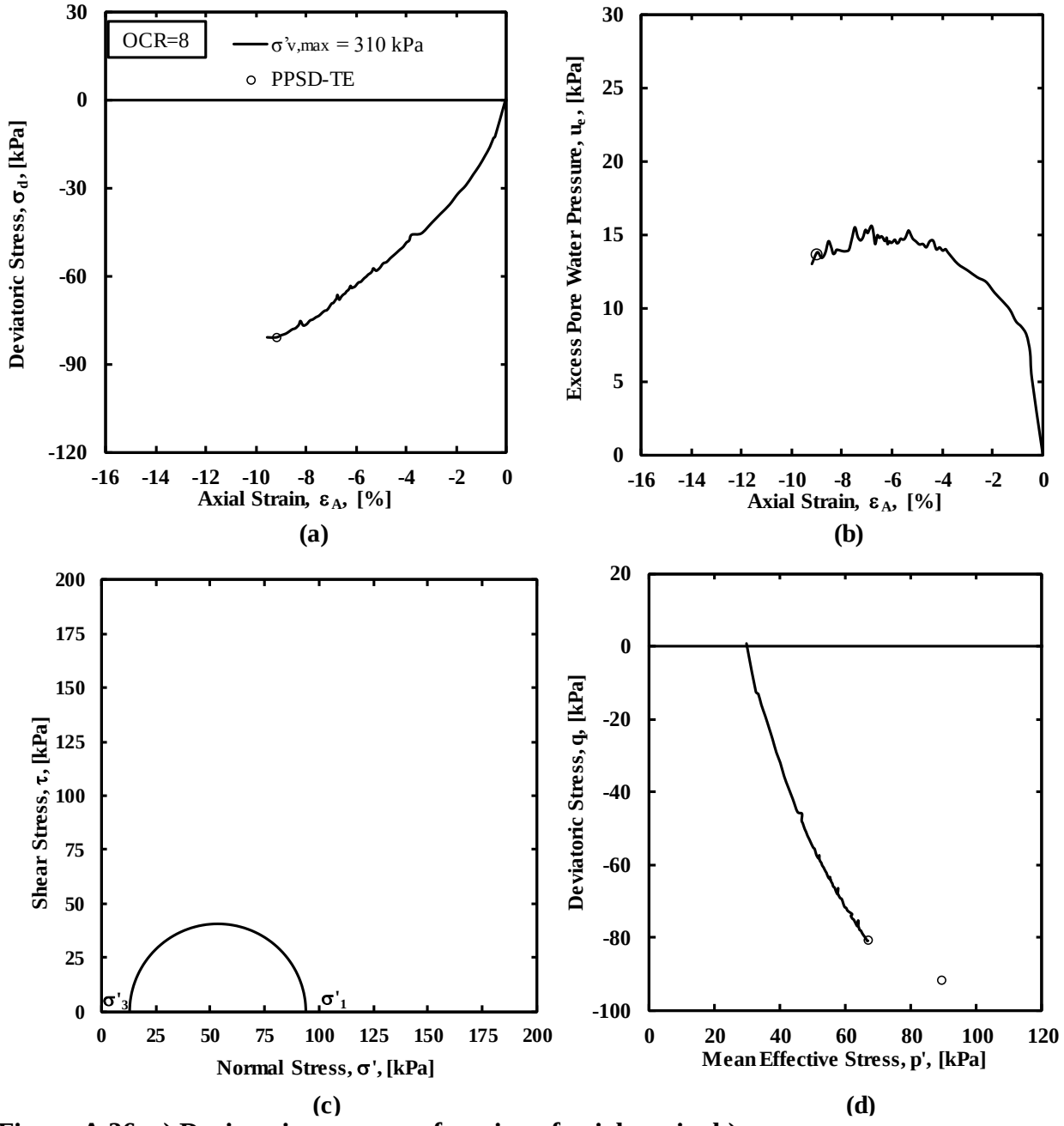

Figure A.36. a) Deviatoric stress as a function of axial strain, b) excess pore water pressure as a function of axial strain, c) Mohr circle, and d) Cambridge p-q stress path for the TE test at OCR=8 and $\sigma'_{v,max}$=310 kPa.

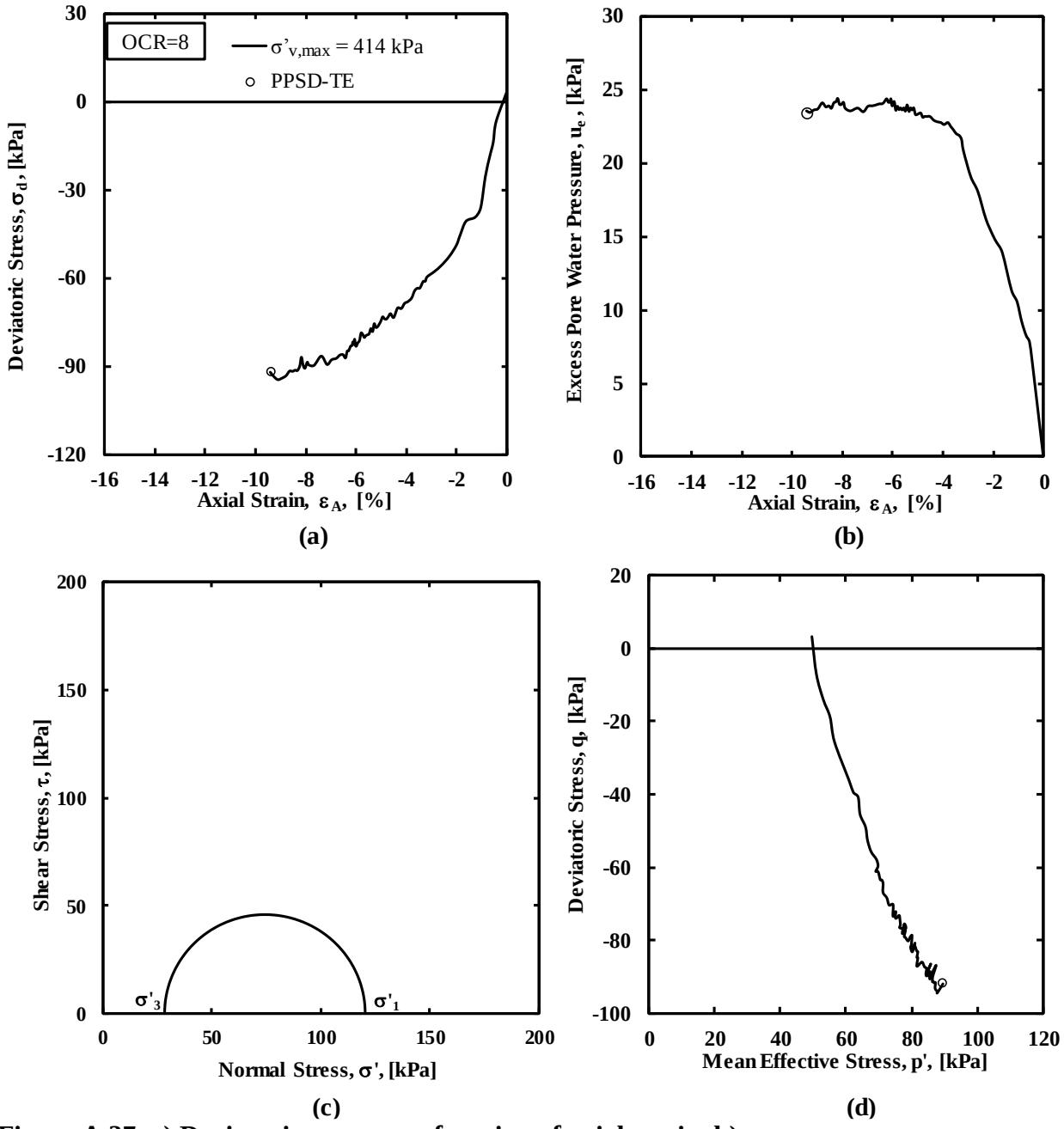

Figure A.37. a) Deviatoric stress as a function of axial strain, b) excess pore water pressure as a function of axial strain, c) Mohr circle, and d) Cambridge p-q stress path for the TE test at OCR=8 and $\sigma'_{v,max}$=414 kPa.

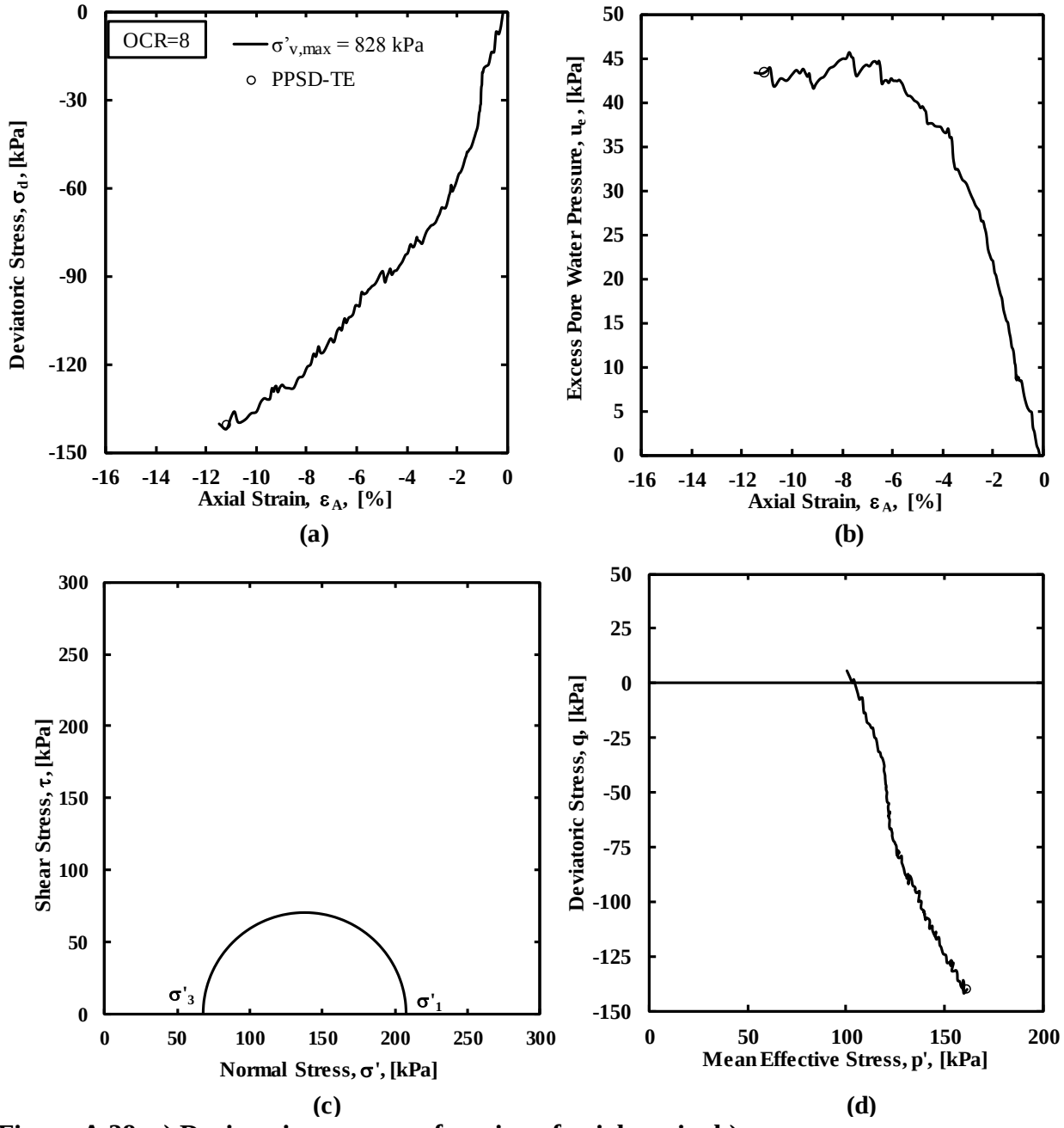

Figure A.38. a) Deviatoric stress as a function of axial strain, b) excess pore water pressure as a function of axial strain, c) Mohr circle, and d) Cambridge p-q stress path for the TE test at OCR=8 and $\sigma'_{v,max}$=828 kPa.

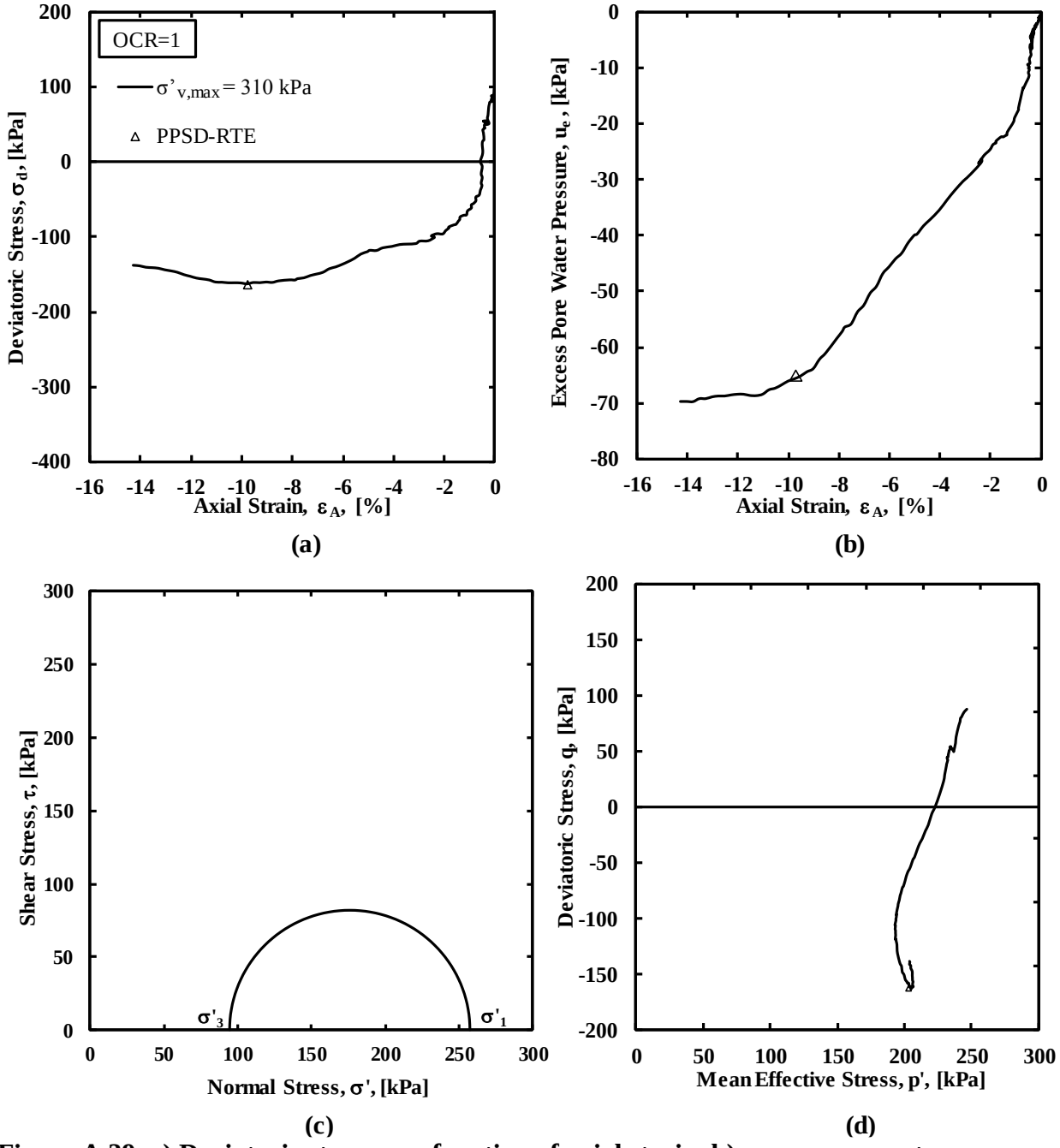

Figure A.39. a) Deviatoric stress as a function of axial strain, b) excess pore water pressure as a function of axial strain, c) Mohr circle, and d) Cambridge p-q stress path for the RTE test at OCR=1 and $\sigma'_{v,max}$ =310 kPa.

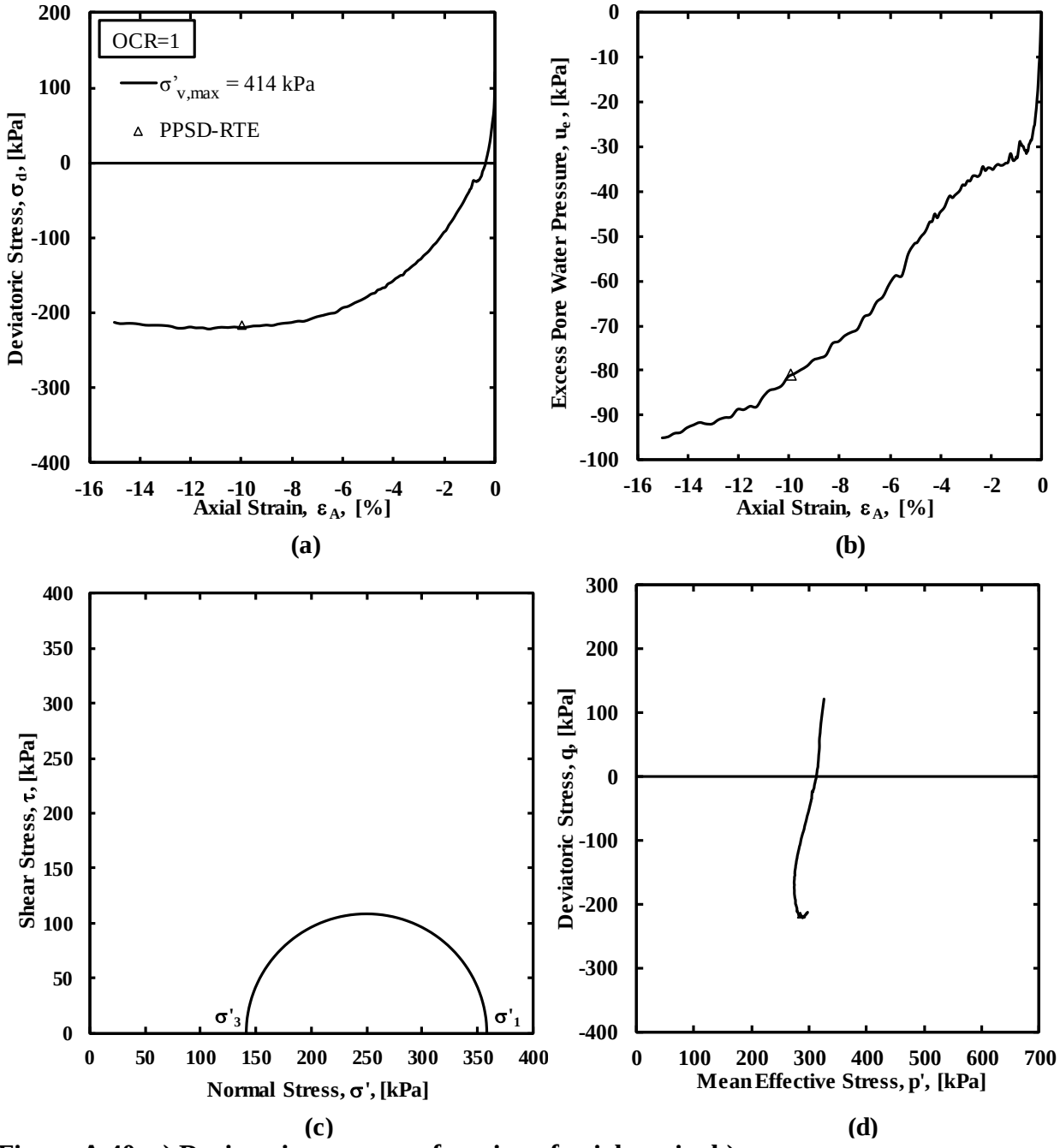

Figure A.40. a) Deviatoric stress as a function of axial strain, b) excess pore water pressure as a function of axial strain, c) Mohr circle, and d) Cambridge p-q stress path for the RTE test at OCR=1 and $\sigma'_{v,max}$ =414 kPa.

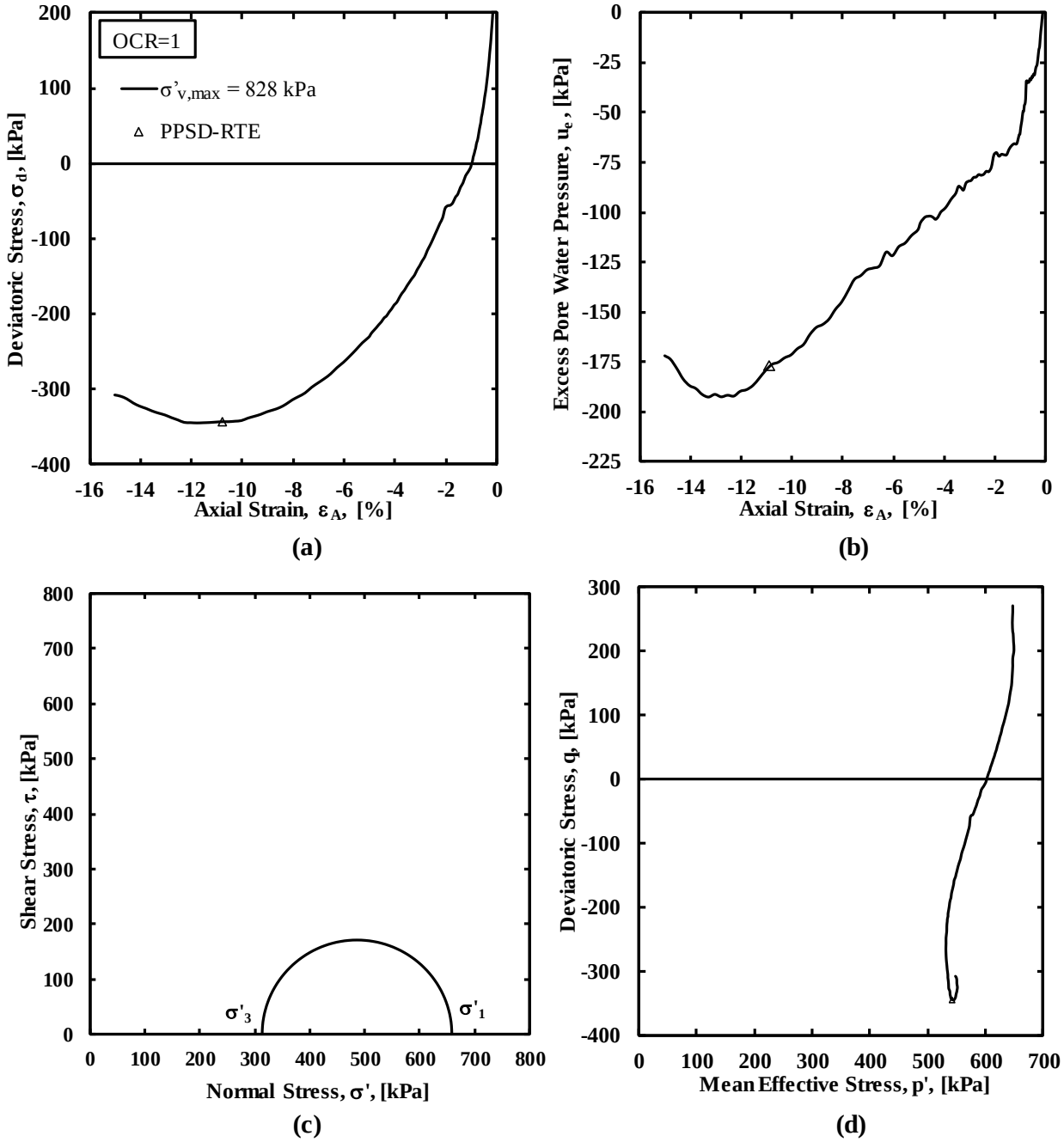

Figure A.41. a) Deviatoric stress as a function of axial strain, b) excess pore water pressure as a function of axial strain, c) Mohr circle, and d) Cambridge p-q stress path for the RTE test at OCR=1 and σ'$_{v,max}$=828 kPa.

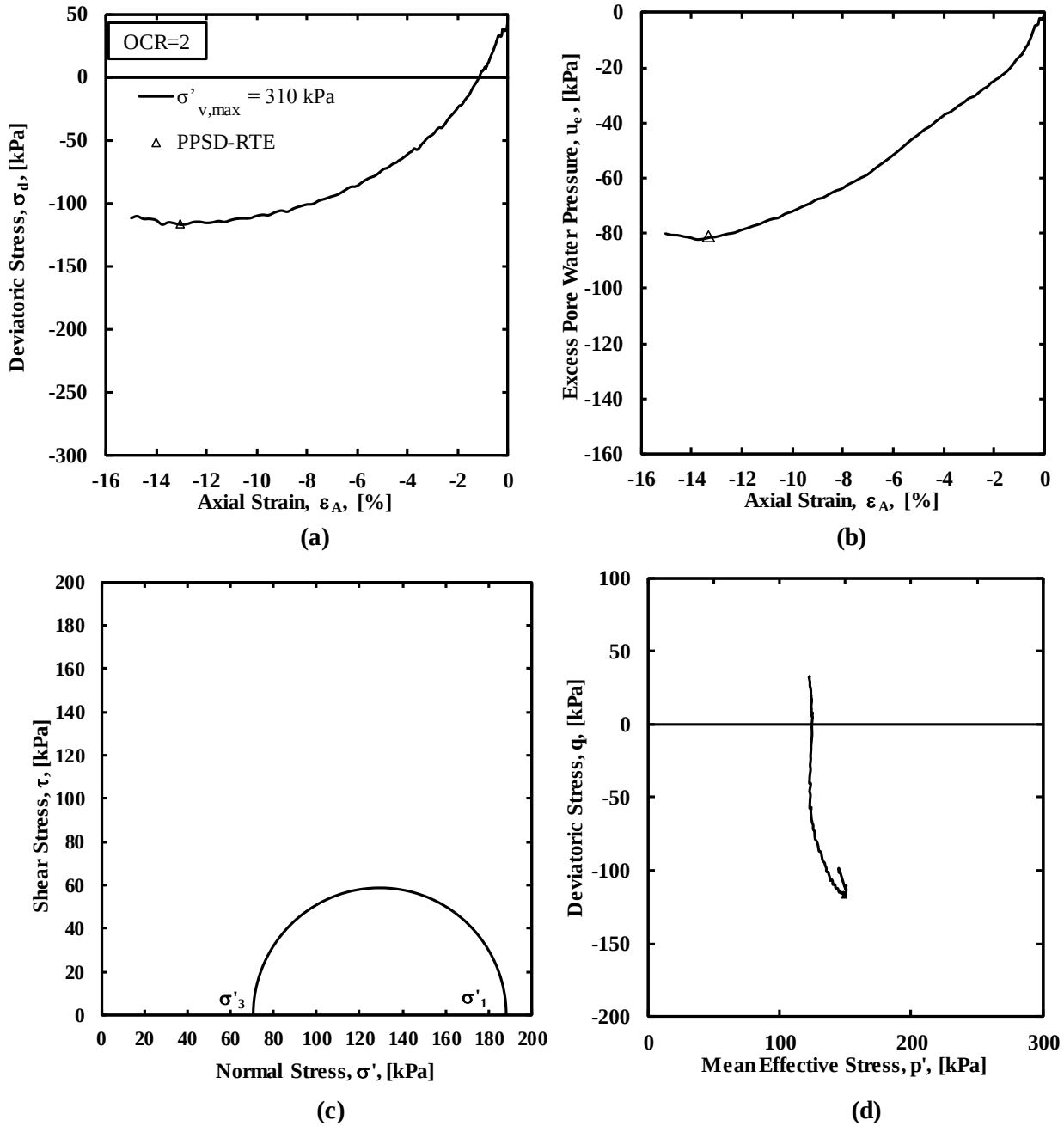

Figure A.42. a) Deviatoric stress as a function of axial strain, b) excess pore water pressure as a function of axial strain, c) Mohr circle, and d) Cambridge p-q stress path for the RTE test at OCR=2 and $\sigma'_{v,max}$=310 kPa.

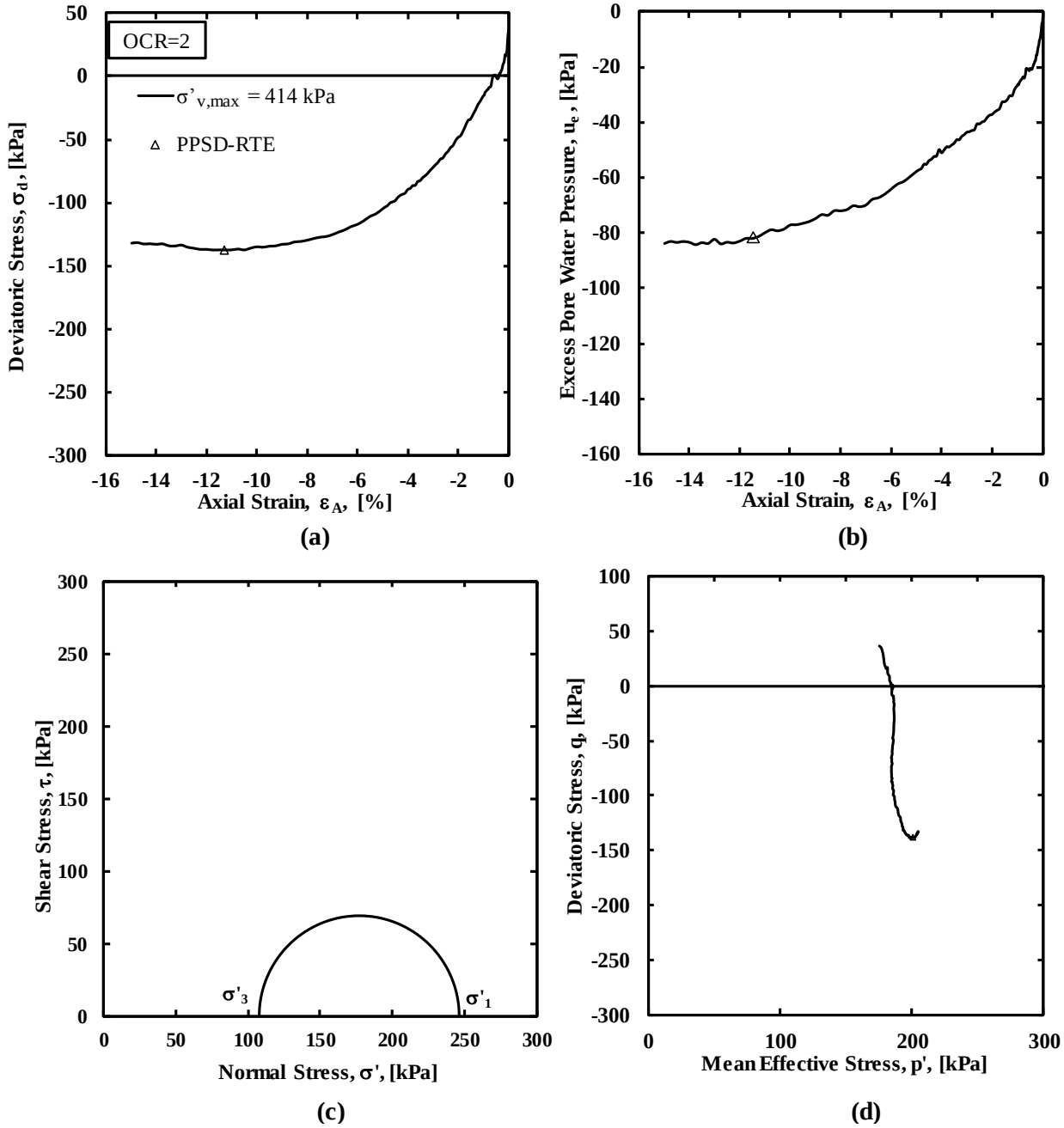

Figure A.43. a) Deviatoric stress as a function of axial strain, b) excess pore water pressure as a function of axial strain, c) Mohr circle, and d) Cambridge p-q stress path for the RTE test at OCR=2 and $\sigma'_{v,max}$=414 kPa.

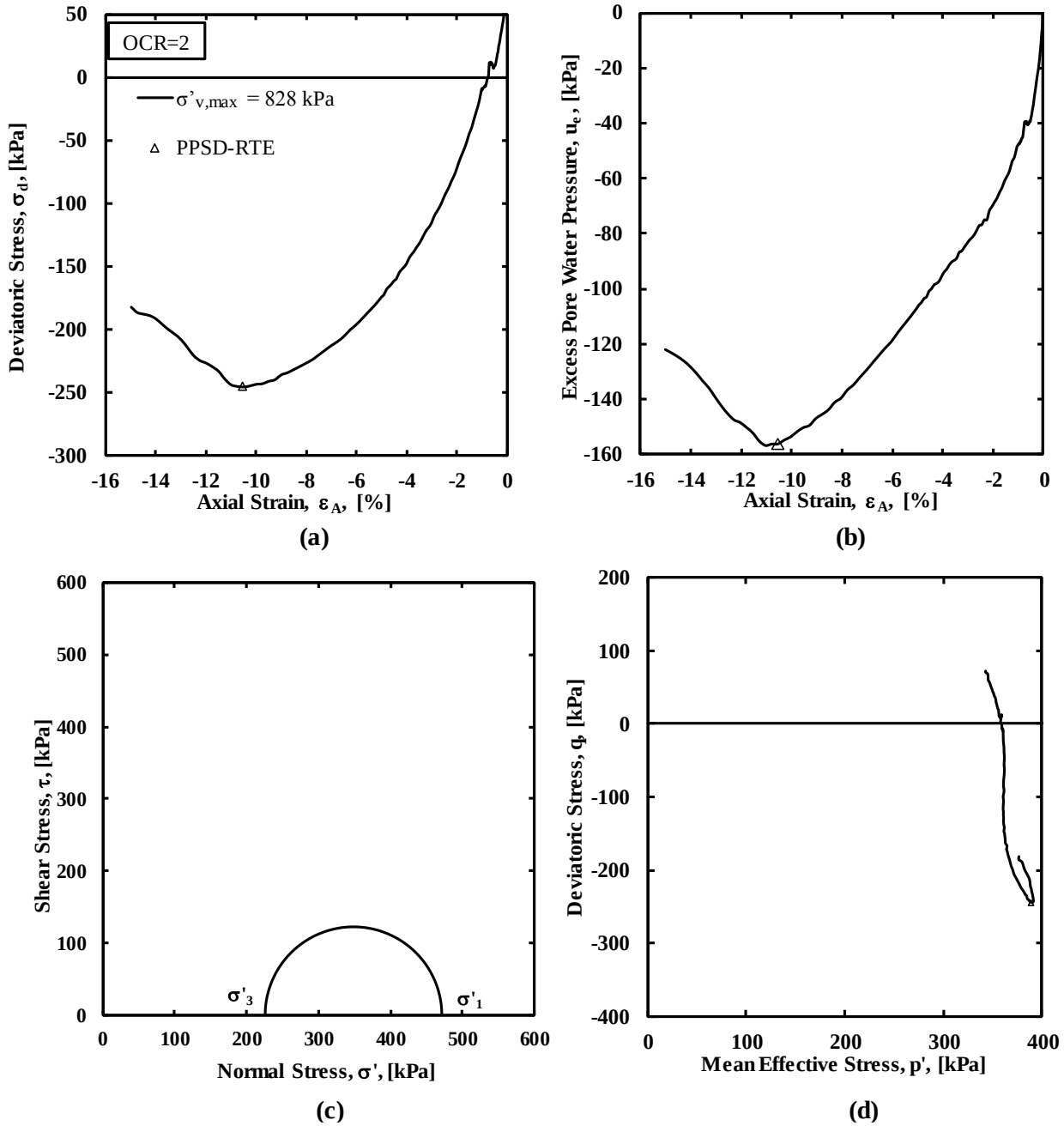

Figure A.44. a) Deviatoric stress as a function of axial strain, b) excess pore water pressure as a function of axial strain, c) Mohr circle, and d) Cambridge p-q stress path for the RTE test at OCR=2 and σ'$_{v,max}$=828 kPa.

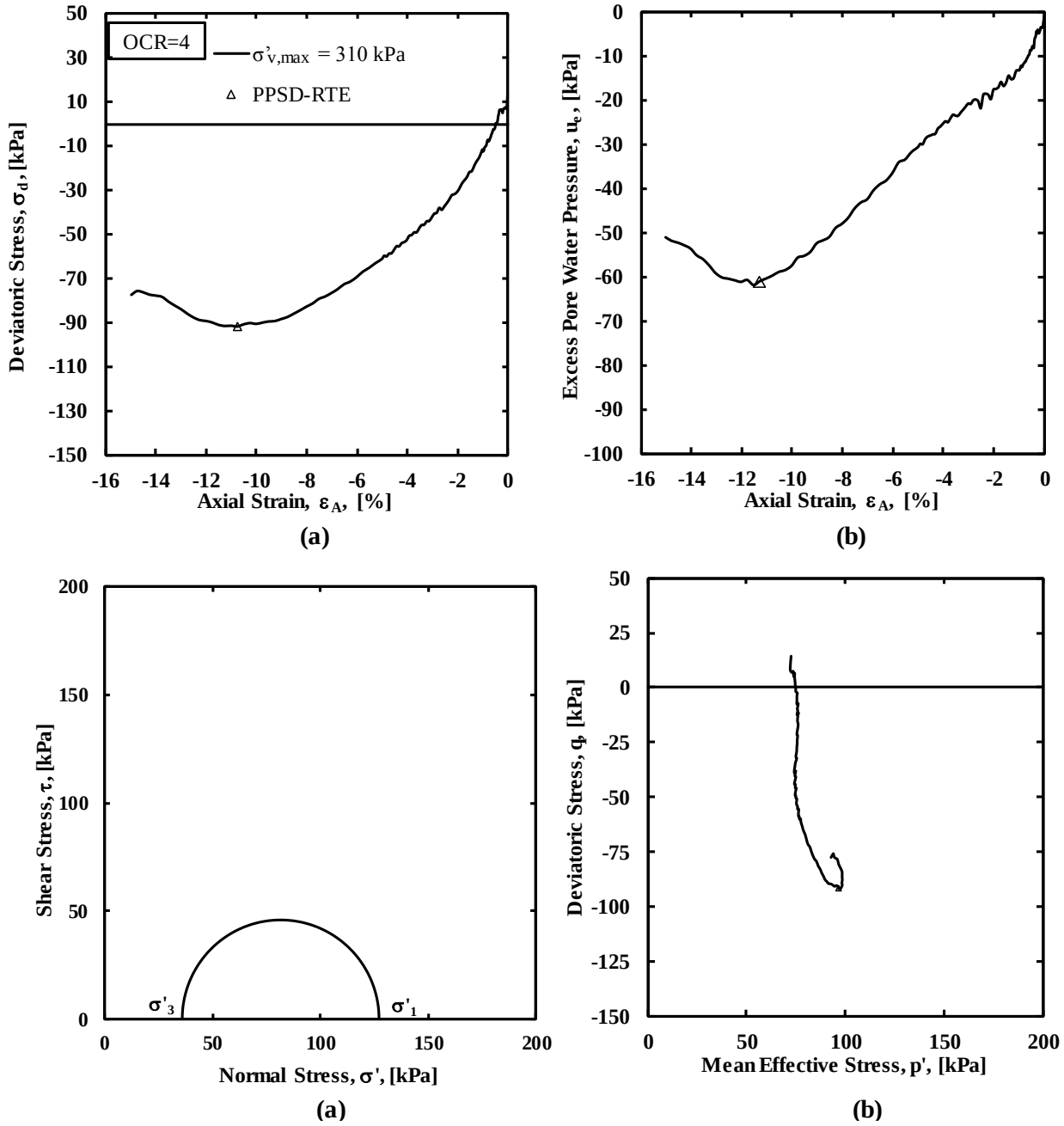

Figure A.45. a) Deviatoric stress as a function of axial strain, b) excess pore water pressure as a function of axial strain, c) Mohr circle, and d) Cambridge p-q stress path for the RTE test at OCR=4 and $\sigma'_{v,max}$=310 kPa.

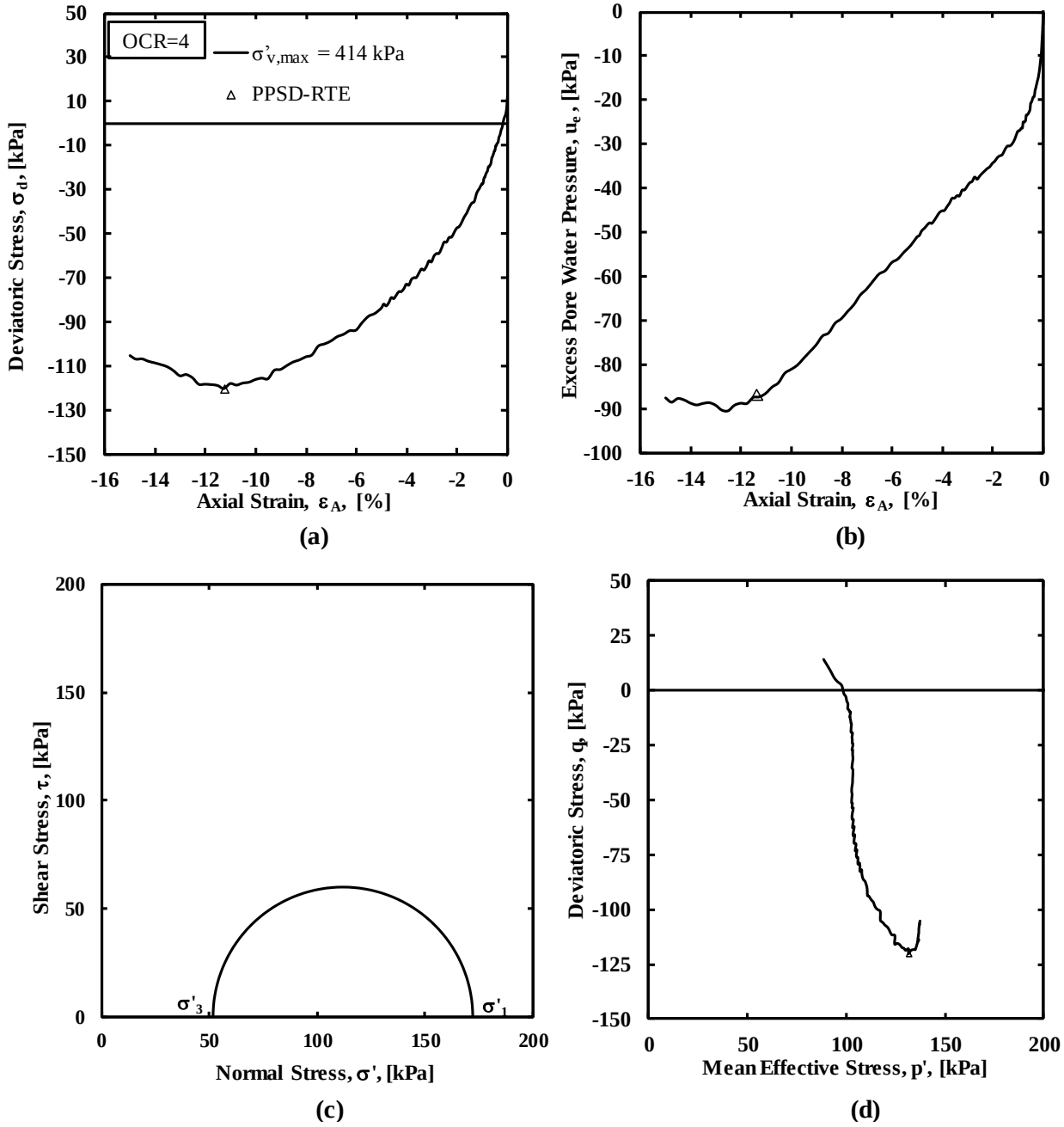

Figure A.46. a) Deviatoric stress as a function of axial strain, b) excess pore water pressure as a function of axial strain, c) Mohr circle, and d) Cambridge p-q stress path for the RTE test at OCR=4 and $\sigma'_{v,max}$=414 kPa.

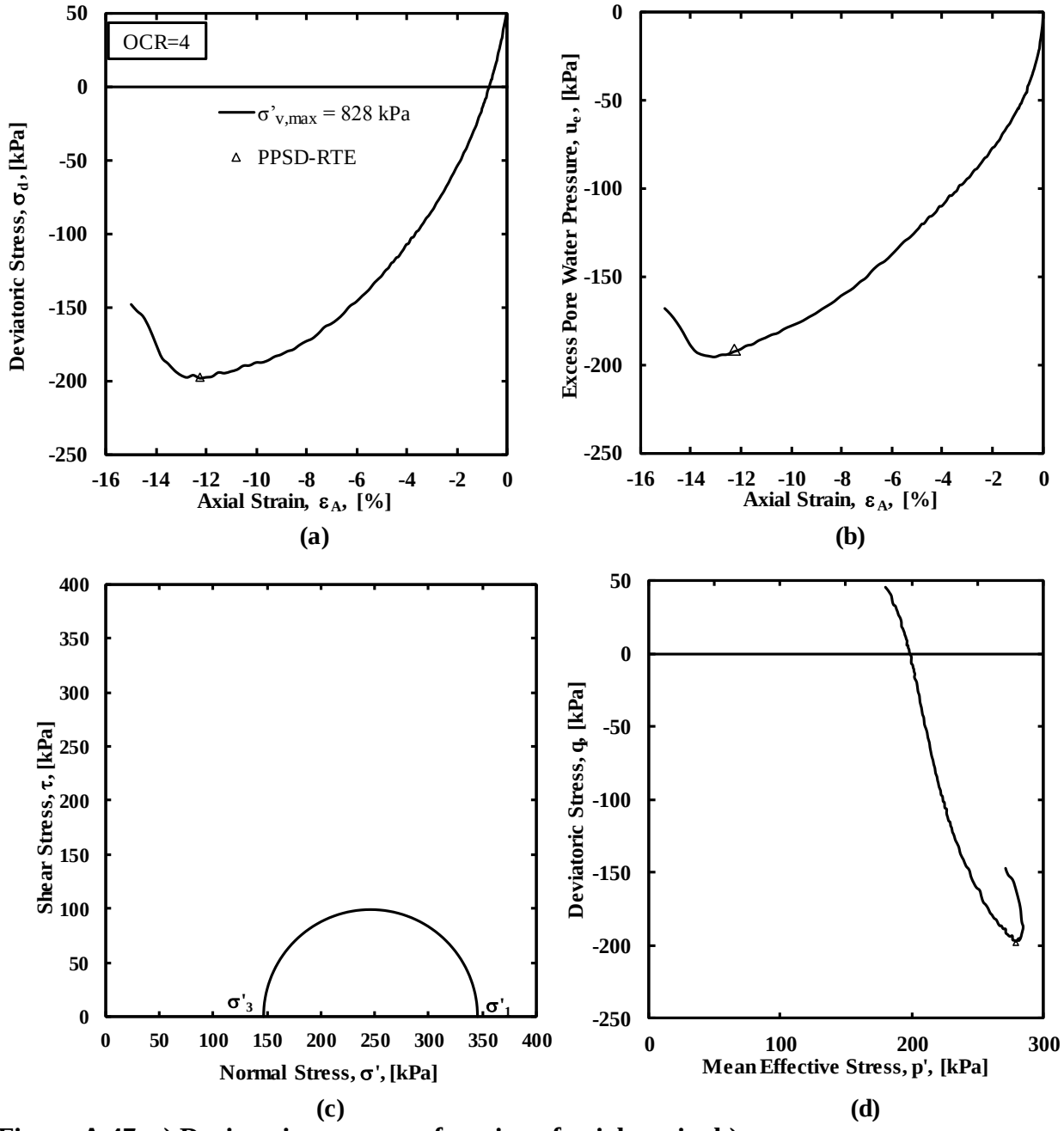

Figure A.47. a) Deviatoric stress as a function of axial strain, b) excess pore water pressure as a function of axial strain, c) Mohr circle, and d) Cambridge p-q stress path for the RTE test at OCR=4 and $\sigma'_{v,max}$=828 kPa.

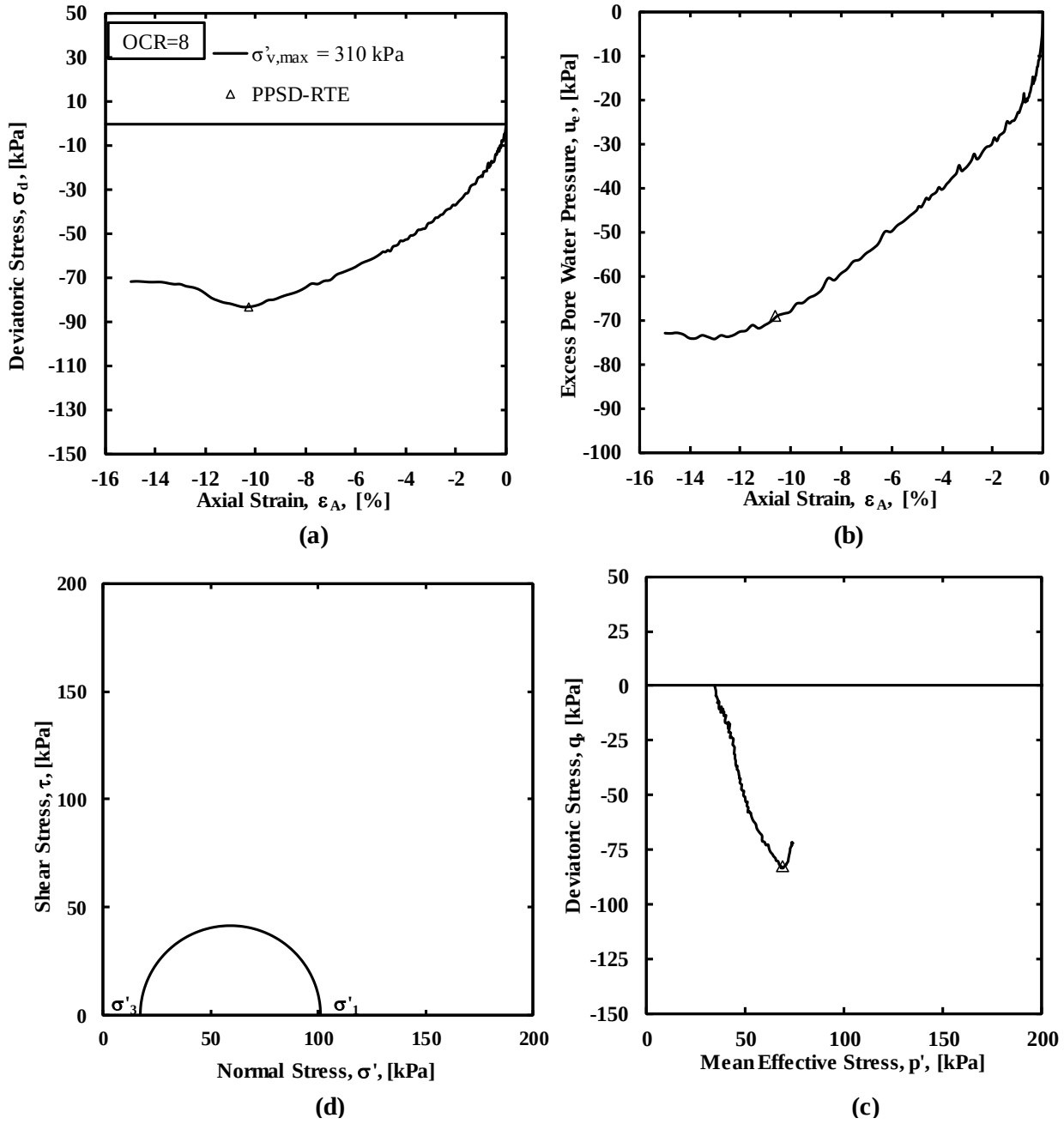

Figure A.48. a) Deviatoric stress as a function of axial strain, b) excess pore water pressure as a function of axial strain, c) Mohr circle, and d) Cambridge p-q stress path for the RTE test at OCR=8 and $\sigma'_{v,max}$=310 kPa.

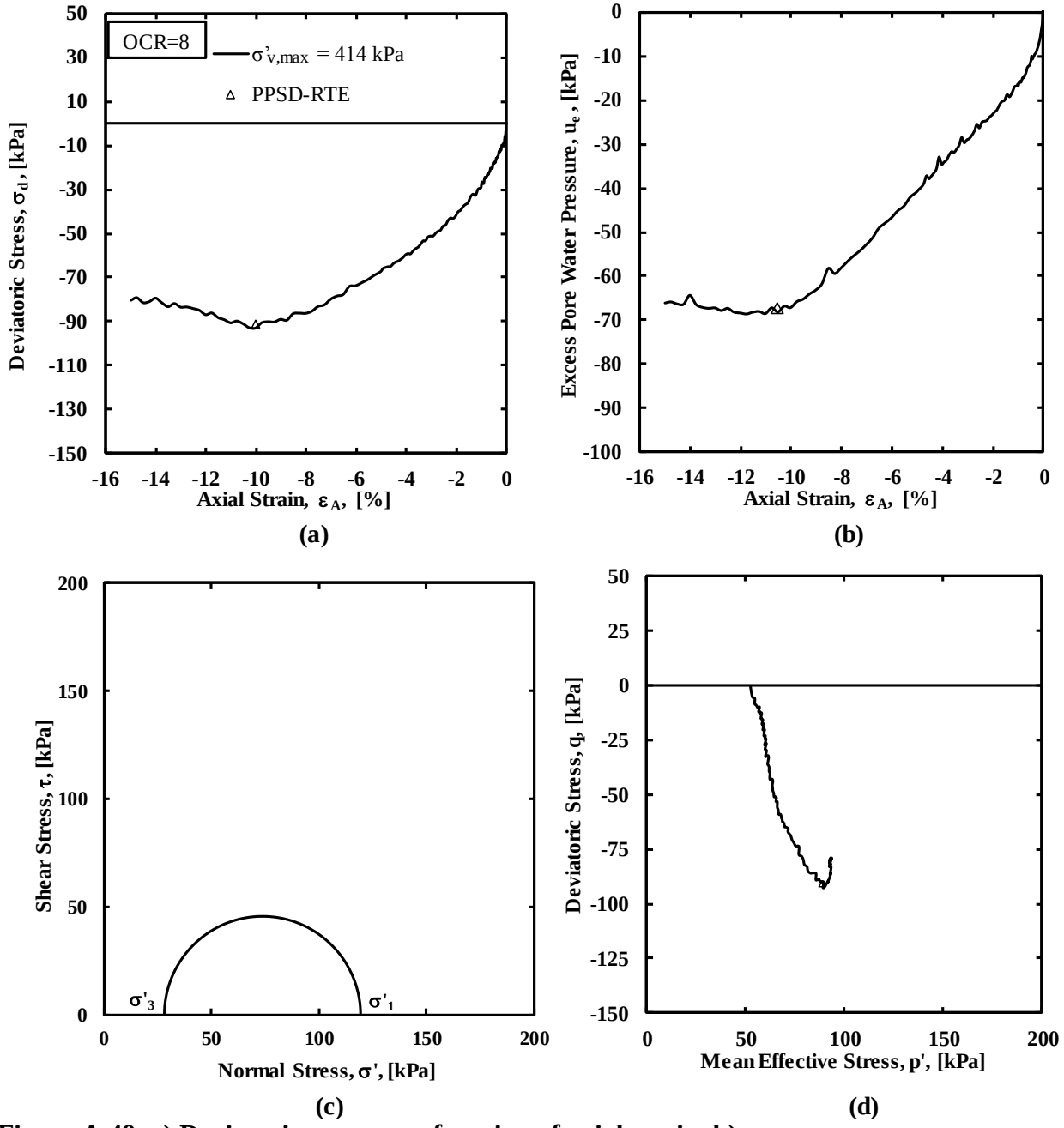

Figure A.49. a) Deviatoric stress as a function of axial strain, b) excess pore water pressure as a function of axial strain, c) Mohr circle, and d) Cambridge p-q stress path for the RTE test at OCR=8 and $\sigma'_{v,max}$=414 kPa.

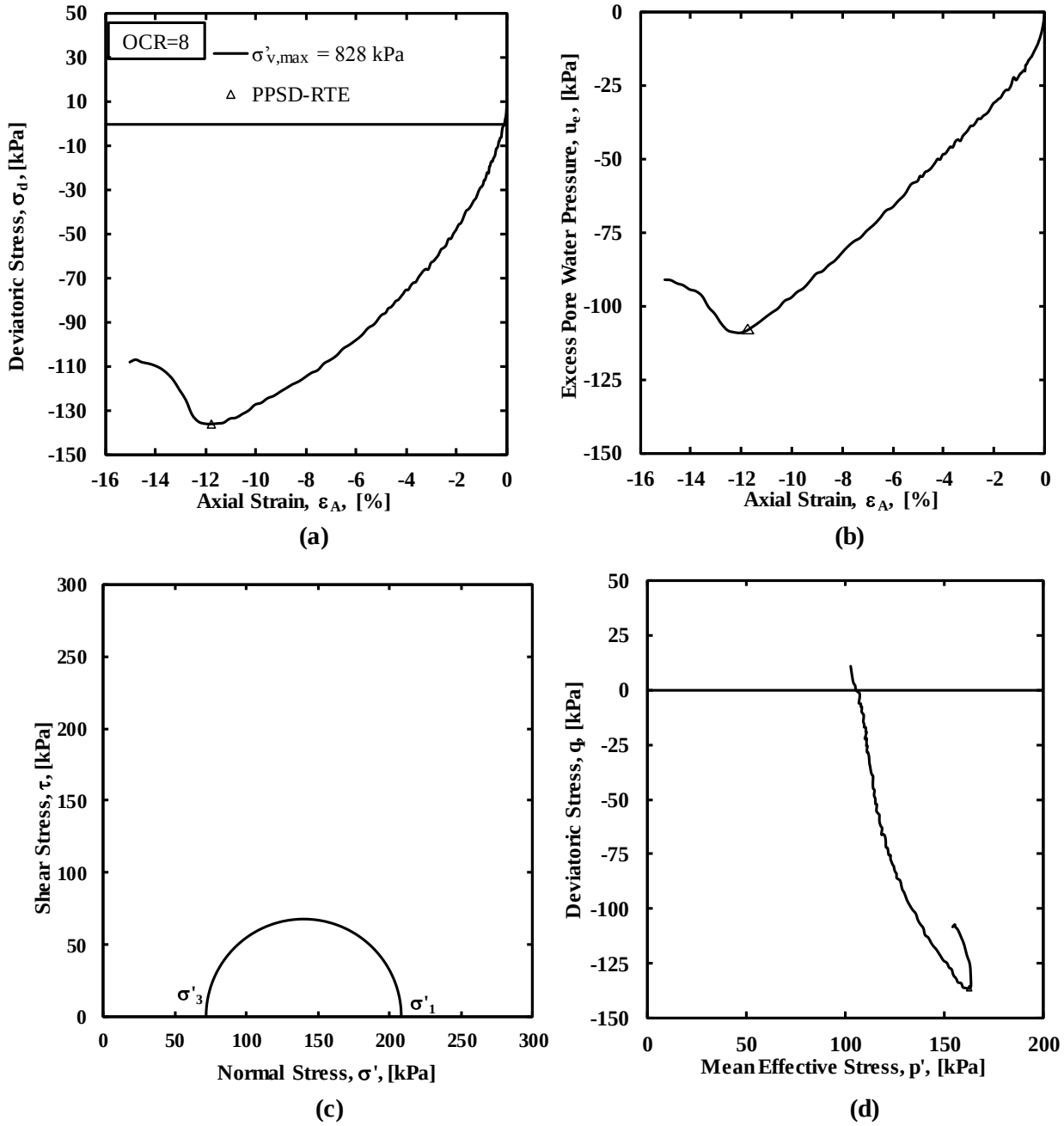

Figure A.50. a) Deviatoric stress as a function of axial strain, b) excess pore water pressure as a function of axial strain, c) Mohr circle, and d) Cambridge p-q stress path for the RTE test at OCR=8 and $\sigma'_{v,max}$=828 kPa.

A.4. Shear Wave Velocity and Shear Modulus Results

Included in this section are the results obtained from the triaxial tests, with bender element measurements, that were performed on kaolinite and illite soil specimens. These results include: 1) measured shear wave velocity as a function of axial stress, 2) shear modulus as a function of axial strain, 3) measured shear wave velocity as a function of void index, 4) shear modulus as a function of void index, and 5) shear modulus as a function of excess pore water pressure.

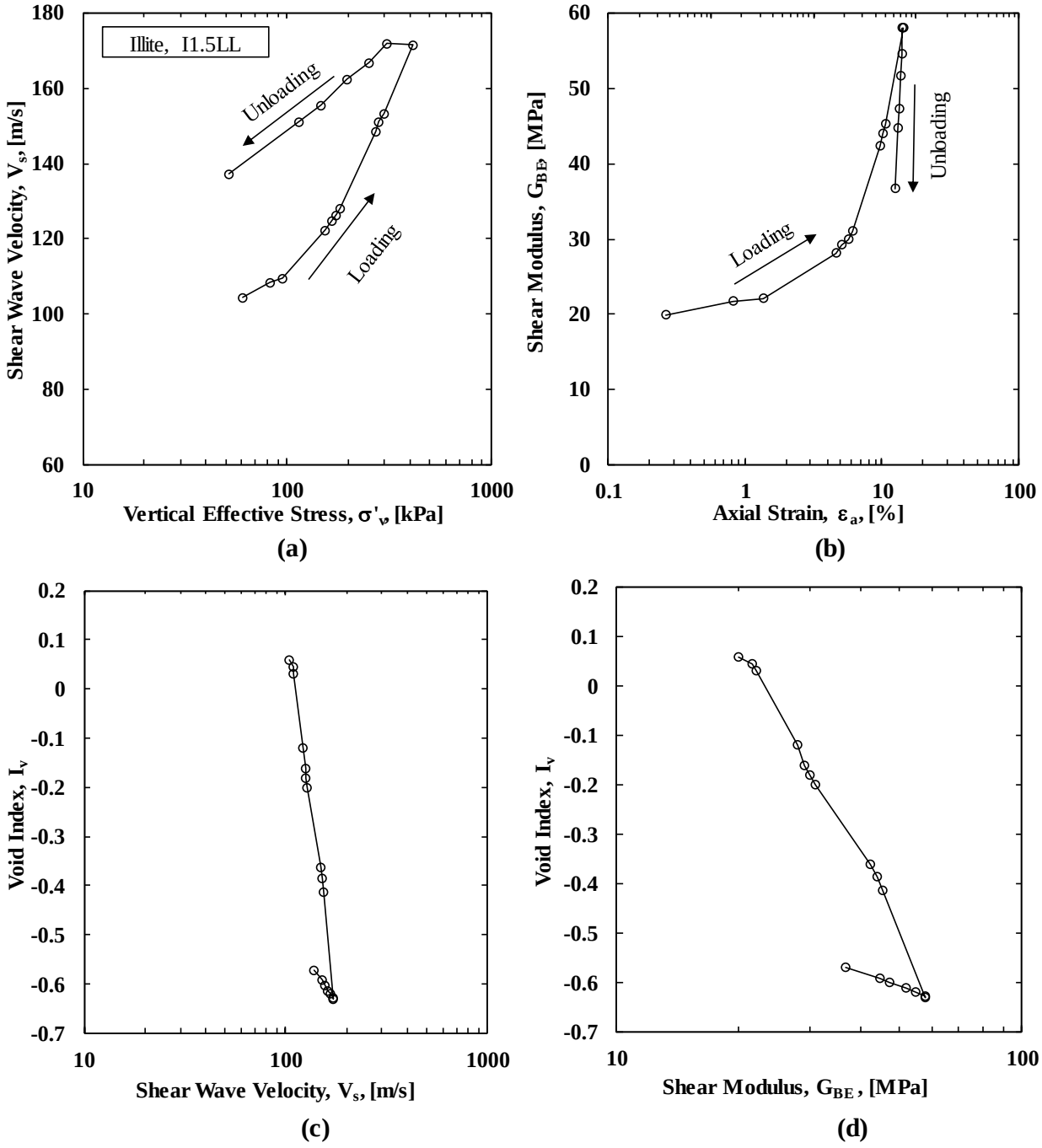

Figure A.51. The small-strain values for reconstituted illite (I1.5LL): a) shear wave velocity-vertical effective stress relationship, b) shear modulus-axial strain relationship, c) shear wave velocity as a function of void index, and d) shear modulus as a function of void index.

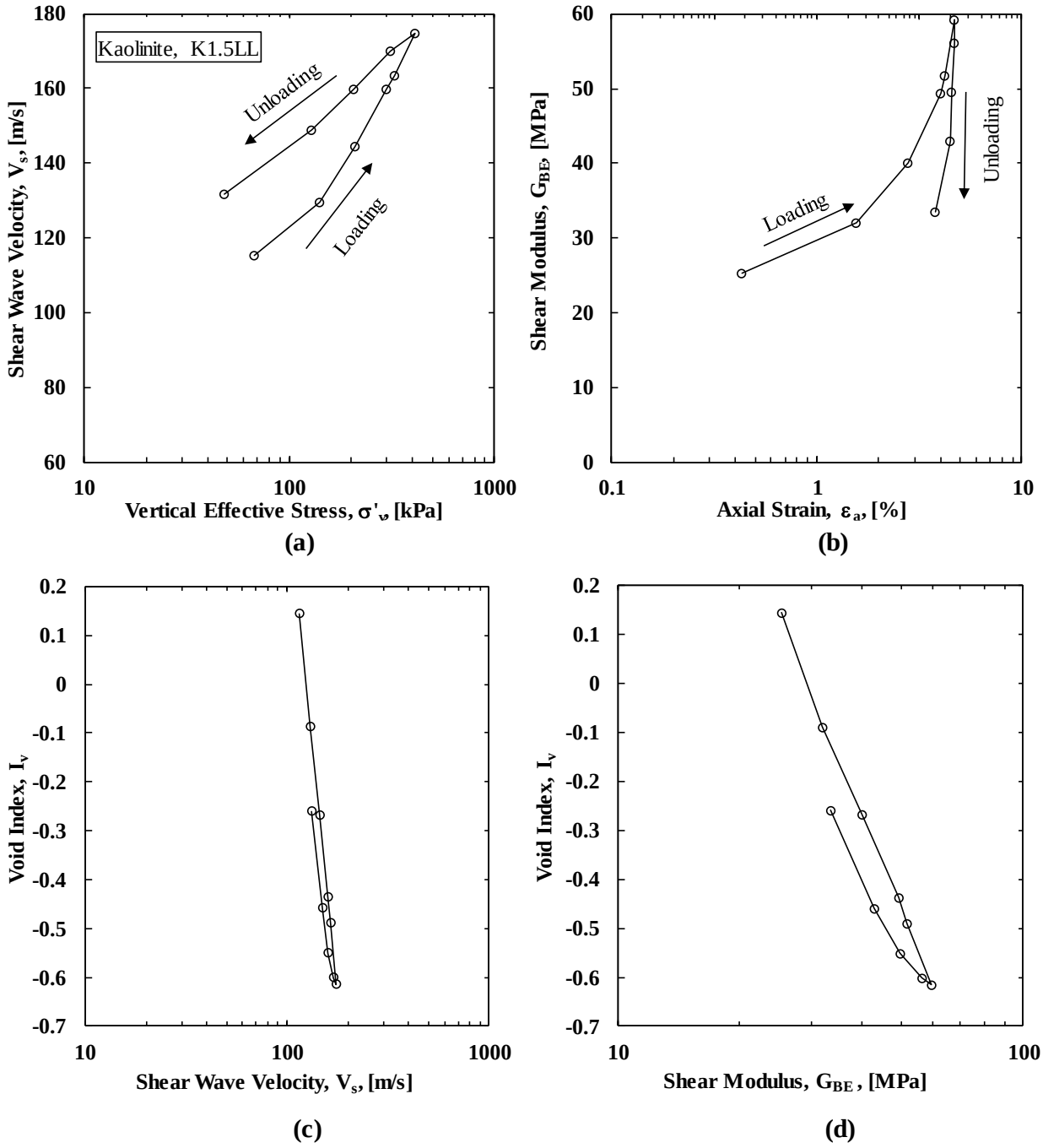

Figure A.52. The small-strain values for reconstituted kaolinite (K1.5LL): a) shear wave velocity-vertical effective stress relationship, b) shear modulus-axial strain relationship, c) shear wave velocity as a function of void index, and d) shear modulus as a function of void index.

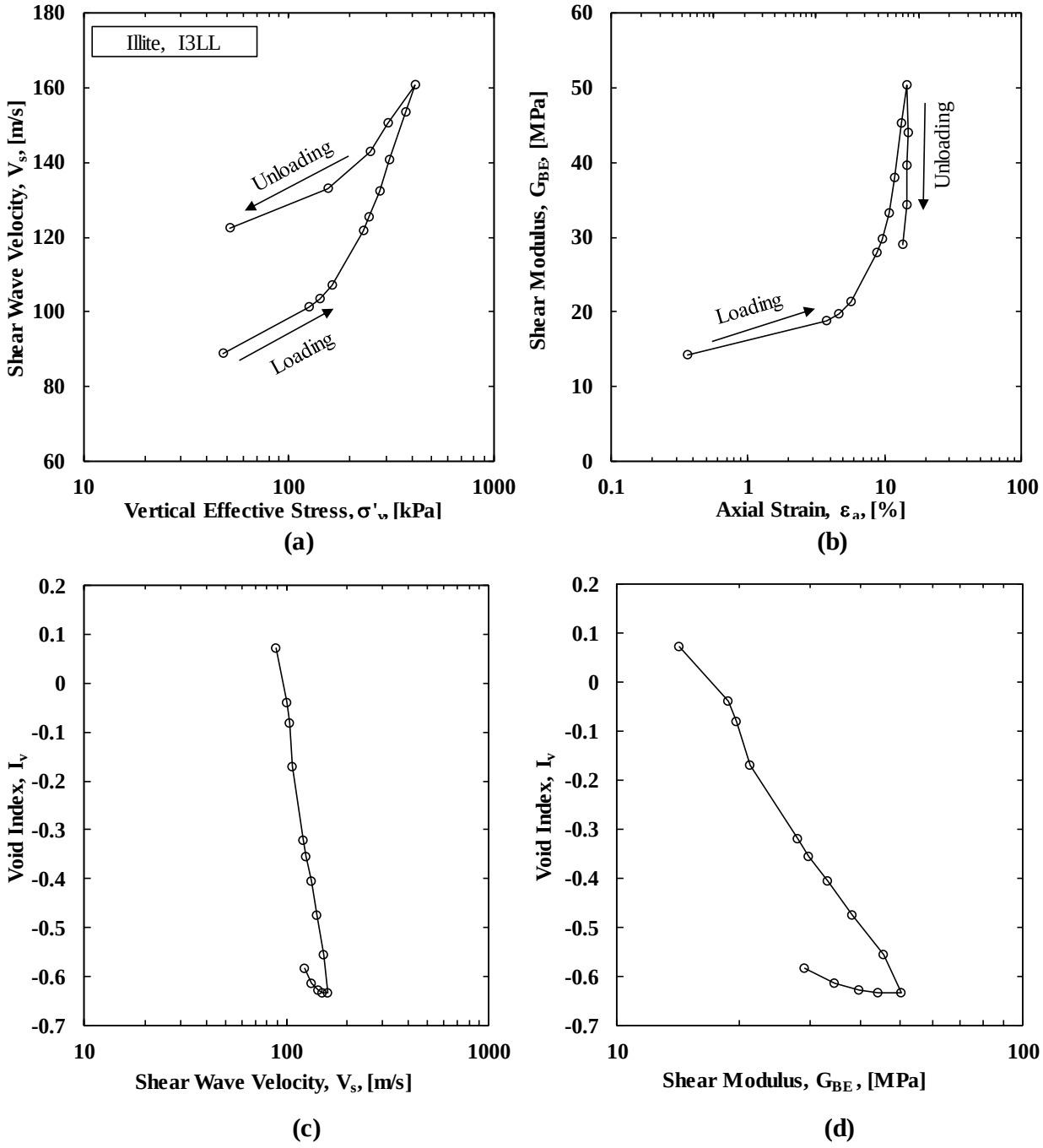

Figure A.53. The small-strain values for reconstituted illite (I3LL): a) shear wave velocity-vertical effective stress relationship, b) shear modulus-axial strain relationship, c) shear wave velocity as a function of void index, and d) shear modulus as a function of void index.

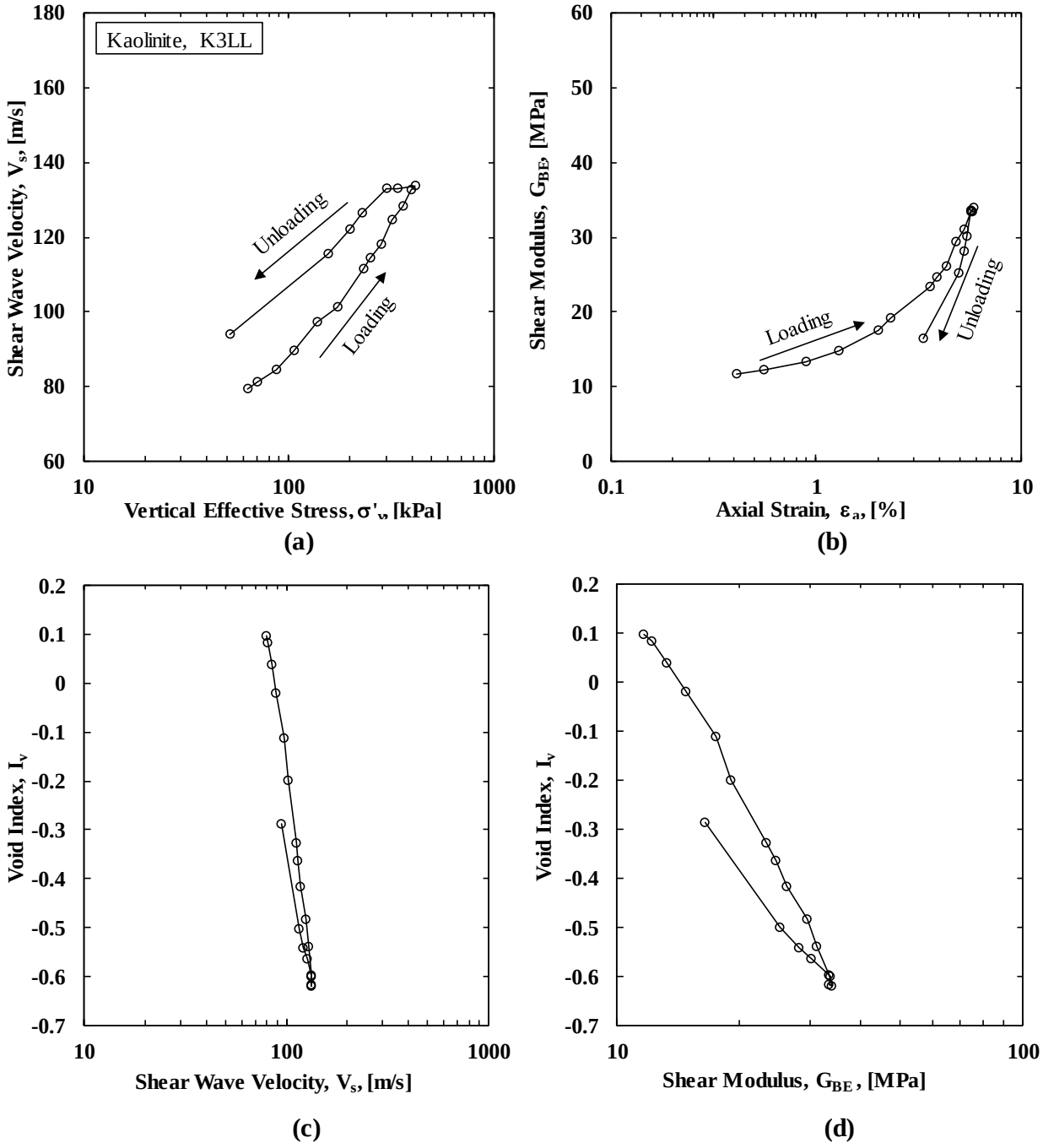

Figure A.54. The small-strain values for reconstituted kaolinite (K3LL): a) shear wave velocity-vertical effective stress relationship, b) shear modulus-axial strain relationship, c) shear wave velocity as a function of void index, and d) shear modulus as a function of void index.

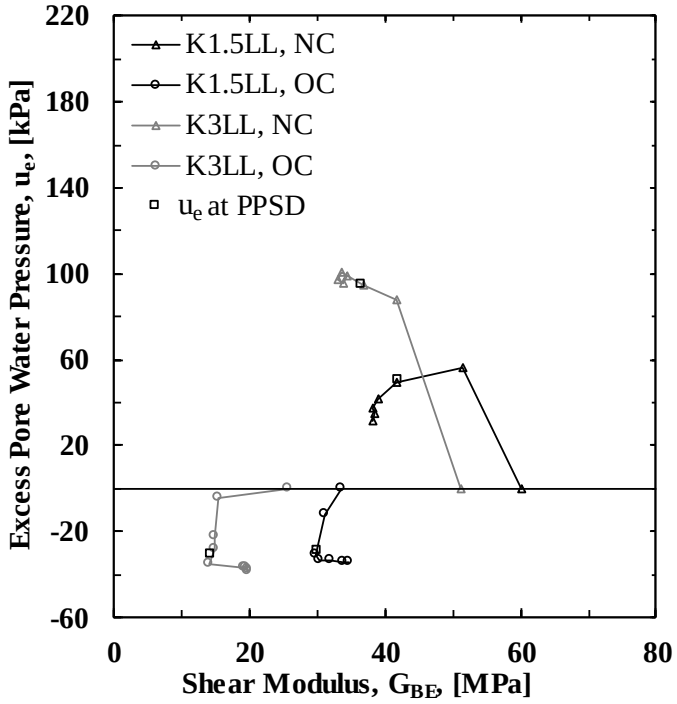

Figure A.55. Shear modulus-excess pore water pressure relationships, during shearing stage, for the kaolinite specimens.

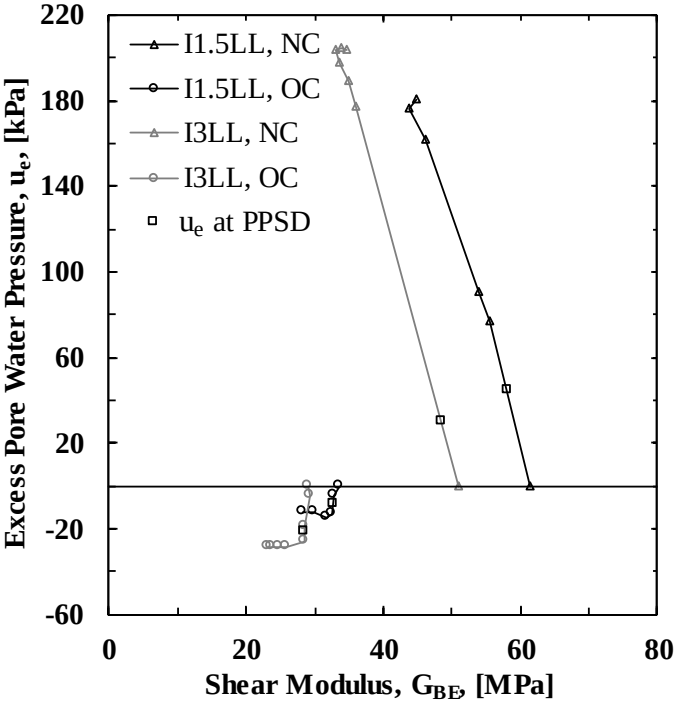

Figure A.56. Shear modulus-excess pore water pressure relationships, during shearing stage, for the illite specimens.